

DUKE POWER COMPANY

POWER BUILDING

422 SOUTH CHURCH STREET, CHARLOTTE, N. C. 28242

WILLIAM O. PARKER, JR.
VICE PRESIDENT
STEAM PRODUCTION

April 8, 1982

TELEPHONE: AREA 704
373-4083

Mr. Harold R. Denton, Director
Office of Nuclear Reactor Regulation
U. S. Nuclear Regulatory Commission
Washington, D. C. 20555

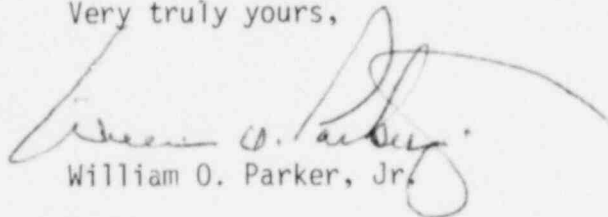
Attention: Ms. E. G. Adensam, Chief
Licensing Branch No. 4

Re: Catawba Nuclear Station
Docket Nos. 50-413 and 50-414

Dear Mr. Denton:

My letter of January 20, 1982 transmitted a list of Action Items which was compiled during a December 15-18, 1981 meeting with the Structural Engineering Branch. Responses to these Action Items are attached except for Items 27, 31, and 32 which will be provided by May 7, 1982.

Very truly yours,



William O. Parker, Jr.

ROS/php
Attachment

cc: (w/o attachment)
J. P. O'Reilly
P. K. Van Doorn
R. Guild
Palmetto Alliance



BOO!

1/1

Aperture Dist.

SEND DRUGS to

Pm

8204160397 820408
PDR ADDCK 05000413
A PDR

1. With respect to groundmotion response spectra, Duke will provide a comparison of the Catawba design with respect to Regulatory Guide 1.60 and address and justify deviations therefrom.

Response:

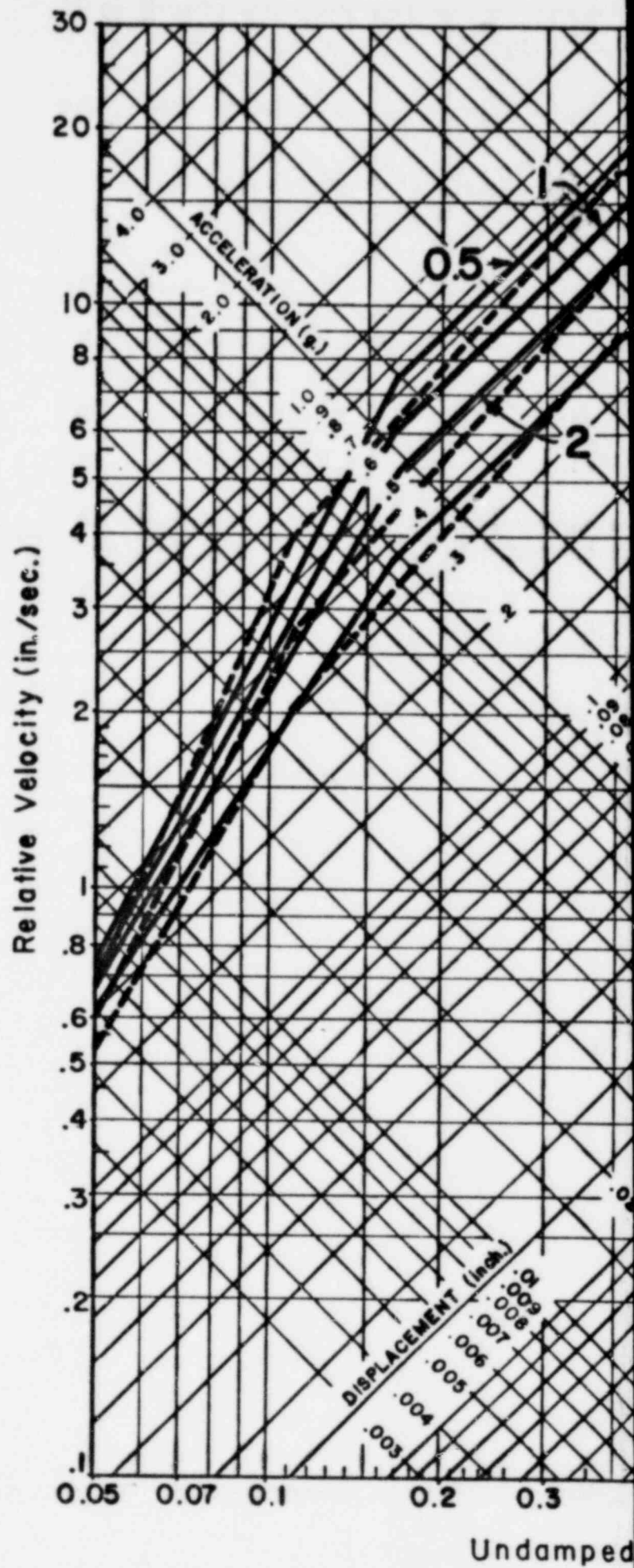
The design ground response spectra obtained from the procedures outlined in Regulatory Guide 1.60 are plotted against the spectra used for the Catawba design in the attached figure.

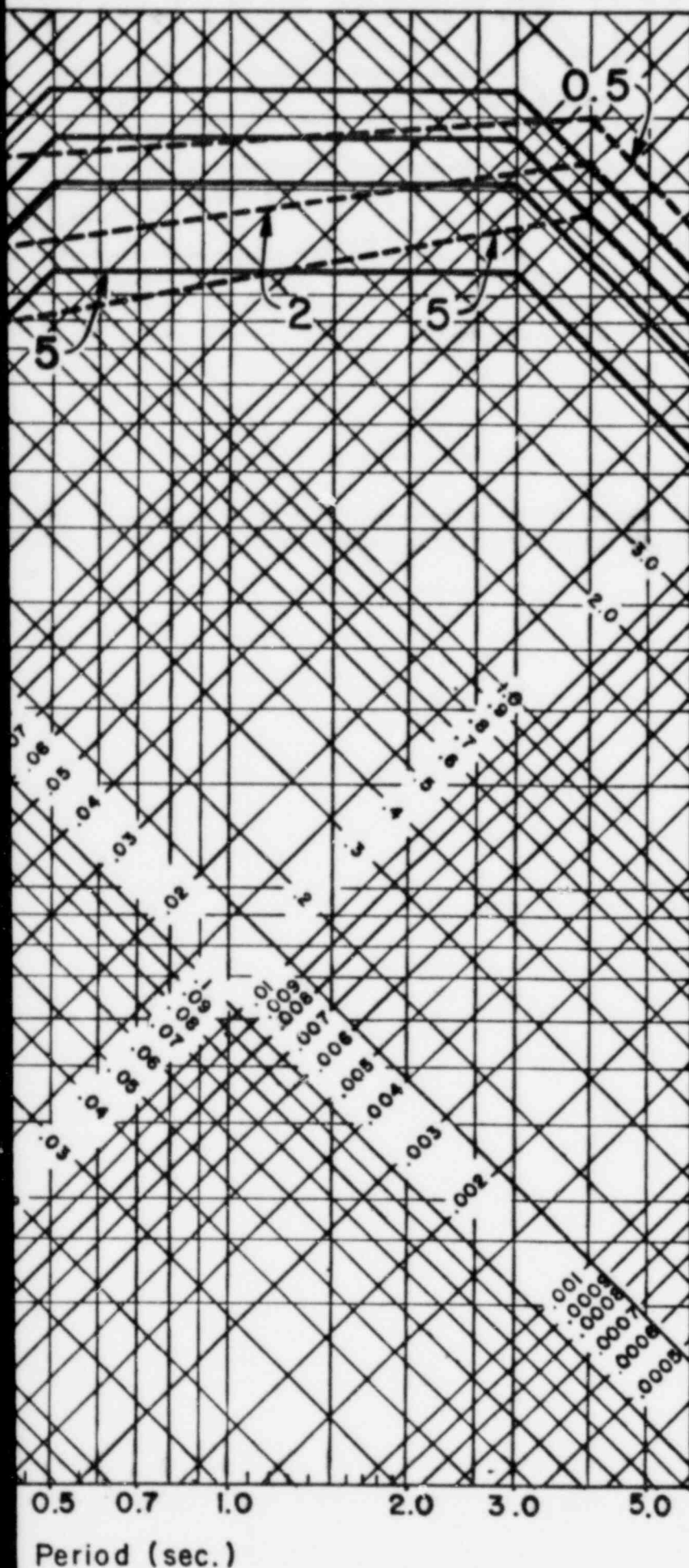
The curves of interest are the 2% and 5% damping curves. The 2% curve is used for welded steel structures and the 5% curve is used for concrete structures. The lowest first mode frequency of any Category one structure is 5.4 cps. Therefore, comparison will be made from the 5.4 cps frequency level and higher.

For the 5% damping curve, the Catawba design acceleration spectra envelopes or equals that resulting from the Regulatory Guide 1.60 criteria.

In the frequency range above 12.5 cps on the 2% damping curve, the Catawba design acceleration spectra equals that resulting from the Regulatory Guide 1.60 criteria. Between 12.5 cps and 7.7 cps, on the 2% curve, the Regulatory Guide criteria envelopes the Catawba design criteria. (The maximum discrepancy is 5% in this frequency range with the average difference being less than 2.5%.) In the frequency range between 7.7 cps and 5.4 cps, the Catawba design acceleration spectra envelopes that resulting from the Regulatory Guide 1.60 criteria.

In conclusion it is noted that the Catawba design response spectra is not based on Regulatory Guide 1.60 criteria but compares very favorably to it.





LEGEND

- Design Spectra
- - - Spectra per Regulatory Guide 1.60

DESIGN RESPONSE SPECTRUM,
 .15g
 CATAWBA NUCLEAR STATION
 FIGURE 2.5.2-7
 OVER PLOT OF REGULATORY
 GUIDE 1.60 USING
 QUESTION 230.3 AT STARTING: .12g

2. Duke will provide a comparison of the key floor response spectra obtained for both a 4% and 5% damping OBE and address and justify deviations.

Response:

The structural damping used at Catawba for Class 1 structures was 5% for both the OBE and SSE seismic conditions. This is the damping to which Duke Power has committed to in both the PSAR and the FSAR, Section 3.7.1.3, and the one to which it is still committed. Regulatory Guide 1.61, implemented after the PSAR review, requires a 4% damping for OBE conditions and 7% for SSE conditions. A comparison will be made between the present criteria and that used for design at Catawba.

Key floor response spectra will be computed for both 4% and 5% structural damping for the OBE seismic condition. The SSE case will not be checked because the Regulatory Guide damping of 7% is in excess of the 5% used in the Catawba design. The attached spectra and Table 2-1 show the results of the above comparison.

Table 2-1 indicates some minor frequency shifts and changes in peak values from +4% to -14.1%. It is felt that since the SSE earthquake controls, the design of plant and components and because the SSE spectra is taken as 15/8 times the OBE spectra, 5% structural damping used in both cases, that the resulting design is conservative and adequate in all cases.

TABULATION OF RESULTS

TABLE 2-1

Fig. No.	Period At Max. Acce.	Max. Acce. 5% Damping (2's)	Max. Acce. 4% Damping (2's)	With 10% Cap.		
				$\Delta\%$ Max. Acce 5% Damping (2's)	$\Delta\%$	
F-4	.11855	.677	.7053	(1)-4.0	.734	4.0
F-13	.11855/.11023	1.068	1.209	-11.7	1.175	-2.8
F-22	.11023	1.760	2.123	-17.1	1.936	-8.8
F-31	.11023/.10911	2.326	2.862	-16.7	2.559	-10.6
F-43	.11023/.07953	6.562	8.242	-20.4	7.218	-12.4
F-100	.1904	.671	.669	.3	.738	10.3
F-109	.0966	1.046	1.219	-14.2	1.151	-5.6
F-118	.0966	1.683	1.958	-14.1	1.851	-5.5
F-130	.0966/.09106	2.101	2.497	-15.9	2.311	-7.4
F-145	.09106	11.575	14.826	-21.9	12.733	-14.1

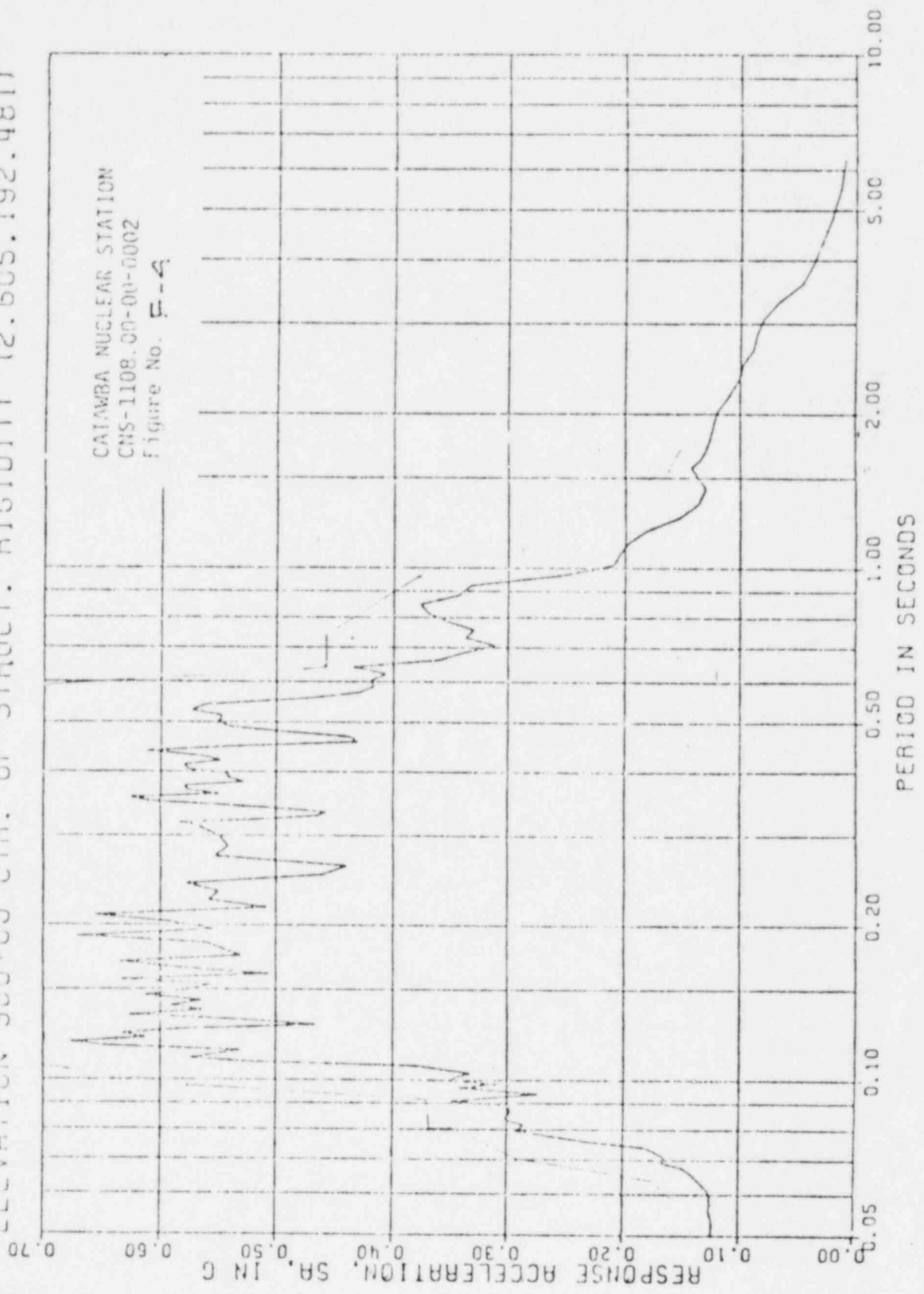
NOTES:

- (1) Pos. values are overage.

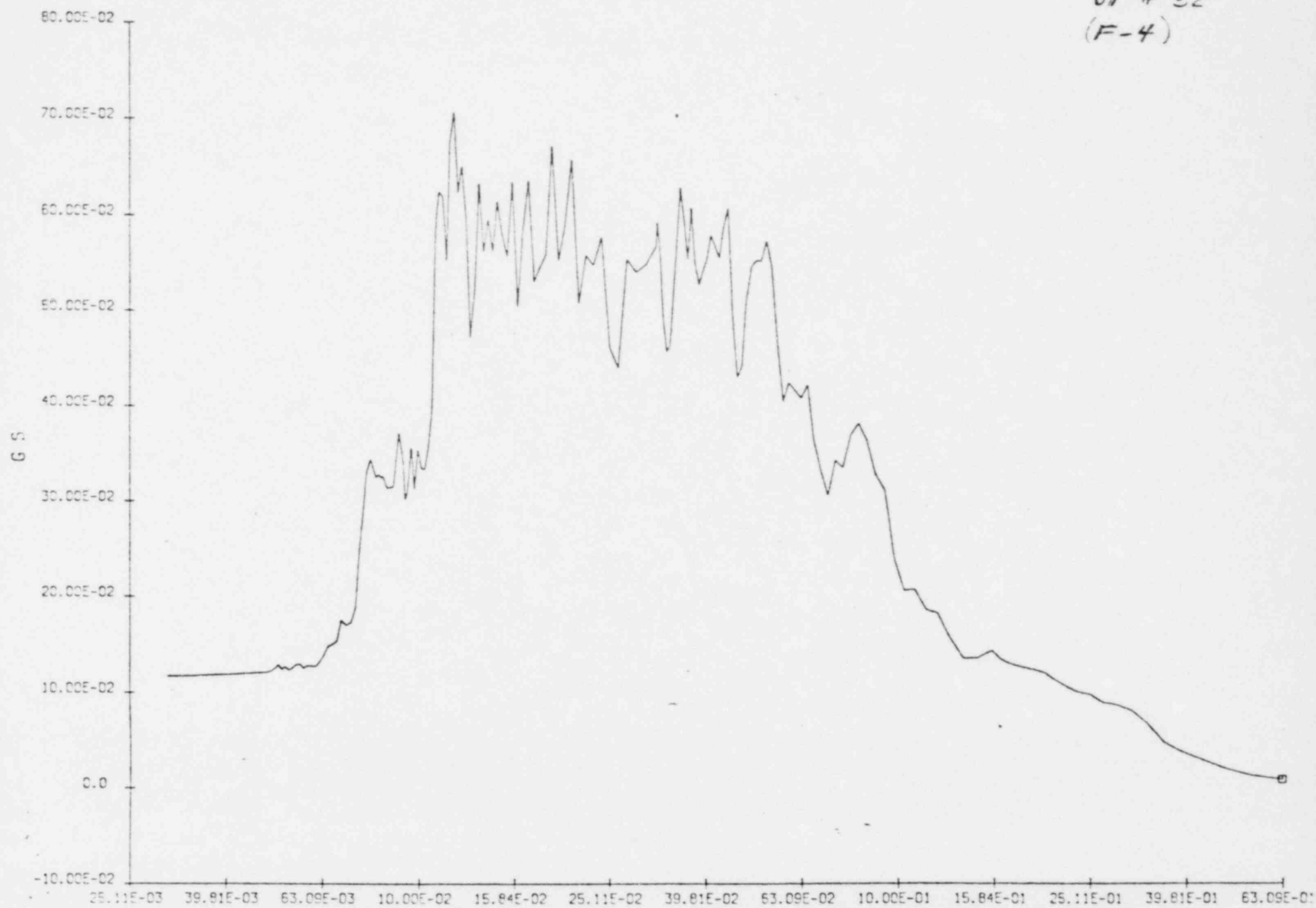
CATAWBA AUX BLDG NOR-SOU (X) EARTHQUAKE

RESPONSE ACCELERATION SPECTRA, DAMPING= 0.005

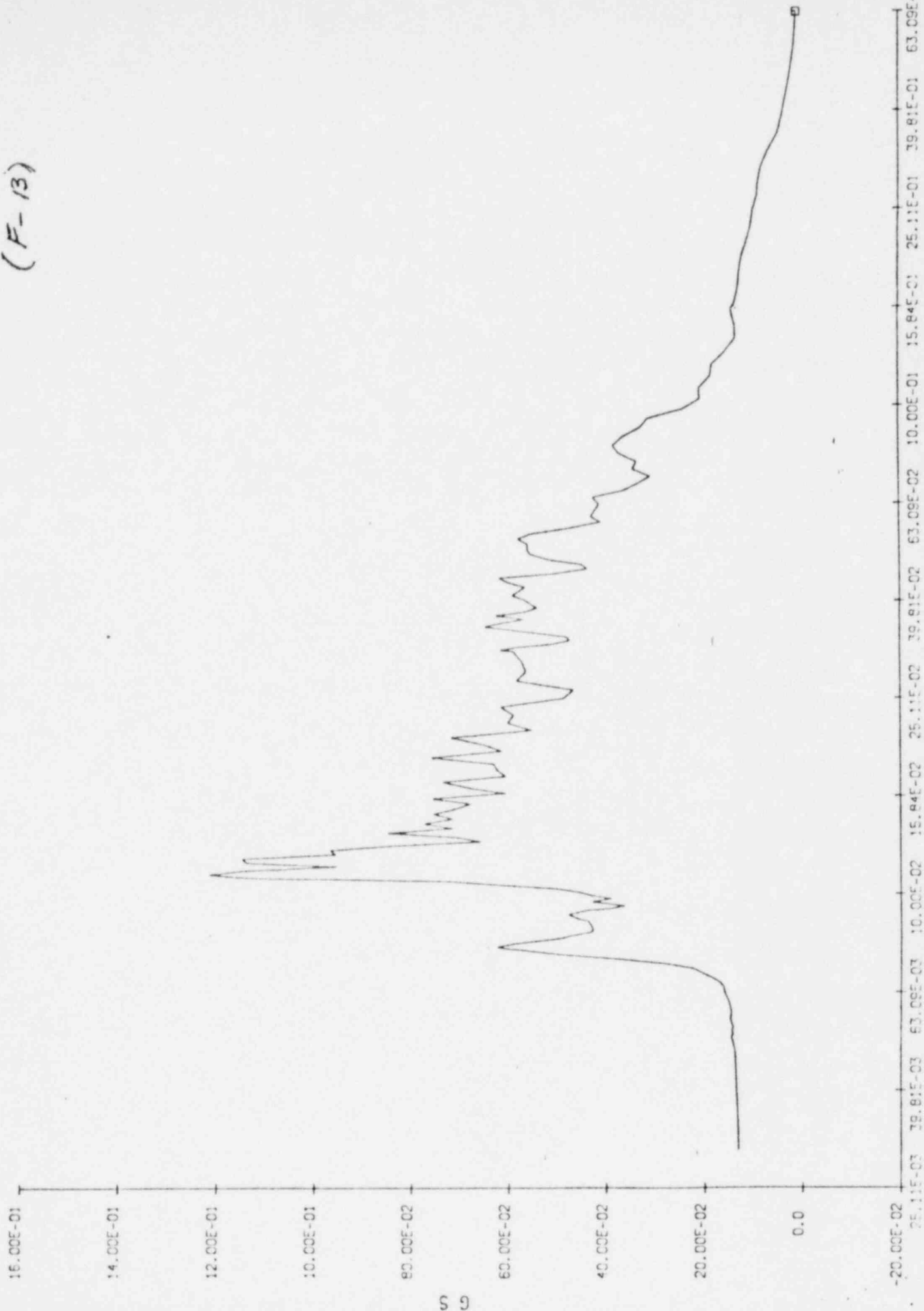
ELEVATION 560+00 CTR. OF STRUCT. RIGIDITY (2.605.192.481)



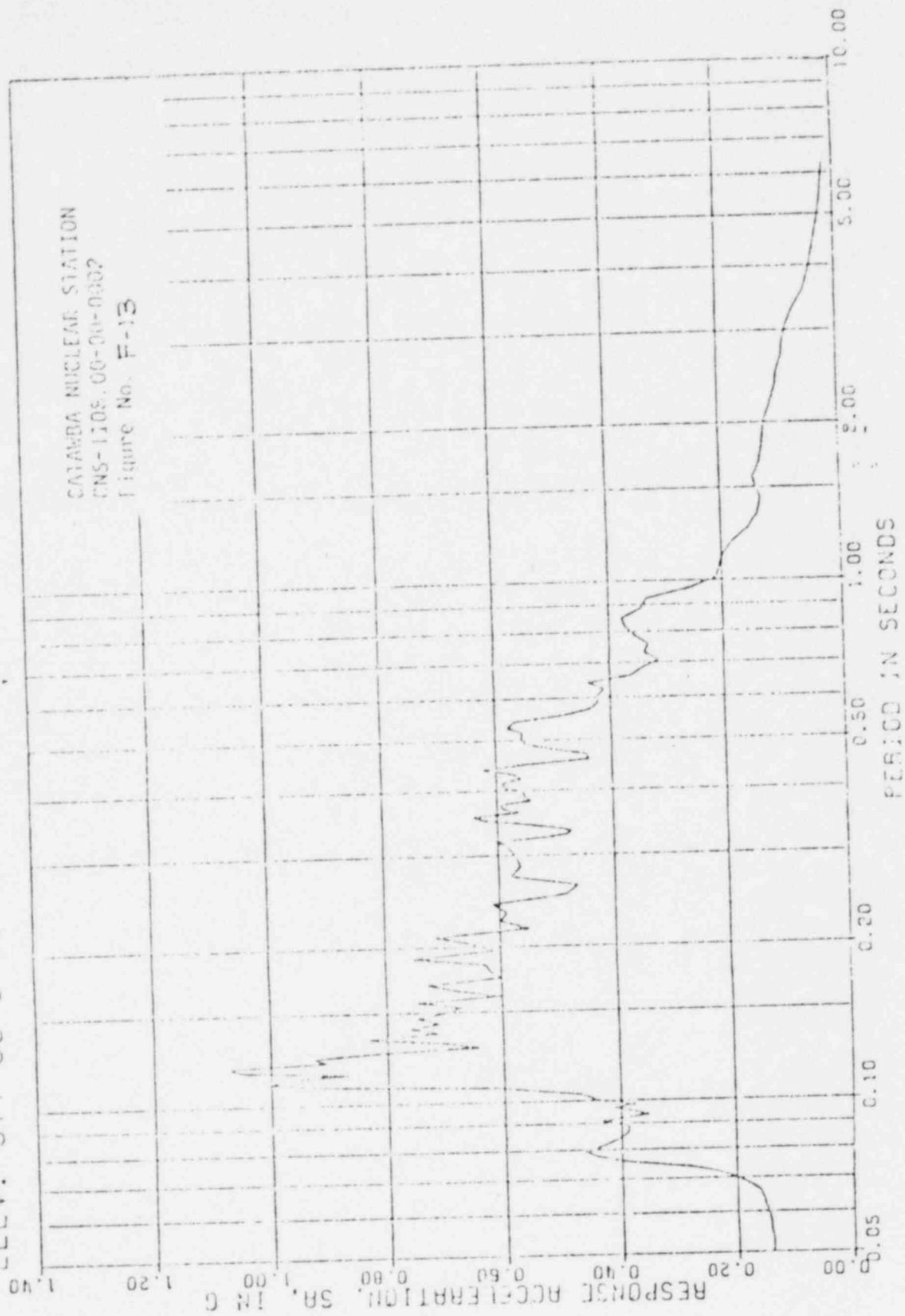
N-S RESPONSE
EL. 560+0
JT # 32
(F-4)



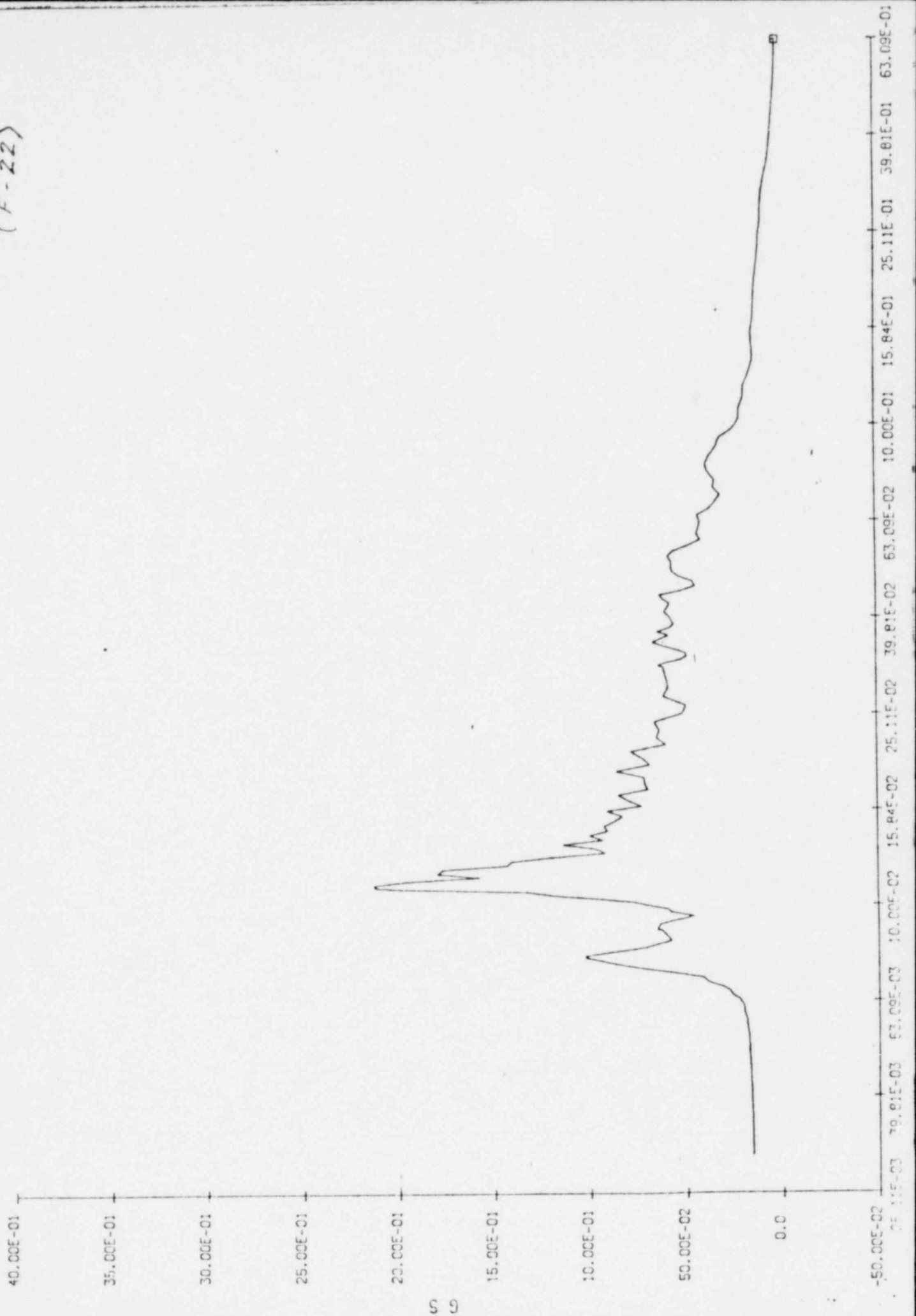
N-S Response
EL 377.0
JT# 52
(F-13)



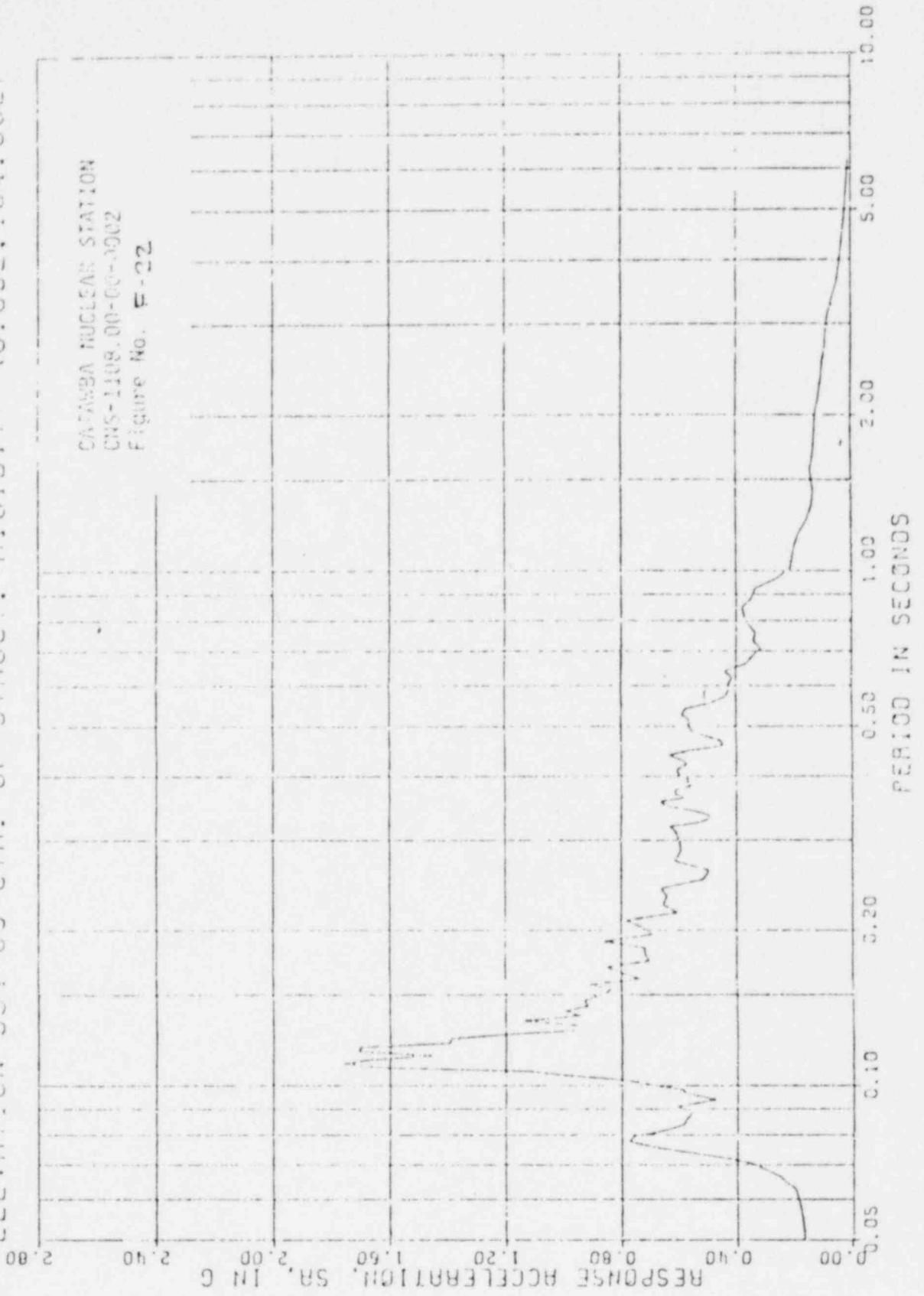
CATAWBA AUX BLDG NCR-SCU (X) EARTHQUAKE
RESPONSE ACCELERATION SPECTRA. DAMPING= 0.005
ELEV. 577+00 CTR. OF STRUCT. RIGIDITY (-0.593, 136.424)



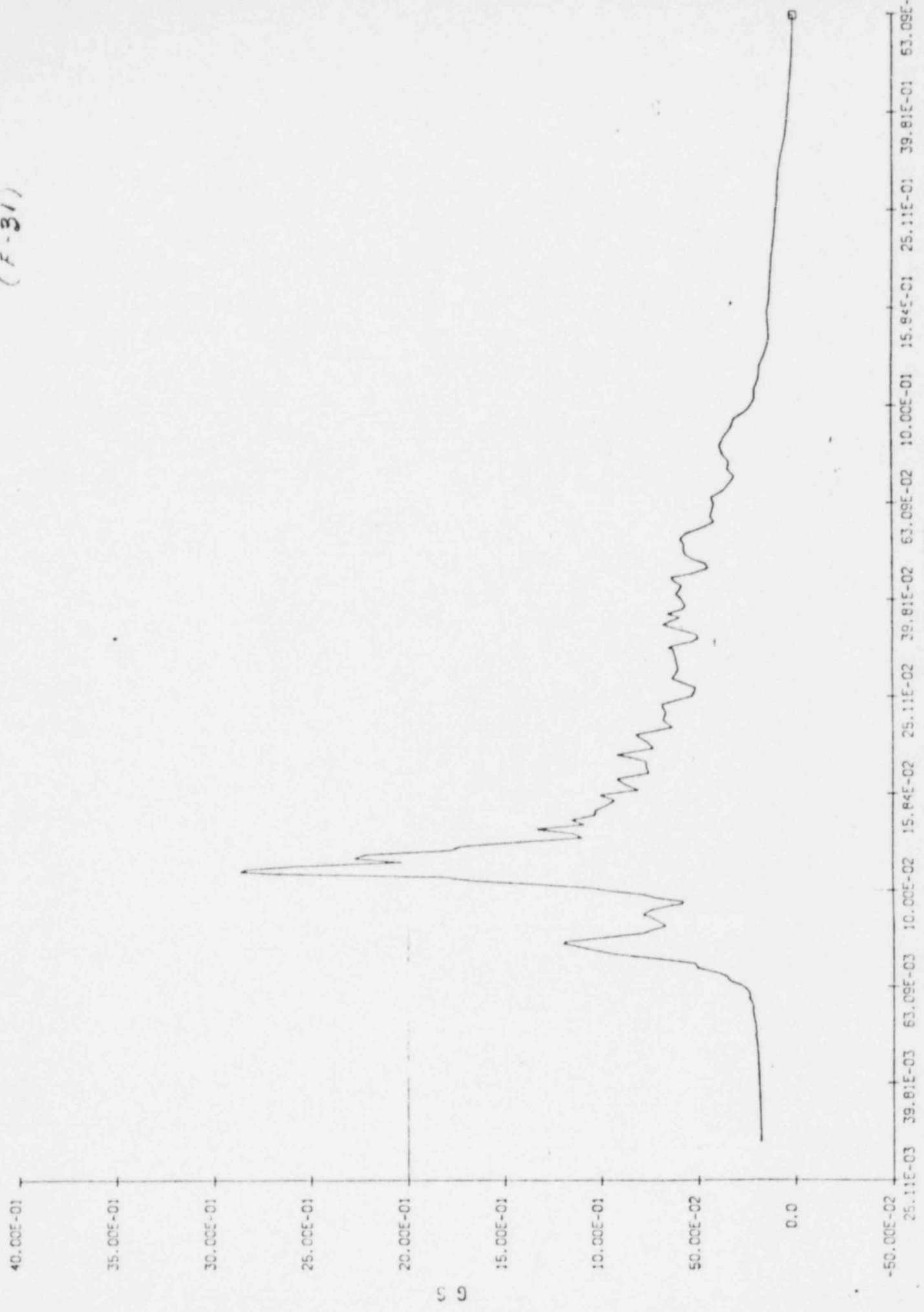
N-S Response
FL 59410
JT 72
(F-22)



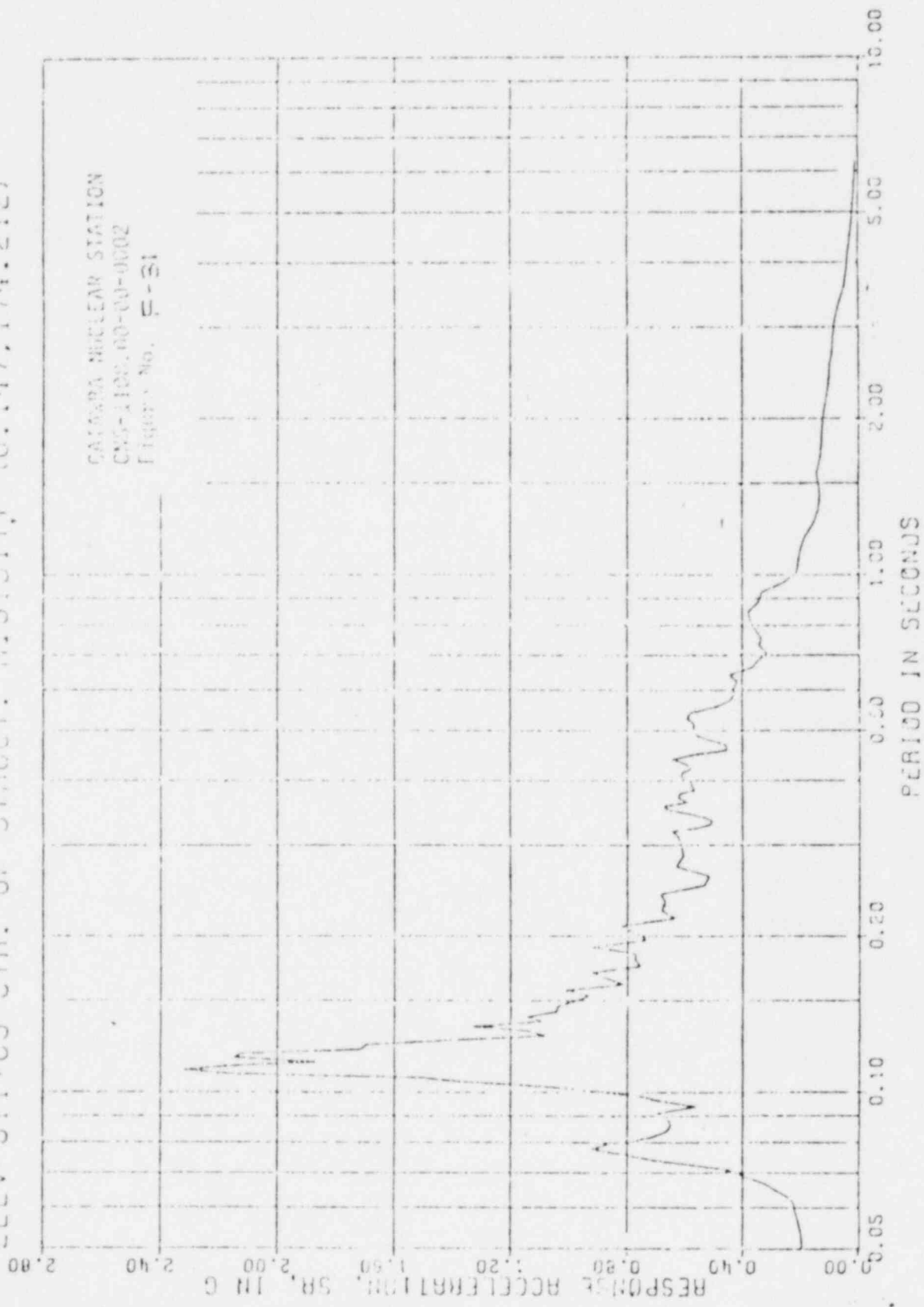
CATANBA AUX SLOG NCR-SCU (X) EARTHQUAKE
RESPONSE ACCELERATION SPECTRA, DAMPING= 0.005
ELEVATION 594+00 CTR. OF STRUCT. RIGIDITY (0.092, 164.082)



N-S Response
FL 61100
JT #91
(F-31)



CATAWBA AUXILIARY BLDG. NORTH-SOUTH (X)
RESPONSE ACCELERATION SPECTRA. DAMPING= 0.005
ELEV 611+00 CTR. OF STRUCT. RIGIDITY (0.147, 174.212)

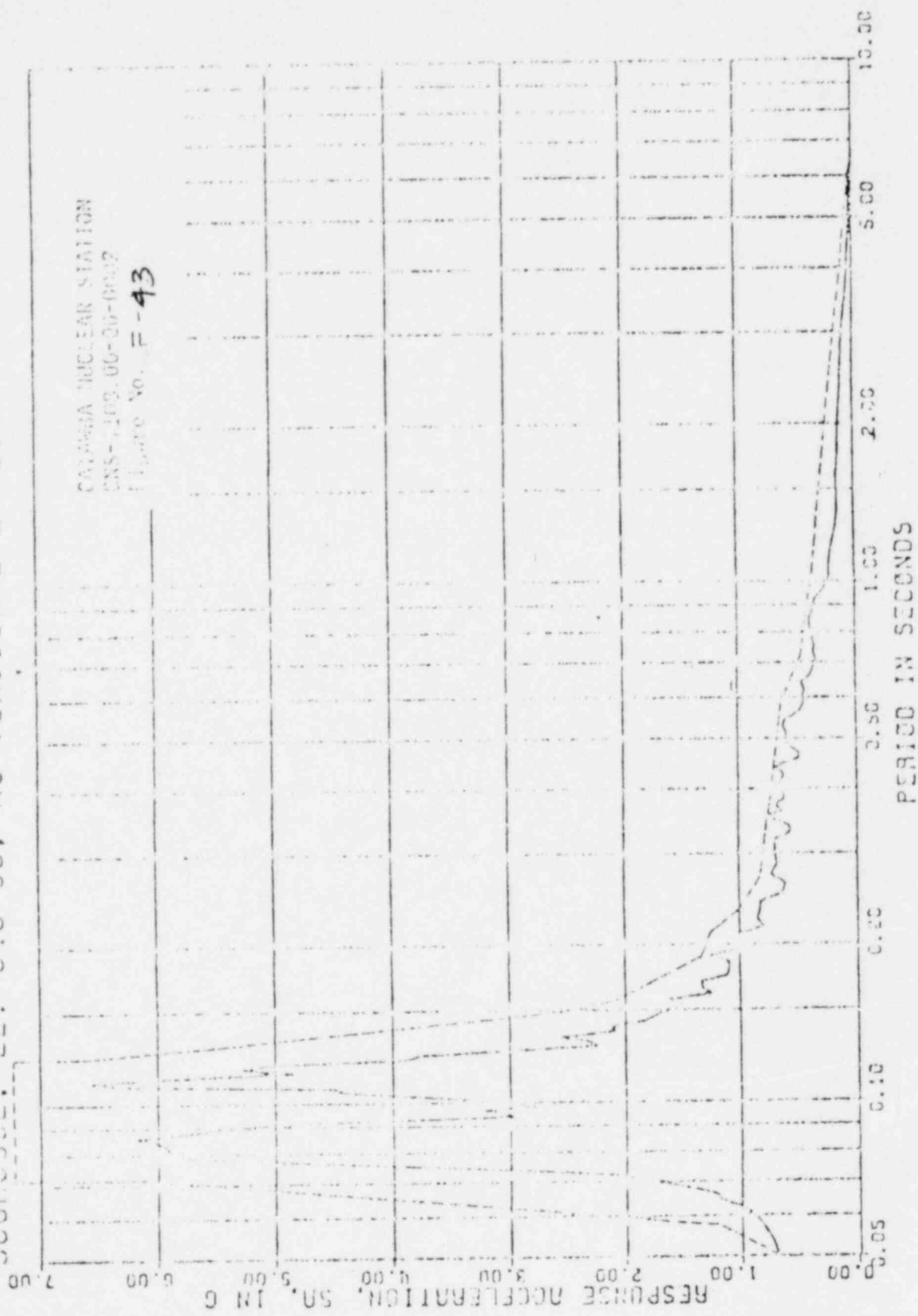


AUX BLDG. NORTH-SOUTH

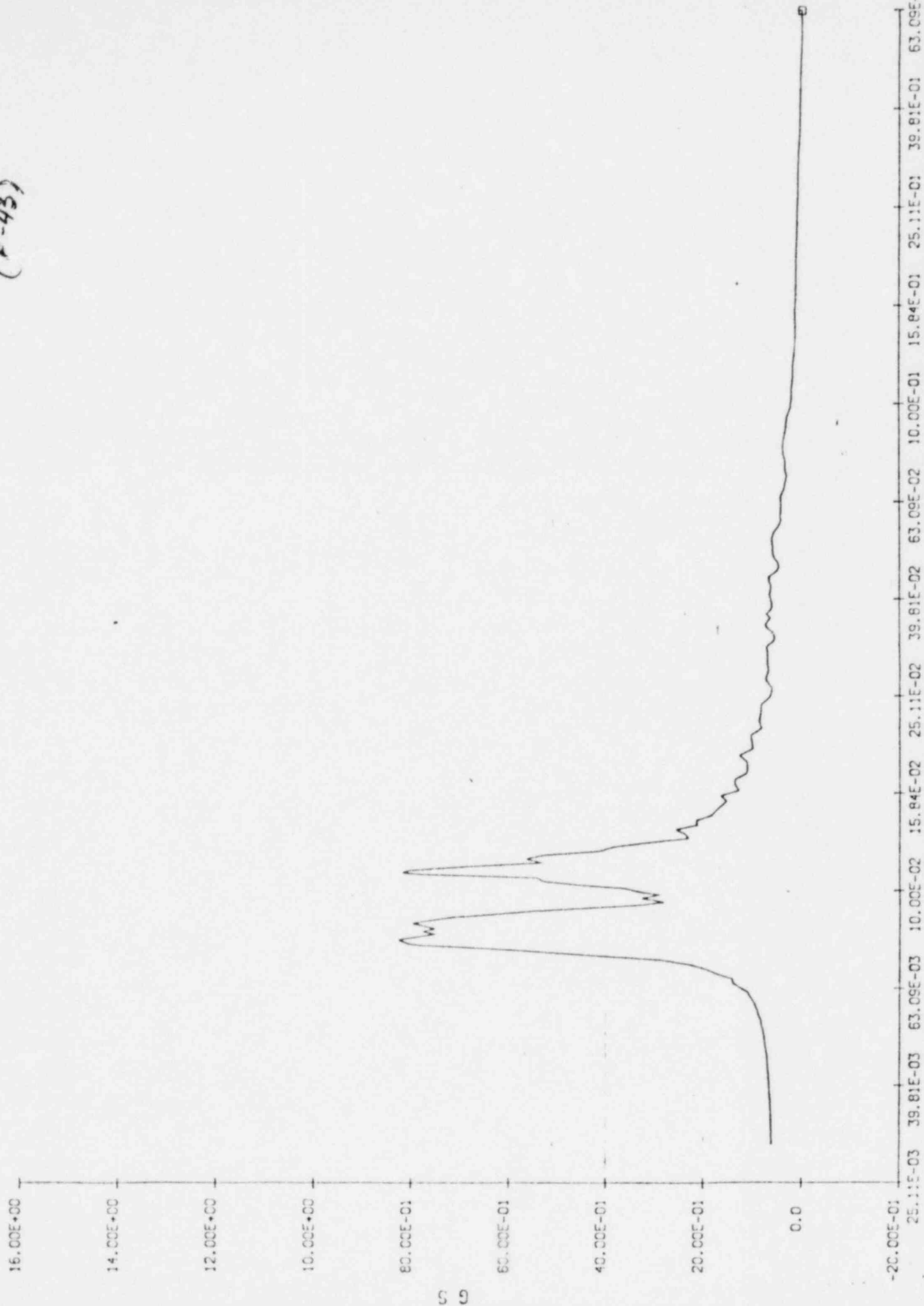
CATSKB9 NUCLEAR STATION

RESPONSE ACCELERATION SPECTRA, DAMPING= 0.005

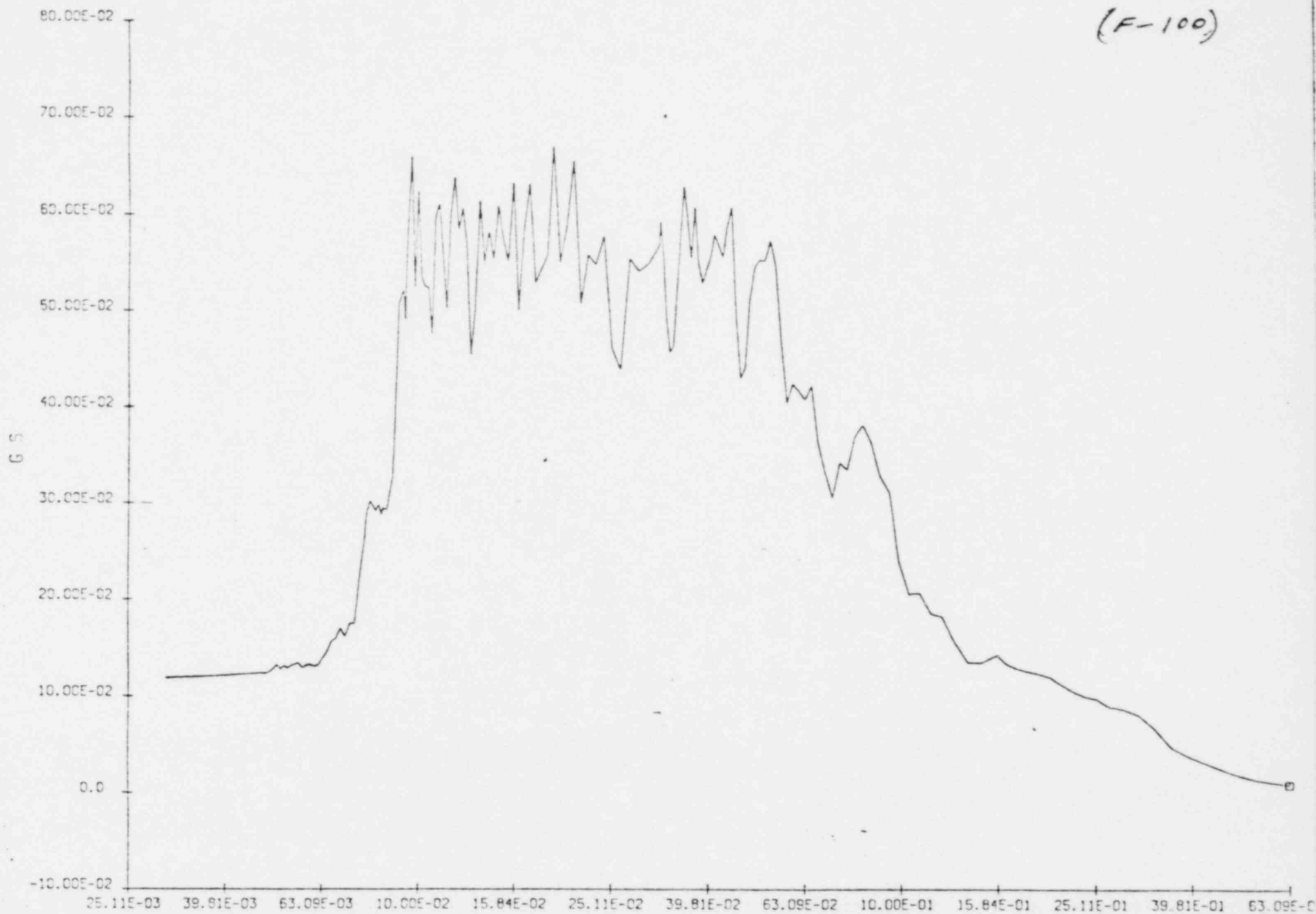
DOCKHOUSE, EL. 048-00, NO TORSIONAL EFFECT



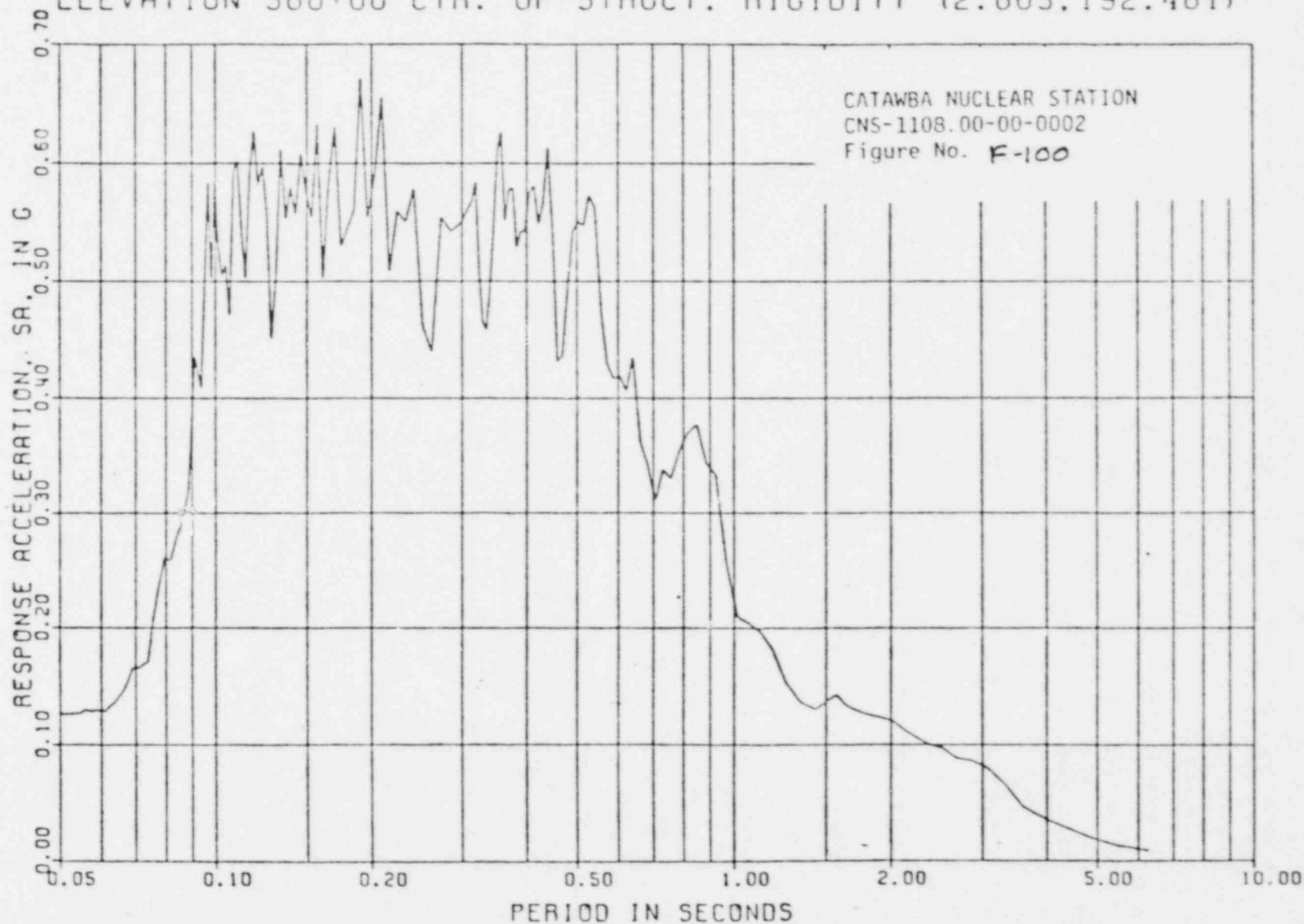
N-S RESPONSE
EL 648+0
JT 15
(F-43)



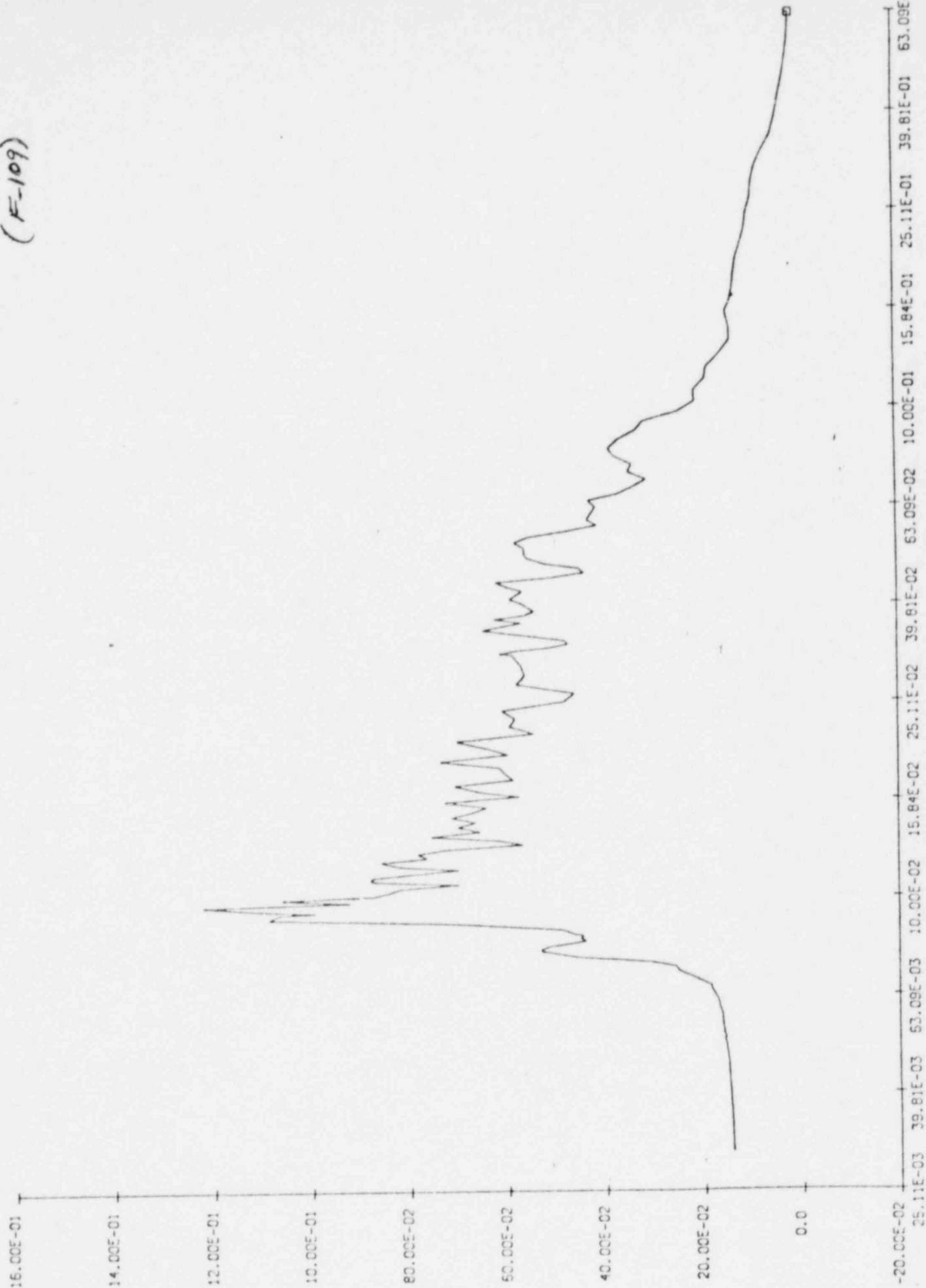
E-W RESPONSE
FL 560+0
JT # 32
(F-100)



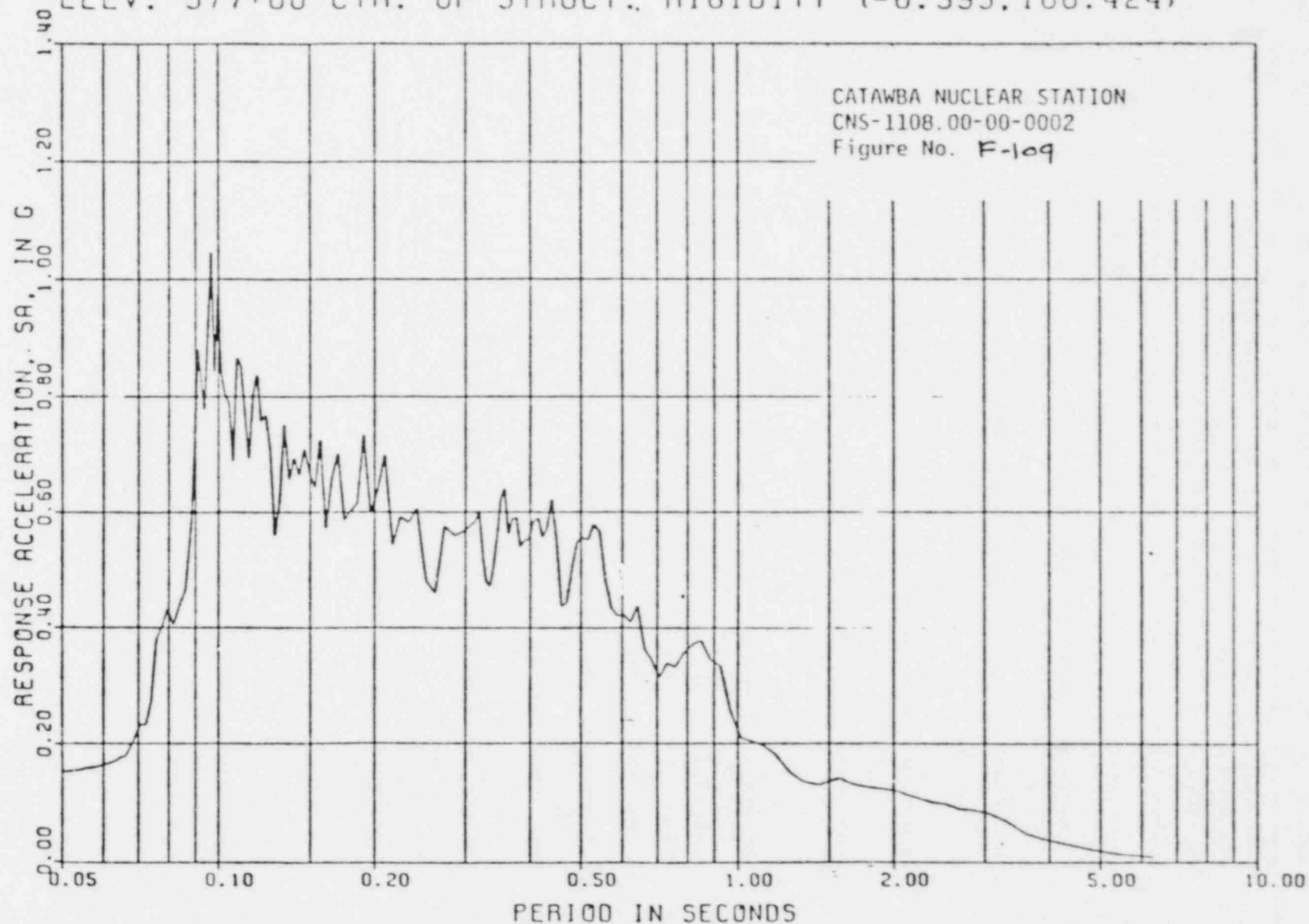
CATAWBA AUX BLDG EAS-WES (Y) EARTHQUAKE
RESPONSE ACCELERATION SPECTRA, DAMPING= 0.005
ELEVATION 560+00 CTR. OF STRUCT. RIGIDITY (2.605,192.481)



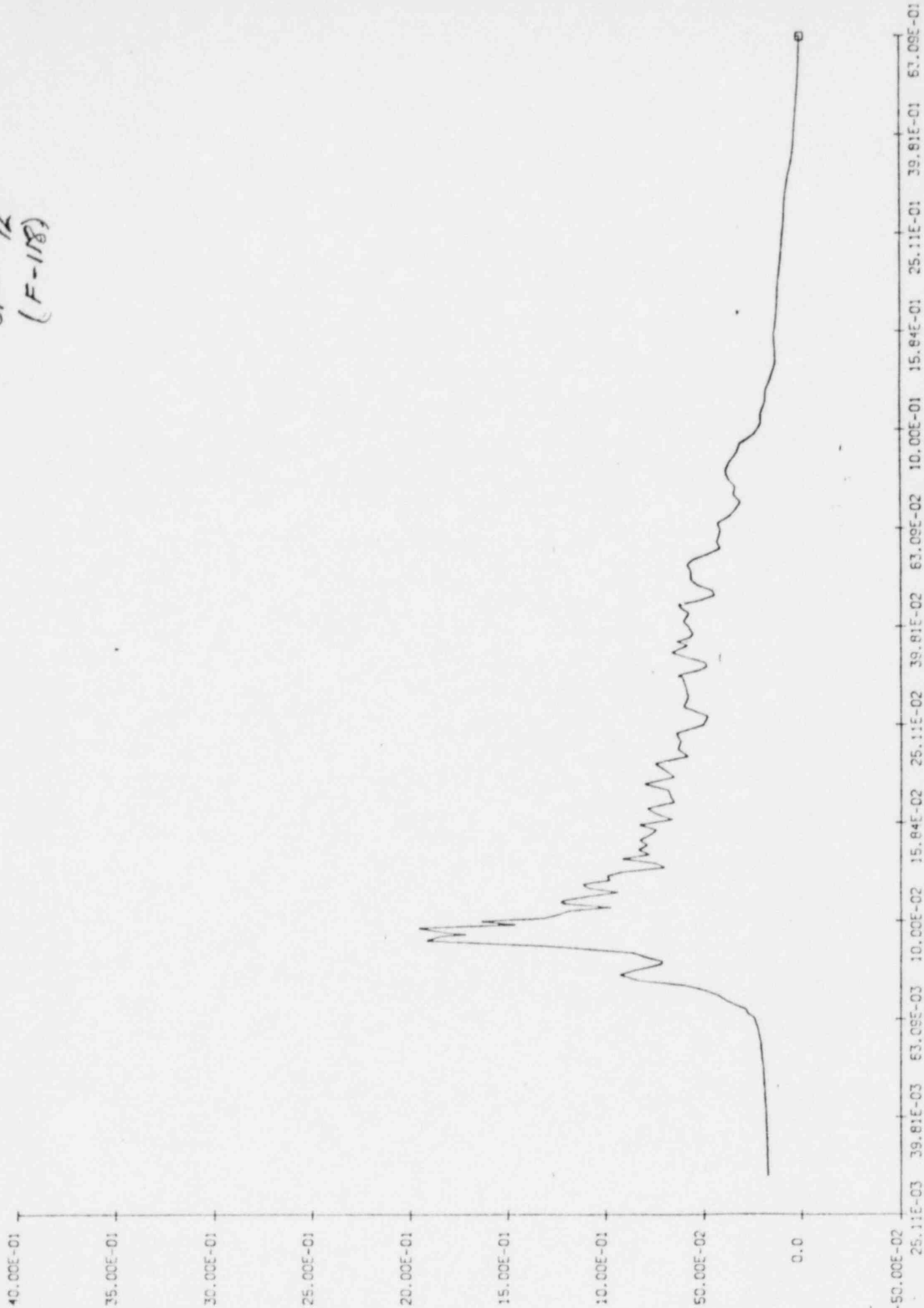
E-W RESPONSE
FL 577-0
IT#52
(F-109)



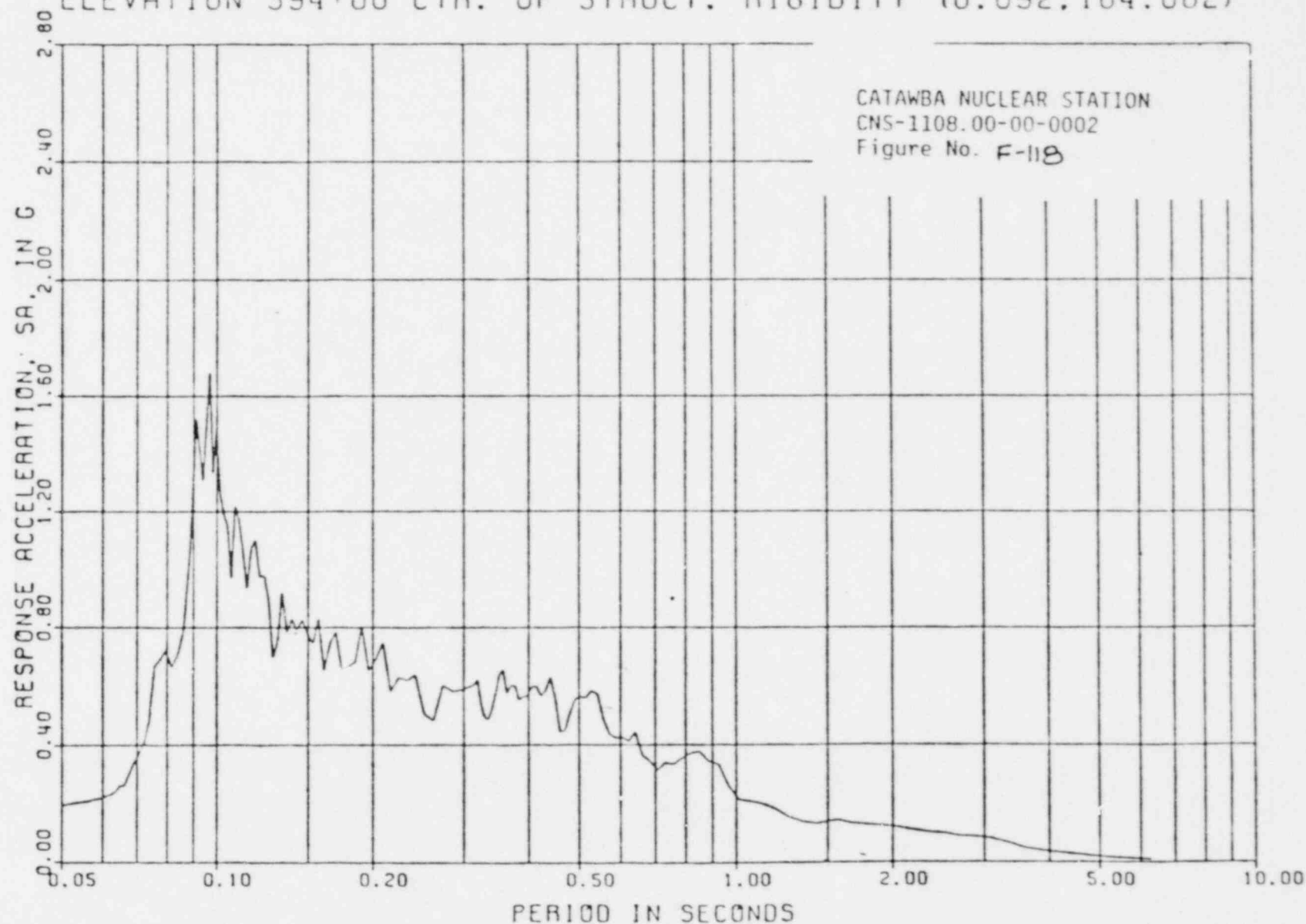
CATAWBA AUX BLDG EAS-WES (Y) EARTHQUAKE
RESPONSE ACCELERATION SPECTRA, DAMPING= 0.005
ELEV. 577+00 CTR. OF STRUCT., RIGIDITY (-0.593,186.424)



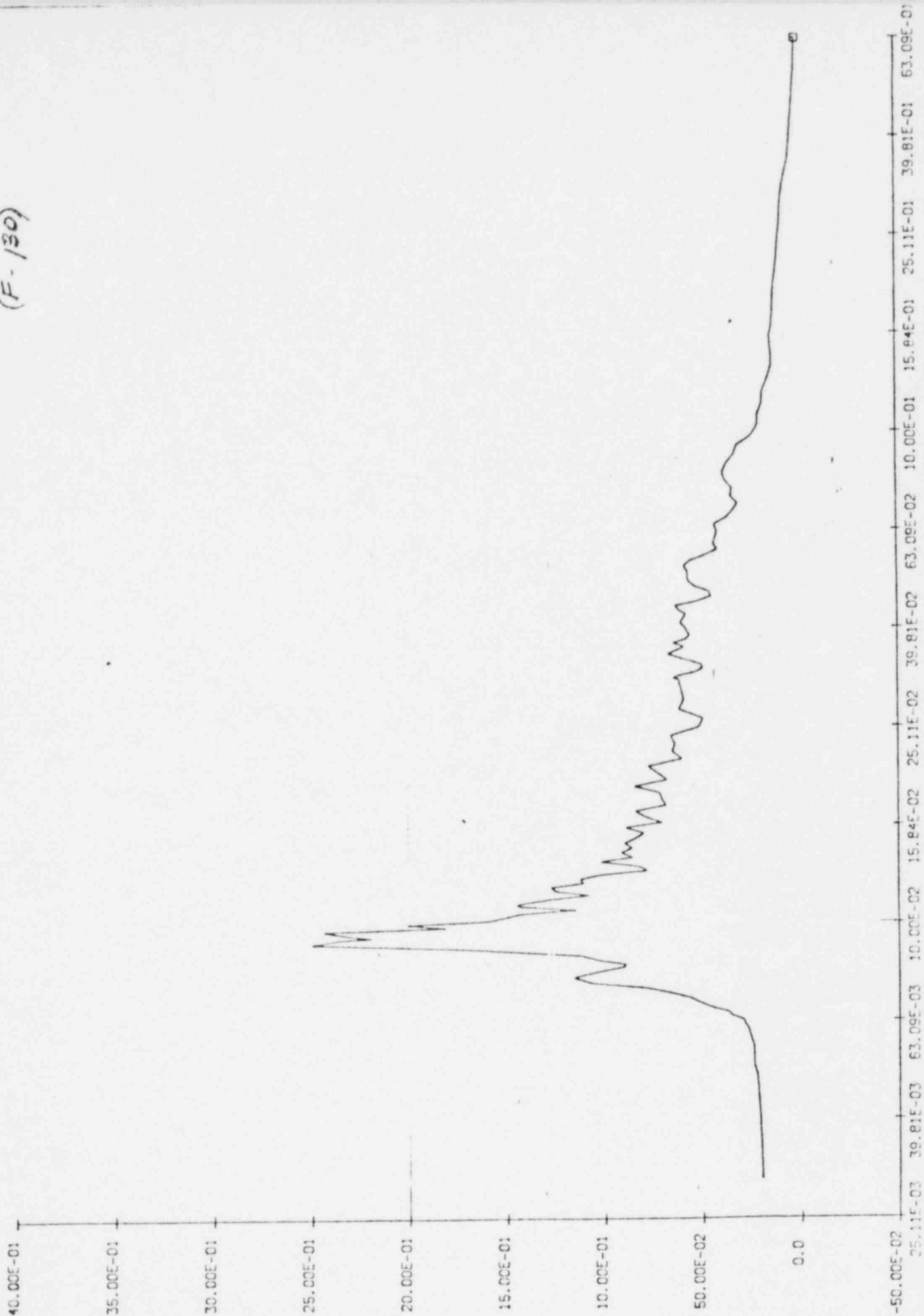
E-W RESPONSE
EL 59410
JT# 72
(F-118)



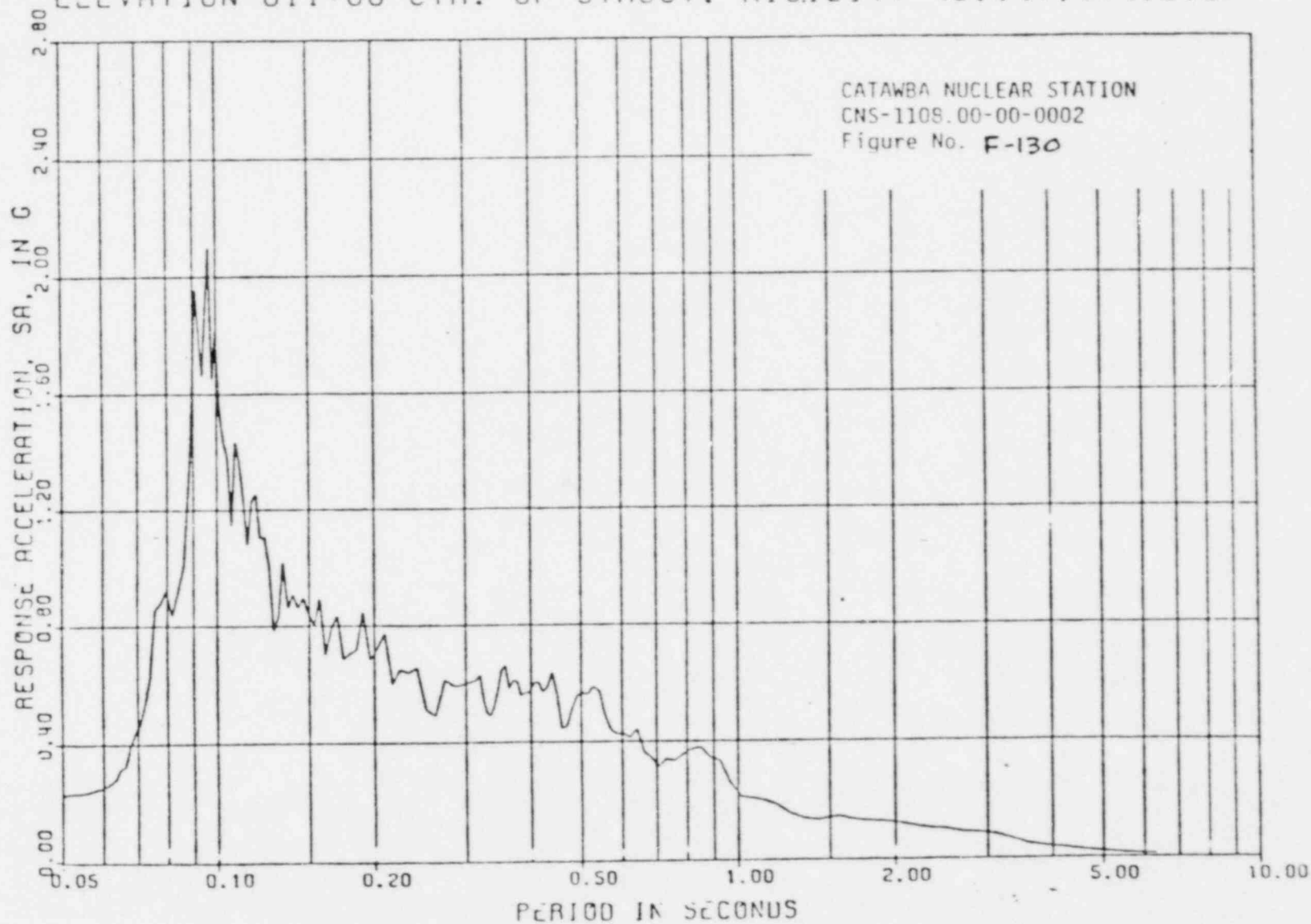
CATAWBA AUX BLDG EAS-WES (Y) EARTHQUAKE
RESPONSE ACCELERATION SPECTRA, DAMPING= 0.005
ELEVATION 594+00 CTR. OF STRUCT. RIGIDITY (0.092,164,082)



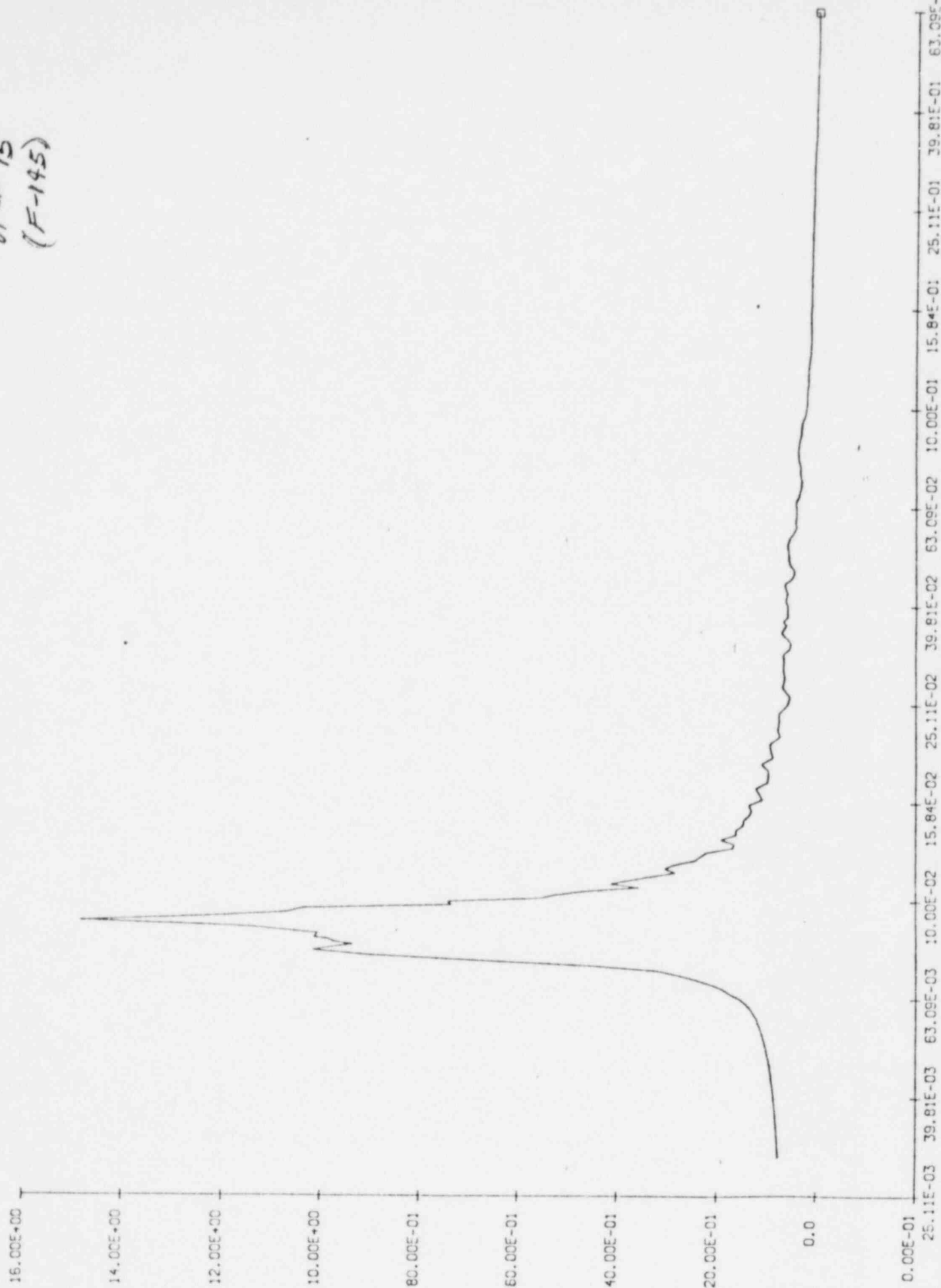
E-W Response
EL 611+0
JT# 91
(F-130)



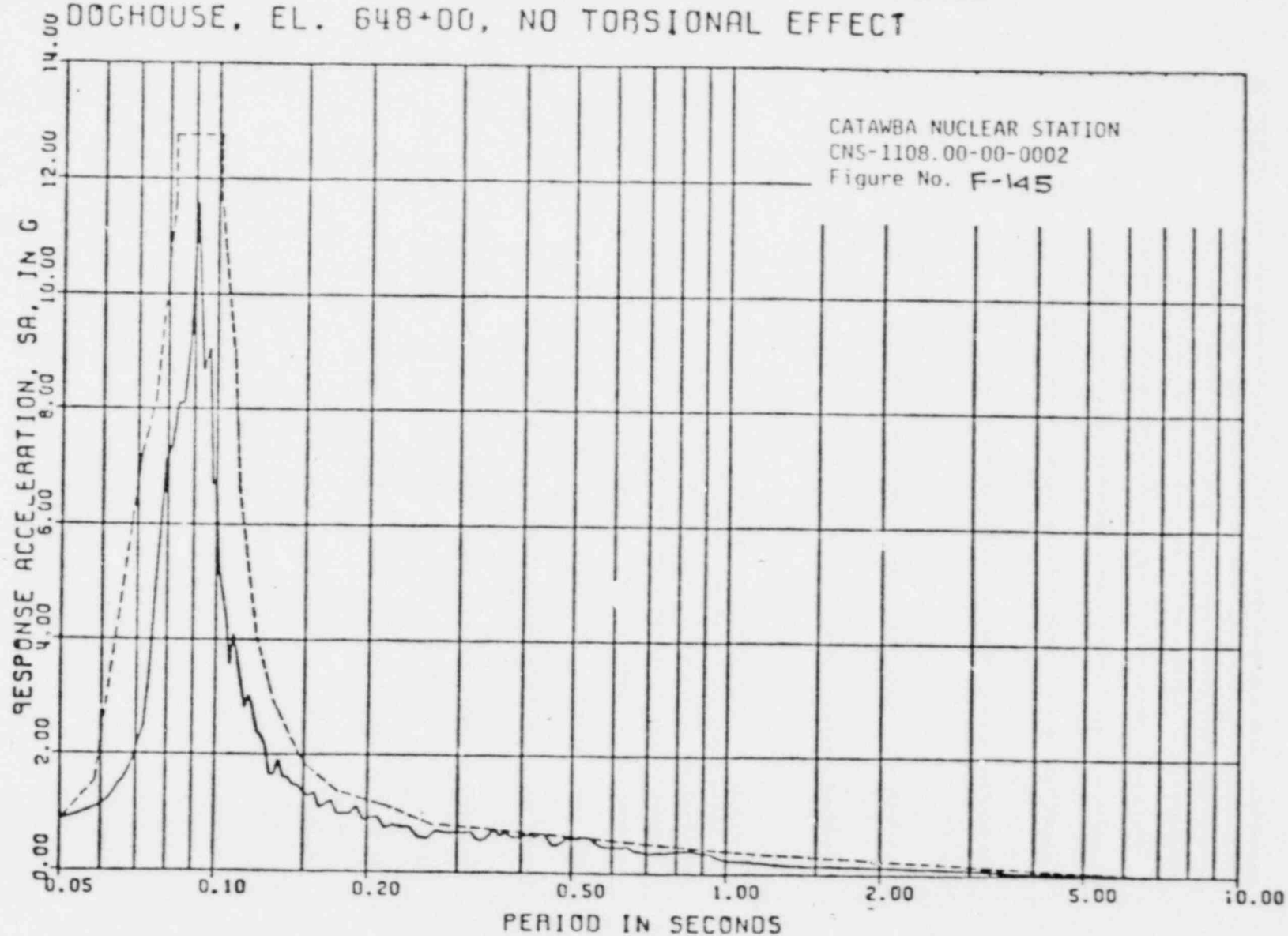
CATAWBA AUXILIARY BLDG. EAST-WEST (Y) EA
RESPONSE ACCELERATION SPECTRA, DAMPING= 0.005
ELEVATION 611+00 CTR. OF STRUCT. RIGIDITY (0.147, 174.212)



E-VI RESPONSE
EL. 648+0
UT # 15
(F-145)



AUX BLDG. EAST-WEST
CATAWBA NUCLEAR STATION
RESPONSE ACCELERATION SPECTRA, DAMPING= 0.005
DOGHOUSE, EL. 648+00, NO TORSIONAL EFFECT



3. Provide a comparison of corrected and uncorrected synthetic time histories (and resultant response spectra) for Cherokee as justification to no base line correction of time histories used for Catawba.

Response:

The Catawba site synthetic time histories were not base line corrected. As justification of this fact, a comparison of the results of both a corrected and uncorrected Cherokee time histories is offered.

The corrected and uncorrected Cherokee time history will be used to compute response spectra in the Catawba Auxiliary Building. The original stick model will be used with the following points:

The roofs of the doghouse and spent fuel pool are used in this comparison because they exhibit the highest response to ground motion.

<u>JOINT</u>	<u>DIRECTION</u>	<u>ELEV.</u>	<u>LOCATION</u>
1	X-Trans	543+0	Base
191	X-Trans	659+0	Spent Fuel Roof
15	X-Trans	648+0	Doghouse Roof
1	Z-Trans	543+0	Base
191	Z-Trans	659+0	Spent Fuel Roof
15	Z-Trans	648+0	Doghouse Roof

NOTES:

(1) Use SD = 5% and RSD = $\frac{1}{2}\%$.

(2) The Cherokee transient is .156 which is an SSE.

Results:

TABLE #1

<u>JOINT</u>	<u>DIRECTION</u>	<u>UNCORRECTED</u>		<u>CORRECTED</u>		<u>$\Delta\%$</u>
		Acce (G's)	Period	Acce (G's)	Period	Acce.
1	X-Trans	1.468	.3855	1.467	.3855	(1)-
191	X-Trans	10.110	.0949	10.103	.0949	-
15	X-Trans	36.876	.0911	36.874	.0911	-
1	Z-Trans	1.468	.3855	1.468	.3855	-
191	Z-Trans	22.413	.1065	22.414	.1065	-
15	Z-Trans	26.598	.0838	26.597	.0838	-

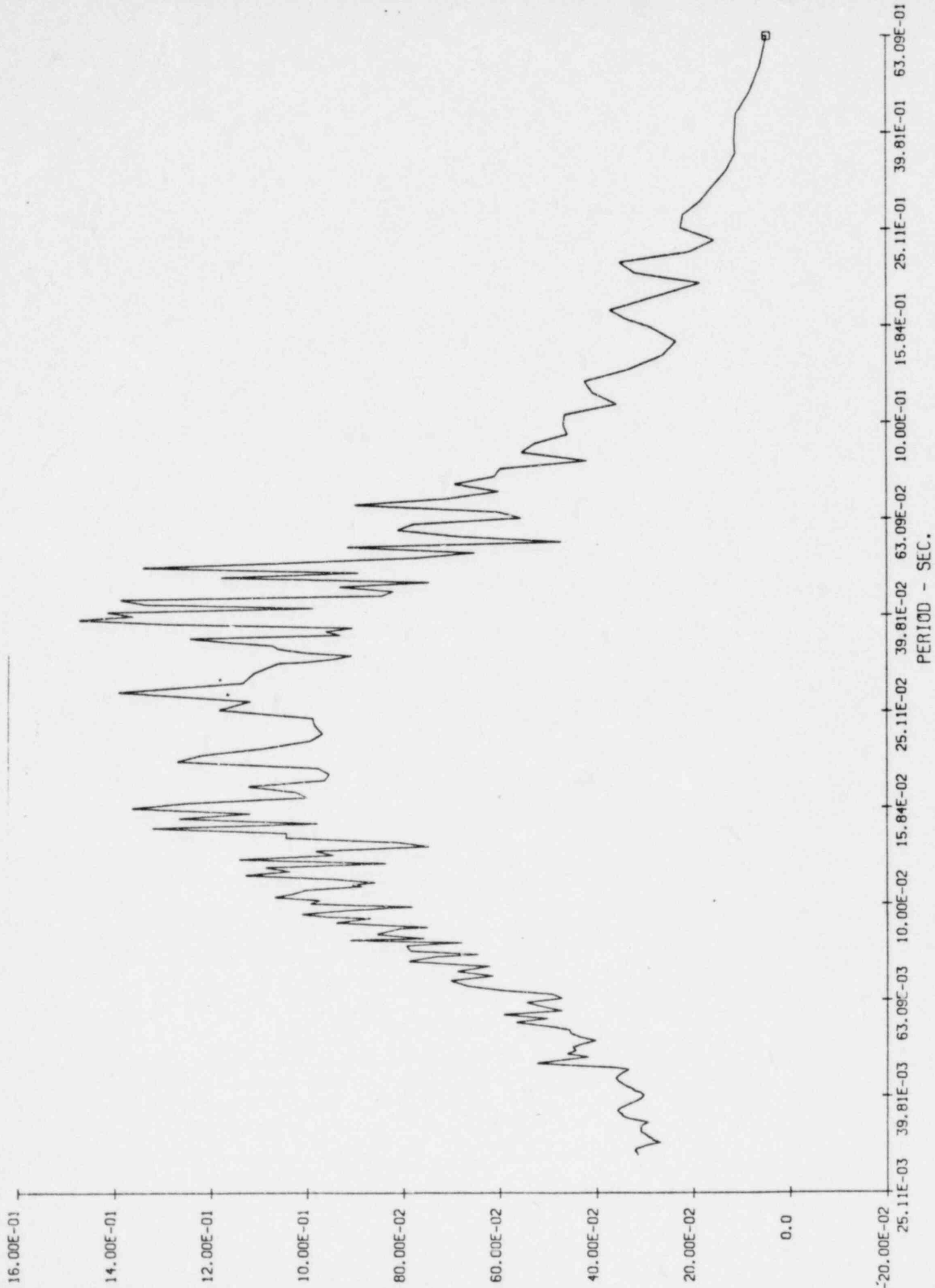
NOTES:

(1) Less than 1%

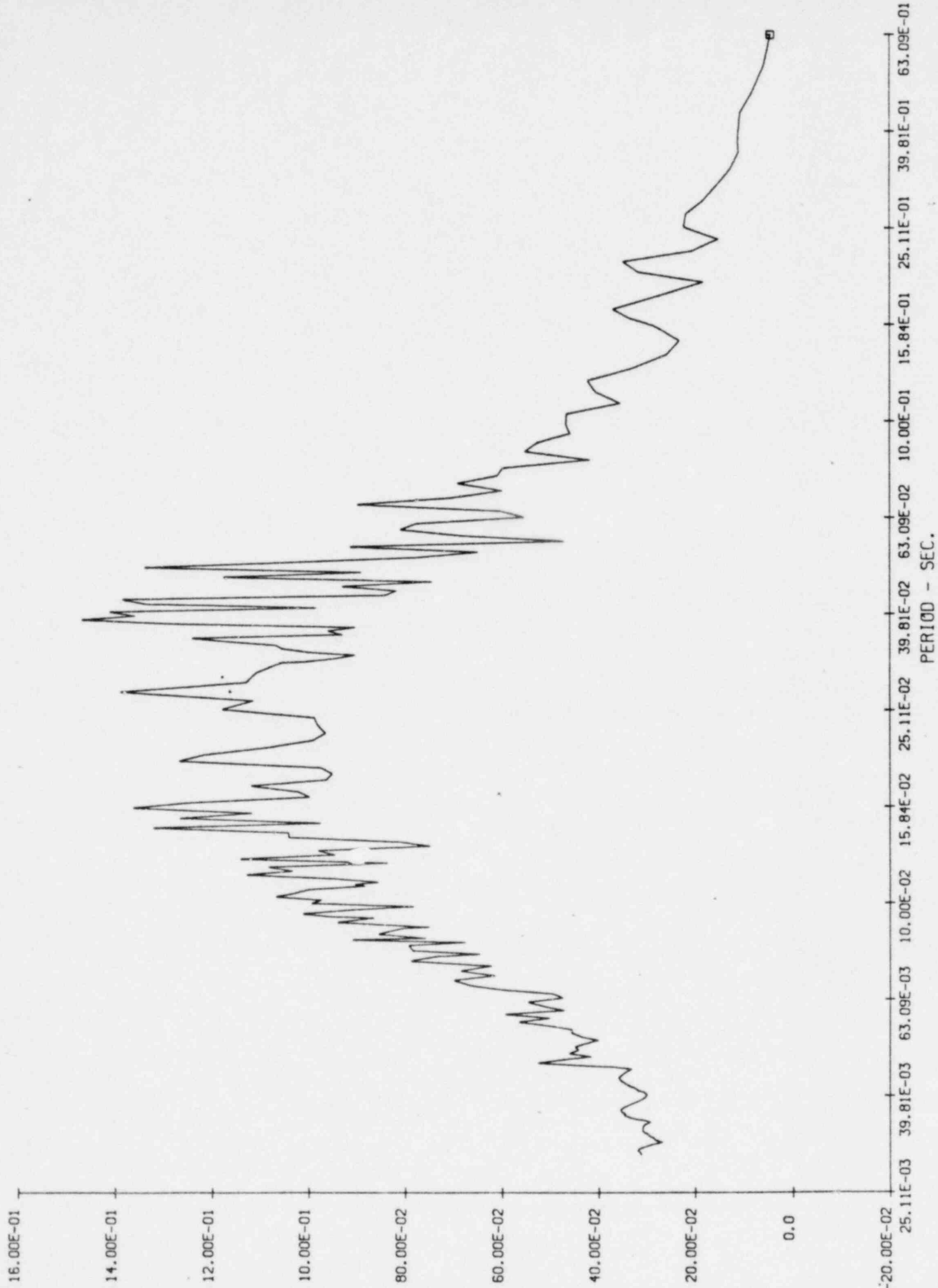
As can be seen from Table #1 above the addition of a base line correction to the time history has negligible effects on the resultant response spectra and there by negligible effects on any design.

See attached response spectra.

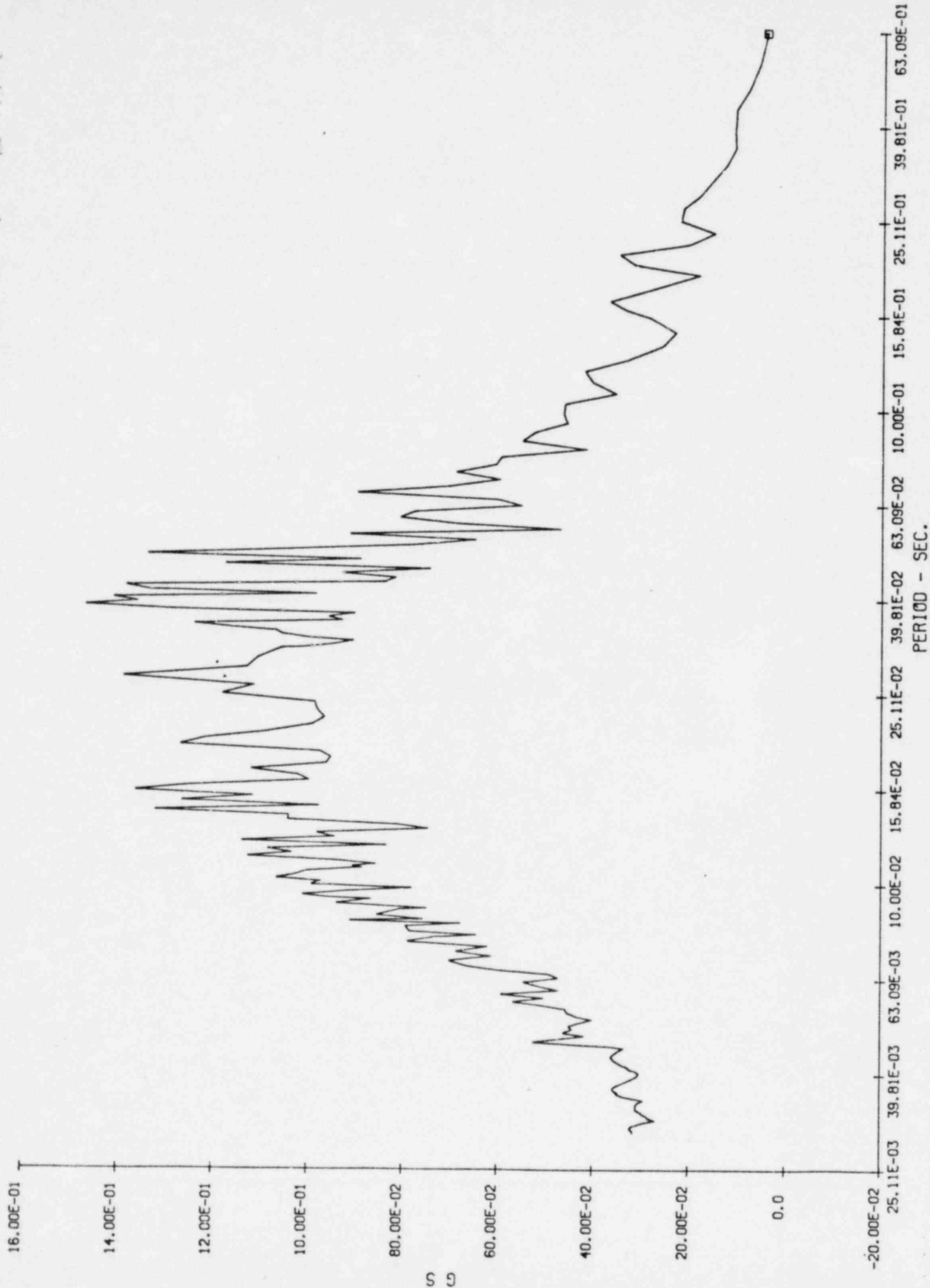
UNCLASSIFIED TAP
71 #1 X-TAP



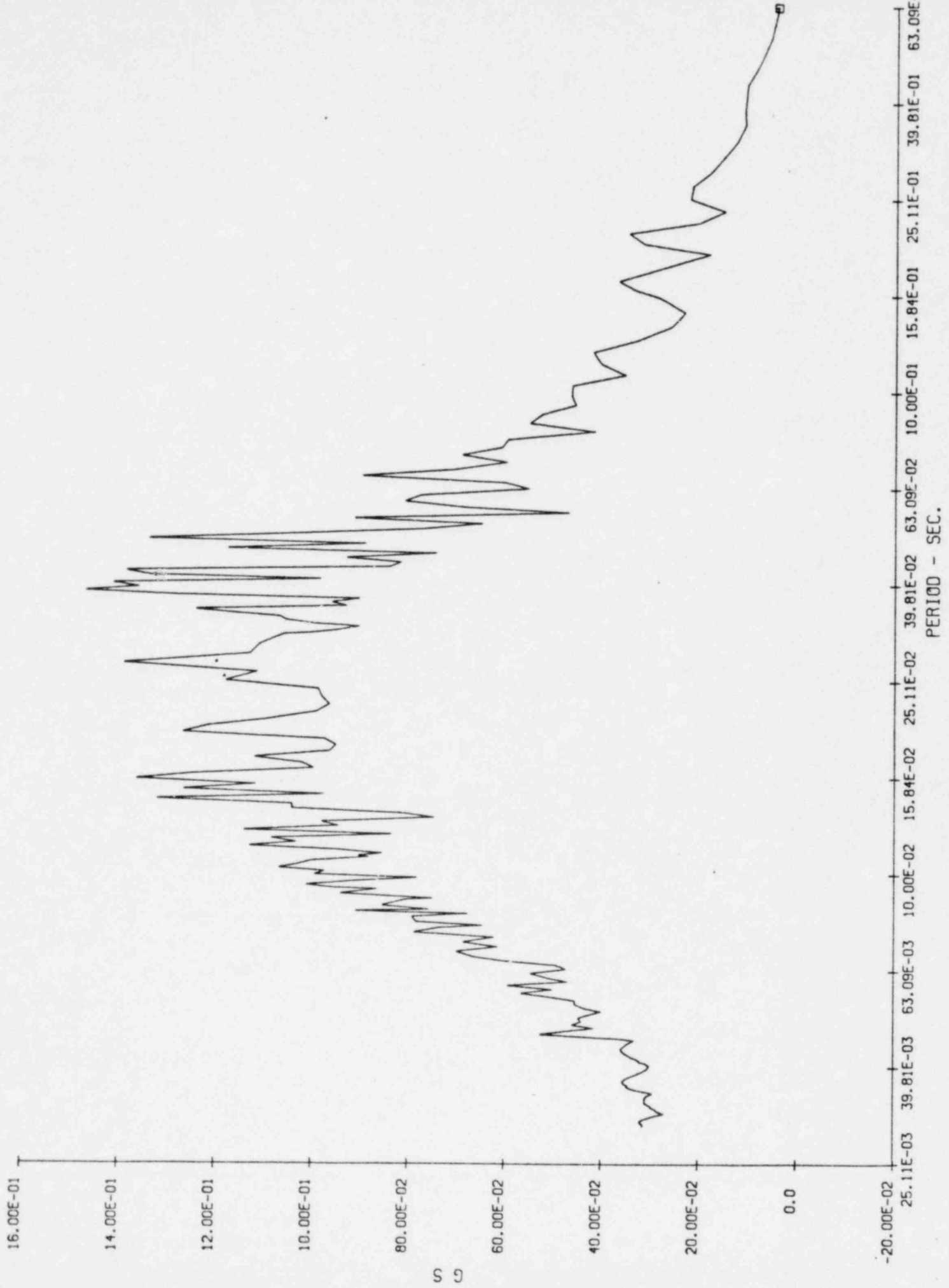
CONFIDENTIAL
JAN 1 1964



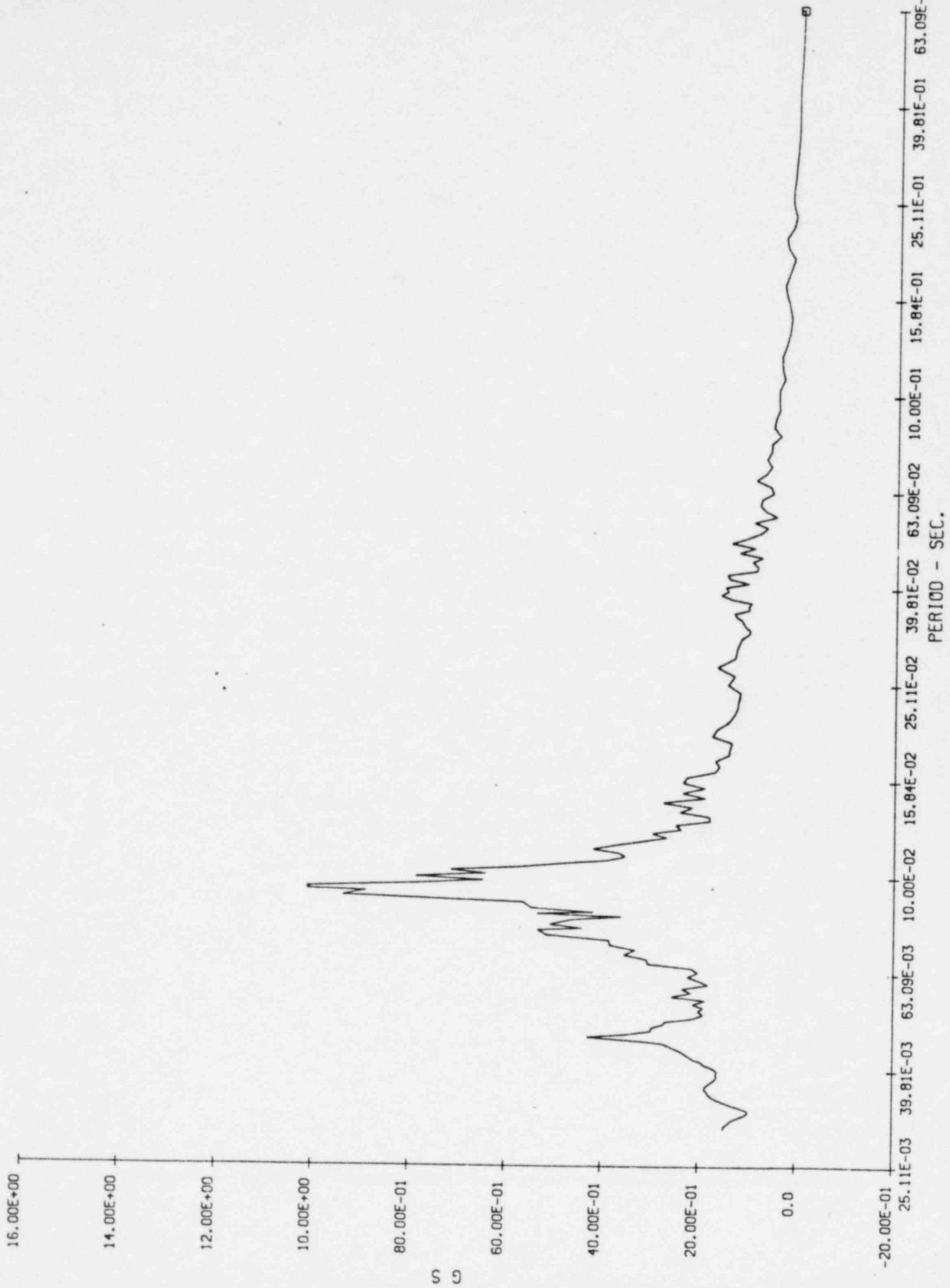
UNCORRECTED - PAPER
07 1 2-1982



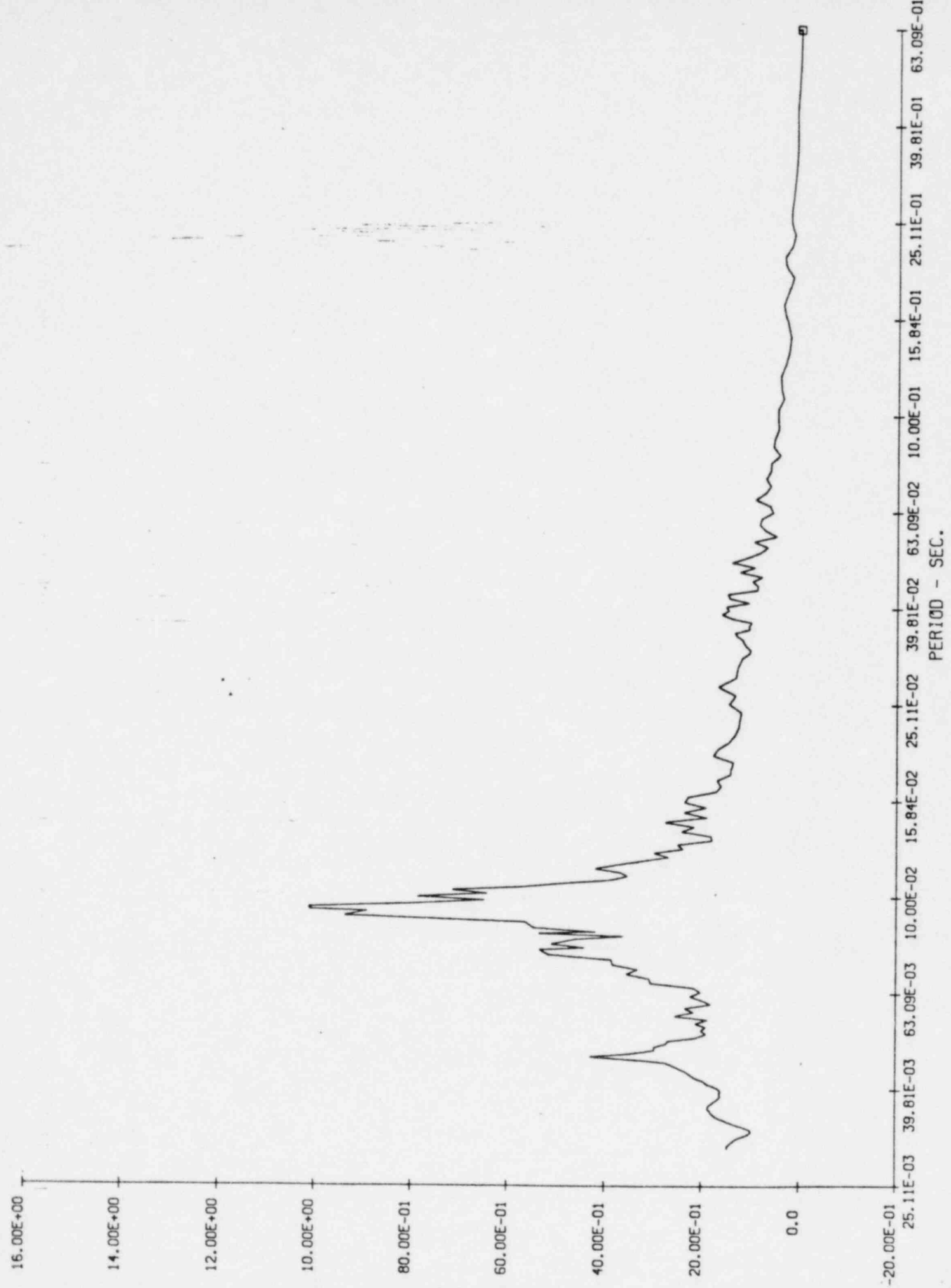
COARDED TRANSMIT
UT # 1 2-7-68



UNCL (2-22) 7000
IT 171 X-7000

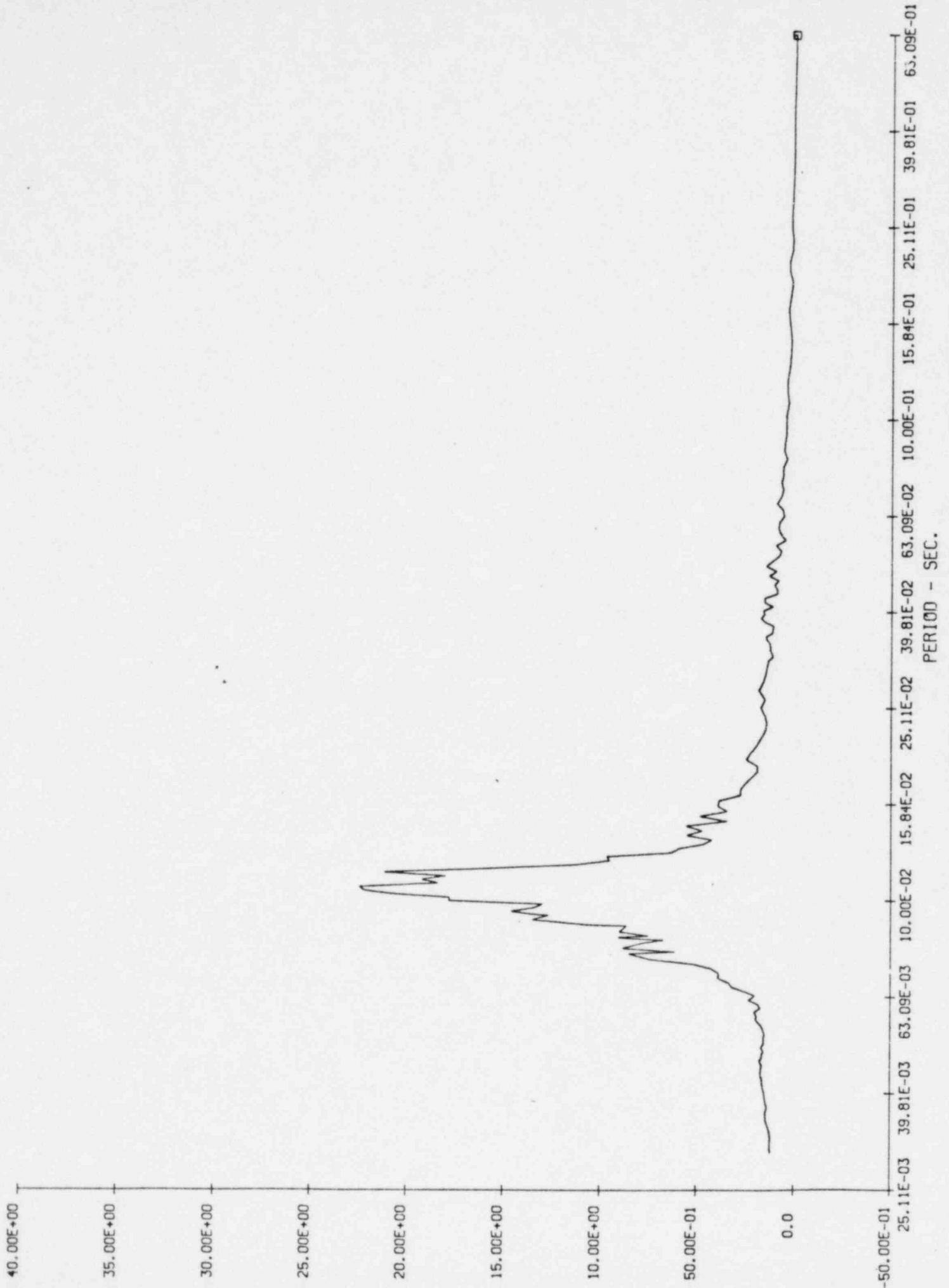


CORRECTED TPO-1A500
IT # 191 X-TRACE



5 9

UNCORRECTED
JT # 191 2.7611



The graph displays a single data series as a continuous line. The vertical axis, labeled 'G S', has major tick marks at -50.00E-01, 0.0, 50.00E-01, 10.00E+00, 15.00E+00, 20.00E+00, 25.00E+00, 30.00E+00, 35.00E+00, and 40.00E+00. The horizontal axis, labeled 'PERIOD - SEC.', has major tick marks at 25.11E-03, 39.81E-03, 63.09E-03, 10.00E-02, 15.84E-02, 25.11E-02, 39.81E-02, 63.09E-02, 10.00E-01, 15.84E-01, 25.11E-01, 39.81E-01, and 63.09E-01. The curve starts near 0.0 at the left edge, remains relatively flat until about 63.09E-03 seconds, then rises sharply to a peak of approximately 22.00E+00 at 10.00E-02 seconds. Following the peak, the curve drops sharply, showing some minor fluctuations, and then gradually decays towards 0.0 as the period increases towards 63.09E-01 seconds.

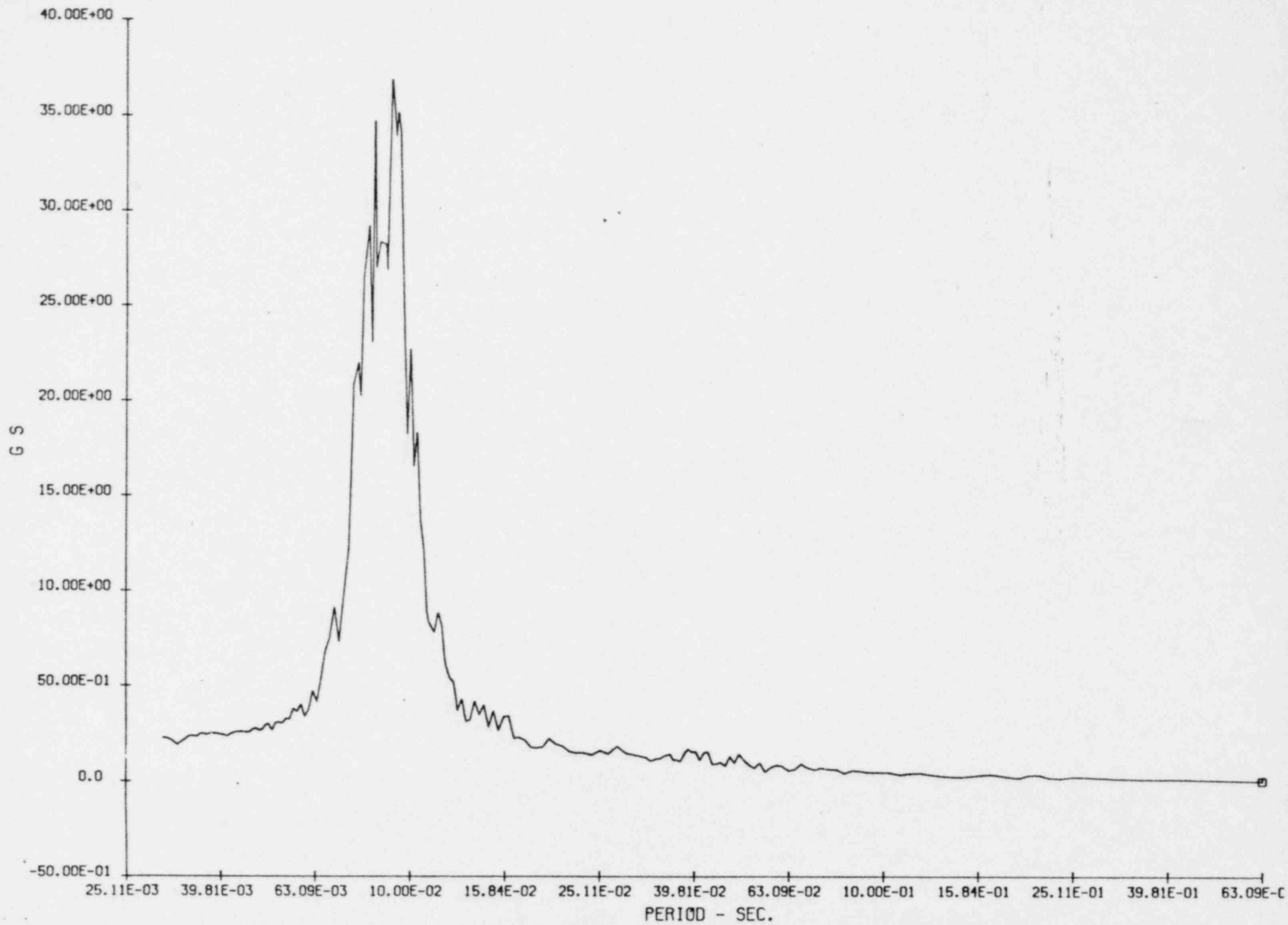
40.00E+00
35.00E+00
30.00E+00
25.00E+00
20.00E+00
15.00E+00
10.00E+00
50.00E-01
0.0
-50.00E-01

25.11E-03 39.81E-03 63.09E-03 10.00E-02 15.84E-02 25.11E-02 39.81E-02 63.09E-02 10.00E-01 15.84E-01 25.11E-01 39.81E-01 63.09E-01

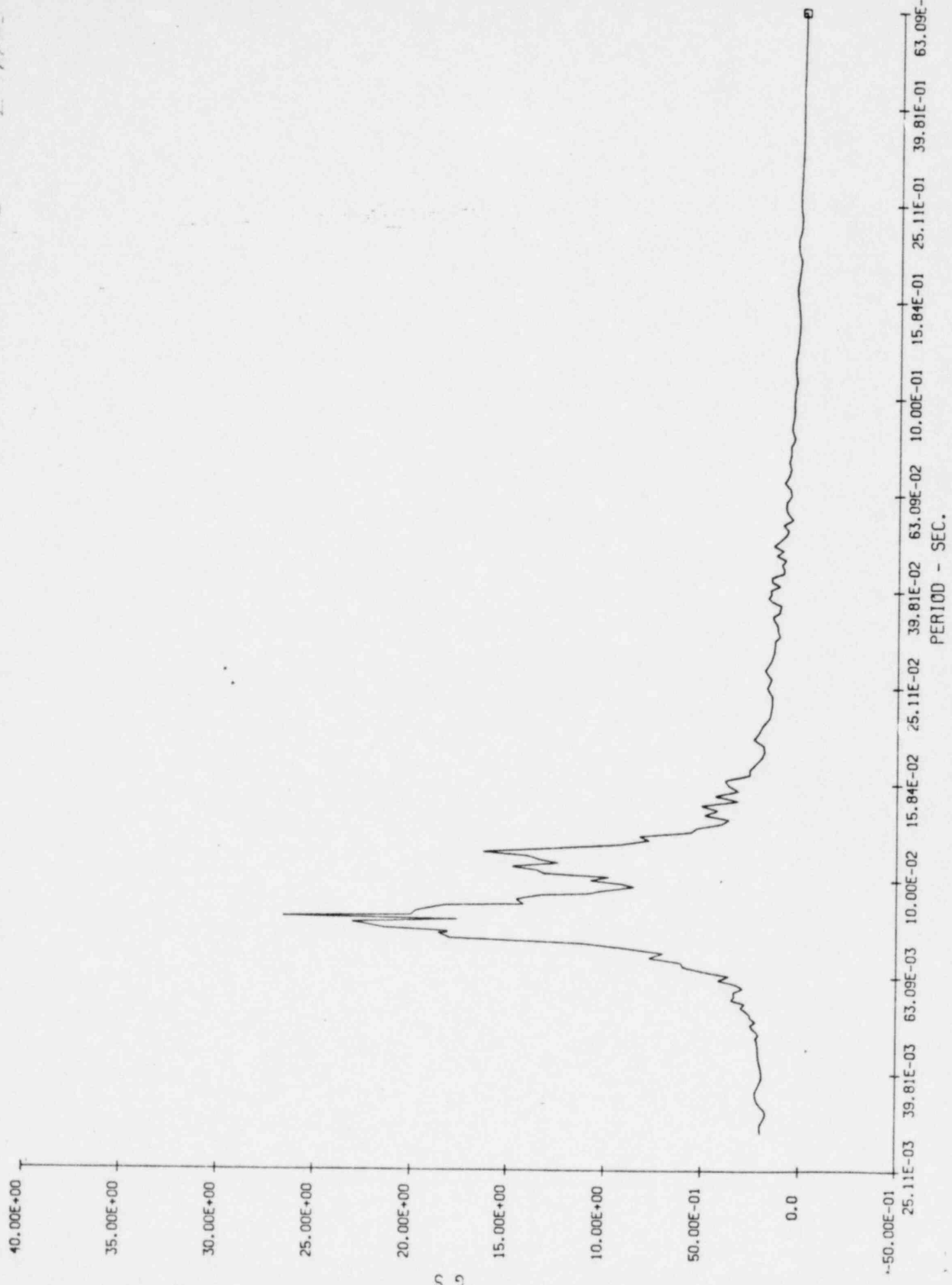
PERIOD - SEC.

PERIOD - SEC.

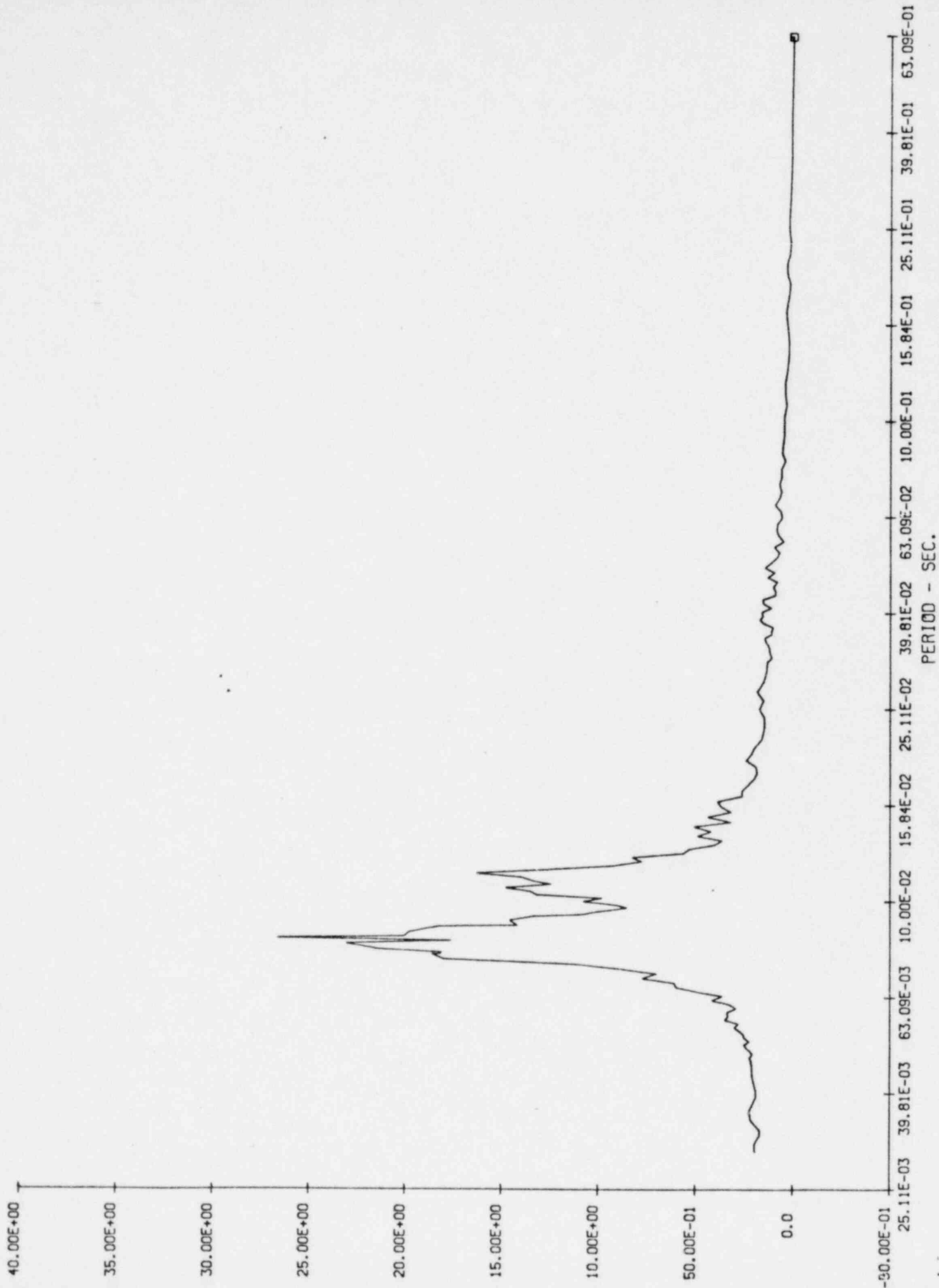
COARACTE
JT * 15



UNCLASSIFIED TRAFFIC
JAN 15 2-77 PM '77



CORRECTION
JUNE 7-1968



4. Provide a discussion of our intent for determining the adequacy of initial design loads (comparing final as-built load to assumed design loads).

Response:

It is the intent of Duke Power to verify the adequacy of our structural building design by comparing the as built loads to the assumed loads used in the initial design.

The various disciplines will submit to the Civil/Environmental Division the magnitude and location of all significant attachments to our structures. The limitations of what magnitude load is submitted will vary depending on which structure is being considered and whether the attachment is made to structural steel or concrete.

Attachments that are of low magnitude are considered individually insignificant when considering overall structural stability. However, to account for the cumulative effect of several small attachment in a given area, a conservative uniform load will be applied in addition to the actual point loads of the significant attachment.

With both the significant point loads and the uniform loads applied, the structural elements of our Category 1 structures will be reanalyzed to insure the as built stresses do not exceed the initial design capacity.

5. Provide justification for not including support stiffnesses of key NSSS components in the seismic model of the interior structure. Also, discuss how the requirements of Standard Review Plan 3.7.2.II-3b are met.

Response:

The original seismic model of the Reactor Building interior structure did not include the stiffnesses of the Nuclear Steam Supply System components. Only the masses of these NSSS components were included in the stick model. This model was accepted as the state of the art at that point in time.

The Standard Review Plan Section (3.7.2) now in effect requires that an approximate model of the NSSS be coupled with the model of the primary supporting structure. The following assumptions were made in the development of the NSSS model:

1. Each steam generator and reactor coolant pump was represented by beam elements located in the proper respective geometric locations.
2. For each steam generator, masses were lumped at each of two support points and at the top.
3. For each reactor coolant pump, masses were lumped at the horizontal support locations.
4. Member properties were varied from magnitudes approximately equal to that of the supporting structure, to three orders of magnitude less than the supporting structure.
5. The steam generators and reactor coolant pump models were connected to the structural model with members which have properties equivalent to the stiffnesses of the actual connection between the building and the equipment.
6. The major loop piping was considered in the composite model.
7. The reactor vessel was not included as a separate item in the model. The centroid of the vessel is approximately at the center of rigidity of the structure (at the support elevation) and the connections to the structure are very stiff. The vessel should behave with the structure. The vessel mass is lumped at the appropriate elevations on the structure.

Figure 1 (attached) shows the resulting model configuration.

A comparison of resulting frequencies is offered below:

MODE	PLANE DIRECTION	FREQUENCIES		HZ.		$\Delta\%$	$\Delta\%$	$\Delta\%$
		ORIG RESULTS	STIFFNESS* 1	2	3	Orig To 1	Orig To 2	Orig To 3
Horiz.	X	7.75	7.83	7.83	7.77	1.03	1.03	.30
Horiz.	Z	6.74	5.98	5.98	5.95	-11.30	-11.30	-11.70
Vert.	Y	19.09	17.95	17.80	16.27	-6.0	-6.76	-14.77

* NOTE: Stiffness value ¹ has member properties equal to that of the supporting structure. Value ² assumes properties 2 orders of magnitude smaller than the supporting structure. Value ³ assumes properties three orders of magnitude smaller than the supporting structure. Refer to assumption 4 above.

A comparison of resulting forces is offered in the following:

FORCE RESULTS	ORIGINAL ANALYSIS	FORCES K & K-FT			$\Delta\%$	$\Delta\%$	$\Delta\%$
		1	STIFFNESS* 2	3	ORIG Vs 1	ORIG Vs 2	ORIG Vs 3
AXIAL	472.9	4470.	5067.	4018.	-5.48	7.15	-15.03
SHEAR Y	10410.	8884.	8970.	8816.	-14.66	-13.83	-15.31
SHEAR Z	10926.	8297.	8461.	8142.	-24.06	-22.56	-25.48
TORSION	63855.	54451.	56066.	57621.	-14.73	-12.20	-9.76
MOMENT Y	811822.	603123.	602467.	594204.	-25.71	-25.79	-26.81
MOMENT Z	767507.	645934.	646045.	645237.	-15.84	-15.83	-15.93

** Results taken at the base of the structure.

Conclusion:

The above comparisons of frequency and forces indicate the interior structure is adequately analyzed and designed. The following observations are made:

- The resulting structural design forces would drop from 10 to 15% over the values used in the original design.
- The resulting response spectra would show a frequency shift of 5 to 10% toward the low frequency side of the curve. The resulting response should fall within the present spectra envelope.

REACTOR PIPING WITH NSSC

C.C.B. STRUCTURE

STEAM GENERATOR
(1770)

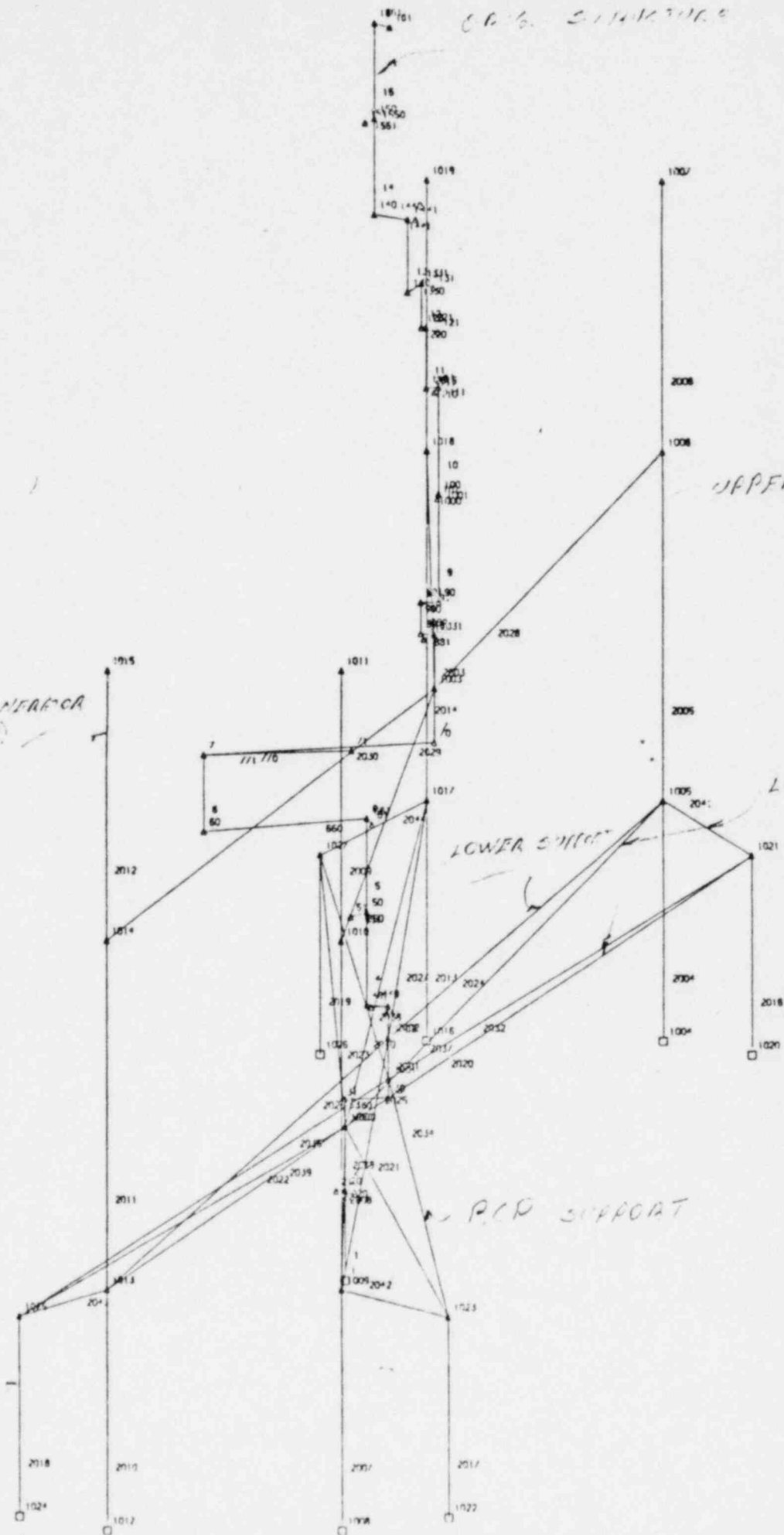
UPPER SUPPORT

LOOP PIPING

LOWER SUPPORT

R.C.P. SUPPORT

R.C.P.
(1770)



6. Provide justification for not considering concrete cracking of the concrete pressure boundaries in the seismic modeling of the interior structure.

Response:

Computer seismic analyses were performed to determine the effect that concrete cracking has on Category I structures (Reference FSAR Section 3.7.2.3.1). To approximate the most conservative case, it was assumed that (1) the cracked moments of inertia equal one-half the gross moments of inertia and (2) all structural members are cracked. Based on these conditions, only small variations in the seismic response result.

7. Determine the effect of including a 5% accidental base dimension eccentricity in the torsional component of the seismic analysis of Category I structures.

Response:

See attached response to question 220.32.

CNS

220.29 Provide description of your procedure to account for three components
(3.7.2.5) of earthquakes in generation of floor response spectra.

Response:

220.30 Provide description of the procedure used in allowing for vertical
(3.7.2.5) flexibility of floors in generation of vertical response spectra.

Response:

220.31 In this section, you have stated that the earthquake ground motions
(3.7.2.6) are assumed to act in one of the horizontal directions and vertical
 direction simultaneously. It is not clear how you have combined the
 responses due to these two motions. Is it by absolute sum method or
 SRSS method? Also, provide a comparison of your method of combining
 two components of earthquakes with the currently acceptable procedure
 of combining all three components with SRSS method. This comparison
 need only be done for one structure which is essentially non-symmetric;
 e.g., internal structure.

Response:

220.32 The present technical position of the staff requires that the acci-
(2.7.2.11) dental torsion, based on eccentricity of minimum 5% of the base dimen-
 sion, be included in the design of structures. This is in addition
 to that which results from the actual geometry and mass distribution
 of the building. Either indicate your willingness to comply with
 this position or provide justification for not doing so.

Response:

Standard Review Plan 3.7.2, Seismic Systems Analysis, Part III, Sec-
tion II, states that an acceptable method for accounting for acci-
dental torsion is to add an additional 5% of the maximum building
base dimension to the eccentricity that exists naturally in the
building. This was not done at Catawba because the requirement did
not exist at the time of the initial analysis.

The effect of incorporating this requirement into the Catawba analysis
has been evaluated using the Auxiliary Building as the case study.
The Auxiliary Building was selected because it exhibits the largest
existing eccentricities as well as the largest plan dimensions.

CNS

The resulting increase in moment arm length ranged from 72% to 738% of the natural eccentricity. This increase in moment arm length increased the torsional moment from 24% to 135% over the original analysis results. Additionally, the distribution of this torsion and shear would vary over what was originally designed. Not only are the total torsional values higher, but the higher elevations of the structure would experience higher proportions.

It is Duke's position that the Catawba seismic model accurately depicts exact locations of centers of mass and rotation; and, therefore the 5% conservative increase is not required.

220.33
(3.7.3.5)

Describe how the effects of three components of earthquake are accounted for in determining overturning moments.

Response:

The three components of earthquake are examined in the methods described in Section 3.7.2.6.

8. Provide justification for not considering the effects of closely spaced modes in the seismic analysis of Category I structures.

Response:

Closely spaced modes do not exist in the Category I structures at the Catawba Nuclear Station. The worst condition for closely spaced modes, i.e., largest number in the lowest frequencies, is the Auxiliary Building. Subsequent analysis indicates that the greatest increase in response, due to consideration of these closely spaced modes, is 7.2%, with an average increase of 2.2%. This increase in seismic responses due to closely spaced modes is insignificant when compared with the original seismic responses.

9. Provide verification for all computer programs used in seismic and structural analysis of Category I structures.

Response:

- (1) The following computer programs, used in the seismic and structural analysis of Category I structures, are recognized as programs in the public domain by Civil Engineers.

	PROGRAM ID	PROGRAM NAME	DESCRIPTION
(a)	STRU DL	Mc-Auto- STRU DL	General purpose computer program for linear static and dynamic analysis of elastic structures.
(b)	CGO-260	QUAD 4	This program utilizes a non-linear Finite Element Method approach for analysis of seismic response of earth structures by iteration of dynamic properties for strain compatibility.
(c)	CGO-264	ISBILD	This program utilizes a non-linear Finite Element Method approach for the determination of stresses and strains of embankments. Input is organized for simulation of dam construction.
(d)	ΔXISYM	WILSON- GHOSH	Performs static and dynamic analysis of shells of revolution.
(e)	CIVMSS03	ELAS-75	General purpose finite element computer program for Linear Equilibrium problems for structures.
(f)	SUPERPIPE	N/A	Proprietary program of EDS Nuclear of General Purpose Structural analysis and code checking per ASME Section III and ANSI B 31.1 of piping systems.

- (2) The following computer programs, used in the seismic and structural analysis of Category I structures, were verified using either independent hand calculations, independent computer programs, published results of some combination thereof.

	PROGRAM ID	PROGRAM NAME	DESCRIPTION
(a)	CIVRHB01	N/A	Modified version of Wilson-Ghosh FE Program for static analysis.
(b)	CIVRHB02	N/A	Modified version of Wilson-Ghosh FE Program for dynamic analysis.
(c)	CIVRHB04	N/A	Determine maximum and minimum disposal from results of CIVRHB02.
(d)	CIVRHB05	N/A	Determine maximum and minimum stress intensities from results CIVRHB02.

	PROGRAM ID	PROGRAM NAME	DESCRIPTION
(e)	CIVMSS01	KSHEL1	Computer program for the static analysis of shells or revolution.
(f)	CIVMSS02	KSHEL3	Computer program for the dynamic analysis of shells of revolution.
(g)	CIVASM09	KSHE- DESIGN	Designs reinforcement for concrete shell structures analyzed by KSHEL 1 or KSHEL 2 computer program.
(h)	QTHETA	N/A	Calculates shear Q_x from other stress resultants from KSHEL 2 programs.
(i)	SPECTRA	N/A	Uses STRUDL punch output file of response spectra to produce plots of response spectra with $\pm 10\%$ period envelope. Executed with STRUDL by Procedure Strudraw.
(j)	SPECTEN	N/A	Same as spectra but with additional 10% acceleration envelopes at peak.
(k)	CIVMSS05	LMSDM	Lumped mass system dynamic analysis for seismic excitations. Computer mode shapes, frequencies, time histories and response spectra for a stick model and subsequent versions.
(l)	CGP-203	N/A	This program calculates the structural member properties to be used in a lumped mass seismic model. These properties are computed from the structural elements (walls and columns) at each floor or section.
(m)	CGP-179	N/A	This program calculates the shear force on the structural elements used to calculate the member properties in the lumped mass seismic model.
(n)	CIVDRB01	COLUMN/ WALL INERTIA PRO- PERTIES	Computes the Inertia Properties such as area moment of inertia, areas of cross section, mass moment of Inertia and Centers of Rigidity of the members of Lumped Mass Model used for Seismic Analysis.
(o)	CIVMSS11	N/A	Calculates fourier series time history loads TMD data for transient analysis of Catawba containment.
(p)	CIVMSS06	STRUC- TURAL RESPONSE TO SEISMIC LOADS	Computes the response to a stick model subject to a given ground response spectrum.

10. Provide justification demonstrating negligible amplification assumed in vertical seismic analysis (interior structure, auxiliary building, and steel containment).

Response:

Interior Structure and Auxiliary Building

Structures at Catawba are assumed to be rigid, thus experiencing negligible vertical implication in the vertical direction. This assumption is validated by examining the first mode vertical frequencies of the structural members in question.

Vertical columns and walls quite obviously display extremely high vertical natural frequencies. The more heavily loaded slabs were analyzed to determine their first mode frequencies. The following results were obtained:

<u>Floor Slab</u>	<u>Frequency</u>
Ice condenser Floor	32 cyc/sec
Accumulator Floor	45 cyc/sec
Aux Bldg - 12" thick - 20' span	18 cyc/sec
Aux Bldg - 24" thick - 37' span	18 cyc/sec

Frequencies of this magnitude justify the negligible amplification assumed in the vertical seismic analysis.

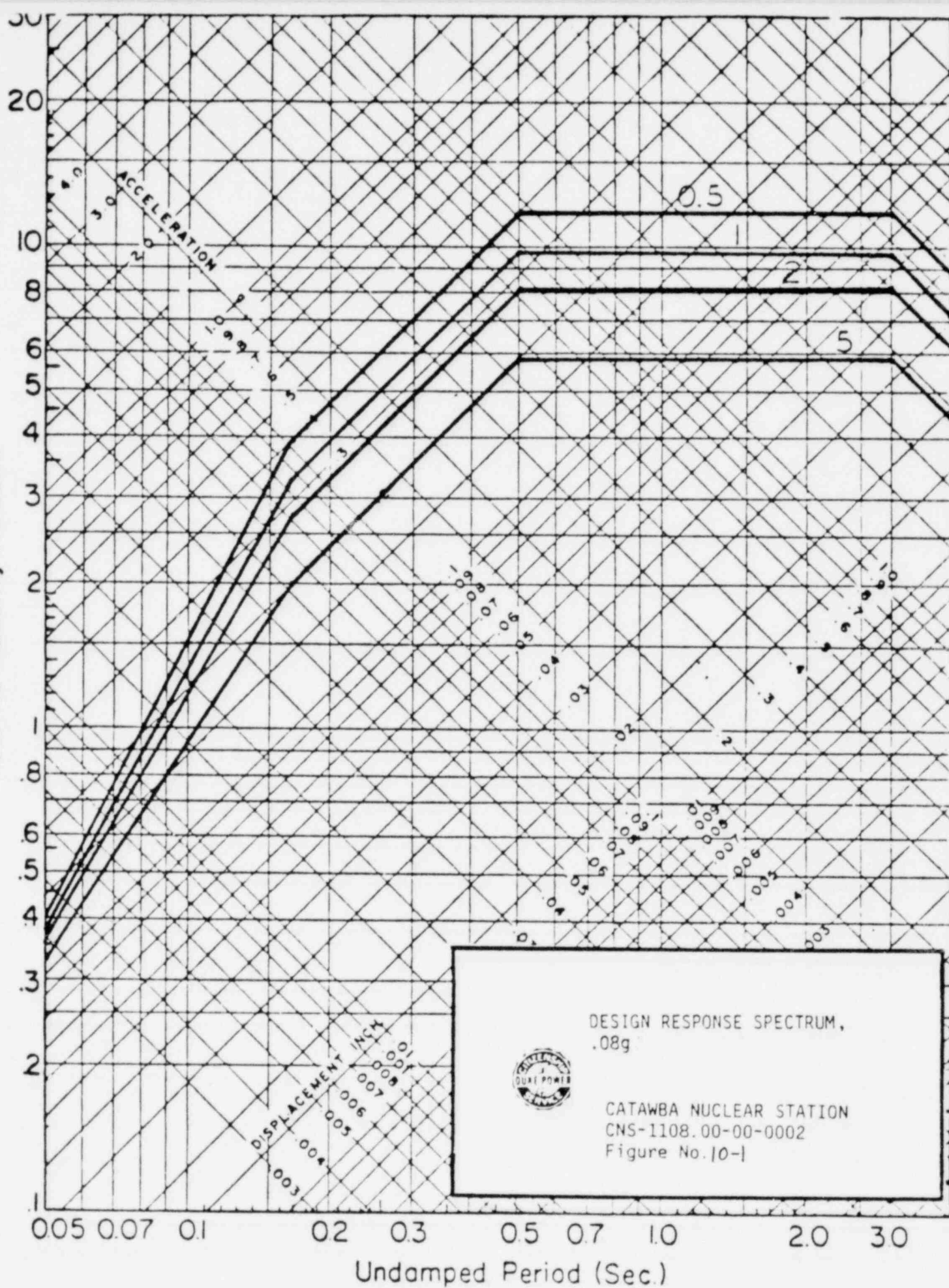
Steel Containment

Ground response spectra for the Operating Basis Earthquake are given in Figure 2 of Specification CNS-1108.00-00-0002, which is included herein as Figure 10-1. Horizontal containment spectra were generated by applying a ground acceleration time history to a lumped mass stick model of the containment shell. The same lumped mass model was used to generate vertical containment spectra, using as input a vertical ground acceleration time history equal to two-thirds of the horizontal ground acceleration time history. The resulting vertical spectra are attached as Figures 10-2 through 10-21. A curve representing two thirds of the horizontal ground response spectrum has been drawn on each figure for comparison purposes.

For a damping ratio of 0.005, several spectra (Figures 10-6, -10, -14, and -18) have isolated peaks in the vicinity of period $T = .05$ sec which exceed the envelope of $2/3$ of ground response. Inspection of FSAR Section 3.7.1.3 reveals that this damping ratio does not apply to the containment vessel or its attachments and therefore this phenomenon has no impact upon design of Category I structures, systems or components.

For a damping ratio of 0.01, a similar occurrence is noted (Figures 10-11, -15, and -19) in the vicinity of $T = .05$ sec. Because of the local nature of these spikes (isolated at $T = .05$ sec) and the low level of accelerations in question (less than $0.02g$), this is not a significant design consideration. All other spectra are enveloped by two-thirds of the horizontal ground response. Therefore, the assumption of negligible amplification in vertical analysis of the steel containment and its attachments is acceptable.

Relative Velocity (in./sec.)



DESIGN RESPONSE SPECTRUM,
.08g



CATAWBA NUCLEAR STATION
CNS-1108.00-00-0002
Figure No. 10-1

CATAWBA CONTAINMENT VESSEL - SEISMIC
VERTICAL RESPONSE TO OBE (.08G) AT EL 593.42
RESPONSE ACCELERATION SPECTRA, DAMPING= 0.0050

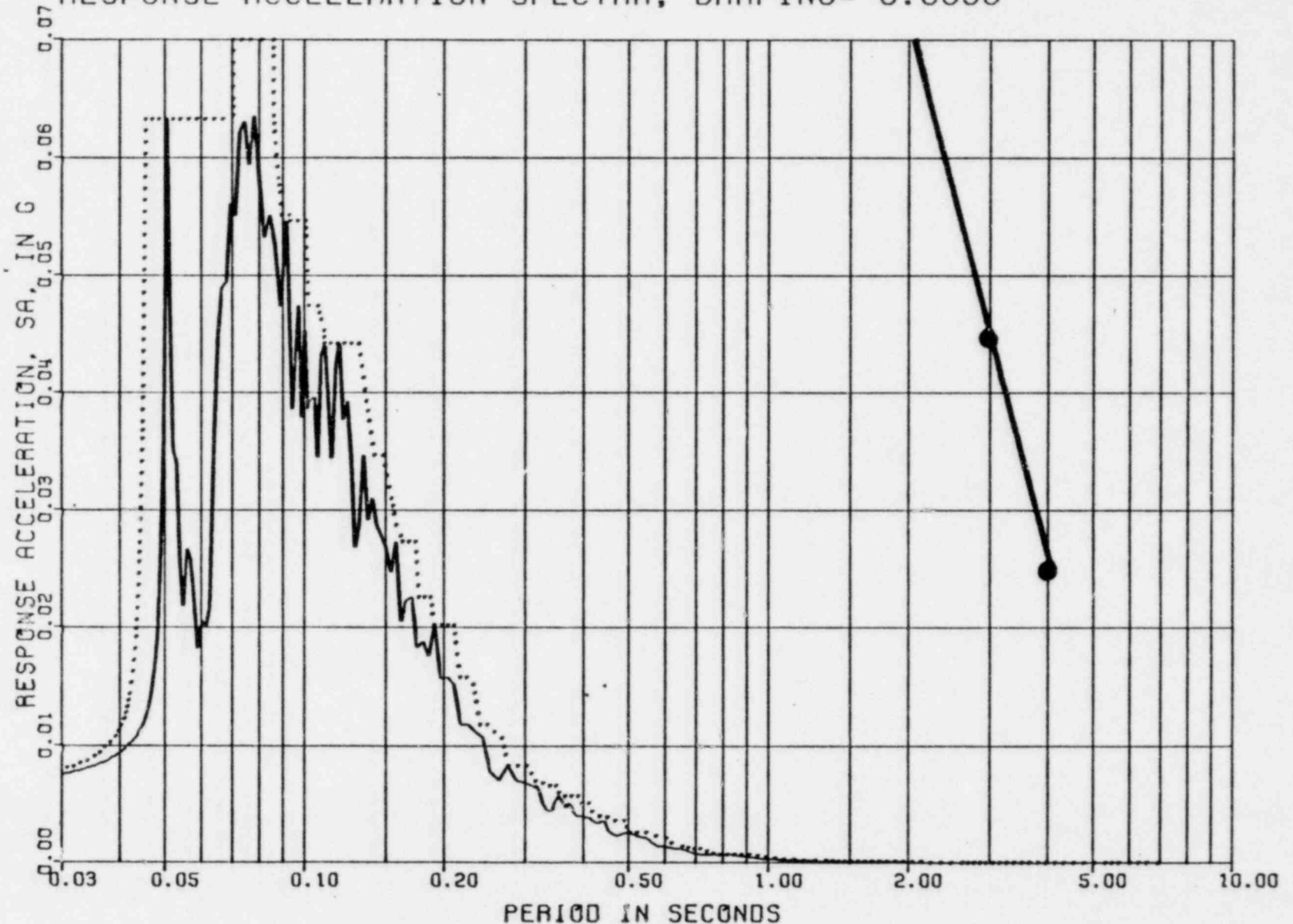


Figure 10-2

CATAWBA CONTAINMENT VESSEL - SEISMIC
 VERTICAL RESPONSE TO OBE (.08G) AT EL 593.42
 RESPONSE ACCELERATION SPECTRA, DAMPING= 0.0100

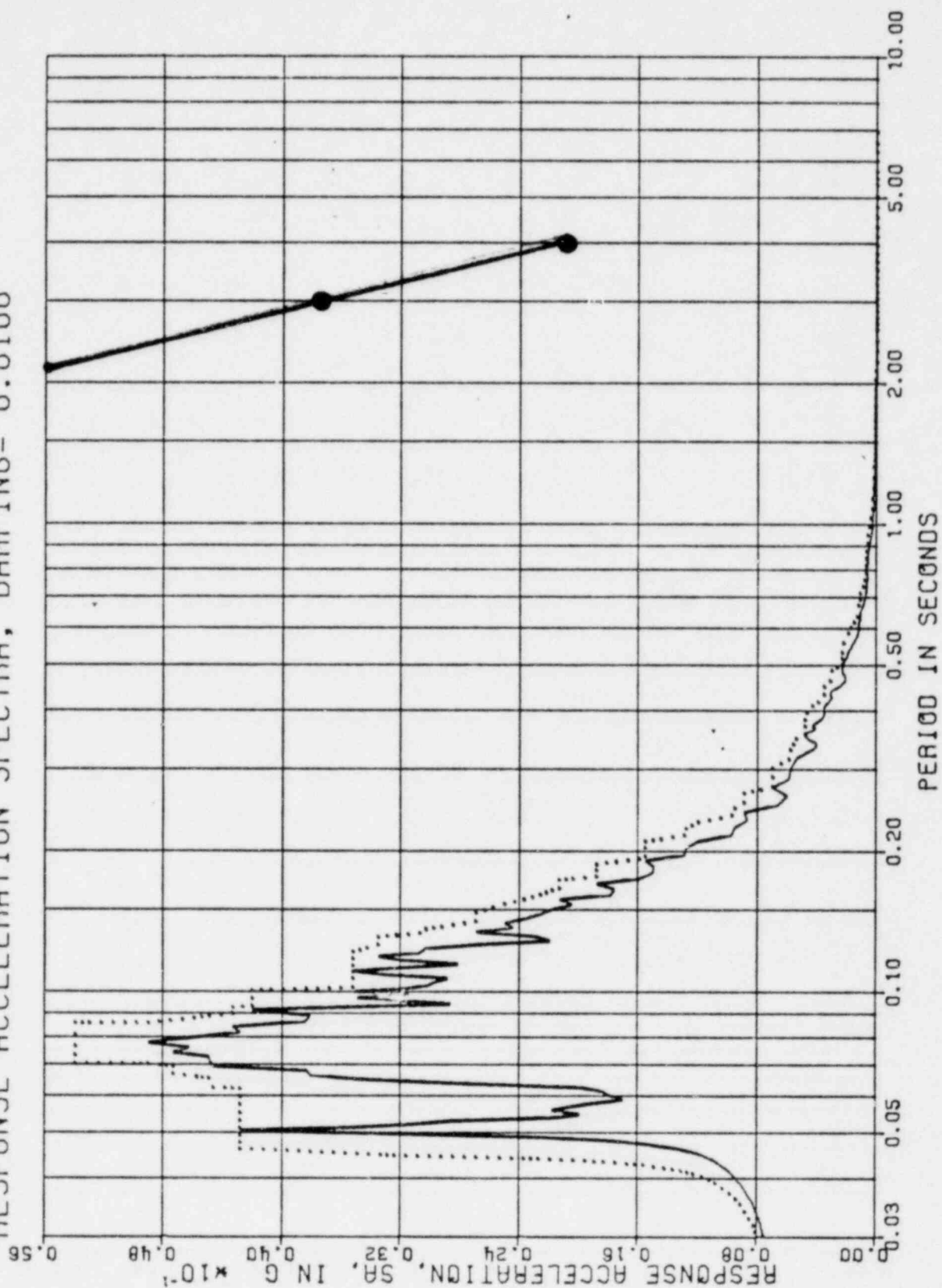


Figure 10-3

CATAWBA CONTAINMENT VESSEL - SEISMIC
VERTICAL RESPONSE TO OBE (.08G) AT EL 593.42
RESPONSE ACCELERATION SPECTRA, DAMPING= 0.0200

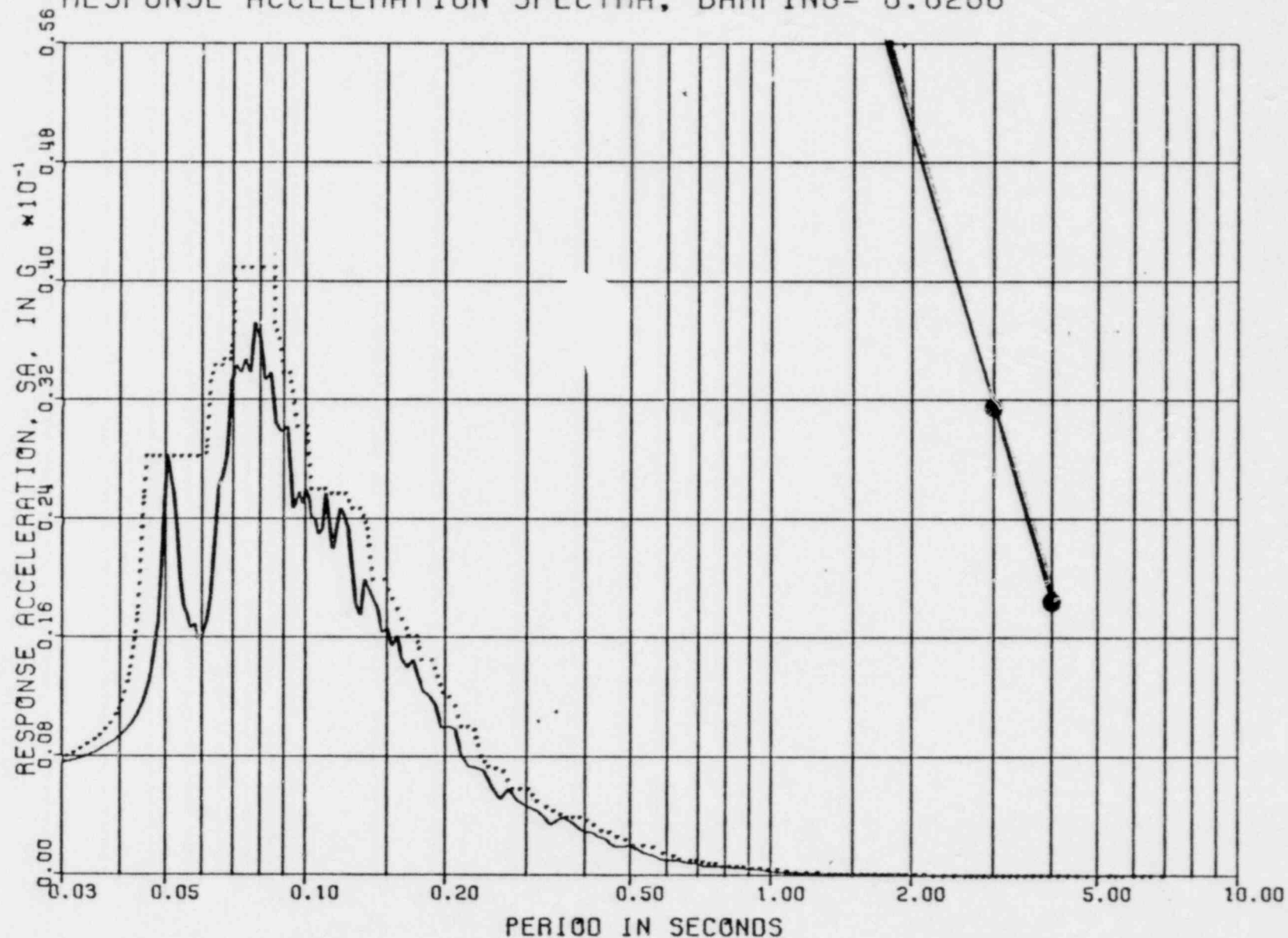


Figure 10-4

CATAWBA CONTAINMENT VESSEL - SEISMIC
 VERTICAL RESPONSE TO OBE (.08G) AT EL 593.42
 RESPONSE ACCELERATION SPECTRA, DAMPING= 0.0500

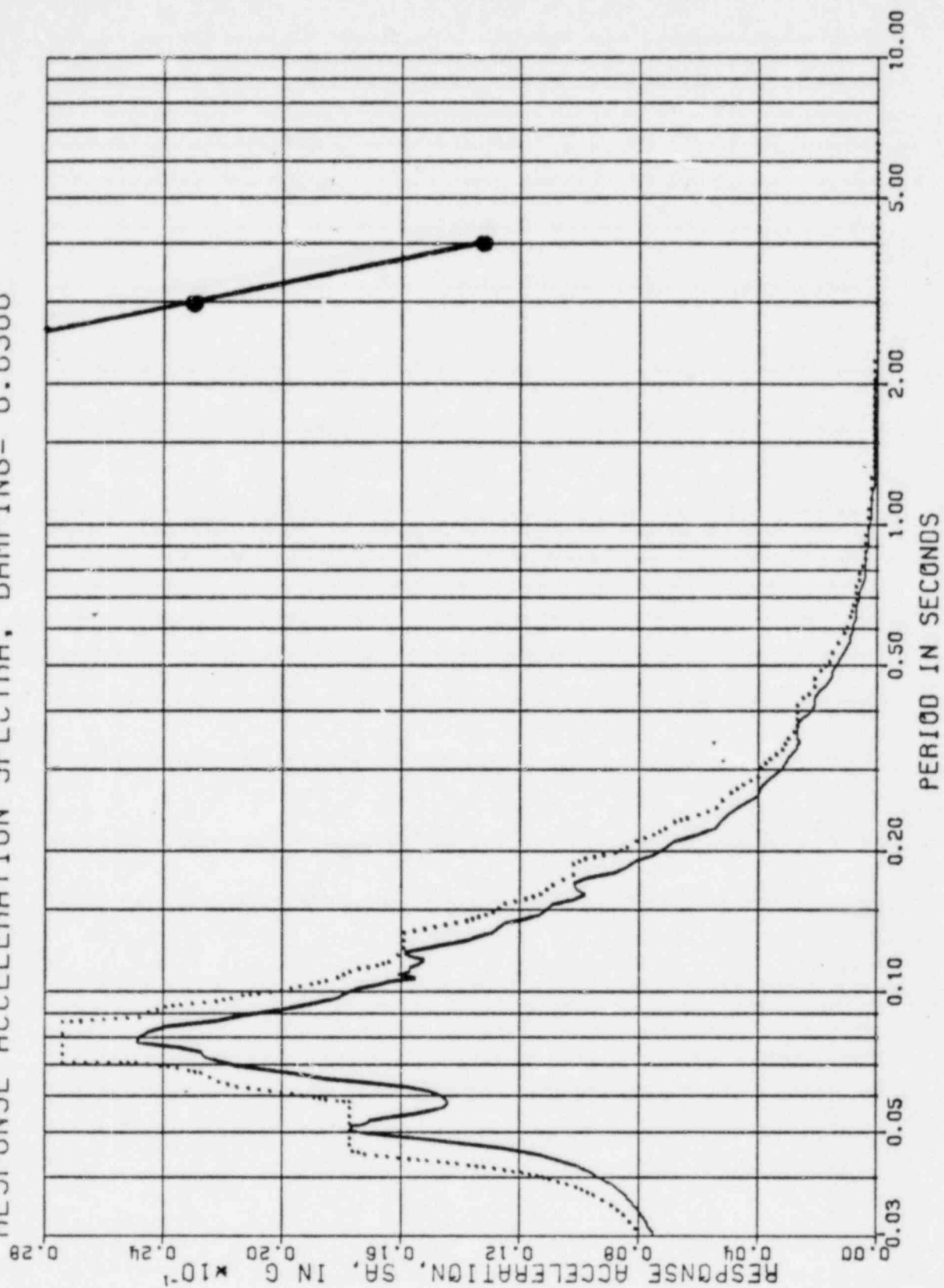


Figure 10-5

CATAWBA CONTAINMENT VESSEL - SEISMIC
VERTICAL RESPONSE TO OBE (.08G) AT EL 619.42
RESPONSE ACCELERATION SPECTRA, DAMPING= 0.0050

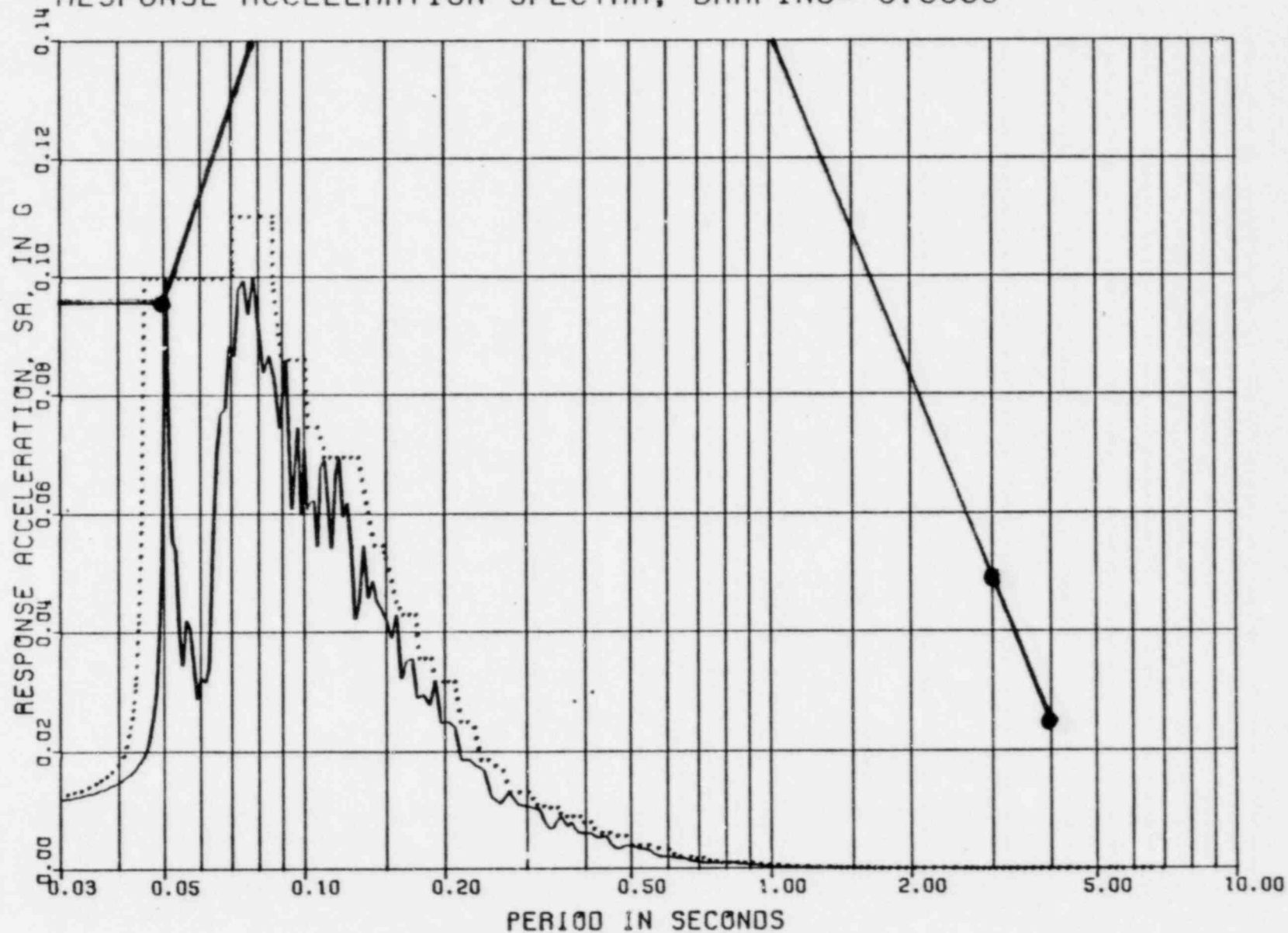


Figure 10-6

CATAWBA CONTAINMENT VESSEL - SEISMIC
 VERTICAL RESPONSE TO OBE (.08G) AT EL 619.42
 RESPONSE ACCELERATION SPECTRA, DAMPING= 0.0100

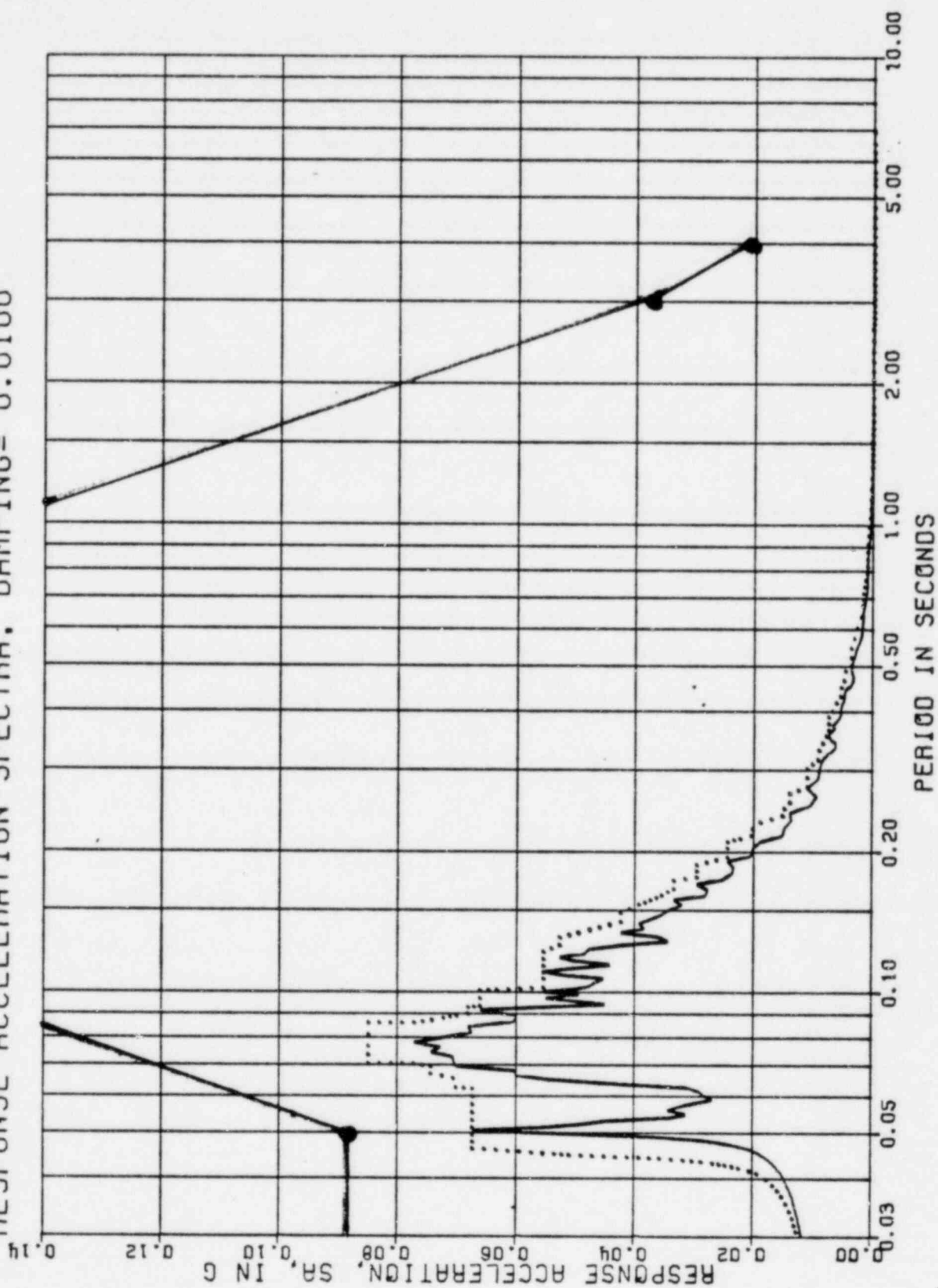


Figure 10-7

CATAWBA CONTAINMENT VESSEL - SEISMIC
 VERTICAL RESPONSE TO OBE (.08G) AT EL 619.42
 RESPONSE ACCELERATION SPECTRA, DAMPING= 0.0200

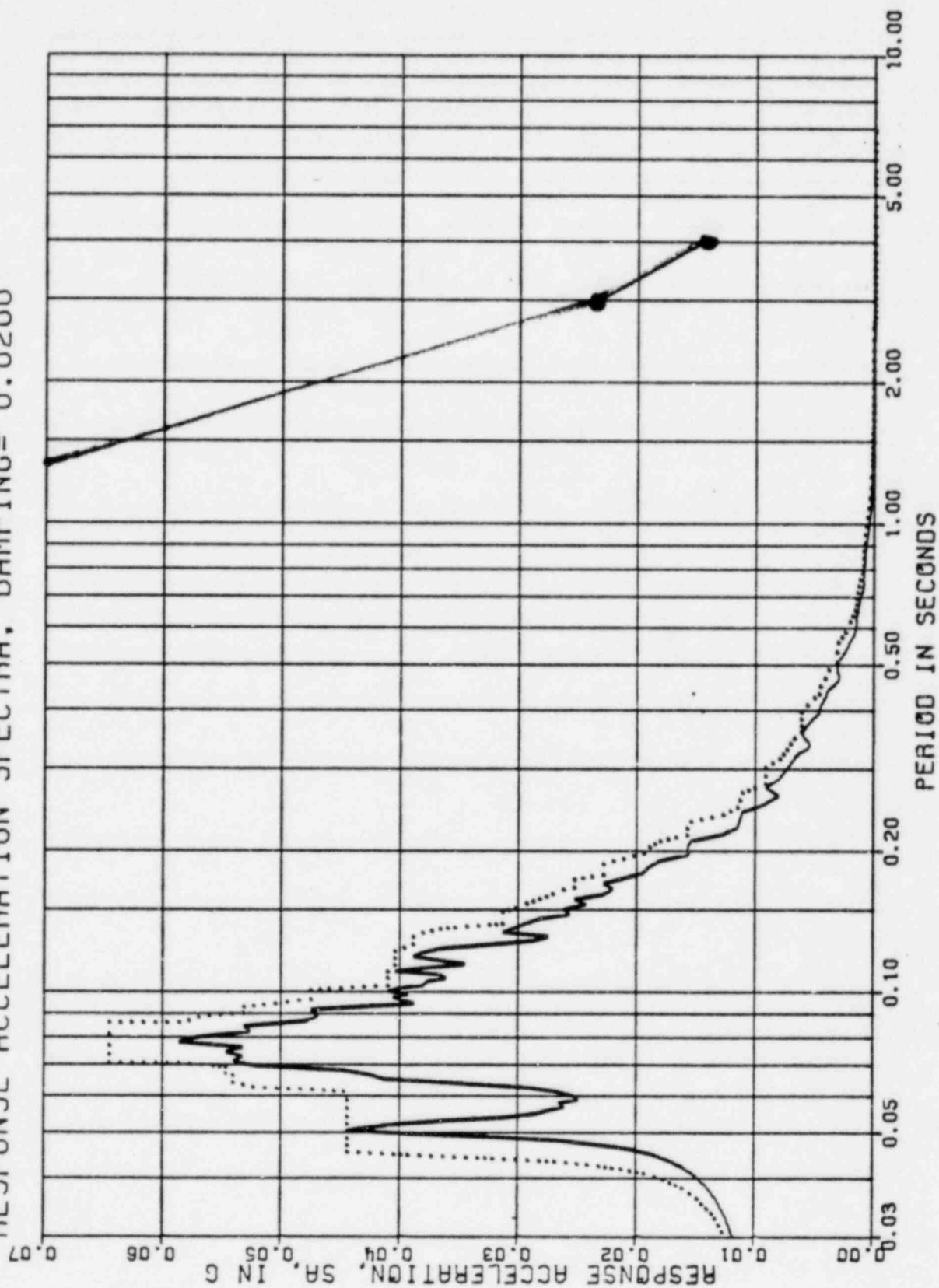


Figure 10-8

CATAWBA CONTAINMENT VESSEL - SEISMIC
 VERTICAL RESPONSE TO OBE (.08G) AT EL 619.42
 RESPONSE ACCELERATION SPECTRA, DAMPING= 0.0500

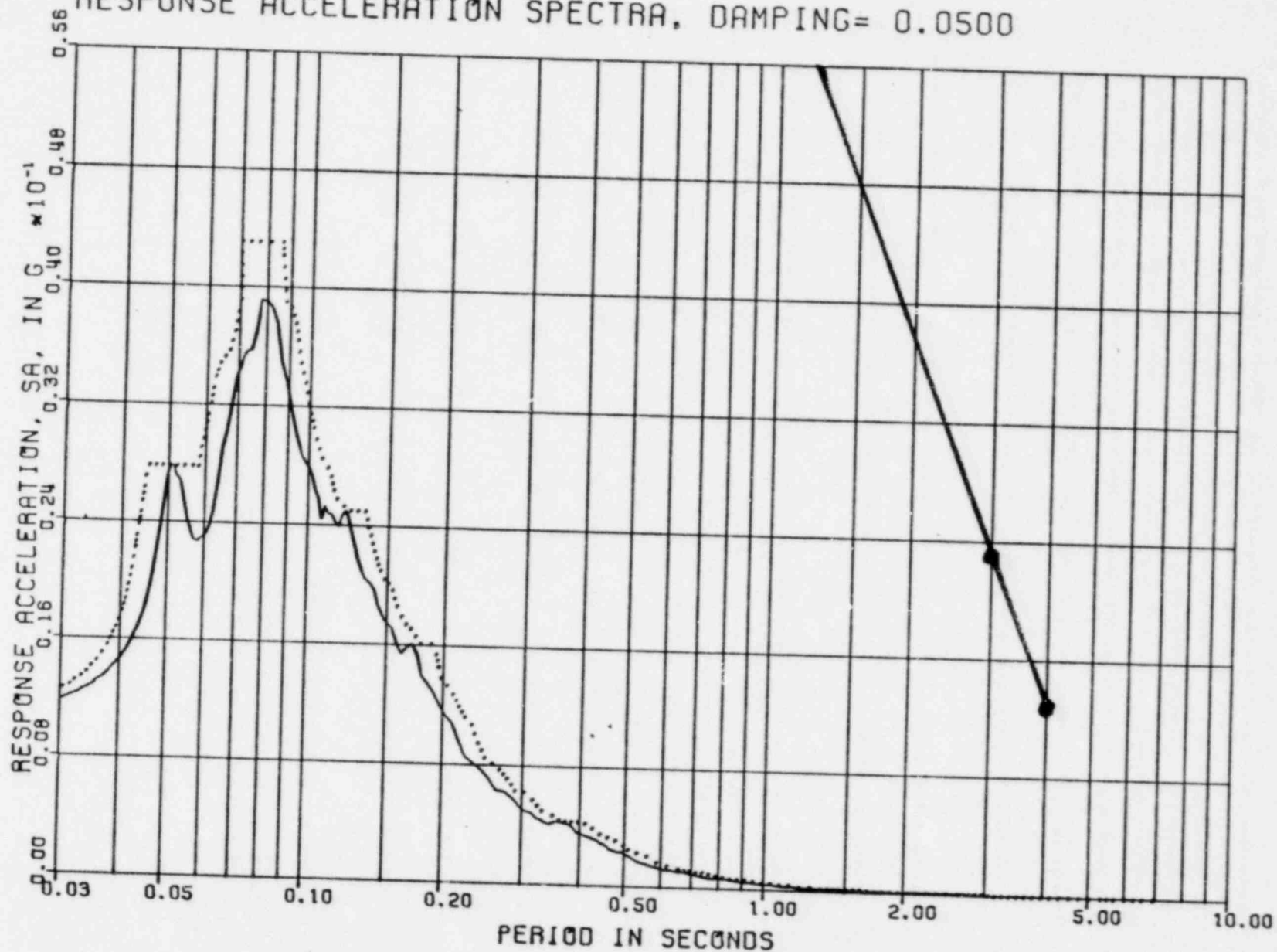


Figure 10-9

CATAWBA CONTAINMENT VESSEL - SEISMIC
 VERTICAL RESPONSE TO OBE (.08G) AT EL 663.75
 RESPONSE ACCELERATION SPECTRA, DAMPING= 0.0050

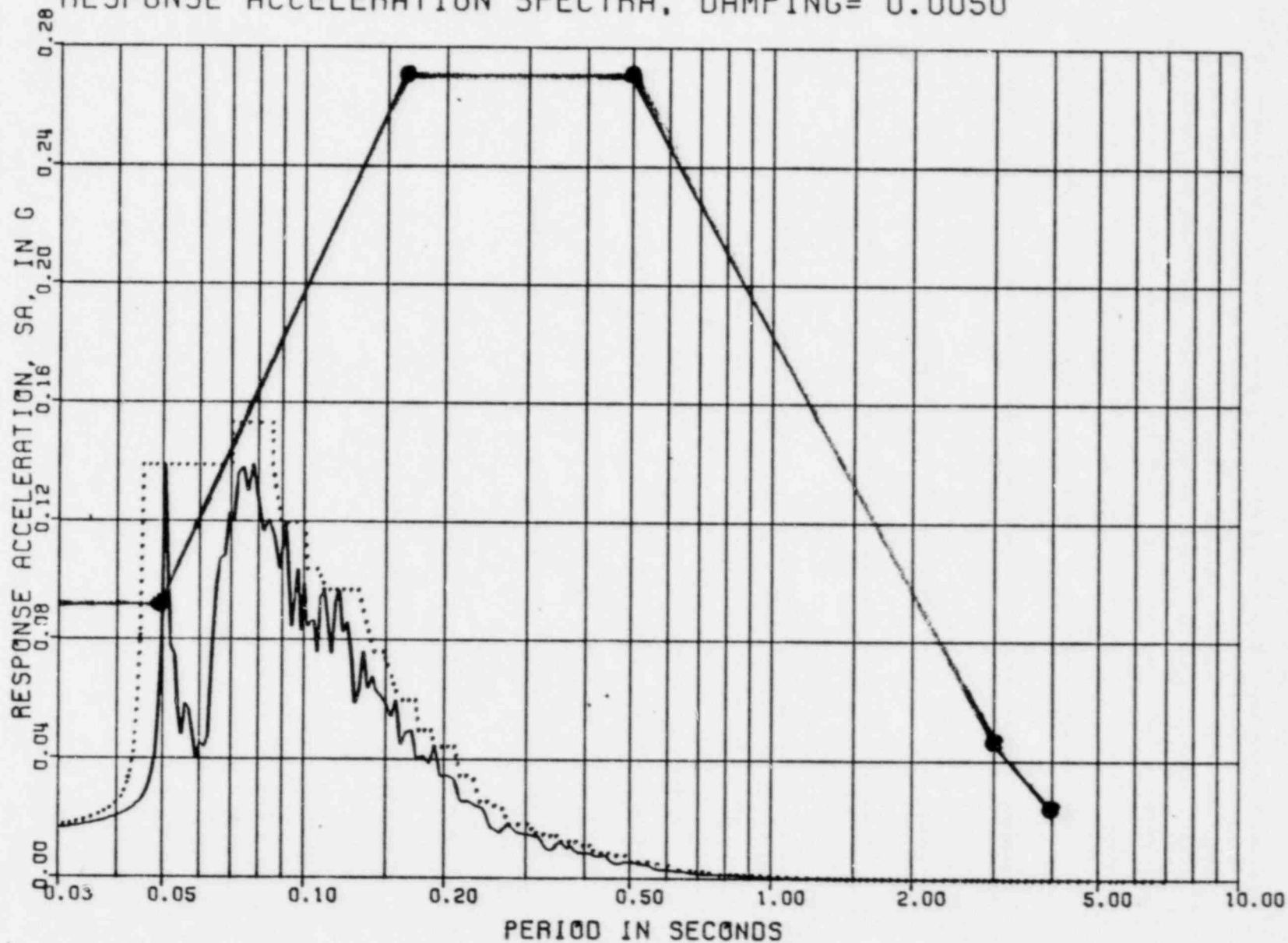


Figure 10-10

CATAWBA CONTAINMENT VESSEL - SEISMIC
 VERTICAL RESPONSE TO OBE (.08G) AT EL 663.75
 RESPONSE ACCELERATION SPECTRA, DAMPING= 0.0100

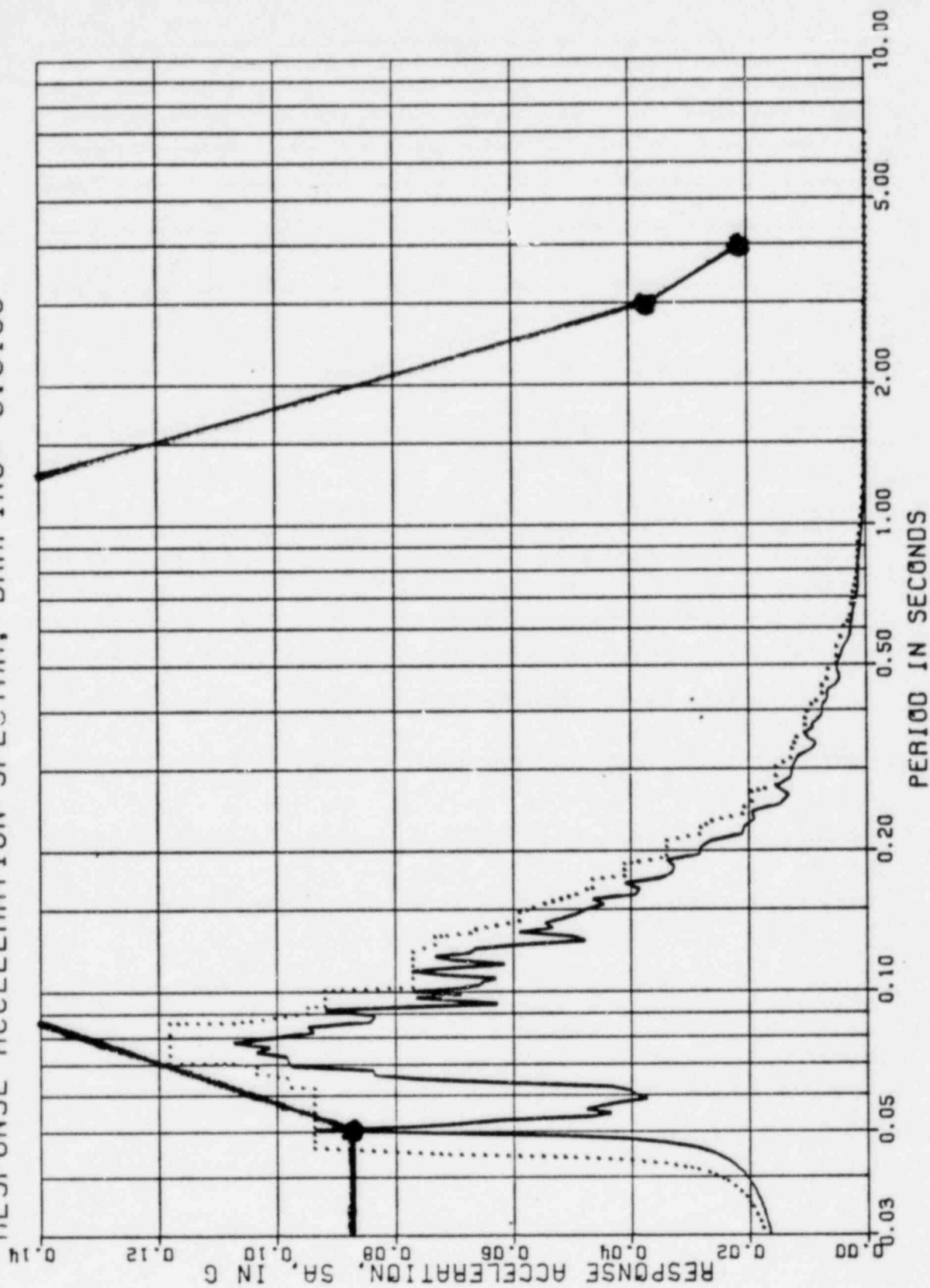


Figure 10-11

CATAWBA CONTAINMENT VESSEL - SEISMIC
VERTICAL RESPONSE TO OBE (.08G) AT EL 663.75
RESPONSE ACCELERATION SPECTRA, DAMPING= 0.0200

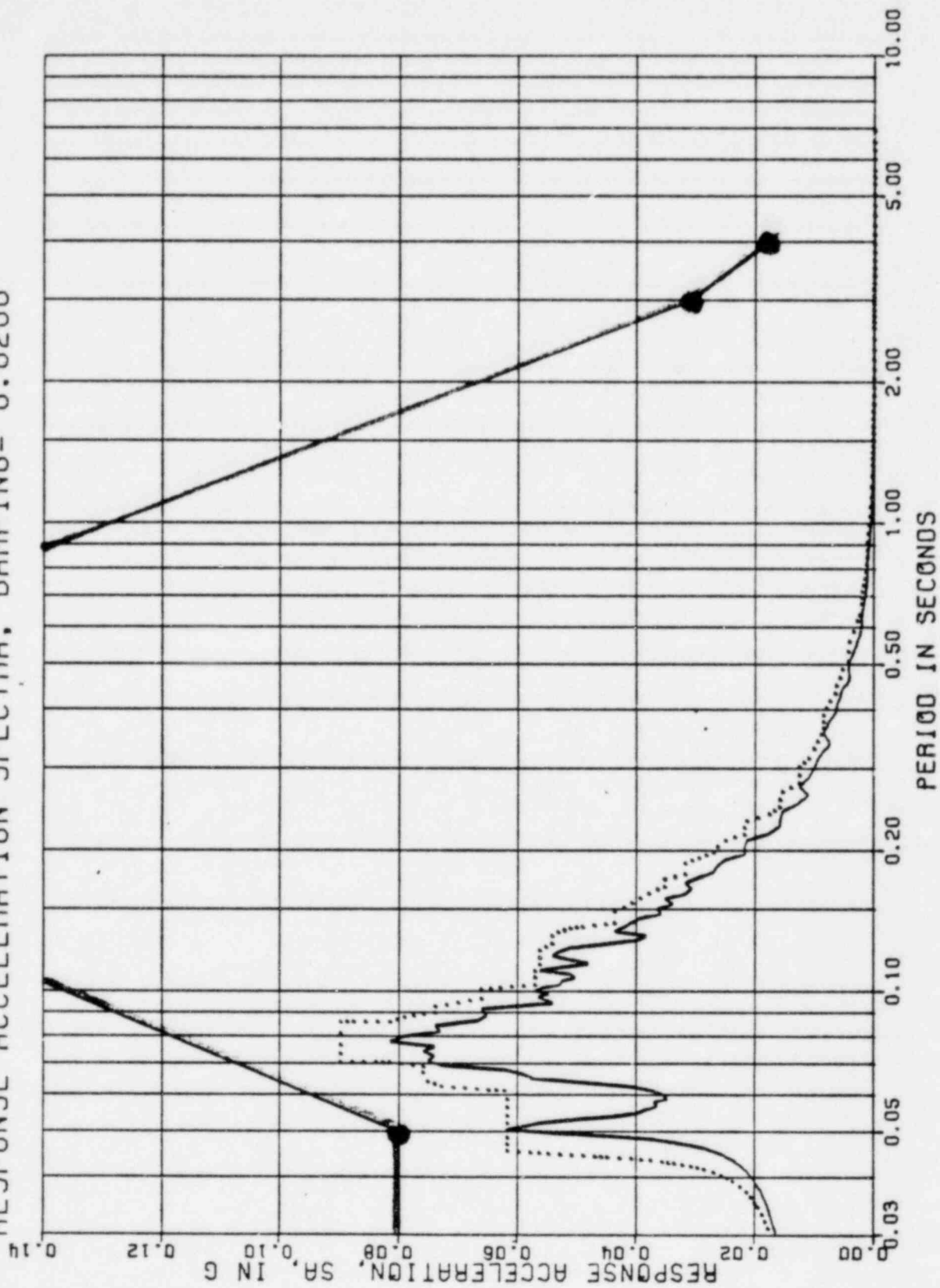


Figure 10-12

CATAWBA CONTAINMENT VESSEL - SEISMIC
VERTICAL RESPONSE TO OBE (.08G) AT EL 663.75
RESPONSE ACCELERATION SPECTRA, DAMPING= 0.0500

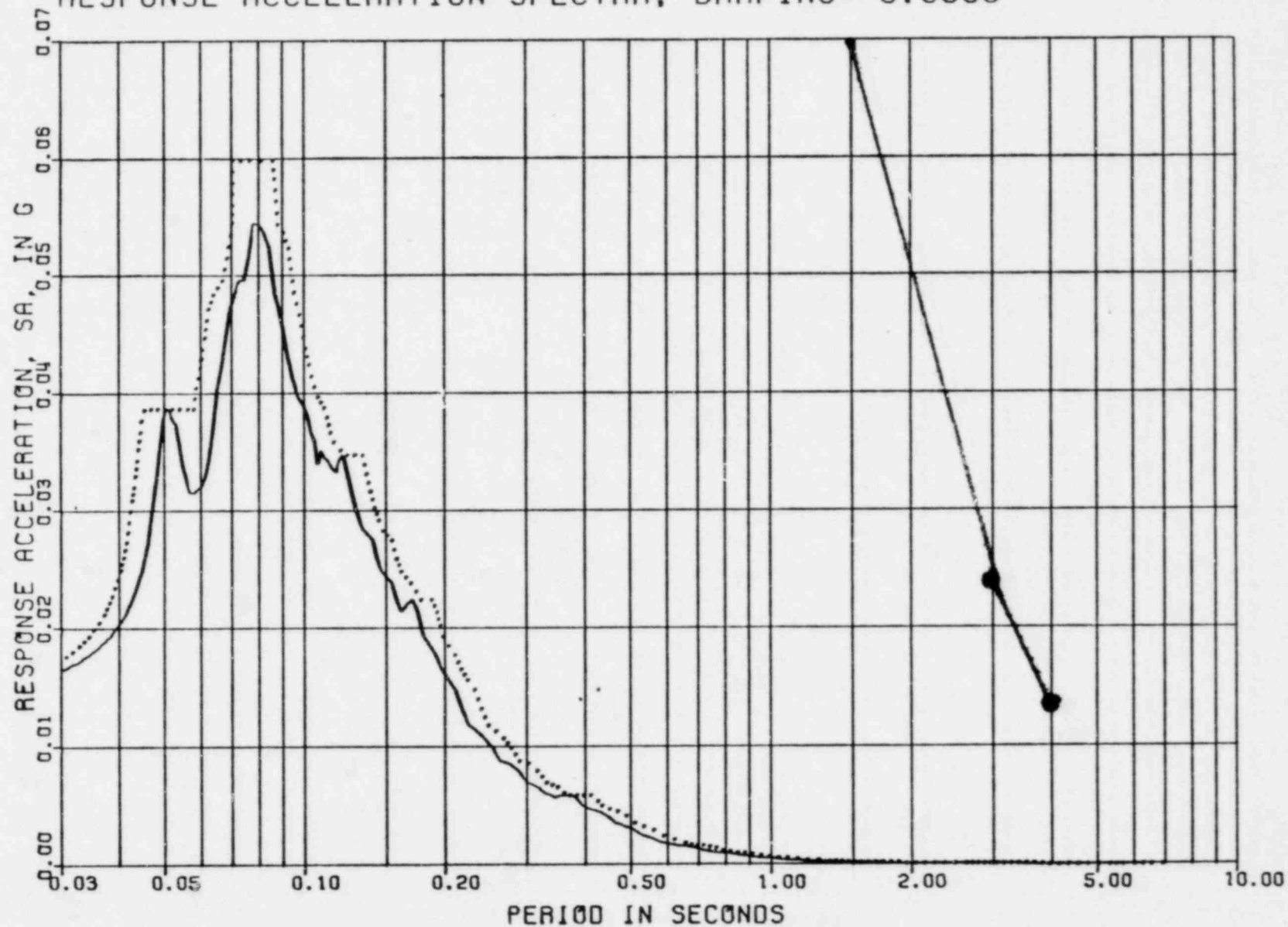


Figure 10-13

CATAWBA CONTAINMENT VESSEL - SEISMIC
VERTICAL RESPONSE TO OBE (.08G) AT EL 688.05
RESPONSE ACCELERATION SPECTRA, DAMPING= 0.0050

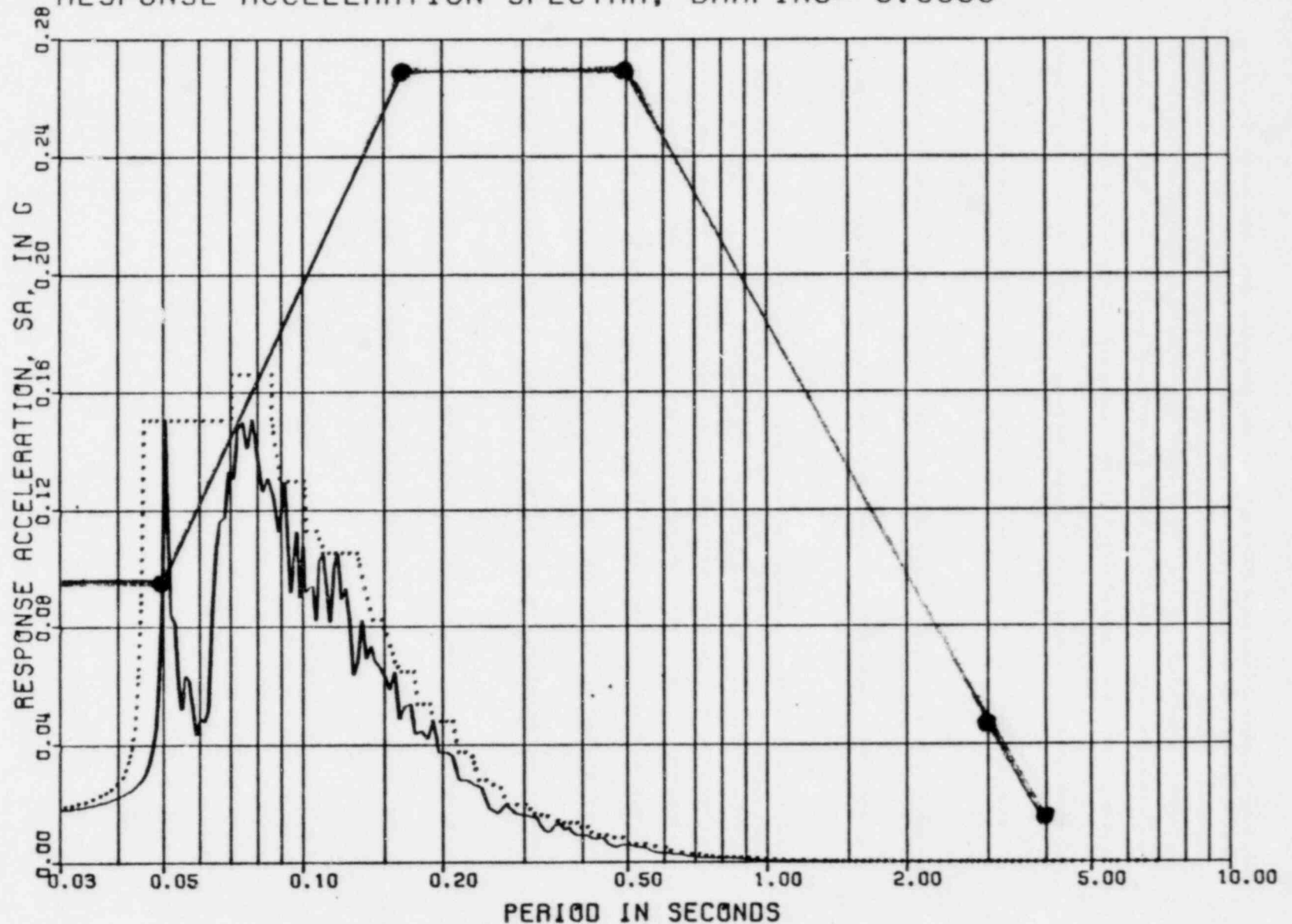


Figure 10-14

CATAWBA CONTAINMENT VESSEL - SEISMIC
 VERTICAL RESPONSE TO OBE (.08G) AT EL 688.05
 RESPONSE ACCELERATION SPECTRA, DAMPING= 0.0100

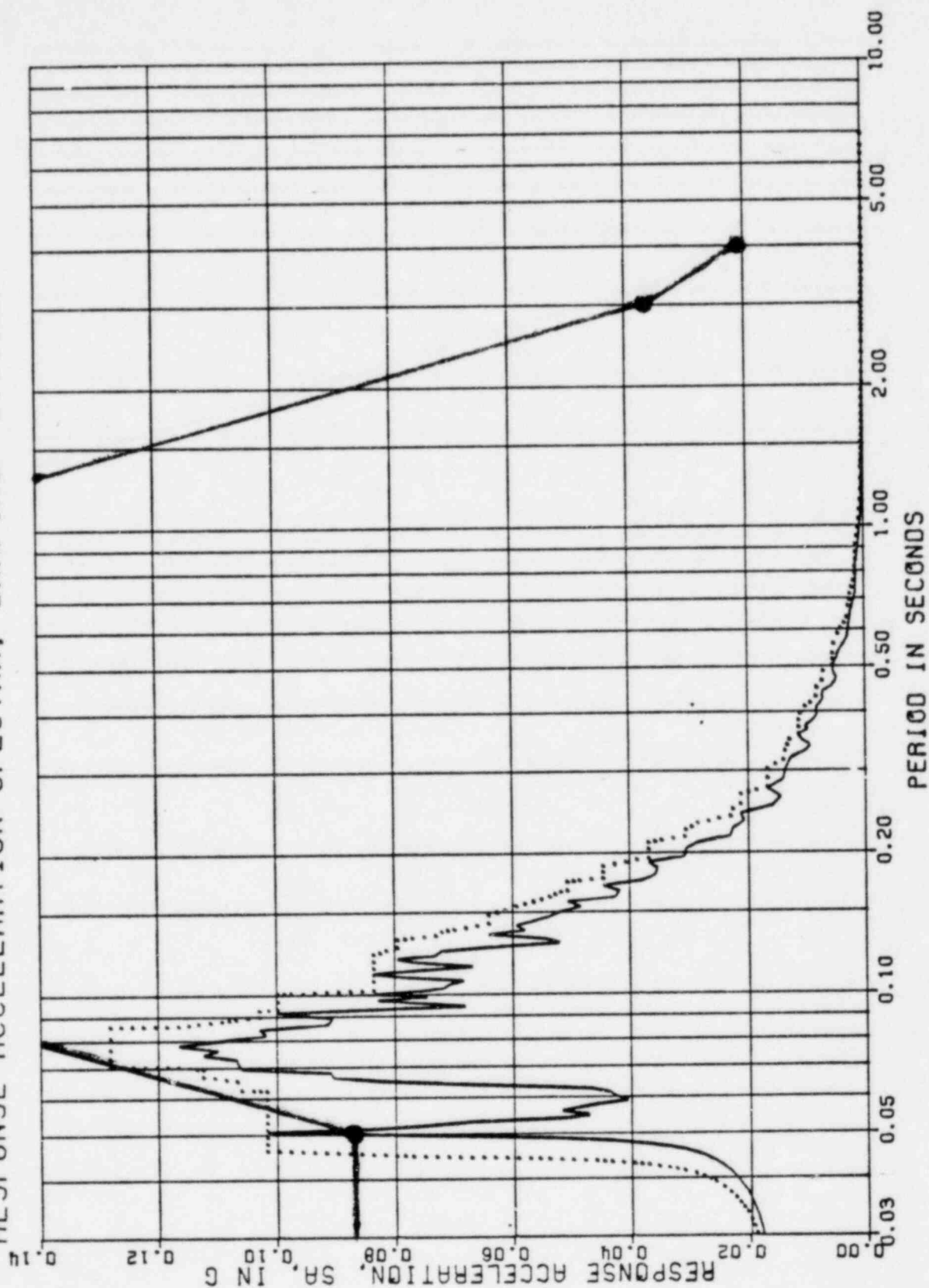


Figure 10-15

CATAWBA CONTAINMENT VESSEL - SEISMIC
 VERTICAL RESPONSE TO OBE (.08G) AT EL 688.05
 RESPONSE ACCELERATION SPECTRA, DAMPING= 0.0200

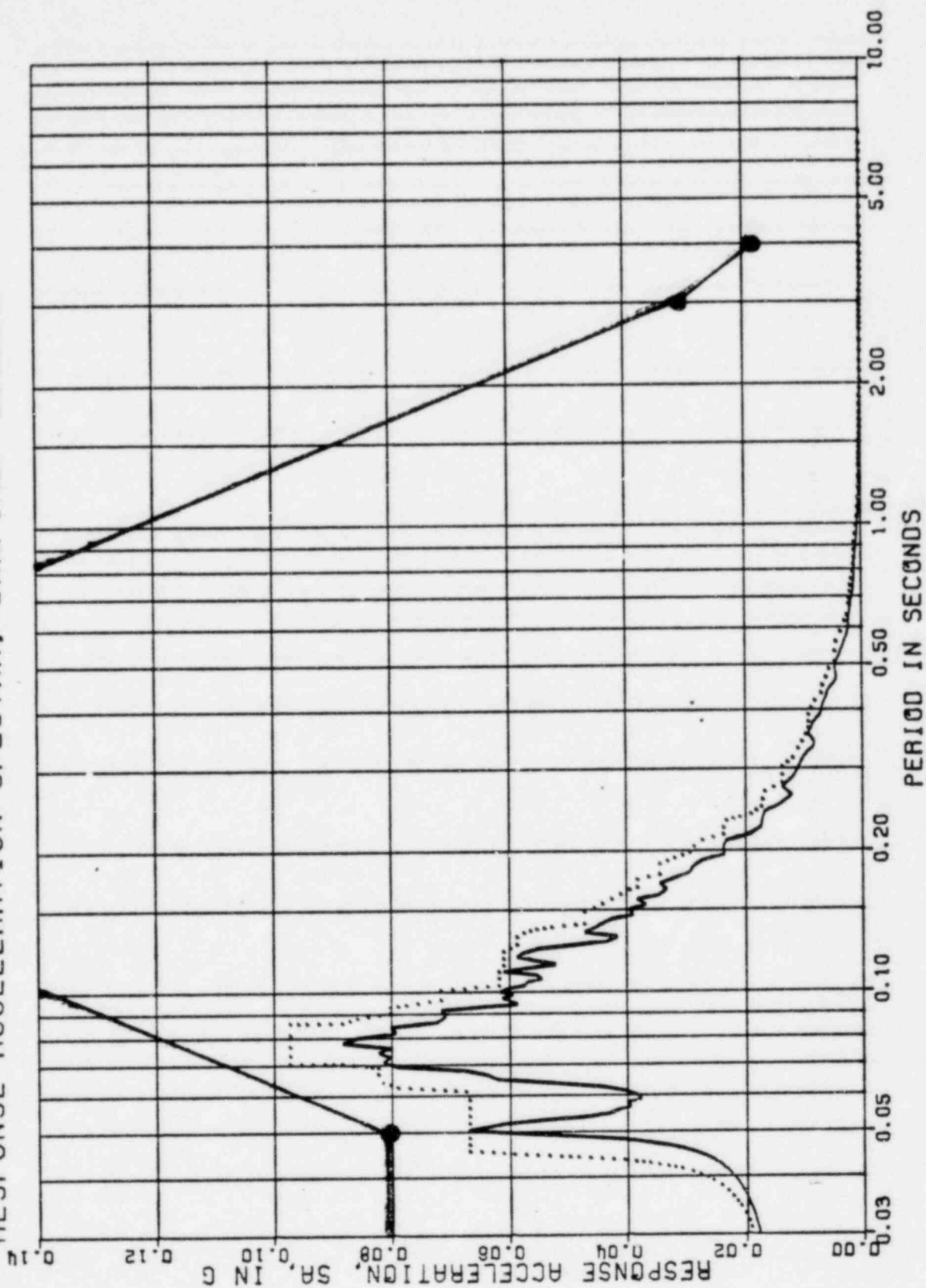


Figure 10-16

CATAWBA CONTAINMENT VESSEL - SEISMIC
VERTICAL RESPONSE TO OBE (.08G) AT EL 688.05
RESPONSE ACCELERATION SPECTRA, DAMPING= 0.0500

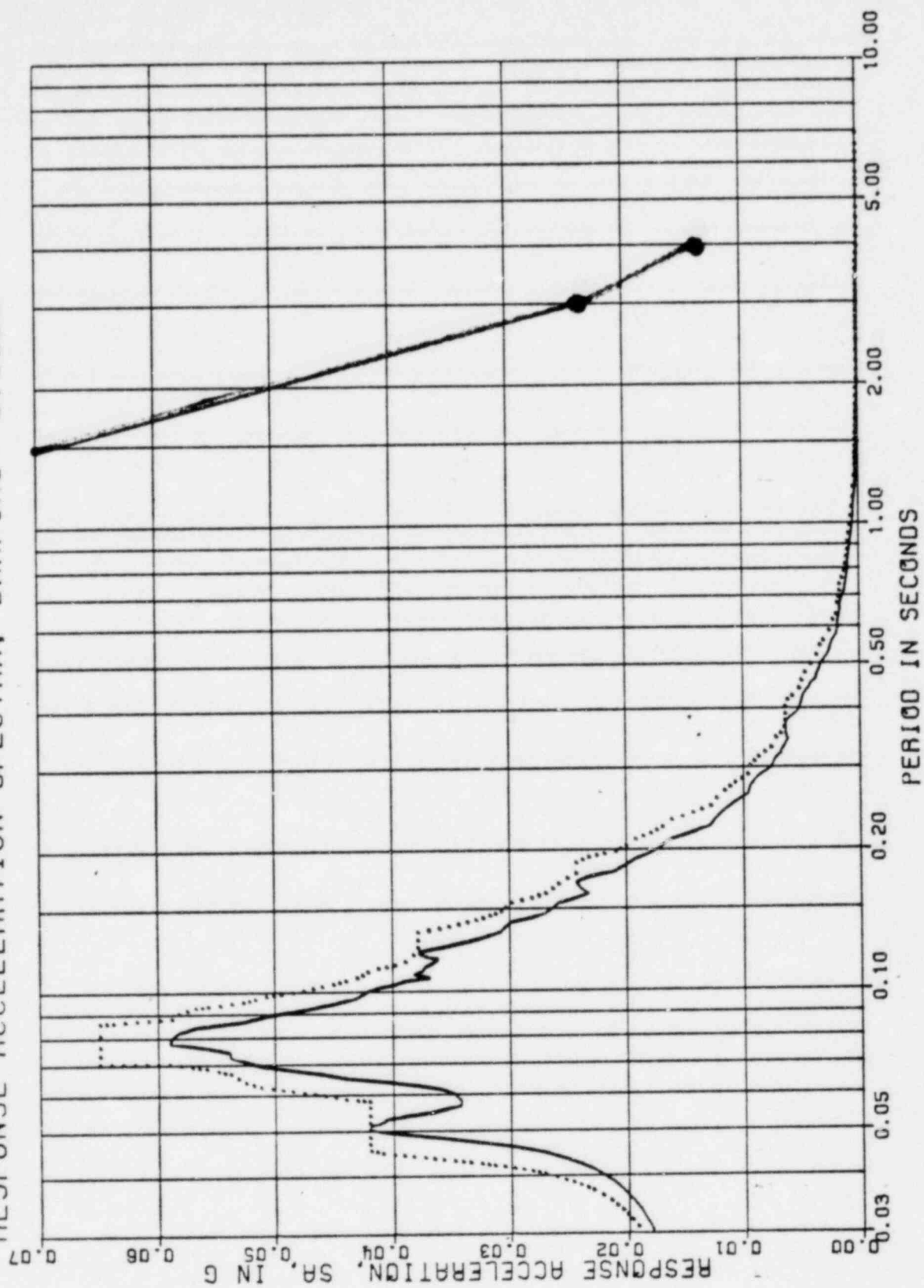


Figure 10-17

CATAWBA CONTAINMENT VESSEL - SEISMIC
 VERTICAL RESPONSE TO OBE (.08G) AT EL 710.85
 RESPONSE ACCELERATION SPECTRA, DAMPING= 0.0050

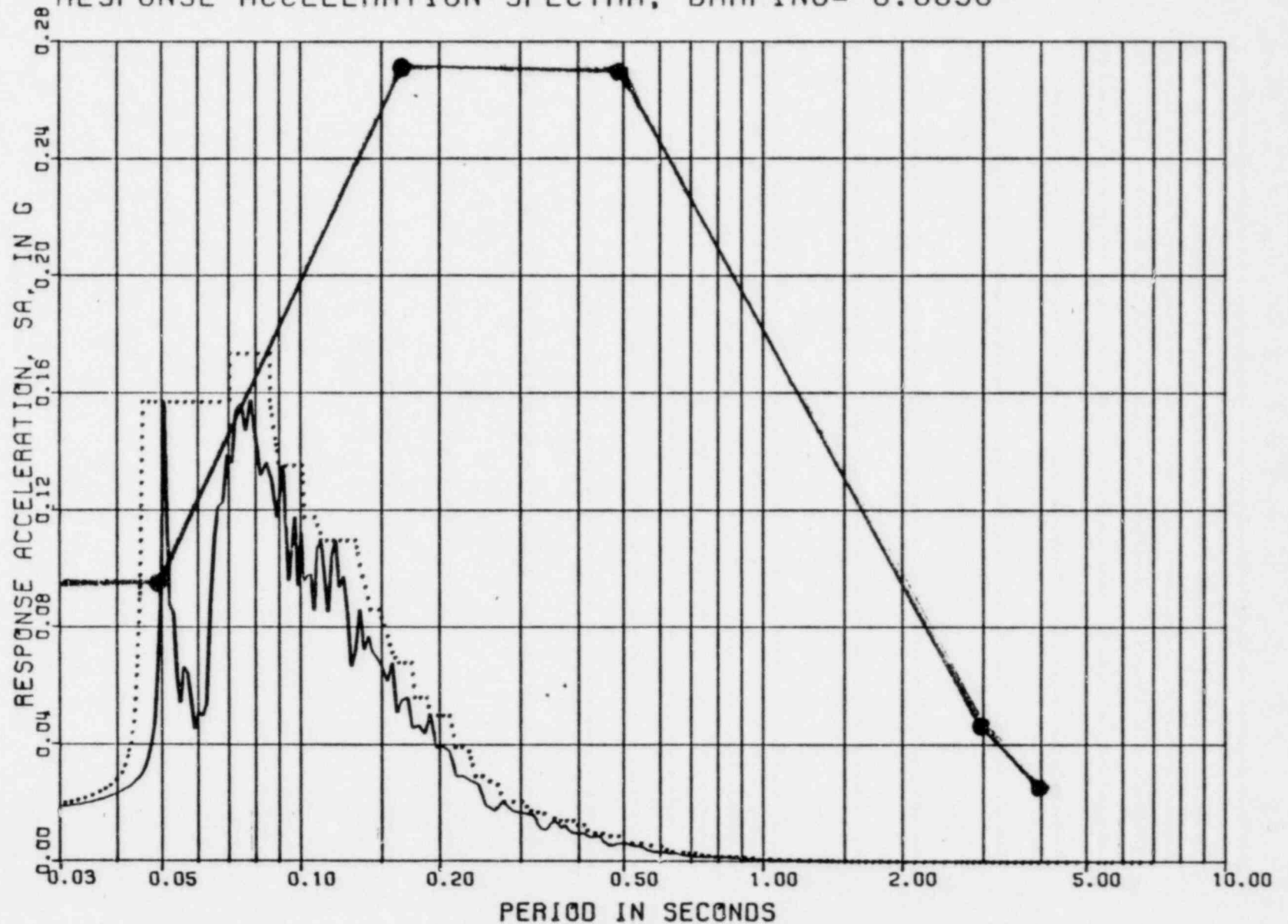


Figure 10-18

CATAWBA CONTAINMENT VESSEL - SEISMIC
 VERTICAL RESPONSE TO OBE (.08G) AT EL 710.85
 RESPONSE ACCELERATION SPECTRA, DAMPING= 0.0100

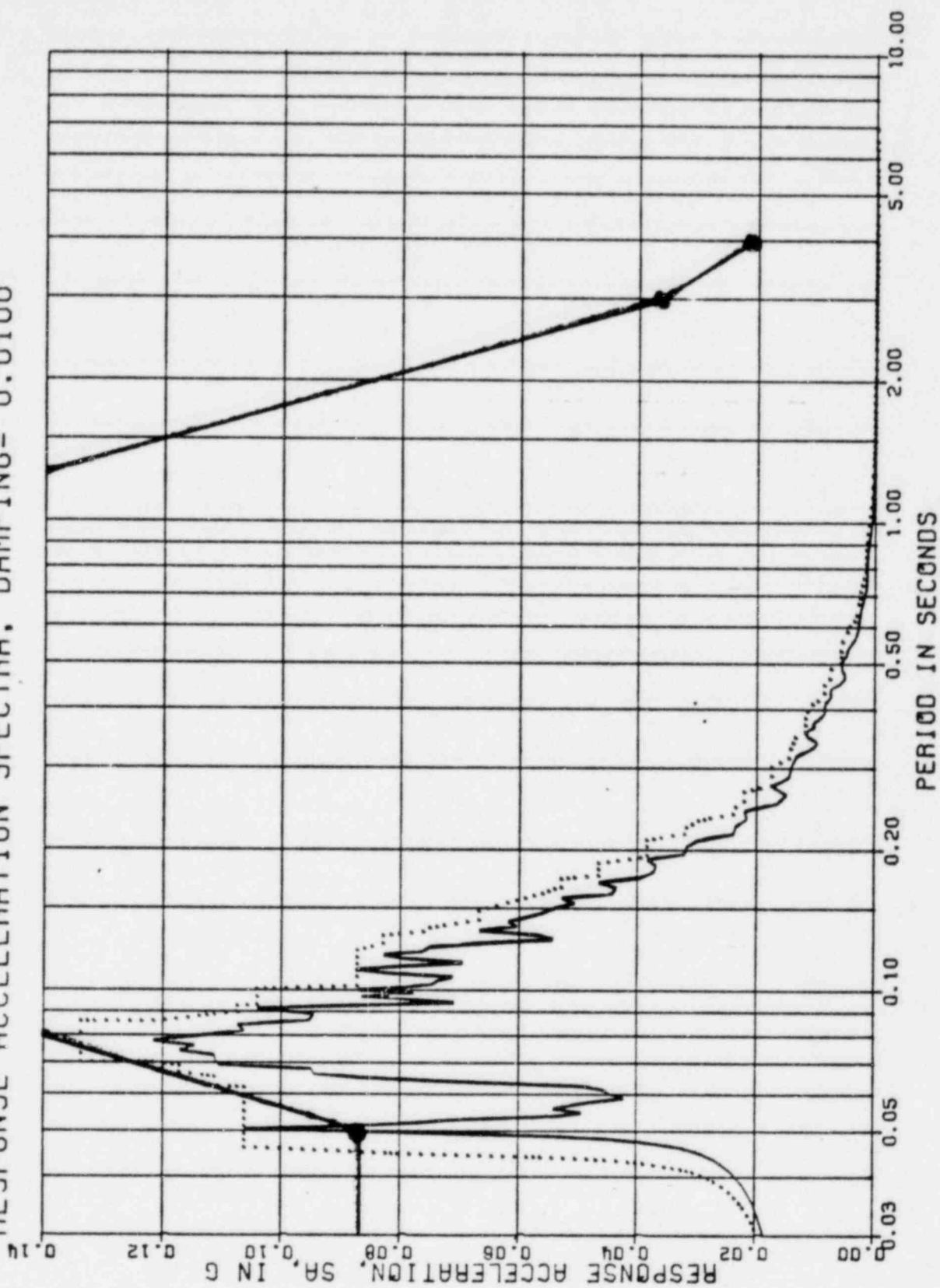


Figure 10-19

CATAWBA CONTAINMENT VESSEL - SEISMIC
 VERTICAL RESPONSE TO OBE (.08G) AT EL 710.85
 RESPONSE ACCELERATION SPECTRA, DAMPING= 0.0200

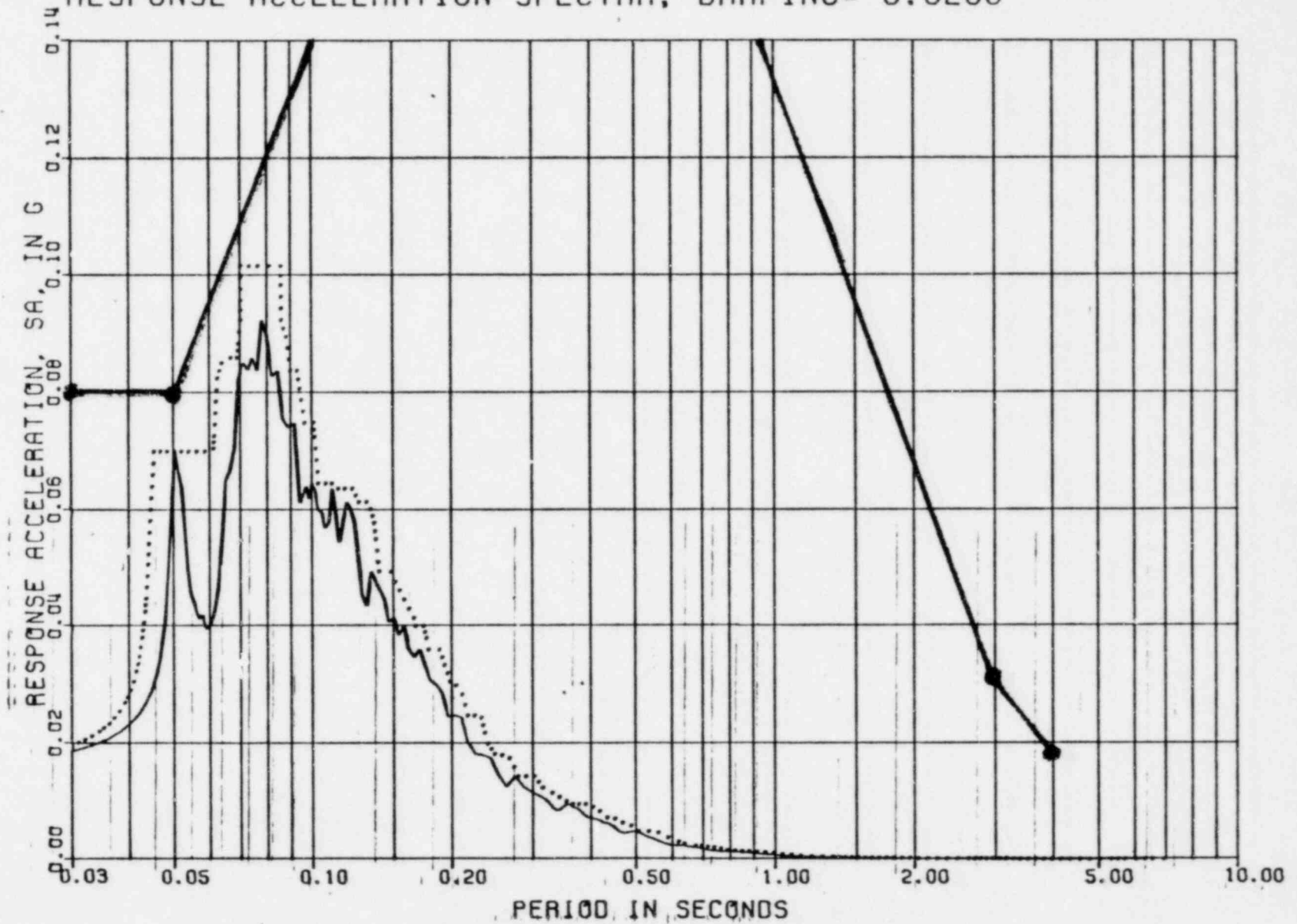


Figure 10-20

CATAWBA CONTAINMENT VESSEL - SEISMIC
VERTICAL RESPONSE TO OBE (.08G) AT EL 710.85
RESPONSE ACCELERATION SPECTRA, DAMPING= 0.0500

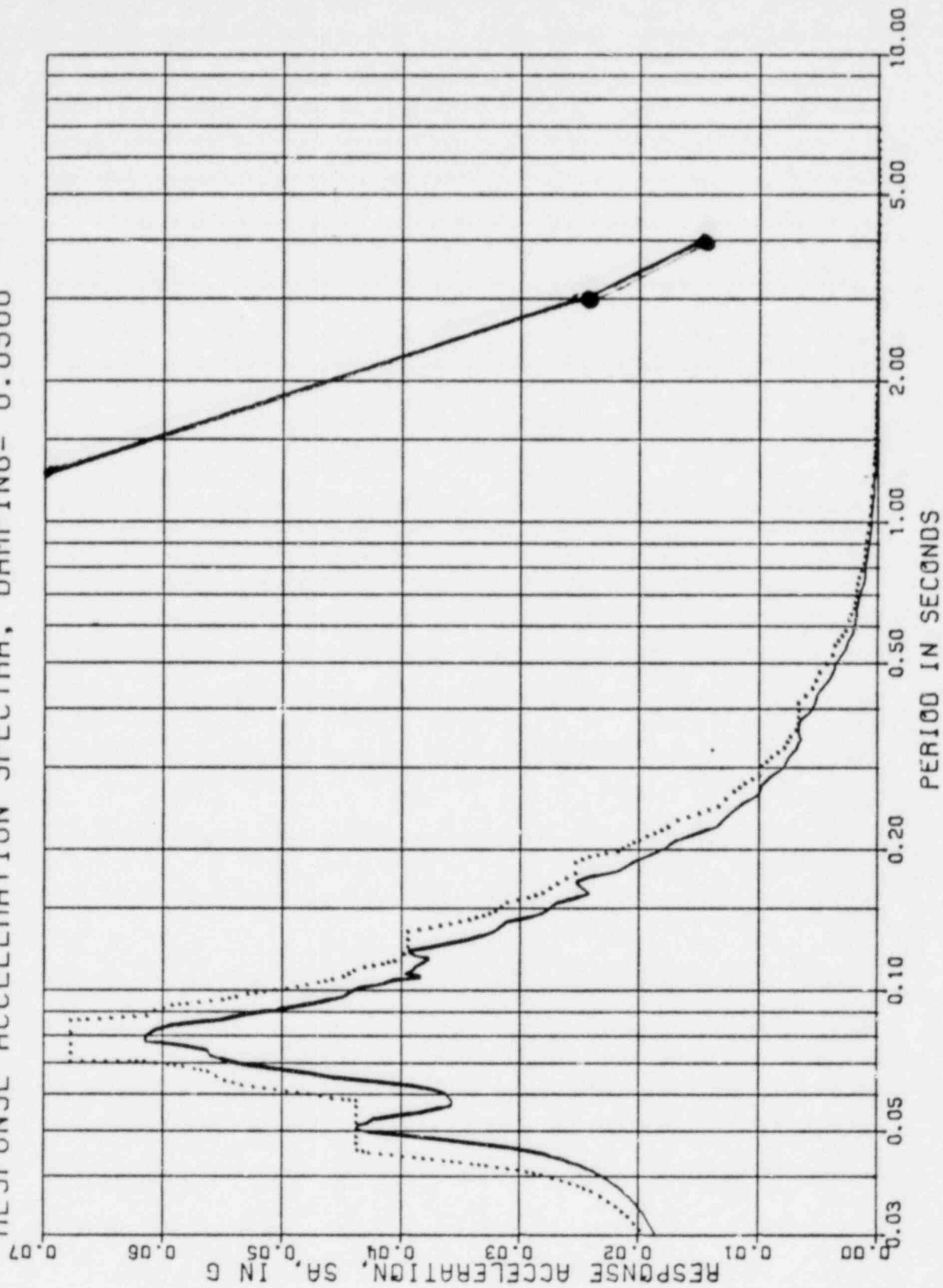


Figure 10-21

11. Compare ACI 349 in conjunction with Regulatory Guide 1.142, to ACI 318 (basis of Duke's design of Category I concrete structures) justify deviations identified in this comparison including considerations of inherent conservatism of the structures as appropriate.

Response:

The attached FSAR Table 3.8.1-5 provides a comparison of the Catawba design to that of ACI 349, in conjunction with Regulatory Guide 1.142.

Table 3.8.1-5 (Page 1)

Comparison of Concrete Design Criteria

Code Section	ACI 318	ACI 349	Regulatory Guide 1.142 <u>April 1978</u>	Justification
Chapter 1 General Req.		Requires copies of structural drawings, typical details and specifications be signed by licensed engineer (seal not required). Requires inspection by Owner.	Recommends inspectors be experienced and familiar with ACI and ASTM standards.	Duke complies with ACI 349 in conjunction with Regulatory Guide 1.142.
Chapter 2 Definitions	Massive concrete not specifically mentioned.	Requires areas to be treated as massive concrete to be identified on drawings or specification.		Current practice is in accordance with NRC position.
Chapter 3 Materials	No test reports req'd. Allows use of rail-steel and axel steel bars. Allows Grade 90 bars.	Excludes use of air-entraining Portland Cement. Requires test report on each cement shipment. No cement can be used prior to receipt of 7-day mill test strength. Excludes use of light weight aggregate concrete. Requires use of billet steel reinforcing bars of Grade 60 or less only.		Duke Concrete Specification is in accordance with ACI-349.

Table 3.8.1-5 (Page 2)

Comparison of Concrete Design Criteria

<u>Code Section</u>	<u>ACI 318</u>	<u>ACI 349</u>	<u>Regulatory Guide 1.142 April 1978</u>	<u>Justification</u>
Chapter 4 Concrete Quality	Gives mix design criteria for use in lieu of trial batch method of proportioning mix.	Gives method of determining water/cement ratio for fly ash mixes.		Duke Concrete Specification is in accordance with ACI 349.
	Requires use of Type V cement for sulfate exposure.	Requires use of trial batch method for mix design.		
	Requires 1 strength test/day/concrete class.	Defines sulfate exposure. Allows fly ash mix for sulfate exposure conditions.	Requires test frequency per ANSI N45.2.5-74.	Current practice is in accordance with NRC position.
Chapter 5 Mixing and Placing Concrete		Permits test internal increase by 50 Yd ³ /100 psi lower standard deviation if standard deviation for 30 tests in a class is less than 600 psi.		
		Requires construction specifications specifically state.		Duke Concrete Specification is in accordance with NRC position.
		1. Method of cleaning construction joints. 2. Method of curing. 3. Method of controlling temperature for hot weather concreting.		

Table 3.8.1-5 (Page 3)

Comparison of Concrete Design Criteria

<u>Code Section</u>	<u>ACI 318</u>	<u>ACI 349</u>	<u>Regulatory Guide 1.142 April 1978</u>	<u>Justification</u>
Chapter 5 (cont'd)	Allows placement of concrete without removal of water from place of deposit at the discretion of the owner.	Same as 318.	Requires removal of water before placement.	
	Allows partially hardened or contaminated concrete to be used at discretion of the Engineer.	Same as 318.	Prohibits use of such material.	
Chapter 6 Form work, Embedded pipes, and construction	Requires pressure test of embedded pipe to 50% above max pressure (150 psi min.) for 4 hours.	Requires pressure test of embedded pipe "in accordance with the applicable standard."	Pressure test shall satisfy requirements of both codes.	Duke complies with the NRC position.
	Limits pressure and temperature of embedded piping to 200 psi and 150°F.	Allows 200° for localized areas. Allows 350° for accident or short term periods. Allows 650° for local areas from fluid jet from pipe failure.		

Table 3.8.1-5 (Page 4)

Comparison of Concrete Design Criteria

<u>Code Section</u>	<u>ACI 318</u>	<u>ACI 349</u>	<u>Regulatory Guide 1.142 April 1978</u>	<u>Justification</u>
Chapter 6 (cont'd)		Allows higher temperatures if supported by test results.		
	Requires vertical construction joints to be wetted and coated with cement grout before placing next lift.	Requires all joints be shown on plans or approval by engineer. Defective or contaminated concrete to be removed. Vertical joints to be saturated with water. Grout not required.		Duke shows all joints on plans and complys to ACI 318.
Chapter 7 Details of Rein- forcement	Placement tolerances are stricter than ACI 301.	Tolerances on bar placement liberalized to ACI 301 standards. Requires test on full welded splices and full positive connections. Specifies minimum tension lap splice of 12 in. Requires welded splices or positive connections for splicing load-carrying rebar located in regions with member tension normal to splice.		Duke Concrete Specification is in accordance with the NRC position. Current practice is in accordance with ACI-318.

Table 3.8.1-5 (Page 5)

Comparison of Concrete Design Criteria

Code Section	ACI 318	ACI 349	Regulatory Guide 1.142 April 1978	Justification
Chapter 8 Analysis and Design- General Con- siderations	<p>Gives procedure for Alternate Design Method.</p> <p>Allows use of fillers in concrete joist construction.</p>	<p>Eliminates Alternate Design Method.</p> <p>Expands required loadings to include loads applicable to nuclear safety structures.</p> <p>Prohibits use of fillers in concrete joist construction.</p> <p>Requires consideration of dynamic response of concrete structure, foundation, and surrounding soil. Requires following load combinations:</p>	<p>Strength Design Method is not applicable for structures intended as pressure barriers. Designs will be reviewed by NRC on a case-by-case basis.</p>	<p>Current practice is in accordance with NRC position.</p>
Chapter 9 Strength & Service- ability Re- quirements	<ol style="list-style-type: none"> 1. $U = 1.4D + 1.7L$ 2. $U = .75 (1.4D + 1.7L + 1.7W)$ 3. $U = 0.9 + 1.3W$ 4. $U = .75 (1.4D + 1.7L + 1.1E)$ 5. $U = 1.4D + 1.7L + 1.7H$ 6. $U = 0.9 + 1.7H$ 7. $U = 1.4D + 1.7L + 1.4F$ 8. $U = .9D + 1.4F$ 	<ol style="list-style-type: none"> 1. $U = 1.4D + 1.7L + 1.7R_o$ 2. $U^o = 1.4D + 1.4F + 1.7L + 1.7H + 1.7E_o + 1.7R_o$ 3. $U = 1.4D + 1.4F + 1.7L + 1.7H + 1.7W + 1.7R_o$ 4. $U = D+F+L+H+T_o + R_o + E_{ss}$ 5. $U = D+F+L+H+T_o + R_o + W_T$ 6. $U = D+F+L+H+T_a + R_a + 1.25P_a$ 	<ol style="list-style-type: none"> 2. $U = 1.4D + 1.4F + 1.7L + 1.7H + 1.9E_o + 1.7R_o$ 6. $U = D+F+L+H+T_a + R_a + 1.5P_a$ 	<p>Current practice is in accordance with NRC position. Duke's loading combinations are provided in Table 3.8.1-2 of the FSAR</p>

Table 3.8.1-5 (Page 6)

Comparison of Concrete Design Criteria

Code Section	ACI 318	ACI 349	Regulatory Guide 1.142 April 1978	Justification
Chapter 9 (cont'd)				
		7. $U = D+F+L+H+T_a + R_a + 1.15P_a + 1.0 (Y_r + Y_j + Y_m) + 1.15 E_o$		
		8. $U = D+F+L+H+T_a + R_a + 1.0 P_a + 1.0 (Y_r + Y_j + Y_m) 1.0 E_{ss}$		
		9. $U = 0.75 (1.4D + 1.7L + 1.4T_o + 1.7R_o)$	9. $U = .75 (1.4D + 1.7L + 1.7T_o + 1.7R_o)$	
		10. $U = 0.75 (1.4D + 1.4F + 1.7L + 1.7H + 1.7E_o + 1.4T_o + 1.7R_o)$	10. $U = .75 (1.4D + 1.4F + 1.7L + 1.7H + 1.9E_o + 1.7T_o + 1.7R_o)$	
		11. $U = 0.75 (1.4D + 1.4F + 1.7L + 1.7H + 1.7W + 1.4T_o + 1.7R_o)$	11. $U = .75 (1.4D + 1.4F + 1.7L + 1.7H + 1.7W + 1.7T_o + 1.7R_o)$	
		Requires consideration of prestress, crane loads, vibration, impact, shrinkage, creep and differential settlement. For normal loads (Comb. 1 to 3).	Effects of differential settlement should be included in all load combinations.	

Table 3.8.1-5 (Page 7)

Comparison of Concrete Design Criteria

<u>Code Section</u>	<u>ACI 318</u>	<u>ACI 349</u>	<u>Regulatory Guide 1.142 April 1978</u>	<u>Justification</u>
Chapter 9 (cont'd)		<p>When D or L reduces effects of other loads, coefficients shall be .9D and 0L.</p> <p>For combination 7 and 8, local strength can be exceeded for Y_r, Y_j, and Y_m, if no loss of safety-related system results.</p> <p>Allows time-history analysis for pipe-rupture loads (combinations 6, 7, and 8).</p>	<p>For all loading conditions, when any load reduces the effects of other loads, the coefficient for the load is always present and acts simultaneously; otherwise, coefficient = 0.</p> <p>Section strengths must be adequate for forces in comb. 7 and 8 without Y_r, Y_j, and Y_m.</p> <p>Local exceedance of section strength for tornado missiles for comb 5 acceptable provided strength is adequate for forces of combination 5 without tornado missiles.</p>	
Chapter 10 Flexure & Axial Loads		Specifies minimum temperature and shrinkage reinforcing for massive concrete.		Current practice in accordance with NRC position.

Table 3.8.1-5 (Page 8)

Comparison of Concrete Design Criteria

<u>Code Section</u>	<u>ACI 318</u>	<u>ACI 349</u>	<u>Regulatory Guide 1.142 April 1978</u>	<u>Justification</u>
Chapter 11 Shear & Torsion	Specifically addresses openings in slabs.	Gives permissible shear stresses for slabs sub- ject to loads with forces in the plane of the slab (i.e., missile loads) Slab opening section de- leted. Sets allowable shear stress values for punching shear in walls.	Provisions of ACI 318 are acceptable.	Current practice is in accordance with NRC position.
Chapters 12 thru 17		No significant changes.		
Chapter 18 Prestressed Concrete	Maximum water/cement ratio for grout for bonded tendons = 0.5. Requires member tem- perature at time of grouting bonded ten- dons to be above 50°F. Temperature must be maintained above 50° for 48 hours.	Limits w/c ratio to .45. Requires member tempera- ture above 35°F maintained until job cured grout cubes reach 700 psi. Grout tem- perature limited to 90°F during mixing and pumping.		Current practice is in accordance with NRC position since there is no prestressed con- crete at Catawba.
Chapter 19 Shells	Applies only to thin shell concrete struc- tures.	Applies only to the design of shell concrete struc- tures having thicknesses		

Table 3.8.1-5 (Page 9)

Comparison of Concrete Design Criteria

<u>Code Section</u>	<u>ACI 318</u>	<u>ACI 349</u>	<u>Regulatory Guide 1.142 April 1978</u>	<u>Justification</u>
		equal to or greater than 12 in.		
Appendix A Special Provisions for Seismic Design		Not included in ACI-349.	ACI-349 lacks specific requirements to assure ductility of framed structures. Adherence to ACI-318 Appendix A is acceptable.	Current practice is in accordance with NRC position.

12. Provide a description including examples of foundation mat design. Provide a detail of reinforcing design at key locations in this mat. Provide an assessment of the extent the containment mat design and liner design conform to CC-3000 of ASME, Section III, Division 2 Code. For deviations identified, provide justification including discussion of inherent conservatism incorporated in the original design.

Response:

The reactor building foundation mat was designed using the basic strength design method of ACI 318-71. Load combinations and load factors used in the design are as listed in FSAR Table 3.8.1-2 for Category I structures. ASME, Section III, Division II recommends using a working stress design method for service load conditions. Because of this difference in design methods, ASME load factors do not compare to those used for the strength design method in the foundation mat. However, the use of the strength design method and the load combinations and load factors of FSAR Table 3.8.1-2 are acceptable by SRP 3.8.4. For factored loads, ASME and ACI 318-71 both use strength design. For factored loads, ASME contains two additional load combinations which are not listed in FSAR Table 3.8.1-2, but once again the FSAR load combinations and load factors are identical to those of SRP 3.8.4. Aside from the differences listed above, the remainder of ASME, Division II, Subsection CC dealing with design details is essentially the same as ACI 318-71 and was therefore indirectly included in the Catawba foundation mat design.

As for the actual selection of reinforcement, ACI publication SP-17, "Design Handbook" was used. The following is an example of the method used for selecting flexural reinforcement:

From computer analysis, maximum positive moment (tension on top) at the reactor coolant pump embedments is equal to 1432 K.ft/ft in the radial direction.

Using $f'_c = 5 \text{ ksi}$
 $f'_y = 60 \text{ ksi}$

$b = 12"$, $d = 60"$

From "Design Handbook" Table-Flexure 1.3

$$\frac{M_u}{K_u} = \frac{bd^2}{12000} = \frac{12(60)^2}{12000} = 3.6$$

$$K_u = M_u/3.6 = \frac{1432}{3.6} = 398$$

for $K_u = 423$, $p = .0083$ from the table.

therefore:

$$A_s \text{ required} = pbd = .0083 (12) (60) = 5.98 \text{ in}^2/\text{ft}$$

Answer

See attached FSAR Figure 3.8.1-14 for reinforcement details.

DOCUMENT/ PAGE PULLED

ANO. 8204160397

NO. OF PAGES 1

REASON

☐ PAGE ILLEGIBLE

☐ HARD COPY FILED AT. PDR CF

OTHER _____

☐ BETTER COPY REQUESTED ON _____

☒ PAGE TOO LARGE TO FILM

☒ HARD COPY FILED AT. PDR

CF

OTHER _____

☒ FILMED ON APERTURE CARD NO 8204160397-01

13. Provide maximum displacements of adjacent Category I structures and insure that 3 inch gap provided between structures exceeds the cumulative relative displacements of the structure.

Response:

The maximum displacement of adjacent Category I structures, as a result of an SSE occurs at the Spent Fuel Building/Reactor Building and Main Steam Doghouse/Reactor Building interfaces. The interface elevations are 631'+6" and 648'+0", respectively. The maximum displacements are:

	<u>Displacement (ft)</u>	
	EW Quake	NS Quake
Spent Fuel Bldg (631'+6")	2.279×10^{-3}	5.571×10^{-3}
* Reactor Bldg (631'+6")	5.208×10^{-3}	7.457×10^{-3}
Doghouse (648'+0")	11.679×10^{-3}	8.654×10^{-3}
* Reactor Bldg (648'+0")	6.295×10^{-3}	8.861×10^{-3}

Therefore, the maximum cumulative displacement is 17.97×10^{-3} ft (0.216 in), occurring at the Doghouse/Reactor Building interface due to an E-W quake. It should be noted that the maximum displacements occur without respect to a given mode, thus it is highly improbable that the maximum would occur simultaneously. Therefore, the 3 inch gap provided between Category I structures is adequate to insure independent action.

- * Reactor Building displacements are shown in FSAR Figure 3.7.2-17 (N-S) and 3.7.2-18 (E-W).

14. Describe the earthquake analysis methods used in combining the three components, input motions of earthquake and the stability analysis of the reactor building foundation mat.

Response:

In the stability analysis of the reactor building foundation mat, moments, shears, and torsions were calculated for two separate perpendicular (N-S and E-W) earthquakes. Accelerations for these earthquakes were taken from PSAR Figure 2E-4, Amendment 17. Vertical acceleration for each case was taken as 2/3 of the horizontal. The maximum moments, shears, and torsions from either of the two earthquakes were used to determine factors of safety against sliding, overturning, and uplift. These two earthquakes were not considered to act simultaneously.

15. Provide information to confirm that the embedment length of dowels extending from the base mat into the shell is adequate per code requirements.

Reinforcement extending from the shell wall into the base mat consists of 2-#11 bars bundled on the outside face with a minimum embedment length into the mat of 5'-4". The inside face reinforcement consists of single #11 bars with a minimum embedment length of 4'-5". Per ACI 318-71 Section 12.2.2, the basic development length for #11 and smaller bars with less than two bars per bundle equals:

$$\frac{0.04 A_b f_y}{\sqrt{f'_c}} \text{ but not less than } 0.0004 d b f_y$$

For Catawba foundation mat #11 bars:

$$A_b = 1.56 \quad f_y = 60,000 \text{ psi} \quad f'_c = 5000 \text{ psi}$$

Using this information the basic required development length is 52.9 inches which is slightly less than 4'-5".

See FSAR Figure 3.8.1-14 which is attached to item 12 above.

16. Provide a discussion and key calculation sheets of the tangential shear analysis and design of the shield building shell wall.

Response:

The reactor building shell wall was analyzed for loading combinations of FSAR Table 3.8.1-2 using Kalnin's K SHELL program. A description of this program is given in FSAR Section 3.7.2.1.1.1. One of the results of this program is a calculation of in-plane shear stresses. The attached copy of calculation sheets show the stress resultants which were considered in the reactor building design. The design was based upon the results of this program and the provisions of ACI 318-71 using the strength design method. Section 11.16, "special provisions for walls," was included in the design wherever applicable. To assist in the preliminary selection of reinforcement, a FORTRAN program which accepts stress resultants from K SHELL and which utilizes ACI 318-71, was used. The final reinforcement design was repeated with hand calculations to insure the accuracy of the program.

Dev./Station CATAWBA

Unit 1+2

File No. CNC1144.02-3

Subject REACTOR BUILDING DESIGN FOR GENERAL LOADS

By DWJ

Date 4-1-76

Sheet No. 8 of Problem No.

Checked By AH2

Date 5-3-76

CNC1144.02-03-0001

DESCRIPTION OF SHELL DESIGN PROGRAM

THIS PROGRAM DESIGNS REINFORCING FOR A ONE FT. WIDE STRIP OF A SHELL, BASED ON THE ACI CODE 318-71 USING ULTIMATE STRENGTH DESIGN. IT ACCEPTS PUNCHED STRESS RESULTANT OUTPUT FROM EITHER KALNIN'S PROGRAM OR THE Q-THETA PROGRAM. ADDITIONAL INPUT REQUIRED INCLUDES MATERIAL PROPERTIES, CROSS SECTION DIMENSIONS, LOAD COMBINATIONS, AND LOAD FACTORS. ALL INPUT IS IN UNITS OF POUNDS AND INCHES. OUTPUT UNITS ARE THE FOLLOWING:

MERIDIONAL AND CIRCULAR STEEL AREAS

IN^2/FT

Q SHEAR REINFORCEMENT

IN^2/FT^2

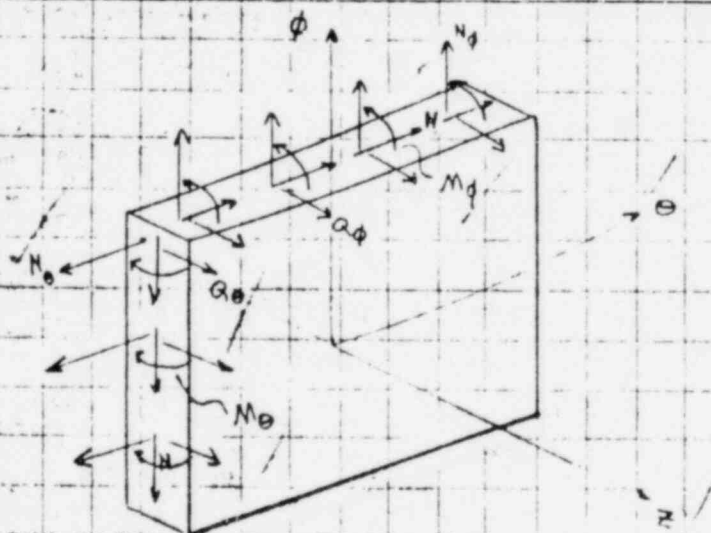
HORIZONTAL N SHEAR REINFORCEMENT

IN^2/FT

VERTICAL N SHEAR REINFORCEMENT

IN^2/FT

ORIENTATION OF STRESS RESULTANTS TO STRIP OF SHELL



Dev./Station CATAWBA

Unit 1+2

File No. CNC 1144.02-3

Subject REACTOR BUILDING DESIGN FOR GENERAL LOADS

By DWJ

Date 4-1-76

Sheet No. 16 of

Problem No.

Checked By

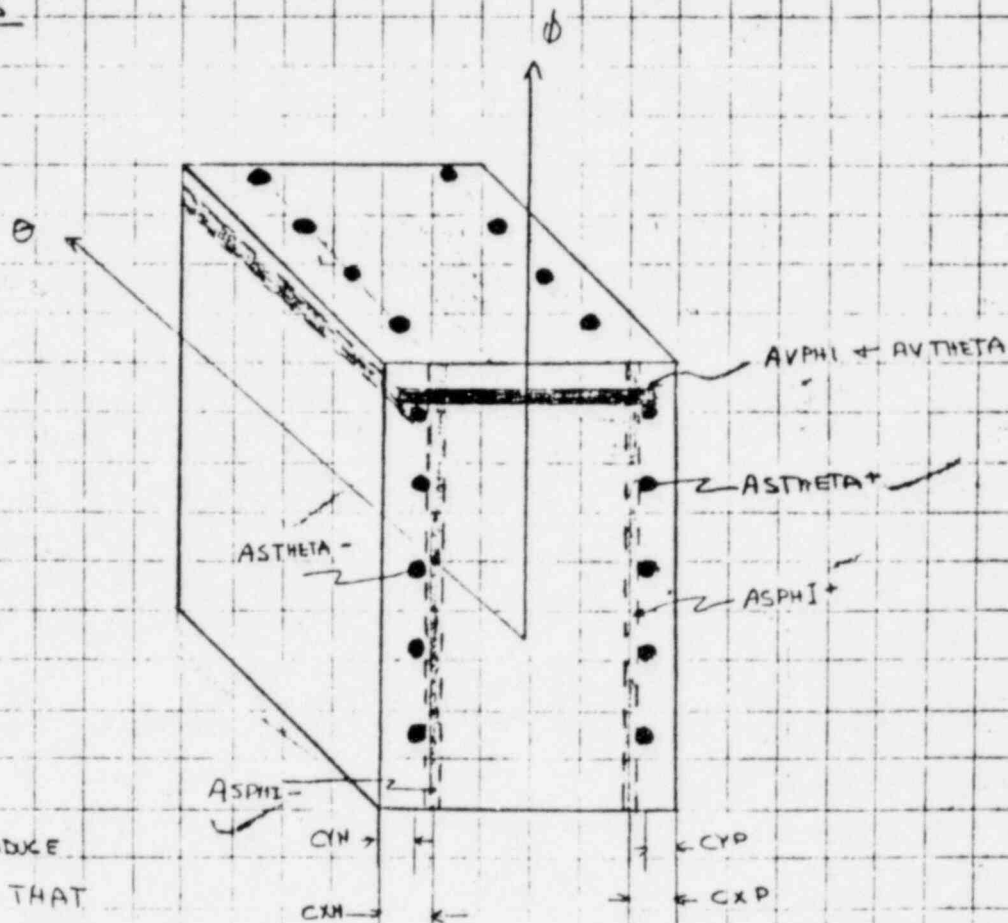
AH2

Date 5/10/76

CNC1144.02-03-0001

DEFINITION OF TERMS

Axis
of
Symmetry



STRESS RESULTANTS THAT PRODUCE
AXIAL TENSION OR BENDING THAT
CAUSES TENSION ON THE OUTSIDE
FACE ARE CONSIDERED POSITIVE.

AVN REINFORCING DESIGNED BY PROGRAM WILL BE ADDED TO
ASPHI- AND ASPHI+ ($\frac{1}{2}$ ON EACH FACE). AVN REINFORCING
DESIGNED BY PROGRAM WILL BE ADDED TO ASTHETA- AND
ASTHETA+ ($\frac{1}{2}$ ON EACH FACE).

Dev./Station CATAWBA

Unit 1+2

File No. 1144.02-3

Subject REACTOR BUILDING DESIGN FOR GENERAL LOADS

By DWJ

Date 4-2-76

Sheet No. 15 of Problem No.

Checked By AHZ

Date 5-10-76

$$\sigma_u = \frac{N}{\phi h t} \quad (11-31) \quad \text{CNC 1144.02-03-0001}$$

$$A_v = \frac{(v_u - v_c) b_w s}{f_y} \quad (11-13) \quad \text{WHERE SPACING (S) IS 12 IN.}$$

THE ABOVE PROCEDURE DESIGNS SHEAR REINFORCING FOR N SHEARS. FOR VERTICAL AXIAL LOADS (N_v), SHEAR REINFORCING WILL BE HORIZONTAL (A_{HN}). FOR HORIZONTAL AXIAL LOADS (N_h), SHEAR REINFORCING WILL BE VERTICAL (A_{VN}). FOR LAYOUT OF THE REINFORCING, A_{VN} WILL BE ADDED TO A_{SPH+} AND A_{SPH-} ($\frac{1}{2}$ ON EACH FACE) AND A_{HN} WILL BE ADDED TO $A_{STHETA+}$ AND $A_{STHETA-}$ ($\frac{1}{2}$ ON EACH FACE). SEE PG 16

Dev./Station CATAWBA

Unit 1+2

File No. CNC 1144.02-3

Subject REACTOR BUILDING DESIGN FOR GENERAL LOADS

By DWV

Date 4-2-76

Sheet No. 14 of Problem No.

Checked By AHZ

Date 5-10-76

CNC 1144.02-03-000

IF $M_p > 0$

$$\sigma_c = \phi (3.5) \sqrt{f_c'} \sqrt{1 + .002 \frac{P_u}{A_g}}$$

OR (CHOOSE SMALLER)

$$\sigma_c = \phi \left[1.9 \sqrt{f_c'} + 2500 \frac{A_s}{b_w d} \left(\frac{V_u}{M_p} \right) \right] \quad (11-4)$$

$$\sigma_u = \frac{V_u}{b_w d} \quad (11-3)$$

$$A_y = \frac{(\sigma_u - \sigma_c) b_w s}{\phi f_y} \quad (11-13)$$

SPACING (S) ASSUMED AT 12 IN

THE ABOVE EQUATIONS DESIGN SHEAR REINFORCEMENT
AS FOLLOWS.FOR ϕ SHEARS \Rightarrow AVPHI IS DESIGNED.FOR θ SHEARS \Rightarrow AVTHETA IS DESIGNED.
(SEE PG. 16)

SHEAR DESIGN FOR IN-PLANE SHEAR (N) IS BASED ON ACI 318-71,
SECTION 11.16 - SPECIAL PROVISIONS FOR WALLS. REINFORCEMENT IS DETERMINED FOR
BOTH THE HORIZONTAL AND VERTICAL DIRECTIONS. THE DIFFERENCE IN THE TWO
IS DUE TO DIFFERENT σ_c DUE TO DIFFERENT AXIAL LOADS. REFERRING TO
ACI 318-71, SECTION 11.16.2: L

FOR AXIAL COMPRESSION

$$\sigma_c = 2 \sqrt{f_c'}$$

FOR AXIAL TENSION

$$\sigma_c = 2 \left(1 + .002 \frac{P_u}{A_g} \right) \sqrt{f_c'}$$

WHERE P_u IS NEG. FOR
TENSION

Dev./Station CATA 13A

Unit 1+2

File No. CNC 1144.02-3

Subject REACTOR BUILDING DESIGN FOR GENERAL LOADS

By DJSJ Date 4-2-76

Sheet No. 13 of Problem No. Checked By AHZ Date 5-10-76

CNC1144.02-03-0001

SHEAR

PERPENDICULAR SHEARS (Q_ϕ AND Q_θ) ARE COVERED BY SECTIONS 11.4.2 - 11.4.4, WITH MODIFICATIONS FOR REVISIONS IN THE AIS SUPPLEMENT. Q_ϕ CORRESPONDING TO M_ϕ IS GIVEN BY KALNIN'S PROGRAM. Q_θ CORRESPONDS TO M_θ AND IS PRESENT ONLY WHEN M_θ VARIES IN THE θ DIRECTION. Q_θ IS NOT GIVEN BY KALNIN'S PROGRAM, BUT CAN BE DETERMINED USING A COMPUTER PROGRAM ESPECIALLY WRITTEN FOR CALCULATING Q_θ (Q-THETA PROGRAM). THE OUTPUT FROM THE Q-THETA PROGRAM CAN BE READILY ACCEPTED BY THIS CONCRETE SHELL DESIGN PROGRAM.

FROM ACI 318-71, SECTION 11.4.2 \rightarrow 11.4.4 ... AND SECTION 11.6.1

1) MEMBERS SUBJECT TO AXIAL TENSION

$$v_c = 2 \left(1 + .002 \frac{P_u}{A_g} \right) \sqrt{f_c'} (\phi) \quad \text{ACI (11-8)} \quad \text{WHERE } P_u \text{ IS NEG. FOR TENSION AND } \frac{P_u}{A_g} \text{ IS EXPRESSED IN PSI}$$

$$v_u = \gamma \frac{V_u}{b_w d} \quad (11-3) \quad \text{(CONSERVATIVE)}$$

$$A_y = \frac{(v_u - v_c) b_w s}{\phi f_y} \quad (11-13) \quad \text{WHERE SPACING (S) IS ASSUMED AT 12"} \quad \phi f_y$$

2) MEMBERS SUBJECT TO AXIAL COMPRESSION

$$M_p = \left[M_u - P_u \left(\frac{4h-d}{8} \right) \right] \left(\frac{1}{d} \right) \quad (11-5) \quad \text{WHERE } P_u \text{ IS POS. FOR COMPRESSION}$$

IF $M_p < 0$

$$v_c = \phi (3.5) \sqrt{f_c'} \sqrt{1 + .002 \frac{P_u}{A_g}} \quad (11-7) \quad \text{WHERE } P_u \text{ IS POS. FOR COMPRESSION}$$

Subject REACTOR BUILDING DESIGN FOR GENERAL LOADS

By DWJ

Date 4-5-76

Sheet No. 24 of Problem No.

Checked By AHZ

Date 5-11-76

CNC 1144.02-03-0001

DESIGN OF AVN OR AHN

(REFER TO PGS 14-15)

$$1.4D + 1.7L \pm 1.01E' =$$

$$1.4D + 1.7L \pm 1.9\left(\frac{9}{15}\right)SSE$$

1) MEMBER SUBJECT TO AXIAL TENSION

USING RESULTS FROM LOADING COMBINATION $(1.4D + 1.7L - 1.01E')$ AT SOIL B = 15°
AND $X = 0.0$ IN. (RUN #1)

$$N_B = 999.8 \frac{lb}{in}$$

$$P_U = \frac{459.3(12)}{1000} = 5.52^k$$

$$\sigma_c = 2 \left(1 \pm 2 \left(\frac{5.52}{36(12)} \right) \right) \sqrt{5000} = 137.81 \text{ psi}$$

$$A_v = \frac{(221.97 - 137.81)(12)(36)}{60,000} = .61 \text{ in}^2$$

AVN FROM PROGRAM = .61 in²

$$N_d = 2417.4 \frac{lb}{in}$$

$$P_U = 29^k$$

$$\sigma_U = 221.97 \text{ psi}$$

$$\sigma_c = 2 \left(1 \pm 2 \left(\frac{29}{12(36)} \right) \right) \sqrt{5000} = 122.43$$

$$A_v = \frac{(221.97 - 122.43)(12)(36)}{60,000} = .717 \text{ in}^2$$

AHN FROM PROGRAM = .72 in²

2) MEMBER SUBJECT TO AXIAL COMPRESSION

USING RESULTS FROM LOADING COMBINATION $1.4D + 1.7L + 1.01E'$ AT SOIL B = 30° AND

$$N_d = -17573.6 \frac{lb}{in}$$

$$P_U = -210.9^k$$

$$N = 8756.7 \frac{lb}{in}$$

(RUN #1)

$$\sigma_U = 286.2 \text{ psi}$$

SINCE $P_U < 0$, $\sigma_c = 2\sqrt{f_c} = 2(10.71) = 141.42 \text{ psi}$

$$A_v = \frac{(286.2 - 141.42)(12)(36)}{60,000} = 1.042 \text{ in}^2$$

AHN FROM PROGRAM = 1.04 in²

CONCLUSION IS THAT PROGRAM DESIGNS REINFORCING IN
ACCORDANCE WITH CONCRETE DESIGN THEORY AND ACI 318-71.

000051852

17. Provide a summary of controlling load combinations in the design forces at key locations of the shield building shell wall.

Response:

The following are the controlling load combinations at various locations in the Catawba reactor building:

Location	Controlling Load Combination
Below grade (Elev. 594)	$1.4D + 1.7L + 1.9E$
Above grade	Tornado missile criteria per PSAR Section 3.5 pmin = .014
Ringbeam (horizontal reinforce.)	Construction loads $1.4D + 1.7L$
Ring beam (vertical reinforce.)	$D+L+We$
Dome (Hoop reinforce.)	$1.4D + 1.7L + 1.9E$
Dome (radial reinforce.)	$D+L+We$

Faulted loads were checked for live load having its full value and being completely absent.

In addition to the load combinations shown above (for the dome), a middle layer of steel was added to satisfy construction load requirements.

18. Provide a description of increase in wind forces to confirm that Duke adheres to Table 5 of ANSI A58.1 and insure that they do not control the design of Category I structures.

Response:

See attached response to Questions 220.13 and 220.14.

3.3 WIND AND TORNADO LOADINGS

All Category I structures, except those structures not exposed to wind, are designed to withstand the effects of wind and tornado loadings, without loss of capability of the systems to perform their safety functions. The following sections provide the basis for the wind and tornado parameters and methods used in meeting the wind and tornado criteria.

3.3.1 WIND LOADINGS

3.3.1.1 Design Wind Velocity

The design wind velocity for all Category I structures is 95 mph, at 30 feet above the nominal ground elevation. According to ASCE Paper No. 3269, "Wind Forces on Structures" (Reference 1), this velocity is the fastest mile of wind with a recurrence interval of 100 years. This reference summarizes existing technical literature on wind velocities' distribution extending back to the early 1800's, and is the basis for the selected wind velocity.

Reference 2 recommends that buildings and structures with a height to minimum horizontal dimension ratio exceeding five should be dynamically analyzed to determine the effect of gust factors. All Category I structures have a height/width ratio of less than five. A gust factor of 1.10 is used for determining wind loads on all Category I structures except the Reactor Building. The wind load on the Reactor Building is determined as a function of the maximum height of the structure using the most severe coastal area criteria of Reference 1. Therefore, the effective velocity pressures used for design of Category I structures meet or exceed the values given in Table 5, Exposure C, of Reference 2. It is also concluded that wind forces on Category I structures are not a controlling load condition in the design.

The vertical distribution of velocity is discussed in Section 3.3.1.2.

3.3.1.2 Determination of Applied Forces

Reference 1 assembles existing information on the factors that determine applied wind loads on structures. Rectangular structures are designed for a wind distribution as defined in Reference 1. The wind pressure distribution, for the Auxiliary Building, Spent Fuel Pool Buildings, New Fuel Storage Buildings, and Doghouse Structures are shown in Figure 3.3.1-2. The wind pressure distributions for the Reactor Buildings above grade, for both the vertical and horizontal profiles are shown in Figure 3.3.1-1.

The wind design pressure magnitude "p" is calculated as follows:

$$p = G_f \times C_{pe} \times f \times v^2$$

where: G_f = Gust factor as defined in Section 3.3.1.1 (not applicable to Reactor Building)

CNS

C_{pe} = The coefficient of the actual pressure distribution on the structure to the dynamic pressure of the free stream as given in ASCE Paper 4933 (Reference 4). The magnitude of C_{pe} is as shown in Figures 3.3.1-1 and 3.3.1-2.

f = The constant obtained from Reference 1 for determining the dynamic pressure of the free stream.

v = The wind design velocity as defined in Section 3.3.1.1.

The Reactor Building design pressure distribution (which is proportional to the distribution of C_{pe} shown in Figure 3.3.1-1) is represented by a Fourier Series. Individual harmonics are analyzed by Kalnin's Computer Program as defined in Section 3.8.1.4, and are combined to produce the stress resultants of the total series.

8220.14 The analysis of building parts and portions is not applicable to the design of Category I structures. The procedures delineated in Reference 4 for determining pressure coefficients for the Reactor Building gives results consistent with those derived using ASCE paper No. 3269 (Reference 1). ASCE paper No. 3269 (Part IV, Enclosed Structure Average Pressure Coefficients for Rounded Roofs) gives average values pressure distributions for segments of circular arches the center half and the windward and leeward quarters. Where, based on Reference 1, Figure 3.3.1-1 utilizes smaller segments resulting in slight variations in coefficient values.

3.3.2 TORNADO LOADINGS

All Category I structures, except those structures not exposed to wind, are designed for tornado loads.

3.3.2.1 Applicable Design Parameters

The design tornado used in calculating tornado loadings is in conformance with Regulatory Guide 1.76 with the following exceptions:

- a. Rotational (Tangential) wind speed is 300 mph.
- b. Translational speed of tornado is 60 mph.
- c. Radius of maximum rotational speed is 240 feet.
- d. Tornado induced negative pressure differential is 3 psi, occurring in three seconds.

The spectrum and characteristics of tornado-generated missiles is covered in Section 3.5.1.4.

EL. 712+3

EL. 698+9

EL. 693+9

EL. 689+6

1.35

IX

VIII

VII

VI

V

IV

III

II

I

1.35

IX

VIII

VII

VI

V

IV

III

II

I

1.35

IX

VIII

VII

VI

V

IV

III

II

I

1.35

IX

VIII

VII

VI

V

IV

III

II

I

1.35

IX

VIII

VII

VI

V

IV

III

II

I

1.35

IX

VIII

VII

VI

V

IV

III

II

I

1.35

IX

VIII

VII

VI

V

IV

III

II

I

1.35

IX

VIII

VII

VI

V

IV

III

II

I

1.35

IX

VIII

VII

VI

V

IV

III

II

I

1.35

IX

VIII

VII

VI

V

IV

III

II

I

1.35

IX

VIII

VII

VI

V

IV

III

II

I

1.35

IX

VIII

VII

VI

V

IV

III

II

I

1.35

IX

VIII

VII

VI

V

IV

III

II

I

1.35

IX

VIII

VII

VI

V

IV

III

II

I

1.35

IX

VIII

VII

VI

V

IV

III

II

I

1.35

IX

VIII

VII

VI

V

IV

III

II

I

1.35

IX

VIII

VII

VI

V

IV

III

II

I

1.35

IX

VIII

VII

VI

V

IV

III

II

I

1.35

IX

VIII

VII

VI

V

IV

III

II

I

1.35

IX

VIII

VII

VI

V

IV

III

II

I

1.35

IX

VIII

VII

VI

V

IV

III

II

I

1.35

IX

VIII

VII

VI

V

IV

III

II

I

1.35

IX

VIII

VII

VI

V

IV

III

II

I

1.35

IX

VIII

VII

VI

V

IV

III

II

I

1.35

IX

VIII

VII

VI

V

IV

III

II

I

1.35

IX

VIII

VII

VI

V

IV

III

II

I

1.35

IX

VIII

VII

VI

V

IV

III

II

I

1.35

IX

VIII

VII

VI

V

IV

III

II

I

1.35

IX

VIII

VII

VI

V

IV

III

II

I

1.35

IX

VIII

VII

VI

V

IV

III

II

I

1.35

IX

VIII

VII

VI

V

IV

III

II

I

1.35

IX

VIII

VII

VI

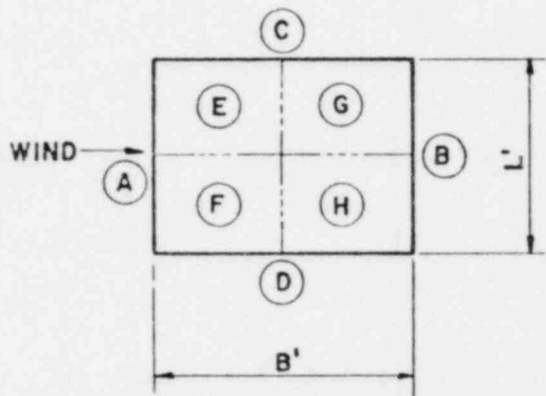
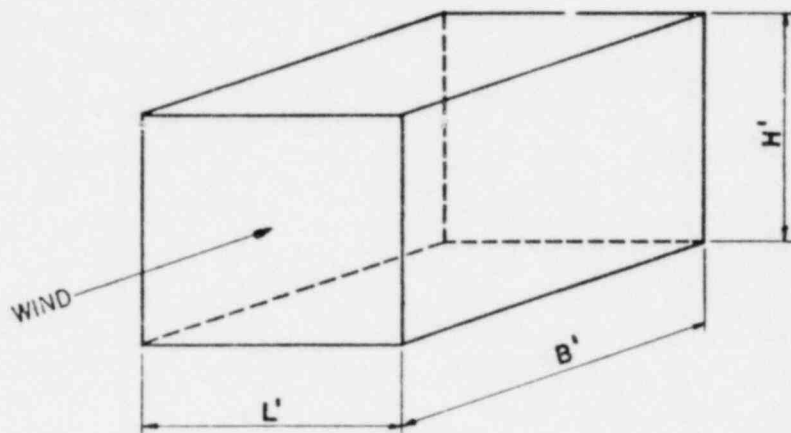
V

IV

III

II

I



PLAN VIEW

STRUCTURE	WIND DIRECTION	COEFFICIENT (Cpe)							
		A	B	C	D	E	F	G	H
AUXILIARY BUILDING	N-S	0.9	-0.3	-0.4	-0.4	-0.8	-0.8	-0.3	-0.3
	E-W	0.9	-0.3	-0.4	-0.4	-0.8	-0.8	-0.3	-0.3
DOGHOUSE STR. & NEW FUEL BLDG.	N-S	0.9	-0.5	-0.7	-0.7	-0.6	-0.6	-0.5	-0.5
	E-W	0.9	-0.5	-0.6	-0.6	-0.7	-0.7	-0.5	-0.5
SPENT FUEL POOL BUILDING	N-S	0.9	-0.5	-0.7	-0.7	-0.6	-0.6	-0.5	-0.5
	E-W	0.9	-0.5	-0.6	-0.6	-0.7	-0.7	-0.5	-0.5

$$p = (Cpe) f v^2$$

$$= (Cpe) (.002558) (95)^2$$

$$= 23.09 (Cpe)$$

$$f = .002558$$

(p. 1150, Ref. 1)

$$v = 95 \text{ mph}$$

$$p = \text{psf}$$

$$p = (G_F) (Cpe) f v^2$$

$$f = 0.002558 \text{ (p. 1150, Ref. 1)}$$

$$v = 95 \text{ mph}$$

$$p = \text{psf}$$

$$G_F = \text{Gust Factor} = 1.10$$



19. Provide additional information in response to FSAR Question 220.34.

Response:

See attached response to Question 220.34.

In all cases, equipment under earthquake loadings is designed to be within code allowable stresses.

Also, as noted in Section 3.7.3.1, rigid equipment/support systems have natural frequencies greater than 33 Hz.

3.7.3.5 Use of Equivalent Static Load Method of Analysis

3.7.3.5.1 For NSSS

The equivalent static load method involves the multiplication of the total weight of the equipment or component member by the specified seismic acceleration coefficient. The magnitude of the seismic acceleration coefficient is established on the basis of the expected dynamic response characteristics of the component. Components which can be adequately characterized as a single degree of freedom systems are considered to have a modal participation factor of one. Seismic acceleration coefficients for multi-degree of freedom systems which may be in the resonance region of the amplified response spectra curves are increased by 50 percent to account conservatively for the increased modal participation.

3.7.3.5.2 Other Than NSSS (Seismic Category I and II Piping only)

The equivalent static load method may be used provided it has been demonstrated that the subsystem is either rigid, or can be adequately and realistically represented as a single degree of freedom system. In this case, the modal participation factor is considered to be one and the equivalent static load is determined by using the peak acceleration of the applicable floor response spectrum at the appropriate value of damping.

The method may also be used, when the dynamic characteristics of the subsystem has not been determined, provided the subsystem can be realistically represented as a simple model. In this case a factor of 1.5 is applied to the peak acceleration of the applicable floor spectrum at the appropriate value of damping.

The relative motion between support points is accounted for in the simplified analysis by using the method described in Section 3.7.3.9.

3.7.3.6 Three Components of Earthquake Motion

Methods used to account for three components of earthquake motion for Westinghouse subsystems are given in Section 3.7.2.6.

For seismic piping other than NSSS, analysis is performed using simultaneous three-direction excitation. Directional responses are combined into a total response by taking the square root of the sum of the squares (SRSS) of individual responses. This method conforms fully to the recommendations of Regulatory Guide 1.92.

20. Provide an assessment of the extent to which Duke's design of steel and concrete pressure barriers conform to the intent of Standard Review Plan 3.8.3, (load combination per CC-3000, ASME; design/analysis per ACI 318).

Response:

Duke Power is in compliance with all applicable parts of Standard Review Plan Section 3.8.3. The load combinations and load factors given in FSAR Table 3.8.1-2 are identical to those set forth in SRP 3.8.3. The Catawba Station utilizes a steel containment vessel (see Questions 220.2, 220.3, 220.4, and 220.9) and therefore is not subject to the requirements of Article CC-3000 of the ASME Boiler and Pressure Vessel Code, Section III, Division 2, "Code for Concrete Reactor Vessels and Containments." Those portions of the internal structure which are concrete, conform to the design/analysis requirements of ACI-318. Concrete portions of the internal structure utilize load combinations which are equivalent or conservative to those specified by CC-3000.

21. With respect to hatch opening analysis provide a discussion and basis for local analysis of hatch support including rationale for selection of model boundaries and design adequacy of section (reinforcing quantities, etc.).

Response:

In order to determine the effects of a large penetration, a STRUDL analysis was performed. A square panel 100 feet on a side was modeled. A 10 ft. radius opening was modeled in one corner.

The purpose of this model was to determine the amount of stress concentration that could be expected near the penetration. Arbitrary loads of 10 k.ft/ft and 10k/ft were applied to the free edges of the model. The results of this analysis showed that the stress combinations near the opening were close to theoretical results found in textbooks for a flat plate with a circular hole subjected to bending and axial loads. ("Theory of Elasticity," 3rd edition, by Timoshenko, "Stress Concentration Design Factors" by R. E. Robertson.)

It was also found that the concentration of stress dissipated rapidly moving away from the opening. Based upon the STRUDL model and theoretical analyses, it was decided that a reasonable design approach would be to reduce the spacing of vertical reinforcement (#11 bars) from 0°-52' of arc to 0°-26' for a distance of approximately 11' from the edge of the opening. This effectively used a stress concentration factor of 2 and doubled the amount of reinforcement in the 11' width on the sides of the equipment hatch. The 11' width is approximately equal to the radius of the equipment hatch.

22. Provide assessment of the impact on surrounding Category I structures due to the failure of the vent stack and demonstrate that safety function of the surrounding structures is not impaired.

Response:

The vent stacks are designed as Category I structures, as per the applicable requirements of FSAR Section 3.8. However, some localized failure may occur as a consequence of tornado missile impacts. If the localized failure results in a portion of the vent stack becoming detached, the maximum possible Kinetic Energy developed by that portion is less than the maximum Kinetic Energy developed by the postulated design basis missiles of FSAR Table 3.5.3-1. Therefore, the safety function of surrounding structures is not impaired.

23. Provide comparison for FSAR Question 220.31 for containment internal structures.

Response:

See attached response to Question 220.31.

CNS

A typical structural mathematical model of the Containment Interior Structure is shown in Figure 3.7.2-1.

Response spectra are generated, for structures that require the generation of response spectra, in the horizontal and vertical direction for structures with modes of vibration less than 20 Hz. For structures with fundamental modes of vibration in a particular direction equal to or greater than 20 Hz, the ground time-history response spectra are used.

When the ground response spectra are used the acceleration values corresponding to 20 Hz are used as a minimum value for the design of piping and components. The acceleration values at 20 Hz are greater than the values corresponding to a rigid system and therefore are conservative.

Typical horizontal response spectra for five elevations of the Containment interior structure are shown in Figures 3.7.2-19 through 3.7.2-23.

TORSIONAL CONTRIBUTION TO FLOOR RESPONSE SPECTRA

When the torsional contribution is significant, as in the case of the Auxiliary Building, floor response spectra are generated at various points of interest of each floor elevation for the horizontal components of earthquake motion. Extra weightless joints, connected to the center of structural rigidity of their respective floor elevations by horizontal members of relatively large stiffness, are added to the three dimensional model to generate spectra at locations near the periphery of the structure.

3.7.2.6 Three Components of Earthquake Motion

A) Structures

The earthquake ground motions are assumed to act in one of two perpendicular horizontal directions simultaneously with motion in the vertical direction. The structure is then designed for the case of vertical and horizontal earthquake motion giving the more severe stresses. The provisions of Regulatory Guide 1.92 are not applicable to the design of the Catawba Nuclear Station structures due to the implementation date of the guide.

A comparison was made for the containment interior structure to determine the effects of going to a three dimensional design philosophy. The original lumped mass model of the interior structure was reanalyzed. The new analysis accounts for all the provisions now found in Regulatory Guide 1.92.

A comparison of design forces for the new three dimensional analysis versus the original two dimensional analysis is provided in Table 3.7.2-3.

The shear values (S_y and S_z) in Table 3.7.2-3 show less than 1% change as a result of including the three dimensional effects. The axial loads (A_x) range from conservative results at the base to results that are not conservative in the upper portions of the structure. When compared to the capacity of the

CNS

structural members, the increases in axial loads are negligible. Consideration of the effects of the three dimensional earthquake add little to the overall design and decrease the overall structural integrity by negligible amounts.

While Regulatory Guide 1.92 is not applicable to Catawba structures, the above comparison demonstrates that the Catawba design meets the intent of this guide.

B) Systems and Components (Westinghouse)

The seismic design of the piping and equipment includes the effect of the seismic response of the supports, equipment, structures, and components. The Westinghouse system and equipment response is determined using three earthquake components, two horizontal and one vertical. The design ground response spectra are the bases for generating these three input components. The damping values used in the analysis are those given in Section 3.7.1.3.

In computing the Westinghouse system and equipment response by response spectrum modal analysis, the methods of Section 3.7.2.7 are used to combine all significant modal responses to obtain the combined unidirectional responses.

For each horizontal direction of shock, the total response is obtained by taking the absolute sum of the combined unidirectional responses for the horizontal and vertical directions. The most conservative results, with each direction of horizontal shock considered, are used to obtain the critical response values.

Table 3.7.2-3

COMPARISON OF TWO DIMENSIONAL VERSUS THREE DIMENSIONAL ANALYSIS

MEM	ELEV	ORIGINAL TWO DIMENSIONAL DESIGN			REVISED THREE DIMENSIONAL DESIGN			Ax	$\Delta\%$ Sy	Sz
		AX ² KIPS	SY KIPS	SZ KIPS	AX KIPS	SY KIPS	SZ KIPS			
								3		1
1	548+0	6039.	10372	10926	4729	10410	10926	28	-	-
2	556+8	5612	10274	10839	4673	10308	10840	20	-	-
3	565+5	4847	9910	10506	4472	9931	10506	8	-	-
4	574+3	4261	9504	10119	4260	9513	10120	-	-	-
5	583+2	3757	9019	9641	4020	9018	9642	-7	-	-
6	592+2	3191	8321	8939	3690	8313	8939	-14	-	-
7	599+6	2565	7367	7914	3196	7357	7914	-20	-	-
8	609+10	2173	6614	7080	2811	6608	7080	-23	-	-
9	612+10	1853	5970	6365	2484	5967	6365	-25	-	-
10	623+2	1345	4831	5126	1944	4838	5125	-31	-	-
11	633+5	1039	3794	4011	1482	3804	4010	-30	-	-
12	639+3	839	3158	3330	1208	3169	3330	-31	-	-
13	643+6	587	2312	2429	854	2323	2429	-31	-	-
14	650+6	328	1375	1438	483	1384	1437	-32	-	-
15	659+8	160	700	732	239	705	732	-33	-	-

NOTES:

- ¹ - Less than 1%.
- ² Ax is D.L. x .13G: .13G is 2/3 of ground response at 20 cps.
- ³ + is over, - is under.

24. Provide the basis for using a coefficient of friction of 1 in the stability analysis of the containment base slab (sliding).

Response:

The reactor building foundation mat is a reinforced concrete slab cast-in-place on solid rock. The friction coefficient for this type slab should be very close to 1. "Analytical and Computer Methods in Foundation Engineering" by Joseph E. Bowles, gives the skin-friction coefficient for concrete placed on compacted dense sand as 0.98. Using a coefficient of friction of 1 gives a factor of safety of 2.8 by a conservative analysis which neglects the effects of passive earth resistance. If a coefficient of friction as low as 0.6 were used, the factor of safety would be greater than 1.5 (as required by FSAR Table 3.8.1-2 and SRP 3.8.5).

USE OF GENERALIZED RING SPRINGS AT ENDS OF PARTS IN KSHEL PROGRAMS

Generalized ring springs mean that at ends of parts Ring Loads can be introduced that are proportional to all four displacements. The Ring Spring matrix connects the forces and displacements as shown. Note that Q_1, Q_2, u_1, u_2 are the rotated forces and displacements, as shown in Figure 5 on p.21 of manual. Such Ring Springs permit the separation of a part from the shell and the replacement of that part by Ring Springs attached to the shell. Such a procedure can be very useful when many branches (ribs) are attached to a shell, or when further branching is required than is admitted

$$\begin{bmatrix} Q_1 \\ Q_2 \\ M_\phi \\ N \end{bmatrix} = \begin{bmatrix} k_{11} & k_{12} & k_{13} & k_{14} \\ k_{21} & k_{22} & k_{23} & k_{24} \\ k_{31} & k_{32} & k_{33} & k_{34} \\ k_{41} & k_{42} & k_{43} & k_{44} \end{bmatrix} \begin{bmatrix} u_1 \\ u_2 \\ \beta_\phi \\ u_\theta \end{bmatrix}$$

in KSHEL programs.

The use of the generalized Ring Springs requires the knowledge of the influence coefficients at the junction of the removed part. If the removed part is a simple one, such influence coefficients can be found in Tables (see Roark, Formulas for Stress and Strain). If not, they have to be calculated with the KSHELL program. The following example illustrates how a conical branch can be replaced by Ring Springs.

Example. The object is to find the stresses in a cylindrical shell with a conical branch (Fig.1). The solution can be obtained by replacing the branch AB by Ring Springs at the end of the first cylindrical part. First we must decide in what direction the Ring Springs will be attached to the cylindrical shell at A. (They can be attached in any direction by prescribing ALFA on Ring Load Card). We choose them in normal and tangential directions to the cyl. shell, so that $ALFA=0$. It will be assumed that the loads on this structure are axisymmetric, and that no surface loads act on the branch AB. We must first find the influence coefficients over the branch AB, which are forces at A produced by unit displacements at A. Thus, we must have the solutions to the three problems for the branch AB alone, by prescribing displacements at A: $u_1=1.0, u_2=\beta_\phi=0$; $u_2=1.0, u_1=\beta_\phi=0$; $\beta_\phi=1.0, u_1=u_2=0$. Because we chose the springs along normal and tangent of the cyl. shell, we must have u_1 and u_2 also in the same directions (see Fig.2). (When running the influence coeff. cases, we must set $ALFL=45$ degrees on Bound. Condition Card; see Fig.5 on p.21 in manual). Note that if there were surface loads on the branch, they should have been included in these three runs. From these three outputs, we must calculate the forces at A in the same direction as u_1 and u_2 , because the output gives N_ϕ and Q , from



Figure 1

Figure 2: A diagram showing the coordinate system for the ring springs at point A. The normal direction is u_1 and the tangential direction is u_2 . The angle between the branch axis and the normal direction is β_ϕ . The shell has a radius $E=1.0$, Poisson's ratio $\nu=0.3$, and thickness $h=0.05$.

Figure 2

$$Q_1 = N_\phi \sin \alpha - Q \cos \alpha \quad Q_2 = -N_\phi \cos \alpha - Q \sin \alpha$$

where α is as shown on Fig.5 in manual. The Ring Spring matrix for branch AB is shown below. The first column represents Q_1, Q_2, M_ϕ , at A when $u_1=1.0$, the second when $u_2=1.0$, etc. Note that the influence coeffs must be obtained for the wave number of the applied loads. For $n>0$, four problems must be solved, including also u_θ .

0.062372	-0.047612	-0.00091283
-0.047612	0.044344	0.00008531
-0.00091283	0.00008531	0.00011765

An identical solution over the cylindrical shell is obtained when the same shell is run with the conical part as an ordinary branch, without any springs.

NOTE: on some machines (especially IBM), accuracy is poor when $E=30 \times 10^6$ and a solution is wanted with, say, $u_1=1.0$. One inch can be a very large displacement. This is especially true for wave numbers like $n=1,2,3$, etc. The way out is to specify for the influence coefficient problems $u_1=0.0001$, and then multiply the solution by 10000. Note that then all the other loads that are acting on the branch must also be divided by 10000.

25. With respect to the seismic k-shell model of containment, assess the impact of considering the shell stiffness with the stiffeners. Insure adequacy of using McGuire stiffness calculation or stiffner properties at Catawba.

Response:

In the seismic analysis of the containment the stiffners were replaced with equivalent springs. To determine the spring rate of a stiffener it was modeled on KSHEL (with fixed boundary conditions at the point of attachment to the containment). Unit displacements were then applied and reactions determined (to be used in calculating stiffners). This method is generally used and accepted (Reference: Vibration Problems in Engineering by Timoshenko, Young and Weaver). It is similar to sub-structuring where the stiffener is de-coupled from the main model and represented by a stiffness matrix. To consider the stiffness of the containment shell in addition to the stiffener would not give a true representation of the actual structure (see also attachment from KSHEL manual on ring springs). The ASME code (Section III, Subsection NE, Article 3133.5) requires the use of part of the shell wall for sizing the stiffener, however this is for determining moment of inertia, etc., only and should not be applied to finite element modeling techniques.

The stiffness properties of the McGuire ring stiffeners were used at Catawba as well. This is acceptable since the stiffeners used at both plants are exactly identical.

26. Provide earthquake analysis results and justify not accounting for vertical stiffeners in that analysis.

Response:

The seismic analysis was run on KSHEL without considering vertical stiffeners. As a check, the problem was run using the Wilson Ghosh program using a model containing orthotropic material properties to account for the vertical stiffeners. The stress resultants at various points on the shell are listed in the attached Table 26-1 for comparison. As can be seen, higher stress resultants are obtained from KSHEL, so the results of this program are acceptable without including vertical stiffeners in the model.

TABLE 26-1

LOCATION (Elevation)	KSHEL					WILSON-GHOSH				
	N ϕ (lb/in)	N θ (lb/in)	M ϕ (m-lb/in)	M θ (in-lb/in)	Shear (lb/m)	N ϕ (lb/in)	N θ (lb/in)	M ϕ (in-lb/in)	M θ (in-lb/in)	Shear (lb/in)
20.40"	1467	322	11	4	812	1099	210	29	9	603
224.60"	1228	48	10	3	795	922	34	3	1	591
405.80"	1018	43	9	3	762	764	38	3	1	566
653.00"	744	144	7	2	685	562	63	5	2	514
1013.00"	400	212	7	2	507	306	109	5	2	390
1318.60"	187	259	7	2	297	144	200	5	2	242
122.30°	71	96	1	1	131	52	127	0	0	98
167.63°	23	38	1	0	25	16	32	1	1	20

NOTE: (1) Elevation of base is 0.

(2) Elevations in dome are measured in degrees of arc ($90^\circ + \phi$ from dome-cylinder junction at El. 1341").

The results tabulated in the above Table under $\Delta\%$ Ax indicate that the axial loads generated from the 3D earthquake range from 27% conservative at the base to 83% unconservative in the upper levels of the spent fuel pool. Note that the more critical areas of design, base mat and low level supporting walls, are very conservative. The upper level results basically represent large increases in relatively small response values. It is felt that the design is more than adequate and can withstand these increases easily.

The Table results under columns $\Delta\%$ Sy and $\Delta\%$ Sz indicate that for the most part the shear values from the 3D analysis are within 1% of the values from the original analysis. Notable exceptions exist only in the upper portions of the spent fuel pool. Here again the walls, as designed, are more than adequate and will withstand these increases easily.

For a discussion of 3D effects on the generator or response spectra see Dukes answer to Question 3.12 of the FSAR.

Comparison of individual member results used in design.

ELEMENT ¹ No.	Vx (KIPS) ²	Vy (KIPS) ³	TYPE OF MEMBER	RMS Vx & Vy	$\Delta\%$ Vs Max Shear	CAPACITY (KIPS) ⁴	NOTES
1	1199.3	90.8	Q Line Wall	1202.7K	-	3218.K	
2	2.4	2.7	3' x 3' Col.	3.6K	25%	84.K	
22	1339.2	106.0	N Line Wall	1343.4K	-	3765.K	
108	8517.0	11287.0	Spent Fuel Base	14140.0K	25%	27530.K	29' x 87' Pool Base
12	11.5	399.6	Wall	400.0K	-	1030.K	
86	38.0	605.0	53 Line Wall	606.0K	-	1030.K	
166	454.1	36.3	F Line Wall	456.0K	-	1287.K	
10	2.5	2.7	3' x 3' Col.	3.7K	37%	84.K	
29	2.5	2.7	3' x 3' Col.	3.7K	37%	84.K	
157	511.3	39.5	E Line Wall	513.0K	-	1400.K	
62	955.7	69.1	E Line Wall	958.0K	-	2478.K	
60	511.3	39.4	E Line Wall	513.0K	-	1400.K	
239	32.3	428.3	49 Line Wall	430.0K	-	1126.K	
199	1445.5	11.4	A Line Wall	1446.0K	-	3400 K	
202	2.8	2.7	3' x 3' Column	3.9K	39%	84.K	
211	1.9	1.0	3' x 3' Column	2.2K	16%	84.K	
242	2.8	2.8	3' x 3' Column	4.0K	43%	84.K	

NOTES:

- ¹ Element number per CNC-1189.01-23-0001 Volume 9 of 22, Elevation 543+0 to 560+0.
- ² Shear + Torsional Shear from "X" Axis Shock.
- ³ Shear + Torsional Shear from "Y" Axis Shock.
- ⁴ Capacities based on 3000 psi plain concrete.

The above shear values were assigned, to the elements that compose the structure, based on their relative stiffness in the direction of the

particular shock. As would be expected, the major stiffening elements (walls) carry approximately 90% of the building shear. These elements show less than a 1% change when 3D earthquake effects are included.

The members which show sizeable increases are those which have approximately the same stiffness in both directions. All members in this category, as well as those above, have strengths far in excess of what is required to support these increased loads.

The above discussion confirms that the intent of Regulatory Guide 1.92 is met.

The response to Question 220.19 was provided in FSAR Revision 4.

Portions of the Reactor Building shell and dome are modeled using a space frame finite elements model subject to the tornado missile loads. The results of these analyses in terms of resulting forces, moments and shears are combined with other loadings on the structure as specified in Table 3.8.1-2.

After demonstrating that the postulated missiles would not penetrate the barrier, an equivalent static load, concentrated at the impact area, was determined from which the structural response of the barrier, in conjunction with other design loads, was evaluated using conventional design methods. The response of a structure to missile impact depends largely on the location of impact (midspan of a slab, or near the support), on the dynamic properties of the target and missile, and on the kinetic energy of the missile. The collision is assumed to be plastic, that is, all of the kinetic energy of the missile is absorbed into structural strain energy. However, energy losses due to missile deformation and local penetration are considered when applicable.

For missiles 1 through 5, the impact force is calculated based on the following formula from Reference 7:

$$F_i = \frac{WV^2}{gx}$$

where

F_i = force of impact (lb)
 W_i = weight of fragment (lb)
 V = velocity of impact (ft/sec)
 g = acceleration of gravity (ft/sec²)
 x = penetration (ft)

For missile 6, the derivation of a force-time history is calculated based on the following formula from Reference 8:

$$F(t) = 0.625 V_s W_m \sin 2Dk \quad (0 \leq t \leq 0.0785 \text{ sec})$$

$$F(t) = 0 \quad (t > 0.0785 \text{ sec})$$

where

t = time from the instant of initial contact (sec)
 $F(t)$ = time-dependent force on target (lb)
 V_s = striking velocity of the automobile (ft/sec)
 W_m = weight of automobile (lb)

The ductility ratio (μ) is defined as the ratio of the maximum acceptable displacement ($\Delta\mu$) at failure to the corresponding displacement (Δy) at initial yield (Reference 9). The ductility ratio ranges from 1.0 for a completely brittle structure, to 100.0 for a very ductile structure. For moderately brittle structures, $\mu=3$ to 5; for moderately ductile structures, $\mu=10$ to 30 (Reference 10). The ductility ratio for reinforced concrete

structures depends on the quantity of reinforcement, on the relative quantities of tensile and compressive steel, the compressive strength of concrete the yield stress of steel reinforcement, and the structural behavior of the member under consideration (i.e., whether it is a beam, column, or shear wall). Structures designed in accordance with ACI-328-71 generally have adequate ductility. In critical areas, however, ductility of the structure may be further improved to assure adequate rotational capacity of the members and redistribution of moments in the structure by use of one of the following:

Q
220.19

- a. Compressive reinforcement
- b. Closed stirrups to confine the concrete
- c. Under-reinforced sections
- d. High strength concrete
- e. Reinforcement bars with lower yield stress

The ductility ratio used in the analysis and design of concrete structures does not exceed 10 unless it can be shown by elasto-plastic analysis, considering both local and overall collapse of the structure, that various elements of the structure have adequate strength and rotational capacity required for the redistribution of moments over the entire structure.

28. Provide analysis results and confirm that the intent of Regulatory Guide 1.92 provisions covering the three component earthquake combination is met. Also, respond to Question 220.19.

Response:

The original seismic design concept at Catawba and the one to which Duke is committed, is described in FSAR Section 3.7.2.6. Additional analytical work was performed to confirm that the intent of Regulatory Guide 1.92 covering the three component combination of earthquake motion is met. The reanalysis, in this case, was completed for the Auxiliary Building using the original seismic model. This new analysis was composed of all the provisions now in Regulatory Guide 1.92. This analysis will be referred to as the 3D analysis.

Results of the 3D analysis versus the original analysis for the base of the structure are:

Original Analysis			3D Analysis			$\Delta\%$		
Axial Load	Shear Y	Shear Z	Axial Load	Shear Y	Shear Z	Ax	Sy	Sz
25665.K	40394.K	35738.K	20246.K	40524.K	35833.K	27	(1)	-

(1) - less than 1%.

The above results indicate that the respective directional shears increase less than 1% over the original design forces while the axial load originally used is 27% conservative. When the results of the 3D earthquake are used in the stability analysis the following results are obtained:

Min. safety factor against overturning = 4.37

Min. safety factor against sliding = 6.38

Results of the 3D analysis versus the original analysis by structural elevation:

Elev.	ORIGINAL ANALYSIS (KIPS)			3D ANALYSIS (KIPS)			$\Delta\%$ (1)		
	Axial Load	Shear Y	Shear Z	Axial Load	Shear Y	Shear Z	Ax	Sy	Sz
543+0	25665.	40394.	35738.	20246.	40524.	35833.	27	-	-
551+6	23556.	39853.	35308.	19931.	39956.	35377.	18	-	-
560+0	18366.	37369.	33484.	18358.	37369.	33456.	-	-	-
568+5	16824.	36084.	32502.	17679.	36053.	32444.	-5	-	-
577+0	11329.	29677.	27380.	14205.	29615.	27337.	-20	-	-
585+6	10392.	28150.	26121.	13441.	28099.	26102.	-23	-	-
594+0	6059.	19093.	18595.	8952.	19134.	18675.	-32	-	-
602+6	5153.	16909.	16807.	7938.	16973.	16884.	-35	-	-
611+0(2)	466.	1764.	3608.	1610.	2056.	3767.	-71	-14	-
631+6(2)	149.	732.	1822.	860.	923.	1940.	-83	-21	-
611+0(3)	311.	2273.	1505.	791.	2322.	1526.	-61	-2	-
619+0(3)	201.	2019.	1331.	600.	2063.	1341.	-67	-	-
634+0(3)	80.	1445.	1033.	309.	1457.	1037.	-74	-	-

(1) - less than 1%.

(2) Upper levels of spent fuel pool

(3) Upper levels of doghouse.

29. For the containment vessel, respond to FSAR Question 220.28 dealing with peak widening.

Response:

Attached is the response to FSAR question 220.28 previously submitted in Revision 4. This response is applicable to the containment vessel as well as to other structures in the plant.

structures. The non-Category I structures with sufficient mass to possibly impair the integrity of Seismic Category I structures or components upon collapse are analyzed to prevent their failure in the direction of a Seismic Category I structure under SSE conditions in a manner such that the margin of safety of these structures is equivalent to that of Seismic Category I structures. The collapse of any non-Category I structure, not analyzed to prevent their failure under SSE conditions, will not impair the integrity of Seismic Category I structures or components.

3.7.2.9 Effects of Parameter Variations on Floor Response Spectra

To take into account possible variations in structural properties, damping, soil or rock properties, and soil structure interaction, the calculated floor response spectrum is enveloped to cover a ± 10 percent shift in period and a 10 percent increase in peak response.

Q 220.28 The provisions of Regulatory Guide 1.122 are not applicable to the design of Catawba structures due to the Regulatory Guide implementation date. The requirements of Regulatory Guide 1.122 typically result in slightly more conservative values for the off-peak regions and less conservative values for the peak regions of the response spectra. Duke considers the added conservatism in the peak region to be more beneficial than conservatism in the off-peak region. An adjusted design envelope of a typical floor response spectra utilizing the 10 percent period shift is shown in Figure 3.7.2-24.

3.7.2.10 Use of Constant Load Factors

The vertical modes of vibration are considered in the seismic design of structures.

The vertical modes of vibration for the Containment Vessel and Reactor Building are determined as defined in Section 3.7.2.1. The vertical frequencies of these structures are less than 20 Hz and are considered to influence the seismic design. All vertical modes contributing significantly to the seismic loads are used.

Lumped mass structures with vertical modes of vibration less than 20 Hz are designed by performing a dynamic analysis in the vertical direction. The dynamic analysis is performed as defined in Section 3.7.2.1.

Lumped mass structures with vertical fundamental frequencies equal to or greater than 20 Hz are designed as rigid structures with a constant vertical acceleration equal to the acceleration corresponding to 20 Hz on the vertical response spectrum. The acceleration response at 20 Hz is greater than the response of an infinitely stiff structure and is conservative.

The response spectrum used for the design of vertical modes is equal to two-thirds of the horizontal spectrum.

The maximum horizontal and vertical seismic responses are considered to act simultaneously.

30. Specify the exact location of seismic instrumentation and the basis for that selection.

Response:

FSAR Section 3.7.4.2 specifies the exact location of seismic instrumentation at Catawba. In selecting the location and type of instrumentation, the provisions of Regulatory Guide 1.12 Section C were followed closely. Table 3.7.4-1 provides a comparison of Catawba instrumentation and Regulatory Guide 1.12, Section C. Locations where it was judged that the effects of a seismic event would be most significant, the data obtained would be most valuable, and which satisfied the provisions of Regulatory Guide 1.12 were the locations that were used.

Since all major Catawba Category I structures are founded on a common rock foundation, it was felt that top of soil (free field) instrumentation would not provide significant analytical data and was therefore, not provided.

33. In response to question 220.46, compare allowable stresses now used to those allowed by UBS in masonry.

Response:

The allowable stresses used in the design of the Catawba masonry walls are the same as those allowed by the Uniform Building Code.

34. With respect to safety-related masonry walls provide the following:
- A) Provide a list of walls and identify walls that are not built as of 12/18/81. Indicate your commitment that these walls will be designed analyzed and constructed either as reinforced masonry walls or reinforced concrete walls, meeting the applicable standard review plan requirements. For special situations, such as accessibility, where reinforced walls cannot be built, discuss with the staff the need for using unreinforced walls. Discuss and justify. B) For walls which are complete provide the following: insure each wall is analyzed and designed to meet the SEB masonry wall evaluation criteria and justify that design. Includes any fixes which are required to meet the intent of this criteria. As an option, the use of reinforced masonry design approaches may be used to demonstrate conformance with the SEB criteria. Any major differences found in the assessment should be referred to the staff for joint discussion and resolution. C) Fixes and modifications resulting from the above assessment need only be completed prior to the resumption of operation after first refueling. (3/5/82)

Response:

A list identifying those seismic masonry walls that were not completed as of 12/18/81 was submitted to the NRC in Duke's transmittal dated 1/20/82. Those walls on which construction had already begun or on which construction was complete as of 12/18/81 will utilize the existing design philosophy. Those walls for which construction had not begun as of 12/18/81 will be designed, analyzed, and constructed per the agreements resulting from the Duke/NRC meeting of 2/5/82.

The existing Catawba Nuclear Station seismic masonry wall evaluation criteria compares favorably with the SEB Criteria for Safety Related Masonry Wall Evaluation as is illustrated by the following section by section comparison.

Section 1 - General Requirements:

The SEB criteria requires conformance with UBC-1979 in materials, testing, analysis, design, construction, and inspection. The option is given to comply with ACI-531, ATC-3, or NCMA. The materials used in the construction of the masonry walls at Catawba required conformance to the applicable ASTM standards for each material. This is in conformance with the requirements of ACI-531. A QC/QA inspection procedure is in effect for the construction of the seismic masonry walls. Vertical structural steel shapes reinforce the walls between the floor slab and the ceiling above. The masonry spans horizontally between these vertical steel members. Each course of block was reinforced with durowall placed in every bed joint. The durowall increases the overall ductility of the wall unit as well as assisting in the development of flexural capacity, between the vertical steel members.

Section 2 - Loads and Load Combinations:

All of the load combinations listed by the SEB criteria are considered for the Catawba Nuclear Station seismic masonry walls. The seismic masonry walls at Catawba are located such that no wall is subjected to wind loads, thermal stresses, pressure differentials, pipe break, or

jet impingement. The Catawba seismic walls are in fill walls, thereby making the live load negligible. The resulting load combinations are:

1. D
2. D + E
3. D + E'

Section 3 - Allowable Stresses:

As in the SEB criteria, the Catawba criteria uses the allowable stresses from ACI-531-79. The Catawba criteria considers no increase in the allowable stresses for normal and OBE conditions. For the SSE conditions the Catawba criteria claims a 33 percent increase in all allowable stresses. This is in accordance with Section 10.1.7 of ACI-531-79.

Section 4 - Design and Analysis Considerations:

Duke Power Company considered all of the applicable points in this section during the analysis of the Catawba walls.

Response to Concerns Identified in the 2/5/82 Duke/NRC Meeting:

During the previously mentioned meeting, on 2/5/82, between Duke Power Company and the NRC, additional information was requested for ten items. These items are:

1. Examine uncracked moment of inertia vs. cracked moment of inertia in the analysis of masonry walls.
2. Assure our QA/QC procedure meets the applicable requirements of 10CFR Appendix B, (refer to response to Action Item 35).
3. In the above analysis the following damping values should be considered:

uncracked section - 2%

cracked section - 7%
4. Address interstory drift (method of analysis and basis of allowables used in comparison).
5. Address 3 - component earthquake,
6. Assure significant attachments are connected only to structural wide flange shapes.
7. Provide an example of design of structural wide flange shape.
8. Provide comparison between Duke criteria and NRC-SEB criteria for design of safety related masonry block walls (refer to response on previous pages).
9. Provide behavioral assessment of masonry wall under earthquake loading assuming cracked condition.
10. Supply stress contours for analysis examples.

In order to answer these items a series of STRUDL analyses was performed for six typical wall panels at elevation 594+0. These panels were selected for the analysis because they are at the highest elevation where masonry walls are found in the Auxiliary Building and would thereby experience the greatest acceleration for any seismic masonry walls at Catawba. The following table gives the pertinent information for each wall panel:

MODEL	HEIGHT	MASONRY SPAN	BLOCK CONSTRUCTION	ATTACHMENT
R2 Block A	168"	60"	Grouted Core	I
R2 Block B	168"	60"	Hollow Core	II
R2 Block C	180"	80"	Hollow Core	III
R2 Block D	180"	60"	Hollow Core	IV
R2 Block E	168"	80"	Grouted Core	V
R2 Block F	168"	80"	Hollow Core	VI

The attachments contain the specific information for each model, including boundary conditions output, geometry, results, stress contours.

In the STRUDL models, the masonry was represented by plate bending elements with the steel wide flanges represented by plane grid members.

Appropriate boundary conditions were chosen to represent the block spanning between the vertical steel members and the steel members spanning between the floor and ceiling.

Concerns 1, 3, 9 & 10

The masonry stiffness properties (moment of inertia) were determined for both the uncracked and cracked conditions. The uncracked moment of inertia was based upon the net masonry section with the effect of the transformed joint reinforcement being neglected. The cracked section moment of inertia is determined by accepted theory of cracked sections whereby the tensile stresses are considered to be resisted by the reinforcing steel with the masonry only effective in resisting compression. All masonry on the tension side of the neutral axis is ignored.

Analyses were performed for both the cracked and uncracked sections. For the uncracked section 2% critical damping was considered and 5% critical damping was used for the cracked section analysis.

A dynamic analysis was conducted to determine the natural frequencies of the wall. The resulting participation factors indicate the predominance of the first mode of vibration in describing the response of the masonry walls to a dynamic loading. In the frequency range of interest there were no closely spaced modes.

The models were analyzed with a uniform static pressure loading equivalent to seismic inertial load based on the frequency of the wall and corresponding acceleration chosen from the response spectra curve. The response spectra curve used is that representing ceiling above the wall (Elevation 611).

The various uncertainties connected with masonry construction (i.e., mass, material properties) were taken into consideration by making conservative estimates for wall weight, masonry stiffness, and modulus of elasticity.

As the information in the attachments indicates, the seismic masonry walls at Catawba respond in an acceptable manner. The analyses for the uncracked sections indicate stresses in the acceptable region with a single exception being the vertical span bending stresses in the masonry of the panel described in Attachment V. For this particular wall panel, the vertical span bending stresses exceed the allowable, however, the projected minimum rupture stress for the masonry is not exceeded.

The analysis for the cracked sections resulted in horizontal span bending stresses well within the allowable range for each case. The bending stresses in the steel wide flange shapes are well within the allowable range for flexural stress.

These example calculations show that the Catawba masonry construction provides a valid load carrying mechanism and the walls are designed and reinforced to remain within the limits provided by the code under all applicable loading combinations.

Concern 4

The design of seismic masonry walls also considers interstory drift. Attachment VII contains the Catawba interstory drift considerations. The Catawba seismic masonry walls are acceptable for interstory drift effects.

Concern 5

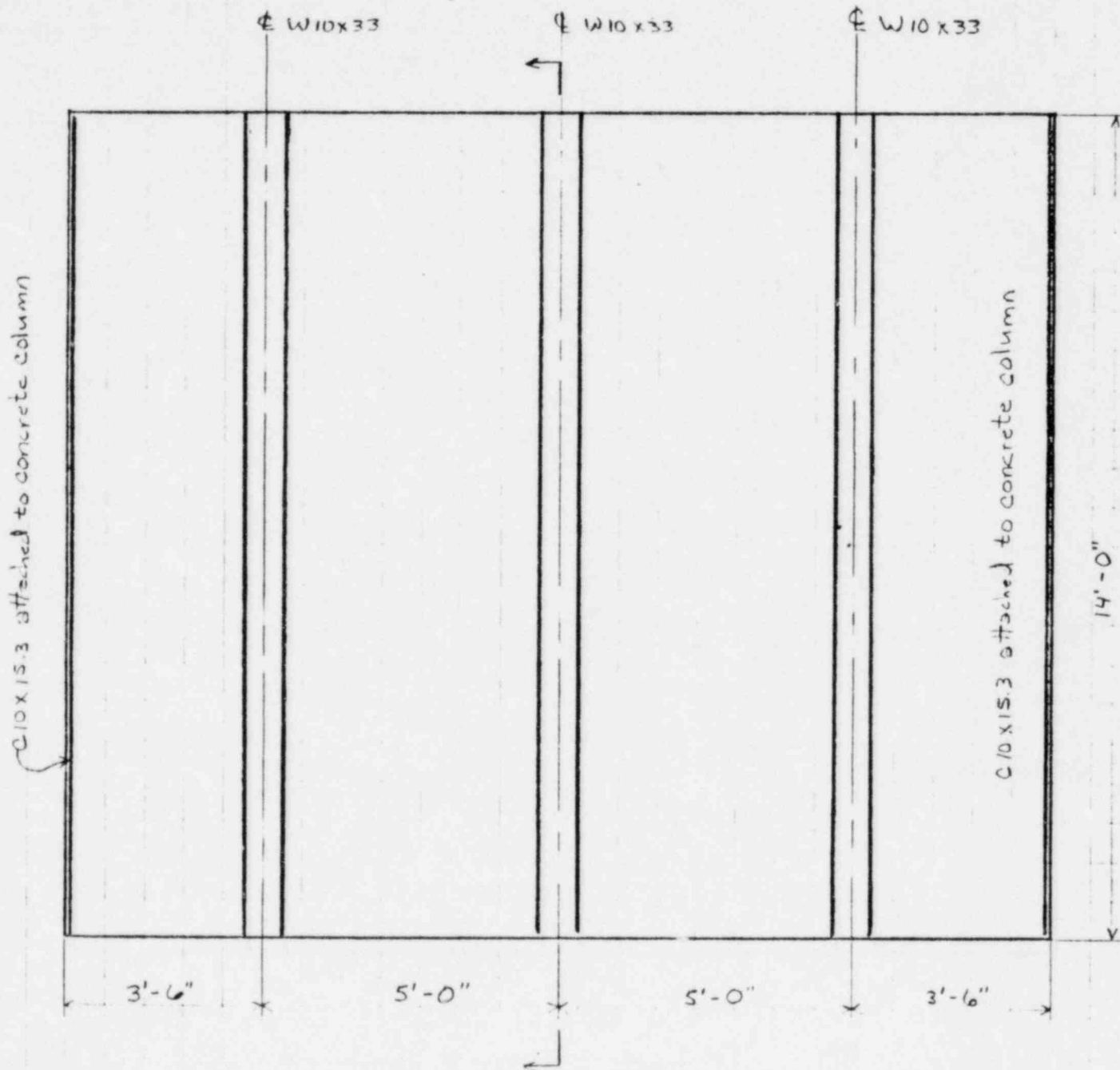
The Catawba masonry walls are designed for a two component earthquake, the vertical and a horizontal component. The net effect of the vertical earthquake component is resulting compression force on the wall, and where conservative this effect is omitted in the analysis of the wall. The walls are in fill panels and there is no fixity between the masonry wall and the primary structure. The effect of two simultaneous horizontal components do not produce additive stresses and analyzing these components independently is considered to be appropriate.

Concern 6

There are no significant attachments to the block itself. The structural steel, which serves as vertical reinforcing to the block wall unit, does have hanger attachments. Each attachment to these structural steel members is reviewed individually to insure that the additional stress does not exceed the allowables.

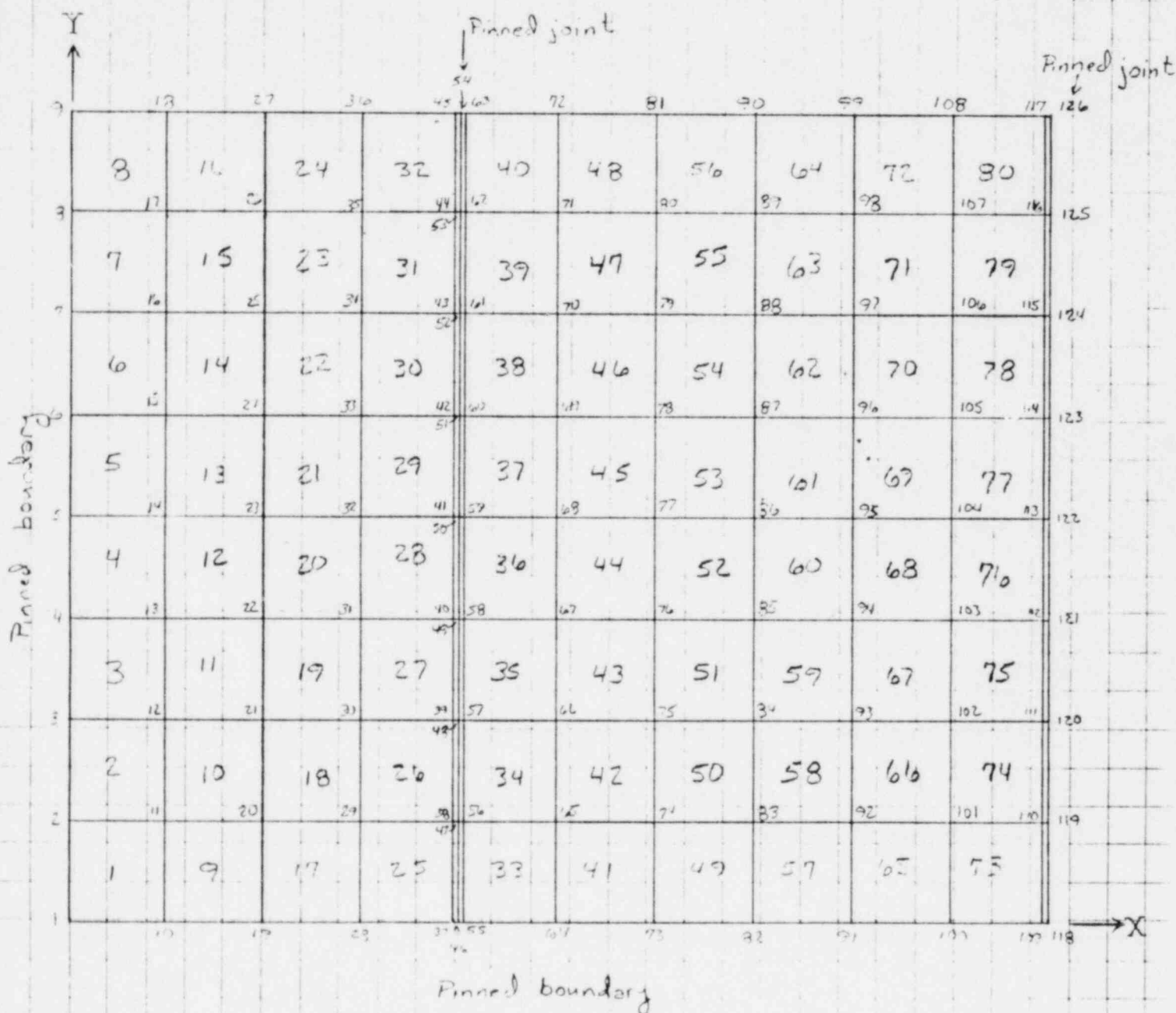
Concern 7

Attachment VIII contains a sample calculation for the design of a structural wide flange.



Attachment I - SHEET 1

Wall Geometry



Attachment I - SHEET 2

Model Grid

This wall panel is of grouted construction. The boundary conditions and member properties along joints 118 thru 126 are adjusted appropriately to take advantage of symmetry in the analysis. The following is an assessment of the results of the analysis for SSE conditions.

	Uncracked Section	Cracked Section
Maximum Horizontal Moment	167 inlb/in	331 inlb/in
Maximum Vertical Moment	313 inlb/in	156 inlb/in
Normal Allowable Moment Horizontal	727 inlb/in	658 inlb/in
SSE Allowable Moment Horizontal	969 inlb/in	877 inlb/in
Cracking Moment Horizontal	2180 inlb/in	N/A
Normal Allowable Moment Vertical	388 inlb/in	N/A
SSE Allowable Moment Vertical	518 inlb/in	N/A
Cracking Moment Vertical	1166 inlb/in	N/A

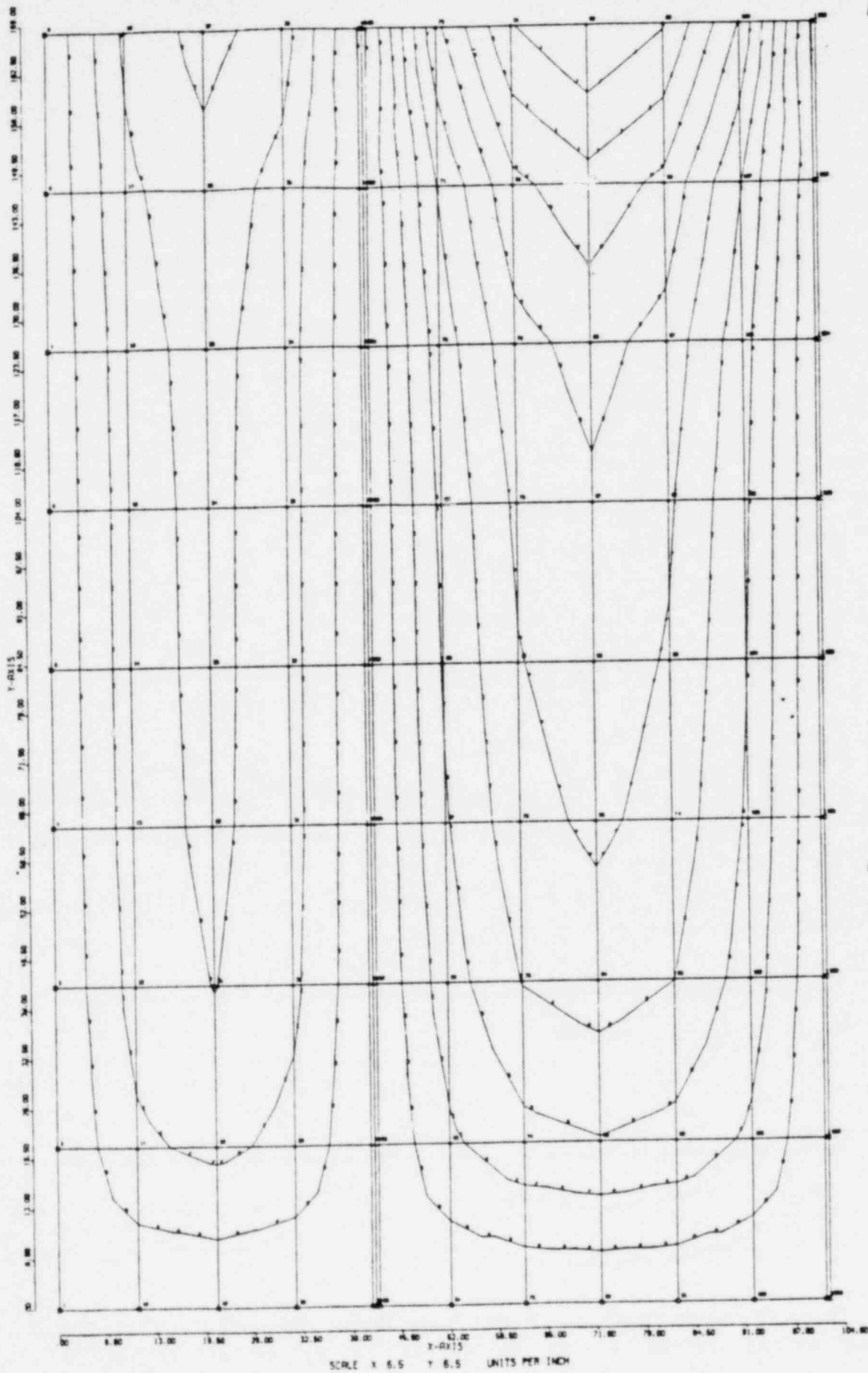
The following four sheets present the stress contours for the wall panel.

Attachment I SHEET 4

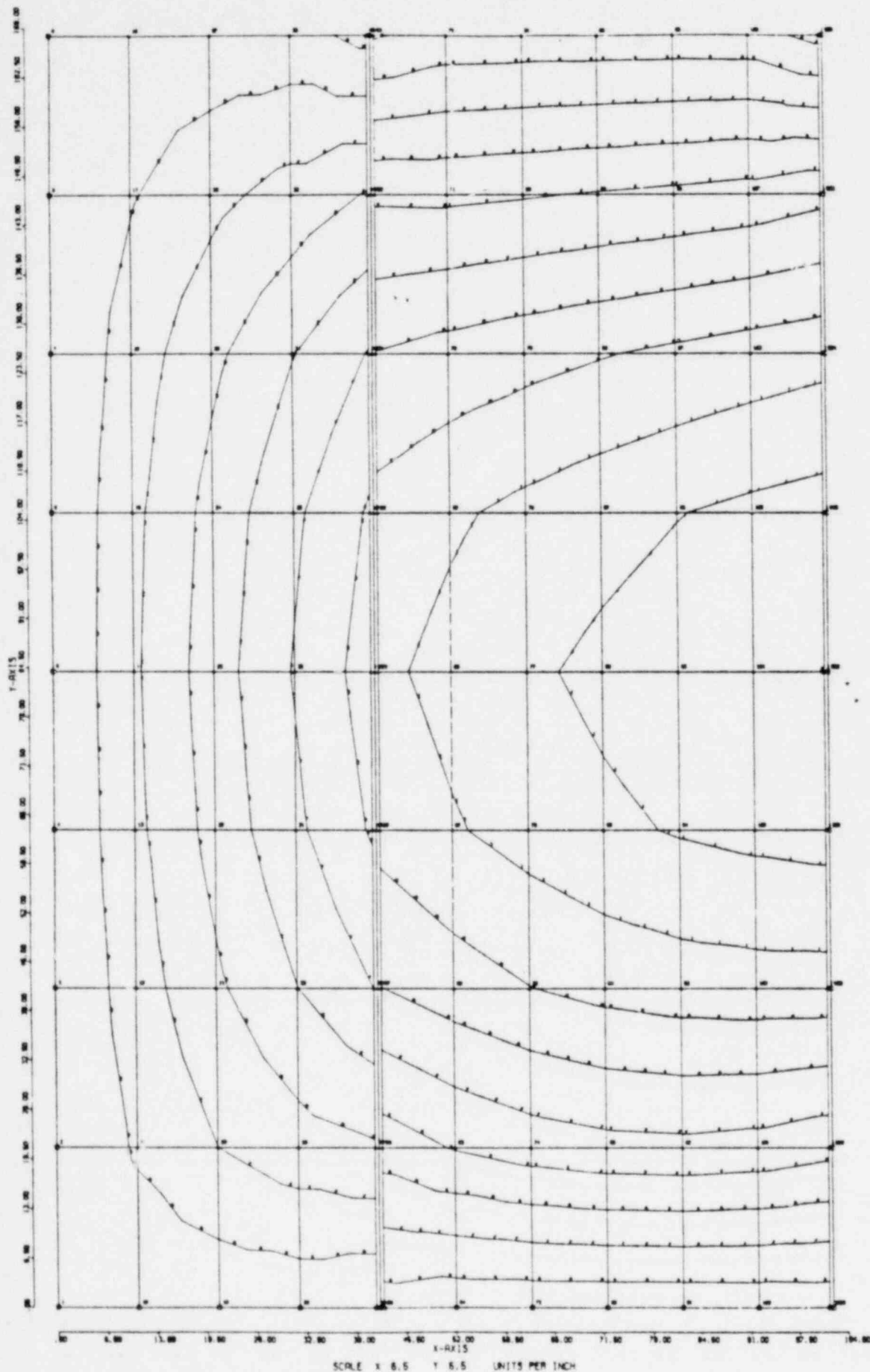
LOADING 1
SURFACE PROFILE
STRESS COUPLES X/
UNITS LB INCH
INTERVAL VALUE

A	0.5
B	1.000E+01
C	7.100E+01
D	1.007E+02
E	1.000E+02
F	1.770E+02
G	2.000E+02
H	2.000E+02
I	2.000E+02
J	1.000E+02
K	1.000E+02

Multiply Interval Values
by 0.47 For SSE



R2BLOCKA UNCRACKED SECTION



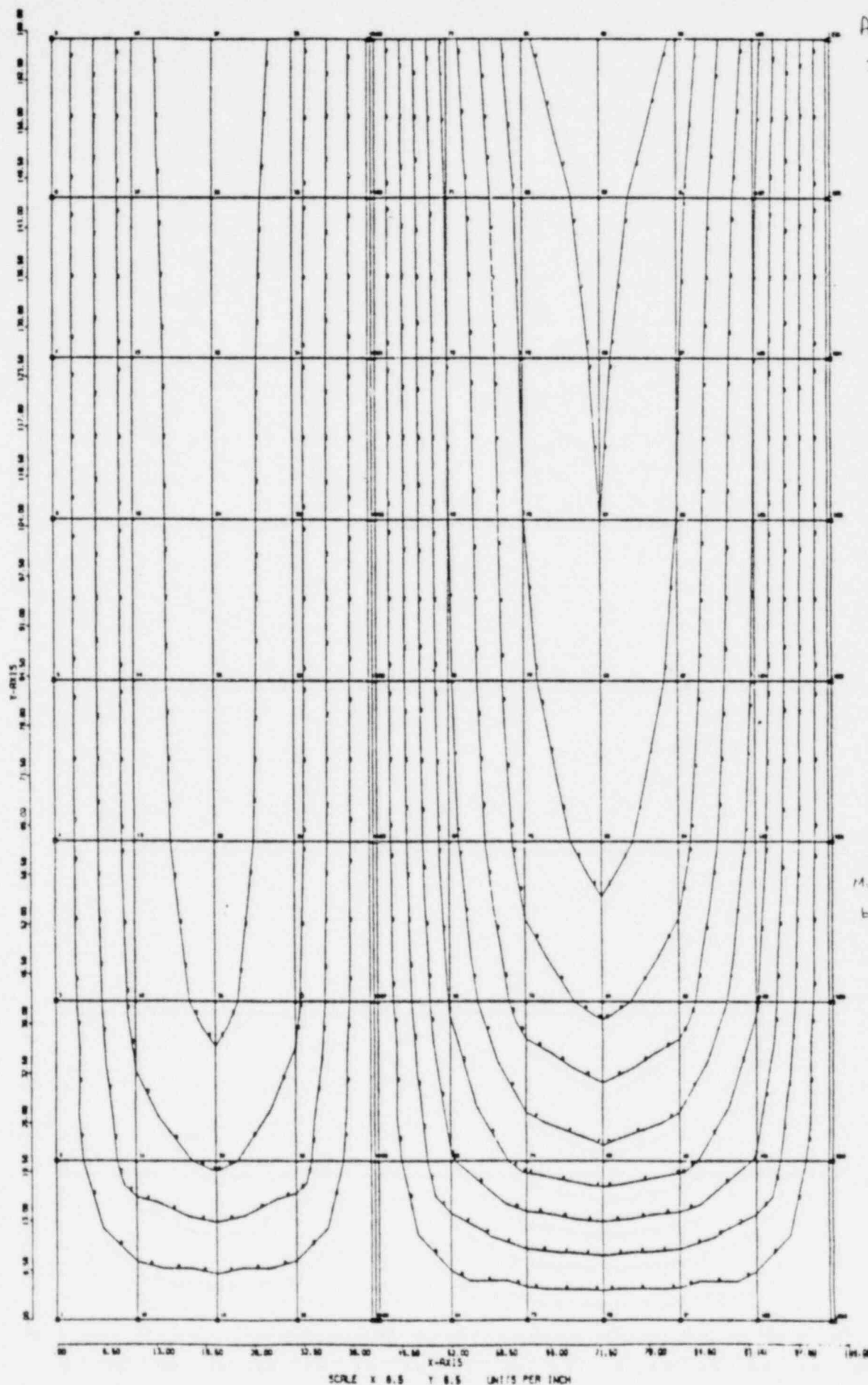
Attn. August I
SHEP

LOADING 1	
SURFACE FIBER	
STRESS COEFFICIENT	
UNITS LB	INCH
INTERVAL	VALUE
1	0.0
2	0.000000
3	0.000000
4	0.000000
5	0.000000
6	0.000000
7	0.000000
8	0.000000
9	0.000000
10	0.000000

Multiply Interval Values
by 0.47 For SSE

R2BLOCKA UNCRACKED SECTION

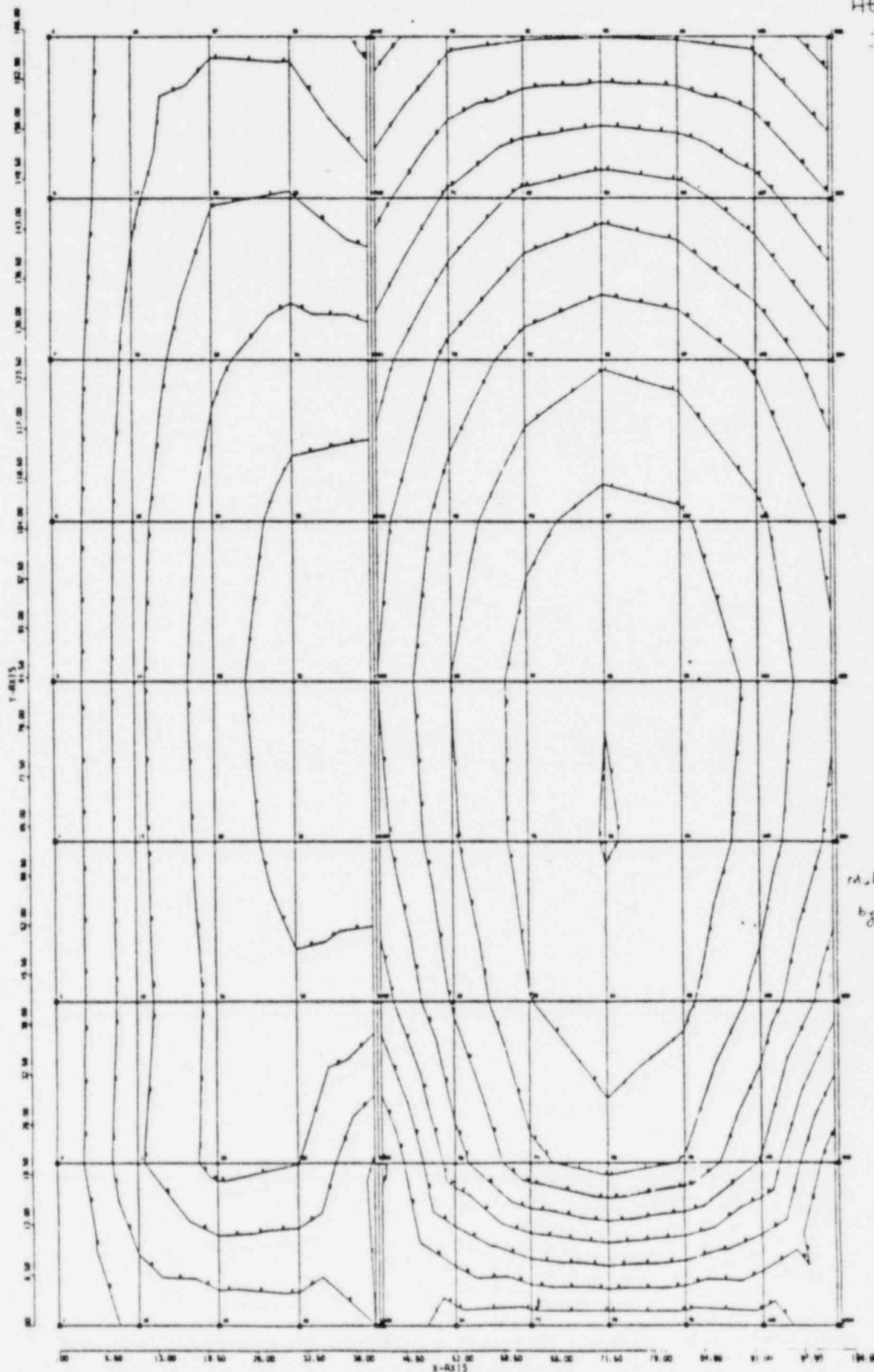
Attachment I
Sheet 6



LOADING	1
SURFACE	POSSIBLE
STRESS COEFFICIENT	4/
UNITS	LB
INTERNAL	VALUE
1	0.0
2	2.0000E-05
3	4.0000E-05
4	6.0000E-05
5	8.0000E-05
6	1.0000E-04
7	1.2000E-04
8	1.4000E-04
9	1.6000E-04
10	1.8000E-04
11	2.0000E-04
12	2.2000E-04
13	2.4000E-04
14	2.6000E-04

Multiply Interval Value
by 1.24 for SSE

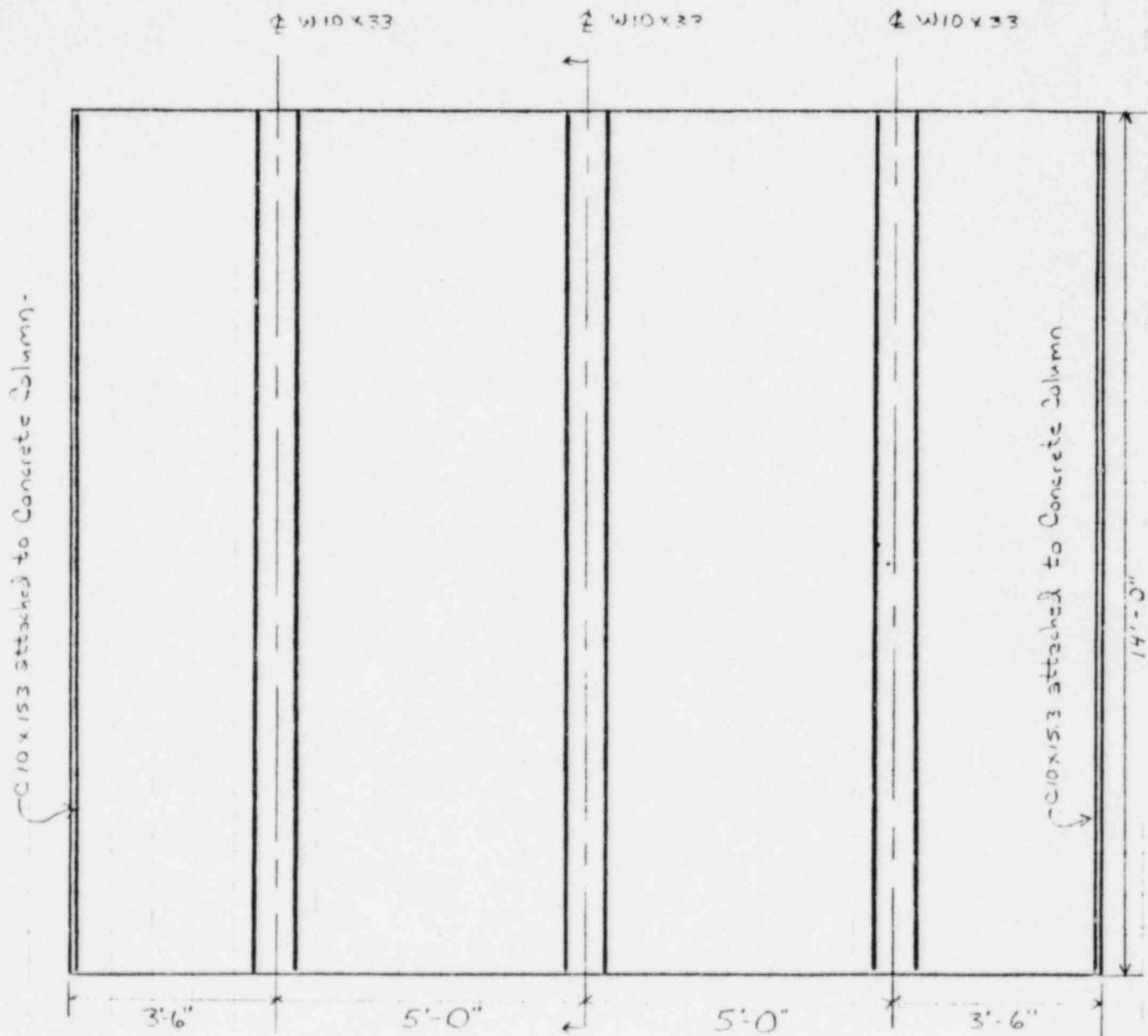
Attachment
Sheet 7



LABELED	1
SURFACE	ATRIANGLE
STRESS COUPLES	1/
UNITS	LB
INTERVAL	VALUE
0	0.0
1	1.24000E-01
2	2.48000E-01
3	3.72000E-01
4	4.96000E-01
5	6.20000E-01
6	7.44000E-01
7	8.68000E-01
8	9.92000E-01
9	1.24000E-00
10	1.48000E-00

Multiply Interval Vol.
by 1.24 For SSE

R2BLOCKA CRACKED SECTION



Attachment II - SHEET 1

Wall Geometry

Model Grid

Attachment II - SHEET - I

Pinned boundary

118	101	100	91	82	73	64	55	46	37	28	19	10	1
119	101	92	83	74	65	56	47	38	29	20	11	2	2
120	102	93	84	75	66	57	48	39	30	21	12	3	3
121	102	94	85	76	67	58	49	40	31	22	13	4	4
122	103	95	86	77	68	59	50	41	32	23	14	5	5
123	103	96	87	78	69	60	51	42	33	24	15	6	6
124	104	97	88	79	70	61	52	43	34	25	16	7	7
125	107	98	89	80	71	62	53	44	35	26	17	8	8
126	108	99	90	81	72	63	54	45	36	27	18	9	9

Pinned boundary

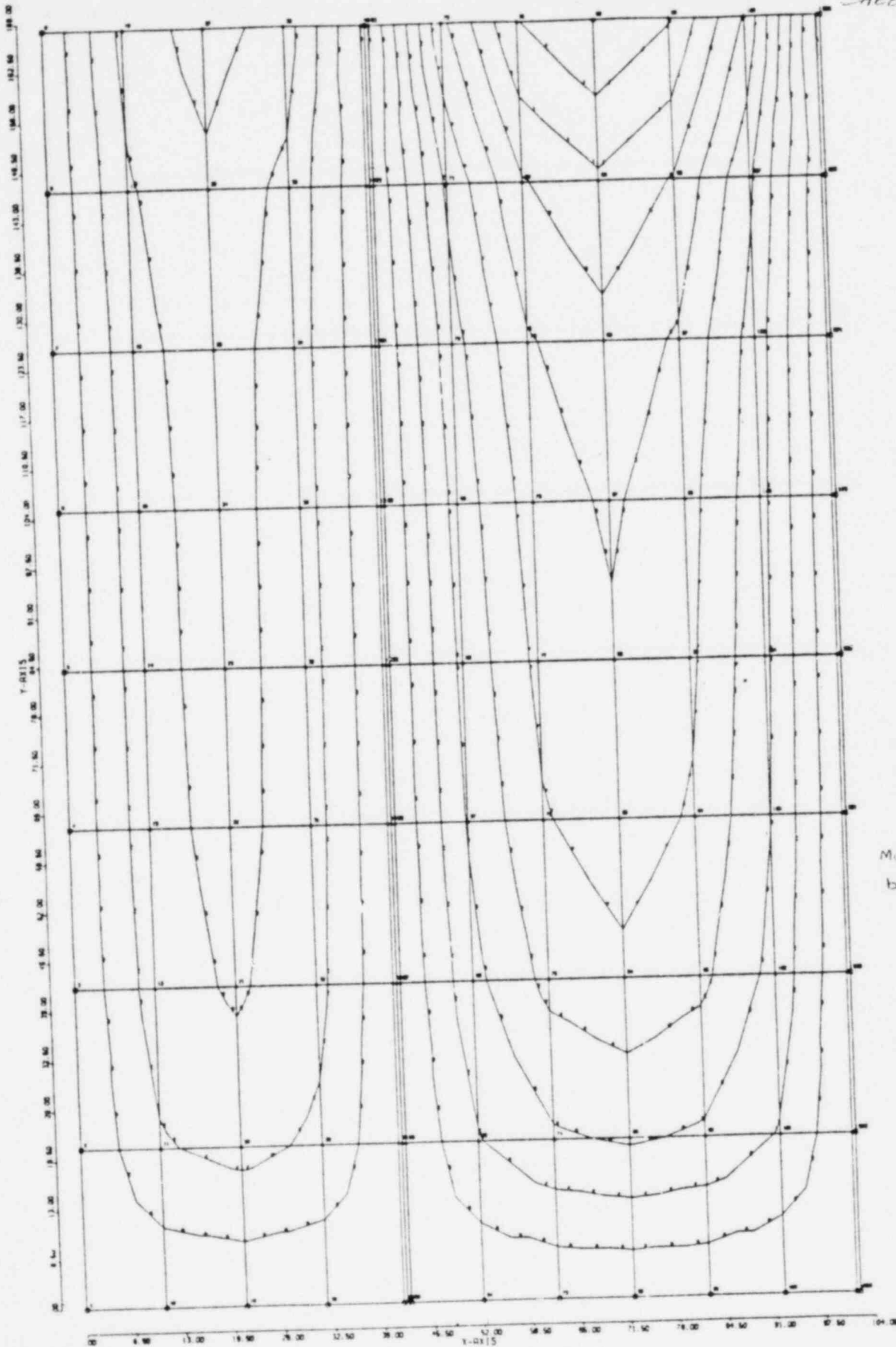
Pinned joint

Pinned joint

This wall panel is hollow core construction. The boundary conditions and member properties along joints 118 thru 126 are adjusted appropriately to take advantage of symmetry in the analysis. The following is an assessment of the results of the analysis for SSE conditions.

	Uncracked Section	Cracked Section
Maximum Horizontal Moment	68 inlb/in	60 inlb/in
Maximum Vertical Moment	116 inlb/in	29 inlb/in
Normal Allowable Moment Horizontal	412 inlb/in	658 inlb/in
SSE Allowable Moment Horizontal	550 inlb/in	877 inlb/in
Cracking Moment Horizontal	1237 inlb/in	N/A
Normal Allowable Moment Vertical	169 inlb/in	N/A
SSE Allowable Moment Vertical	225 inlb/in	N/A
Cracking Moment Vertical	506 inlb/in	N/A

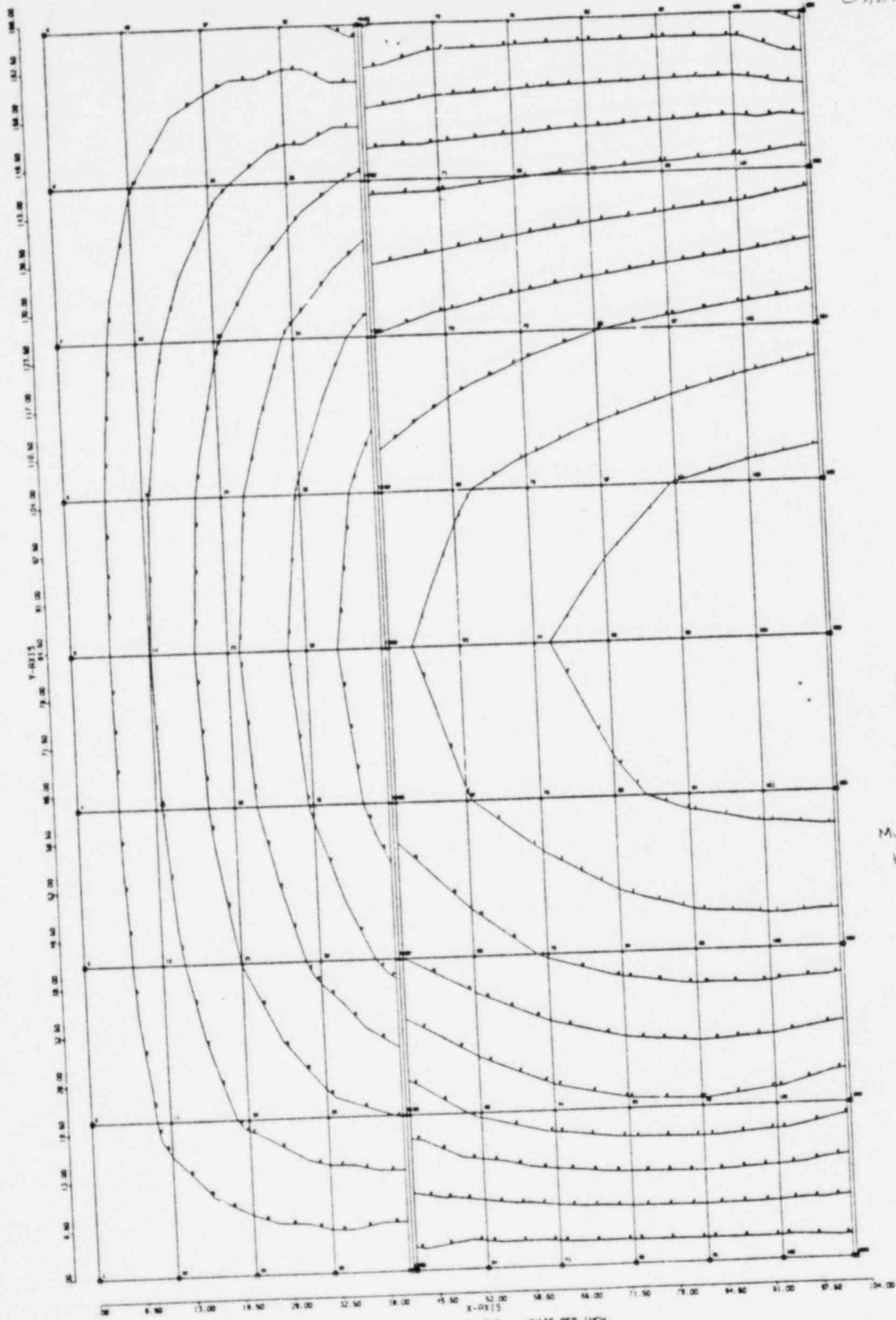
The following four sheets present the stress contours for the wall panel.



LOADING	1
SURFACE	MOBILE
STRESS COUPLES	K
UNITS	LB
INTERVAL	VALUE
0	0.0
1	1.0000E+01
2	1.1111E+01
3	1.2500E+01
4	1.4286E+01
5	1.6667E+01
6	2.0000E+01
7	2.3333E+01
8	2.6667E+01
9	3.0000E+01
10	3.3333E+01
11	3.6667E+01
12	4.0000E+01

Multiply Interval Value
by 0.43 for SSE

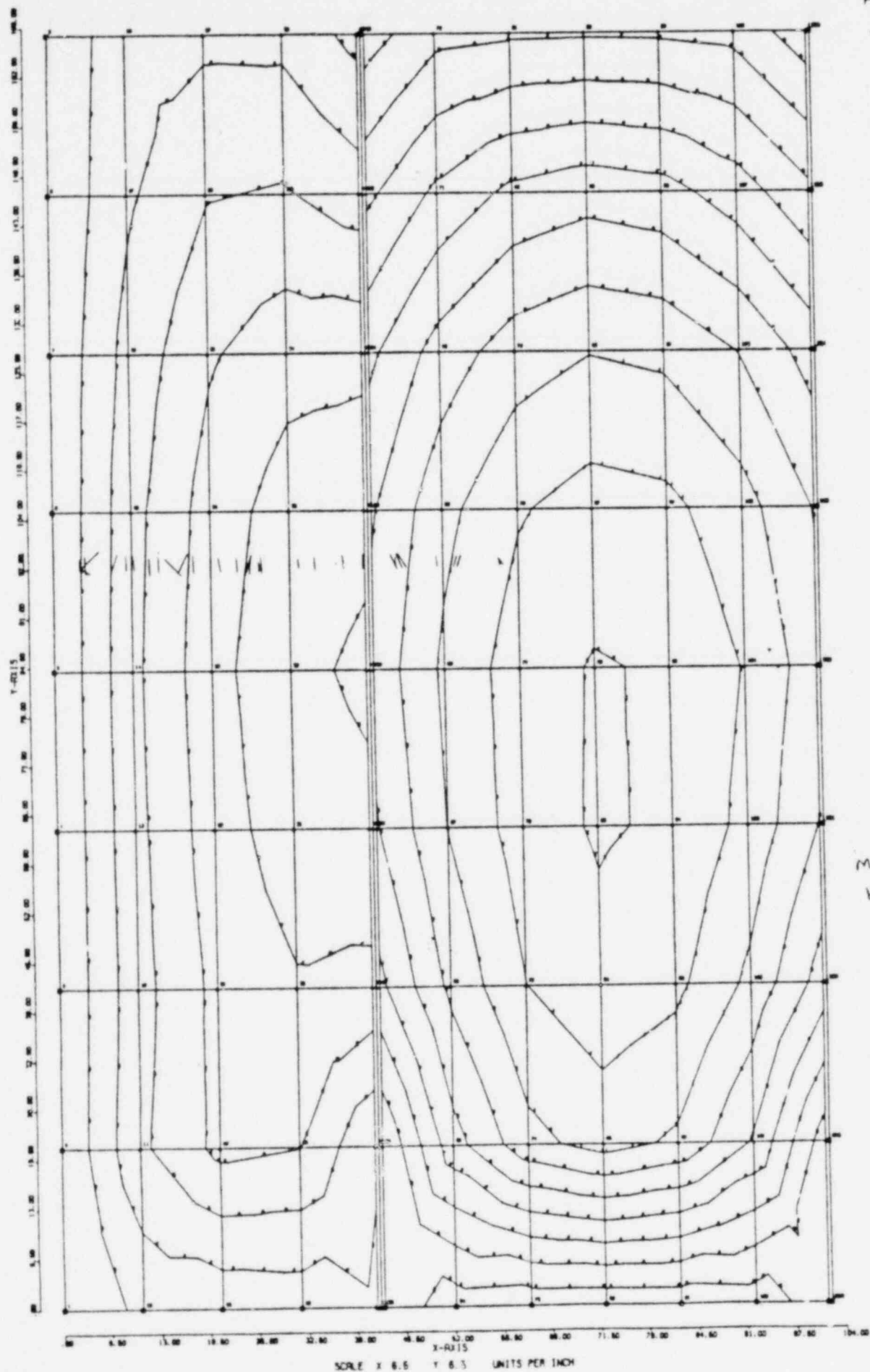
R2BLOCKB UNCRACKED SECTION



LONGITUDINAL	MIDDLE
SURFACE	STRESS COUPLES 1/2
UNITS LB	INCH
INTERVAL	VALUE
0.0	0.0
1.0	0.00000000
2.0	0.00000000
3.0	0.00000000
4.0	0.00000000
5.0	0.00000000
6.0	0.00000000
7.0	0.00000000
8.0	0.00000000
9.0	0.00000000
10.0	0.00000000
11.0	0.00000000
12.0	0.00000000
13.0	0.00000000
14.0	0.00000000
15.0	0.00000000
16.0	0.00000000
17.0	0.00000000
18.0	0.00000000
19.0	0.00000000
20.0	0.00000000
21.0	0.00000000
22.0	0.00000000
23.0	0.00000000
24.0	0.00000000
25.0	0.00000000
26.0	0.00000000
27.0	0.00000000
28.0	0.00000000
29.0	0.00000000
30.0	0.00000000
31.0	0.00000000
32.0	0.00000000
33.0	0.00000000
34.0	0.00000000
35.0	0.00000000
36.0	0.00000000
37.0	0.00000000
38.0	0.00000000
39.0	0.00000000
40.0	0.00000000
41.0	0.00000000
42.0	0.00000000
43.0	0.00000000
44.0	0.00000000
45.0	0.00000000
46.0	0.00000000
47.0	0.00000000
48.0	0.00000000
49.0	0.00000000
50.0	0.00000000
51.0	0.00000000
52.0	0.00000000
53.0	0.00000000
54.0	0.00000000
55.0	0.00000000
56.0	0.00000000
57.0	0.00000000
58.0	0.00000000
59.0	0.00000000
60.0	0.00000000
61.0	0.00000000
62.0	0.00000000
63.0	0.00000000
64.0	0.00000000
65.0	0.00000000
66.0	0.00000000
67.0	0.00000000
68.0	0.00000000
69.0	0.00000000
70.0	0.00000000
71.0	0.00000000
72.0	0.00000000
73.0	0.00000000
74.0	0.00000000
75.0	0.00000000
76.0	0.00000000
77.0	0.00000000
78.0	0.00000000
79.0	0.00000000
80.0	0.00000000
81.0	0.00000000
82.0	0.00000000
83.0	0.00000000
84.0	0.00000000
85.0	0.00000000
86.0	0.00000000
87.0	0.00000000
88.0	0.00000000
89.0	0.00000000
90.0	0.00000000
91.0	0.00000000
92.0	0.00000000
93.0	0.00000000
94.0	0.00000000
95.0	0.00000000
96.0	0.00000000
97.0	0.00000000
98.0	0.00000000
99.0	0.00000000
100.0	0.00000000

Multiply Interval Values
by 0.43 For SSE

R2BLOCK8 UNCRACKED SECTION



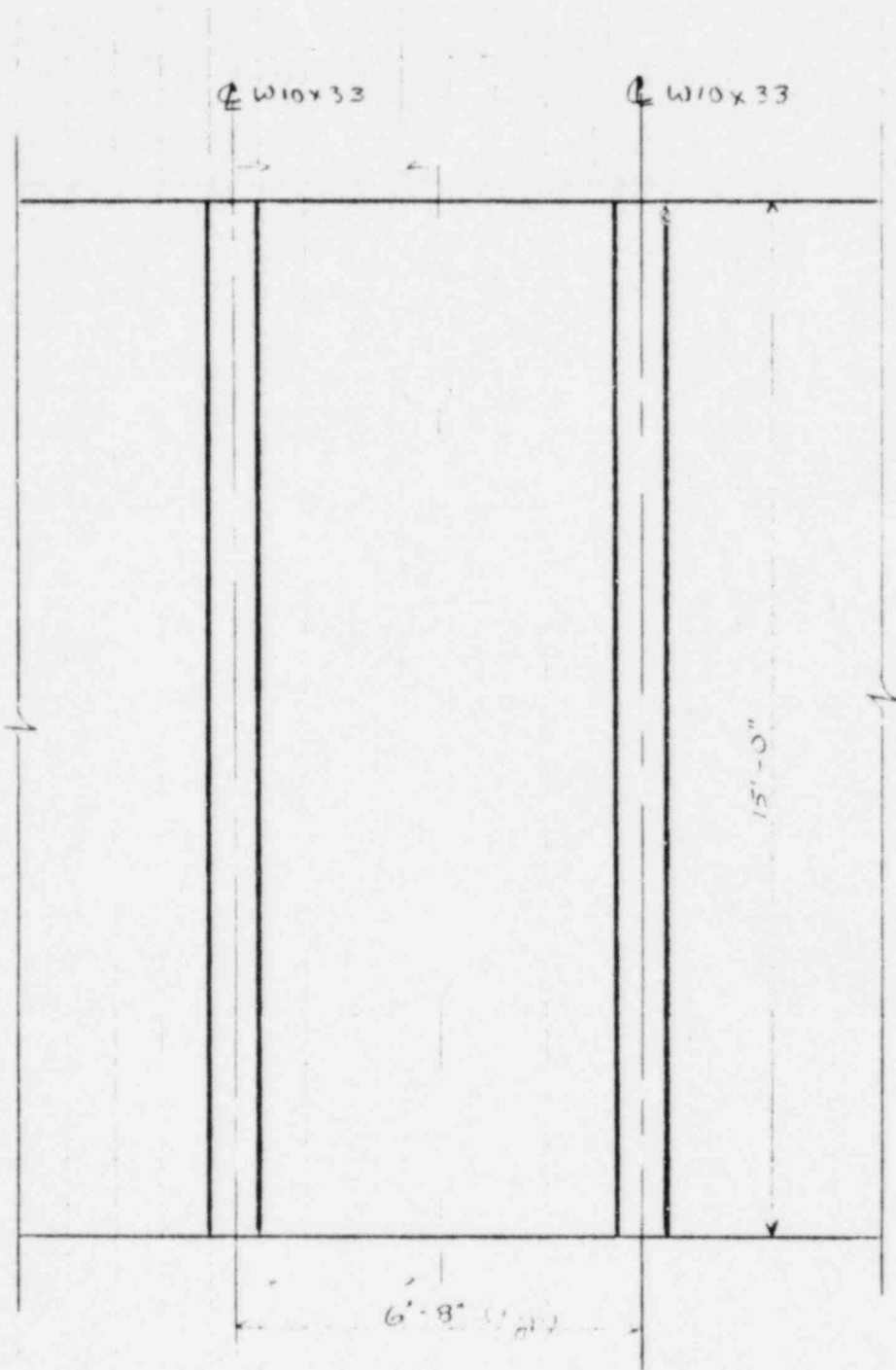
R2BLOCKB CRACKED SECTION

```

LOADING 1
SURFACE NODES
STRESS COMPLEX 1/
UNITS LB INCH
INTERNAL VALUE

```

R2BLOCKB CRACKED SECTION



Attachment III - Sheet 1

Wall Geometry

Pinned joint

56	57	58	59	60
9	18	27	36	
50	51	52	53	54
8	17	26	35	
44	45	46	47	48
7	16	25	34	
38	39	40	41	42
6	15	24	33	
32	33	34	35	36
5	14	23	32	
26	27	28	29	30
4	13	22	31	
20	21	22	23	24
3	12	21	30	
14	15	16	17	18
2	11	20	29	
8	9	10	11	12
1	10	19	28	
1	2	3	4	5

Pinned boundary

Attachment III - SHEET 2

Model Grid

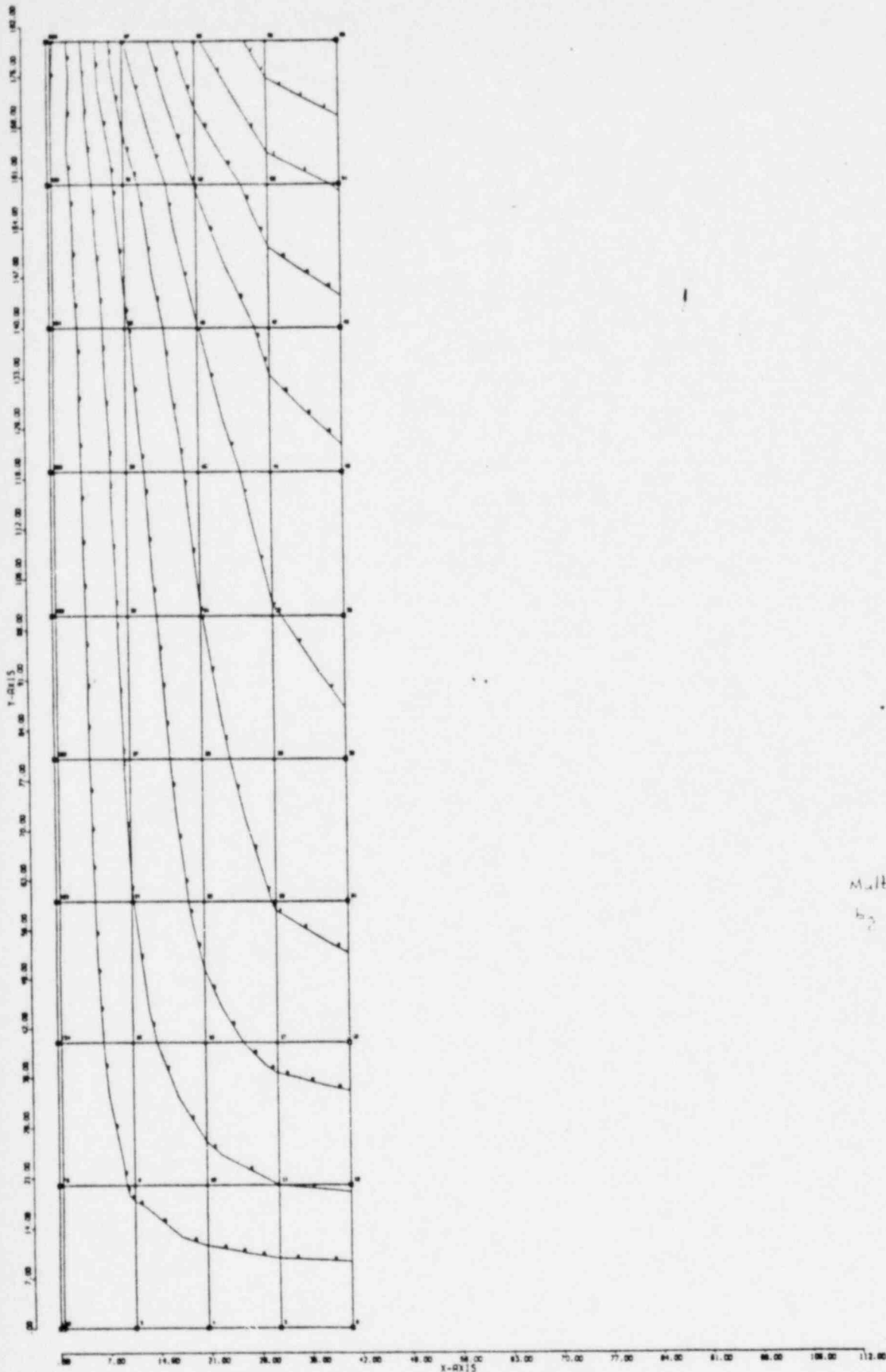
This wall panel is hollow core construction. The boundary conditions and member properties along joints 6 thru 60 by 10 are adjusted appropriately to take advantage of symmetry in the analysis. The following is an assessment of the results of the analysis for SSE conditions.

	Uncracked Section	Cracked Section
Maximum Horizontal Moment	175 inlb/in	314 inlb/in
Maximum Vertical Moment	258 inlb/in	145 inlb/in
Normal Allowable Moment Horizontal	412 inlb/in	658 inlb/in
SSE Allowable Moment Horizontal	550 inlb/in	877 inlb/in
Cracking Moment Horizontal	1237 inlb/in	N/A
Normal Allowable Moment Vertical	169 inlb/in	N/A
SSE Allowable Moment Vertical	225 inlb/in	N/A
Cracking Moment Vertical	506 inlb/in	N/A

The following four sheets present the stress contours for the wall panel.

Attachment III

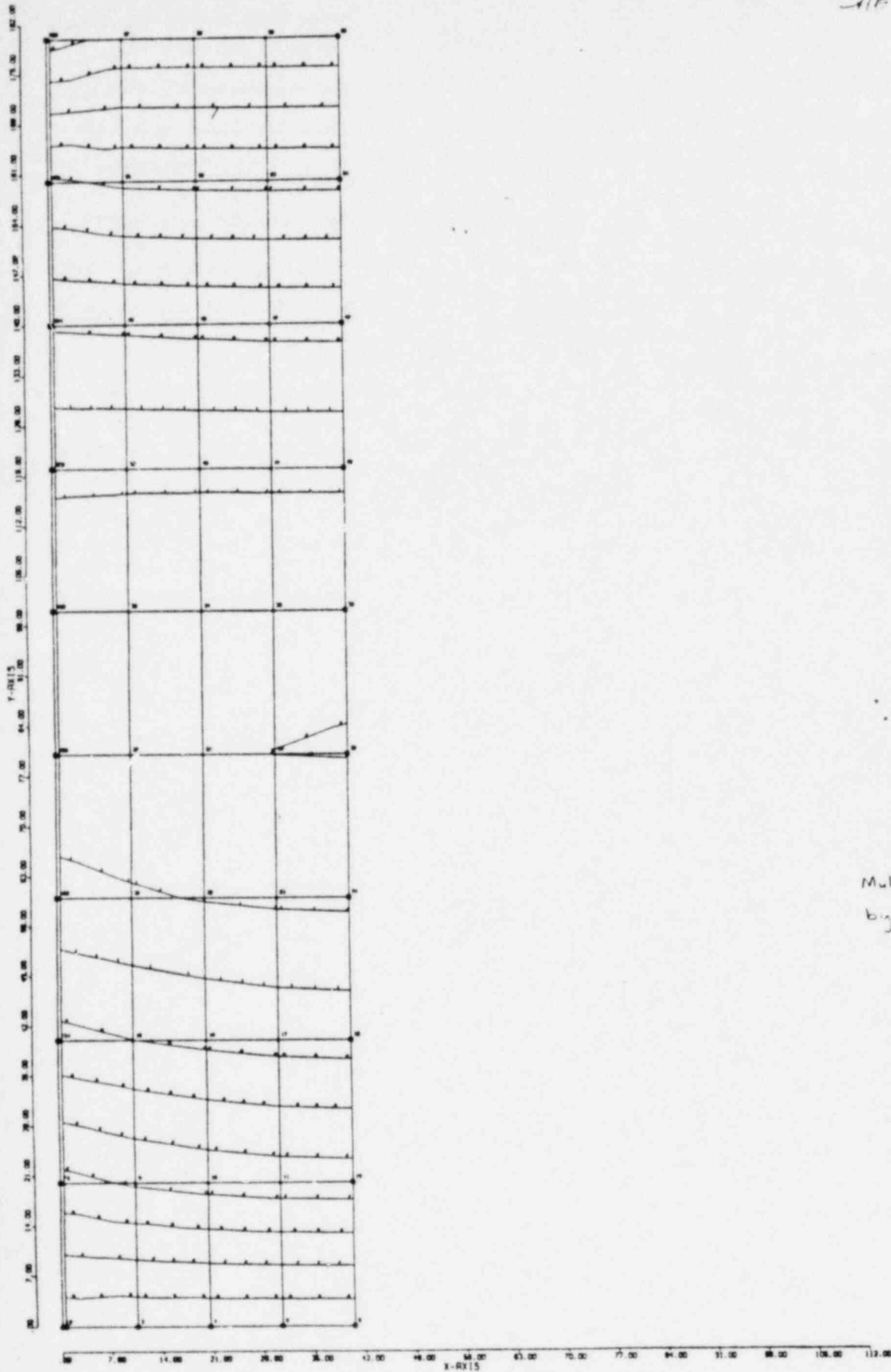
SHEET 1



R2BLOCKC UNCRACKED SECTION

LOCATION	1
SURFACE	MIDDLE
STRESS COUPLES X/	
UNITS LB INCH	
INTERNAL	VALUE
1	0.0
2	0.0
3	0.0
4	0.0
5	0.0
6	0.0
7	0.0
8	0.0
9	0.0
10	0.0
11	0.0
12	0.0
13	0.0
14	0.0
15	0.0
16	0.0
17	0.0
18	0.0
19	0.0
20	0.0
21	0.0
22	0.0
23	0.0
24	0.0
25	0.0
26	0.0
27	0.0
28	0.0
29	0.0
30	0.0
31	0.0
32	0.0
33	0.0
34	0.0
35	0.0
36	0.0
37	0.0
38	0.0
39	0.0
40	0.0
41	0.0
42	0.0
43	0.0
44	0.0
45	0.0
46	0.0
47	0.0
48	0.0
49	0.0
50	0.0
51	0.0
52	0.0
53	0.0
54	0.0
55	0.0
56	0.0
57	0.0
58	0.0
59	0.0
60	0.0
61	0.0
62	0.0
63	0.0
64	0.0
65	0.0
66	0.0
67	0.0
68	0.0
69	0.0
70	0.0
71	0.0
72	0.0
73	0.0
74	0.0
75	0.0
76	0.0
77	0.0
78	0.0
79	0.0
80	0.0
81	0.0
82	0.0
83	0.0
84	0.0
85	0.0
86	0.0
87	0.0
88	0.0
89	0.0
90	0.0
91	0.0
92	0.0
93	0.0
94	0.0
95	0.0
96	0.0
97	0.0
98	0.0
99	0.0
100	0.0
101	0.0
102	0.0
103	0.0
104	0.0
105	0.0
106	0.0
107	0.0
108	0.0
109	0.0
110	0.0
111	0.0
112	0.0

Multiply Internal Values
by 0.60 for SSE

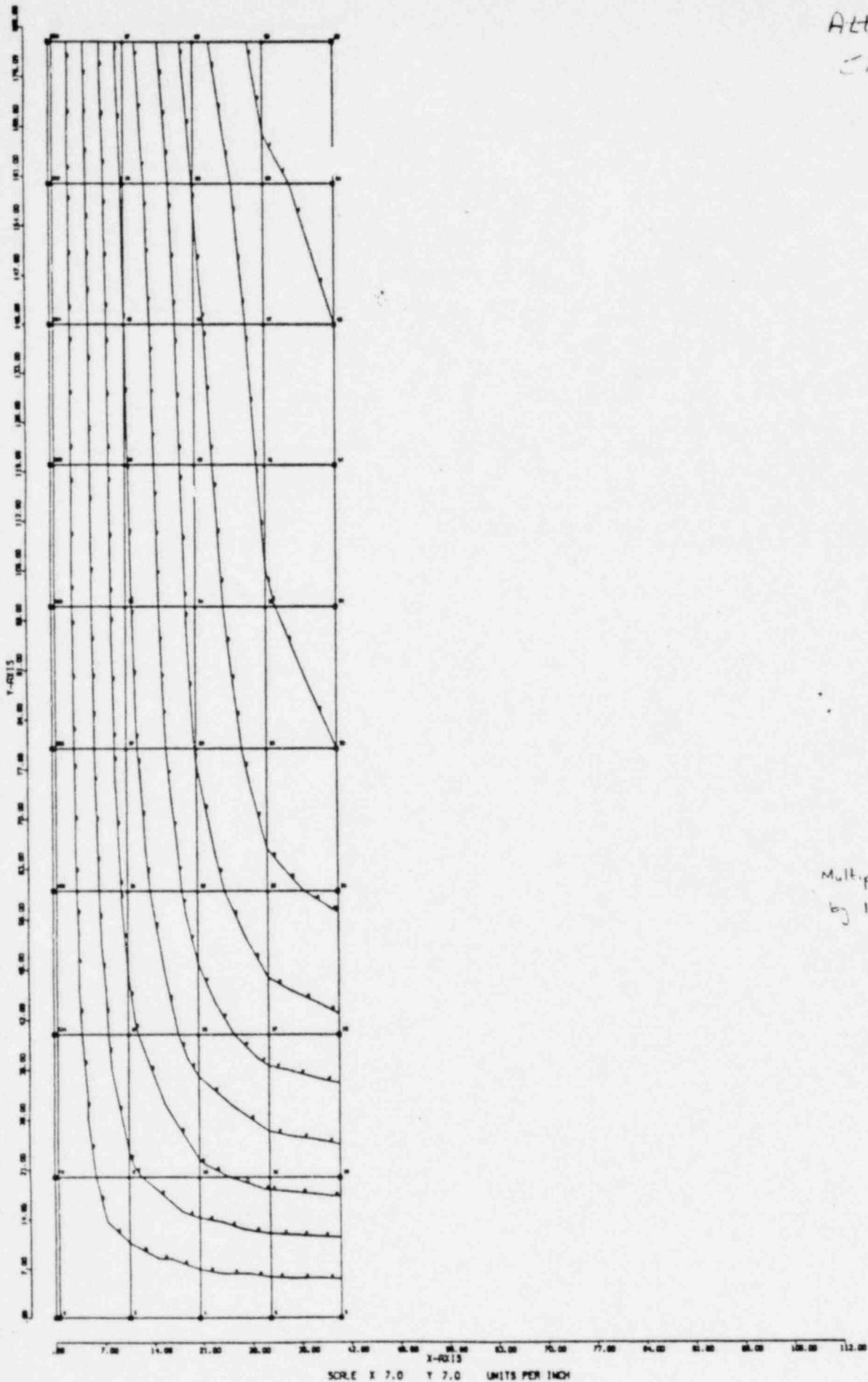


LINE	1
SURFACE	MIDDLE
STRESS COUPLES 1/	
UNITS LB	INCH
INTERVAL	VALUE
A	0.0
B	1.0000E-01
C	8.5700E-01
D	1.0000E-01
E	1.1500E-01
F	1.1500E-01
G	1.1500E-01
H	1.1500E-01
I	1.1500E-01
J	1.1500E-01
K	1.1500E-01

Multiply Interval Values
by 0.160 for SSE

Attachment III

Crack

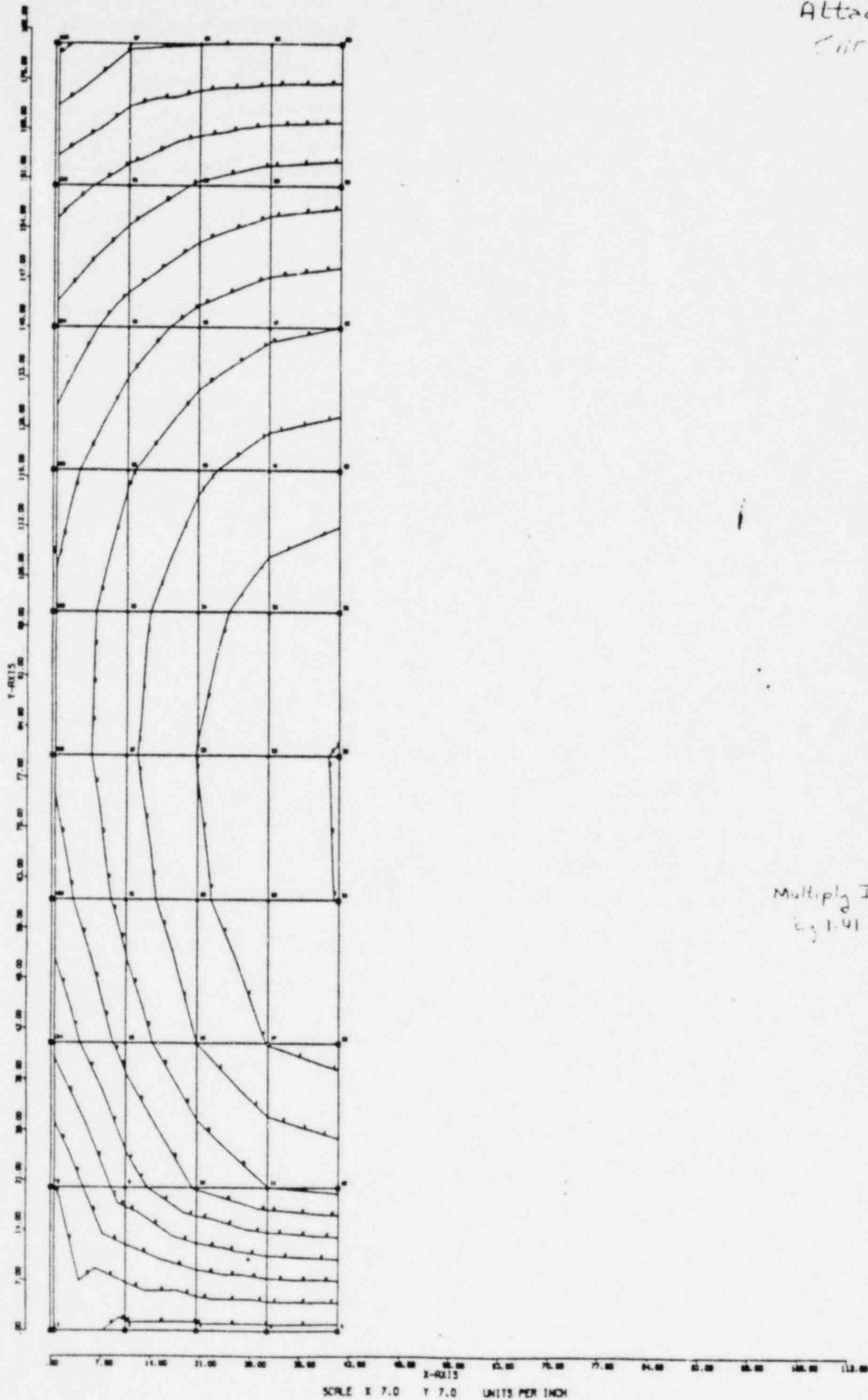


R2BLOCKC CRACKED SECTION

LANDING	1
SURFACE	POSSIBLE
STITCHES	CORRUPUS 1/
UNITS	LB INCH
INTERVAL	VALUE
0	0.0
1	2.0000E-01
2	4.0000E-01
3	6.0000E-01
4	8.0000E-01
5	1.0000E-01
6	1.2000E-01
7	1.4000E-01
8	1.6000E-01
9	1.8000E-01
10	2.0000E-01
11	2.2000E-01
12	2.4000E-01

Multiply Interval Values
by 1.41 for SSE

Attachment III . .
Sheet 7



LONGITUDE	1
SURFACE	MODEL
STRESS	COUPLES Y/
UNITS	LB INCH
INTERVAL	VALUE
1	0.0
2	1.0000E+01
3	2.0000E+01
4	3.0000E+01
5	4.0000E+01
6	5.0000E+01
7	6.0000E+01
8	7.0000E+01
9	8.0000E+01
10	9.0000E+01
11	1.0000E+02

Multiply Interval Values
by 1.41 for SSE

R2BLOCKC CRACKED SECTION

Project Name

Drawn by

Scale

Date

Page

Client

Project No.

Sheet No.

Total



Attachment IV - *Sheet 1*

Wall Geometry

Pinned joint

55	56	57	58	59	60
	9	18	27	36	
49	50	51	52	53	54
	8	17	26	35	
43	44	45	46	47	48
	7	16	25	34	
37	38	39	40	41	42
	6	15	24	33	
31	32	33	34	35	36
	5	14	23	32	
25	26	27	28	29	30
	4	13	22	31	
19	20	21	22	23	24
	3	12	21	30	
13	14	15	16	17	18
	2	11	20	29	
7	8	9	10	11	12
	1	10	19	28	
1	2	3	4	5	6

Pinned boundary

Attachment II Circ. 11

Model Grid

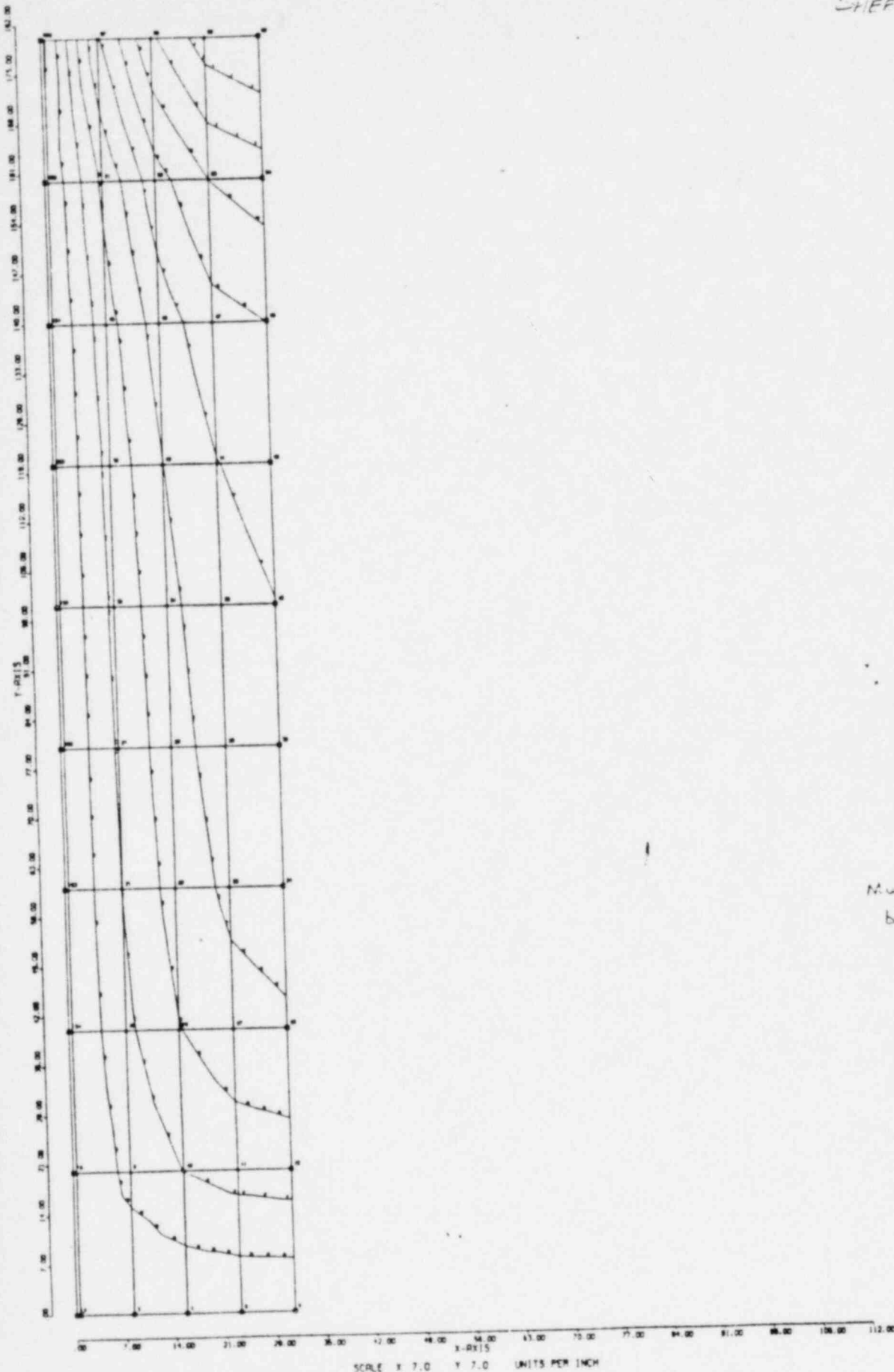
This wall panel is hollow core construction. The boundary conditions and member properties along joints 6 thru 60 by 10 are adjusted appropriately to take advantage of symmetry in the analysis. The following is an assessment of the results of the analysis for SSE conditions.

	Uncracked Section	Cracked Section
Maximum Horizontal Moment	81 inlb/in	100 in lb/in
Maximum Vertical Moment	165 inlb/in	57 in lb/in
Normal Allowable Moment Horizontal	412 inlb/in	658 inlb/in
SSE Allowable Moment Horizontal	550 inlb/in	877 inlb/in
Cracking Moment Horizontal	1237 inlb/in	N/A
Normal Allowable Moment Vertical	169 inlb/in	N/A
SSE Allowable Moment Vertical	225 inlb/in	N/A
Cracking Moment Vertical	506 inlb/in	N/A

The following four sheets present the stress contours for the wall panel.

Attachment IV

SHEET 4

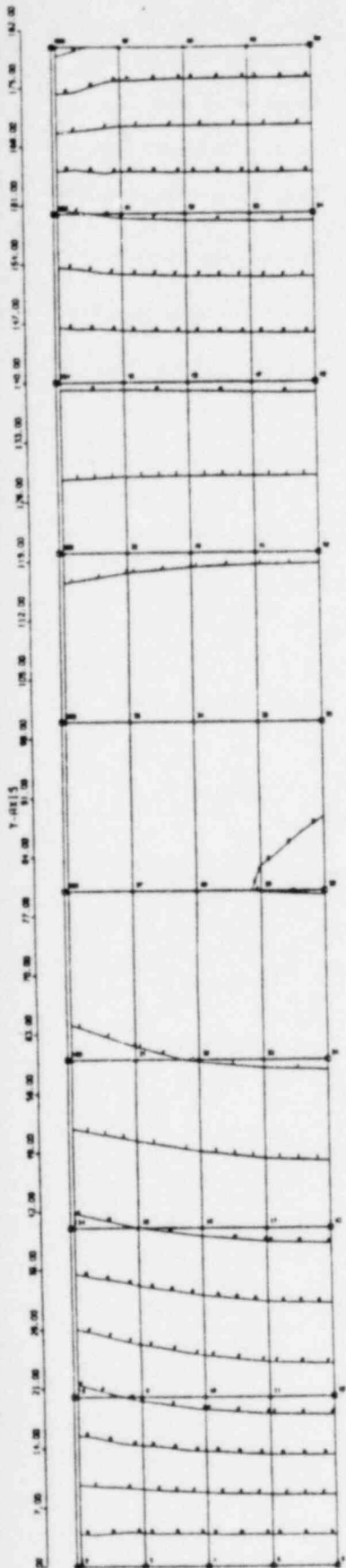


LOADING 1	
SURFACE PITCH	
STRESS COUPLES X	
UNITS	INCH
INTERVAL	VALUE
0	0.0
1	1.7000E-01
2	3.4000E-01
3	5.1000E-01
4	6.8000E-01
5	8.5000E-01
6	1.0200E-01
7	1.1900E-01
8	1.3600E-01
9	1.5300E-01
10	1.7000E-01

Multiply Interval values
by 0.45 for SSE

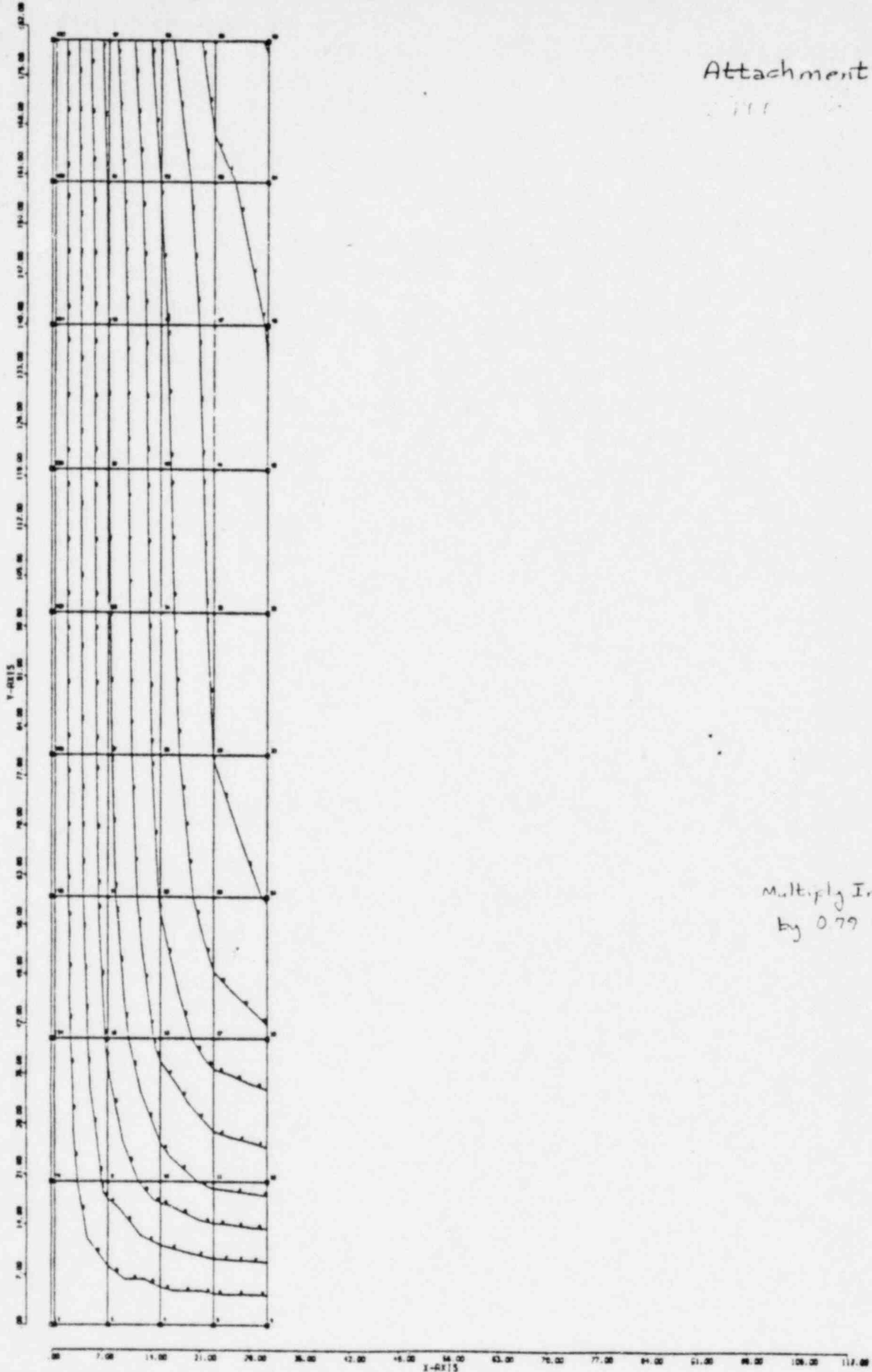
R2BLOCKD UNCRACKED SECTION

Attachment IV



LINE	1	2
SURFACE	1	2
STRESS COEFFICIENTS	1	2
UNITS	LB	INCH
INTERVAL	VALUE	
0	0.0	
1	1.0000E-01	
2	1.1000E-01	
3	1.2000E-01	
4	1.3000E-01	
5	1.4000E-01	
6	1.5000E-01	
7	1.6000E-01	
8	1.7000E-01	
9	1.8000E-01	
10	1.9000E-01	
11	2.0000E-01	
12	2.1000E-01	
13	2.2000E-01	
14	2.3000E-01	
15	2.4000E-01	
16	2.5000E-01	
17	2.6000E-01	
18	2.7000E-01	
19	2.8000E-01	
20	2.9000E-01	
21	3.0000E-01	
22	3.1000E-01	
23	3.2000E-01	
24	3.3000E-01	
25	3.4000E-01	
26	3.5000E-01	
27	3.6000E-01	
28	3.7000E-01	
29	3.8000E-01	
30	3.9000E-01	
31	4.0000E-01	
32	4.1000E-01	
33	4.2000E-01	
34	4.3000E-01	
35	4.4000E-01	
36	4.5000E-01	
37	4.6000E-01	
38	4.7000E-01	
39	4.8000E-01	
40	4.9000E-01	
41	5.0000E-01	
42	5.1000E-01	
43	5.2000E-01	
44	5.3000E-01	
45	5.4000E-01	
46	5.5000E-01	
47	5.6000E-01	
48	5.7000E-01	
49	5.8000E-01	
50	5.9000E-01	
51	6.0000E-01	
52	6.1000E-01	
53	6.2000E-01	
54	6.3000E-01	
55	6.4000E-01	
56	6.5000E-01	
57	6.6000E-01	
58	6.7000E-01	
59	6.8000E-01	
60	6.9000E-01	
61	7.0000E-01	
62	7.1000E-01	
63	7.2000E-01	
64	7.3000E-01	
65	7.4000E-01	
66	7.5000E-01	
67	7.6000E-01	
68	7.7000E-01	
69	7.8000E-01	
70	7.9000E-01	
71	8.0000E-01	
72	8.1000E-01	
73	8.2000E-01	
74	8.3000E-01	
75	8.4000E-01	
76	8.5000E-01	
77	8.6000E-01	
78	8.7000E-01	
79	8.8000E-01	
80	8.9000E-01	
81	9.0000E-01	
82	9.1000E-01	
83	9.2000E-01	
84	9.3000E-01	
85	9.4000E-01	
86	9.5000E-01	
87	9.6000E-01	
88	9.7000E-01	
89	9.8000E-01	
90	9.9000E-01	
91	1.0000E-01	
92	1.1000E-01	
93	1.2000E-01	
94	1.3000E-01	
95	1.4000E-01	
96	1.5000E-01	
97	1.6000E-01	
98	1.7000E-01	
99	1.8000E-01	
100	1.9000E-01	
101	2.0000E-01	
102	2.1000E-01	
103	2.2000E-01	
104	2.3000E-01	
105	2.4000E-01	
106	2.5000E-01	
107	2.6000E-01	
108	2.7000E-01	
109	2.8000E-01	
110	2.9000E-01	
111	3.0000E-01	
112	3.1000E-01	
113	3.2000E-01	
114	3.3000E-01	
115	3.4000E-01	
116	3.5000E-01	
117	3.6000E-01	
118	3.7000E-01	
119	3.8000E-01	
120	3.9000E-01	
121	4.0000E-01	
122	4.1000E-01	
123	4.2000E-01	
124	4.3000E-01	
125	4.4000E-01	
126	4.5000E-01	
127	4.6000E-01	
128	4.7000E-01	
129	4.8000E-01	
130	4.9000E-01	
131	5.0000E-01	
132	5.1000E-01	
133	5.2000E-01	
134	5.3000E-01	
135	5.4000E-01	
136	5.5000E-01	
137	5.6000E-01	
138	5.7000E-01	
139	5.8000E-01	
140	5.9000E-01	
141	6.0000E-01	
142	6.1000E-01	
143	6.2000E-01	
144	6.3000E-01	
145	6.4000E-01	
146	6.5000E-01	
147	6.6000E-01	
148	6.7000E-01	
149	6.8000E-01	
150	6.9000E-01	
151	7.0000E-01	
152	7.1000E-01	
153	7.2000E-01	
154	7.3000E-01	
155	7.4000E-01	
156	7.5000E-01	
157	7.6000E-01	
158	7.7000E-01	
159	7.8000E-01	
160	7.9000E-01	
161	8.0000E-01	
162	8.1000E-01	
163	8.2000E-01	
164	8.3000E-01	
165	8.4000E-01	
166	8.5000E-01	
167	8.6000E-01	
168	8.7000E-01	
169	8.8000E-01	
170	8.9000E-01	
171	9.0000E-01	
172	9.1000E-01	
173	9.2000E-01	
174	9.3000E-01	
175	9.4000E-01	
176	9.5000E-01	
177	9.6000E-01	
178	9.7000E-01	
179	9.8000E-01	
180	9.9000E-01	
181	1.0000E-01	
182	1.1000E-01	
183	1.2000E-01	
184	1.3000E-01	
185	1.4000E-01	
186	1.5000E-01	
187	1.6000E-01	
188	1.7000E-01	
189	1.8000E-01	
190	1.9000E-01	
191	2.0000E-01	
192	2.1000E-01	
193	2.2000E-01	
194	2.3000E-01	
195	2.4000E-01	
196	2.5000E-01	
197	2.6000E-01	
198	2.7000E-01	
199	2.8000E-01	
200	2.9000E-01	
201	3.0000E-01	
202	3.1000E-01	
203	3.2000E-01	
204	3.3000E-01	
205	3.4000E-01	
206	3.5000E-01	
207	3.6000E-01	
208	3.7000E-01	
209	3.8000E-01	
210	3.9000E-01	
211	4.0000E-01	
212	4.1000E-01	
213	4.2000E-01	
214	4.3000E-01	
215	4.4000E-01	
216	4.5000E-01	
217	4.6000E-01	
218	4.7000E-01	
219	4.8000E-01	
220	4.9000E-01	
221	5.0000E-01	
222	5.1000E-01	
223	5.2000E-01	
224	5.3000E-01	
225	5.4000E-01	
226	5.5000E-01	
227	5.6000E-01	
228	5.7000E-01	
229	5.8000E-01	
230	5.9000E-01	
231	6.0000E-01	
232	6.1000E-01	
233	6.2000E-01	
234	6.3000E-01	
235	6.4000E-01	
236	6.5000E-01	
237	6.6000E-01	
238	6.7000E-01	
239	6.8000E-01	
240	6.9000E-01	
241	7.0000E-01	
242	7.1000E-01	
243	7.2000E-01	
244	7.3000E-01	
245	7.4000E-01	
246	7.5000E-01	
247	7.6000E-01	
248	7.7000E-01	
249	7.8000E-01	
250	7.9000E-01	
251	8.0000E-01	
252	8.1000E-01	
253	8.2000E-01	
254	8.3000E-01	
255	8.4000E-01	
256	8.5000E-01	
257	8.6000E-01	
258	8.7000E-01	
259	8.8000E-01	
260	8.9000E-01	
261	9.0000E-01	
262	9.1000E-01	
263	9.2000E-01	
264	9.3000E-01	
265	9.4000E-01	
266	9.5000E-01	
267	9.6000E-01	
268	9.7000E-01	
269	9.8000E-01	
270	9.9000E-01	
271	1.0000E-01	
272	1.1000E-01	
273	1.2000E-01	
274	1.3000E-01	
275	1.4000E-01	
276	1.5000E-01	
277	1.6000E-01	
278	1.7000E-01	
279	1.8000E-01	
280	1.9000E-01	
281	2.0000E-01	
282	2.1000E-01	
283	2.2000E-01	
284	2.3000E-01	
285	2.4000E-01	
286	2.5000E-01	
287	2.6000E-01	
288	2.7000E-01	
289	2.8000E-01	
290	2.9000E-01	
291	3.0000E-01	
292	3.1000E-01	
293	3.2000E-01	
294	3.3000E-01	
295	3.4000E-01	
296	3.5000E-01	
297	3.6000E-01	
298	3.7000E-01	
299	3.8000E-01	
300	3.9000E-01	
301	4.0000E-01	
302	4.1000E-01	
303	4.2000E-01	
304	4.3000E-01	
305	4.4000E-01	
306	4.5000E-01	
307	4.6000E-01	
308	4.7000E-01	
309	4.8000E-01	
310	4.9000E-01	
311	5.0000E-01	
312	5.1000E-01	
313	5.2000E-01	
314	5.3000E-01	
315	5.4000E-01	
316	5.5000E-01	
317	5.6000E-01	
318	5.7000E-01	
319	5.8000E-01	
320	5.9000E-01	
321	6.0000E-01	
322	6.1000E-01	
323	6.2000E-01	
324	6.3000E-01	
325	6.4000E-01	
326	6.5000E-01	
327	6.6000E-01	
328	6.7000E-01	
329	6.8000E-01	
330	6.9000E-01	
331	7.0000E-01	
332	7.1000E-01	
333	7.2000E-01	
334	7.3000E-01	
335	7.4000E-01	
336	7.5000E-01	
337	7.6000E-01	
338	7.7000E-01	
339	7.8000E-01	
340	7.9000E-01	
341	8.0000E-01	
342	8.1000E-01	
343	8.2000E-01	
344	8.3000E-01	
345	8.4000E-01	
346	8.5000E-01	
347	8.6000E-01	
348	8.7000E-01	
349	8.8000E-01	
350	8.9000E-01	
351	9.0000E-01	
352	9.1000E-01	
353	9.2000E-01	
354	9.3000E-01	
355	9.4000E-01	
356	9.5000E-01	
357	9.6000E-01	
358	9.7000E-01	
359	9.8000E-01	
360	9.9000E-01	
361	1.0000E-01	
362	1.1000E-01	
363	1.2000E-01	
364	1.3000E-01	
365	1.4000E-01	
366	1.5000E-01	
367	1.	

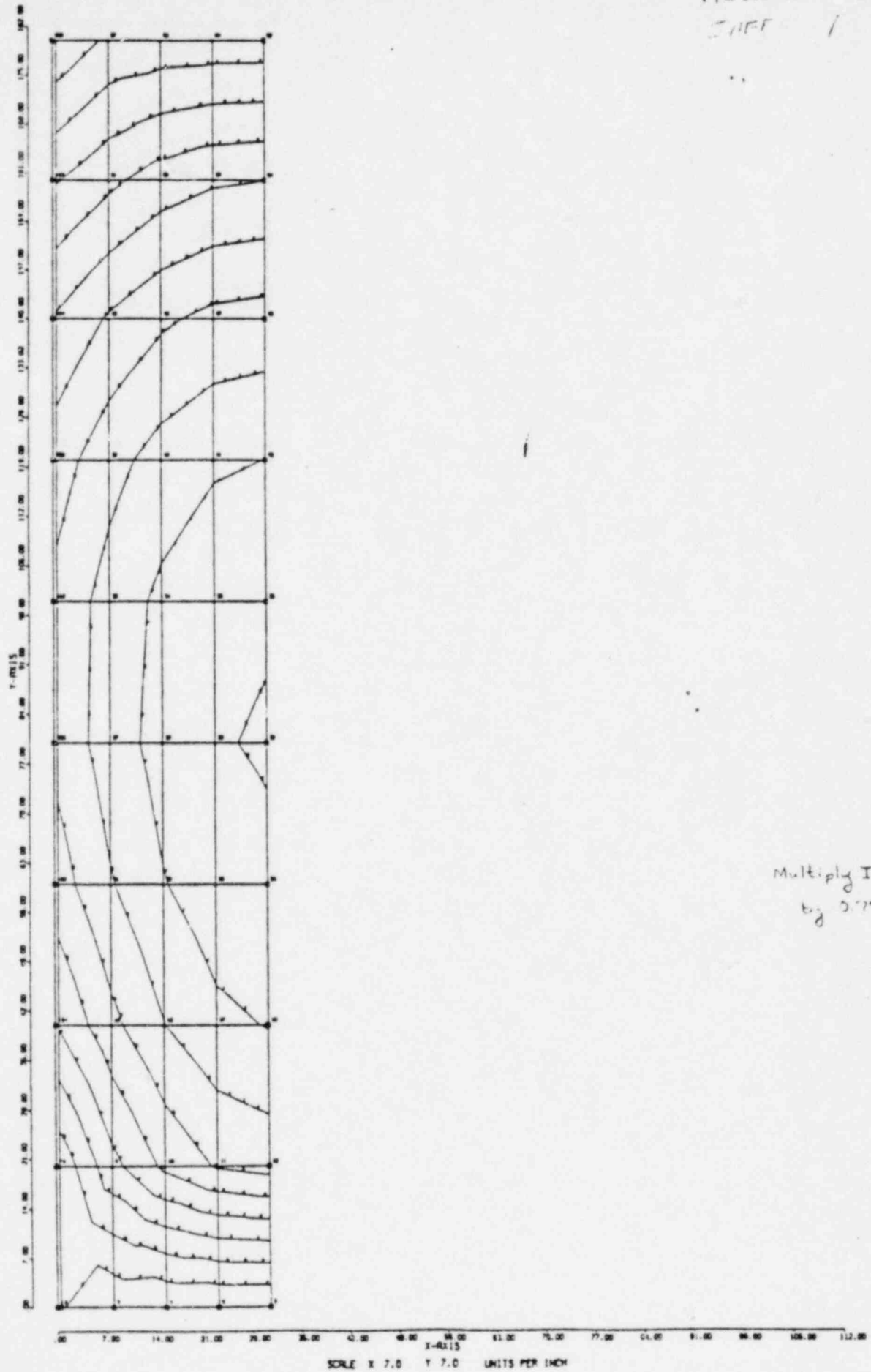
Attachment IV



Multiply Interval Values
by 0.79 for SSE

R2BLOCKD CRACKED SECTION

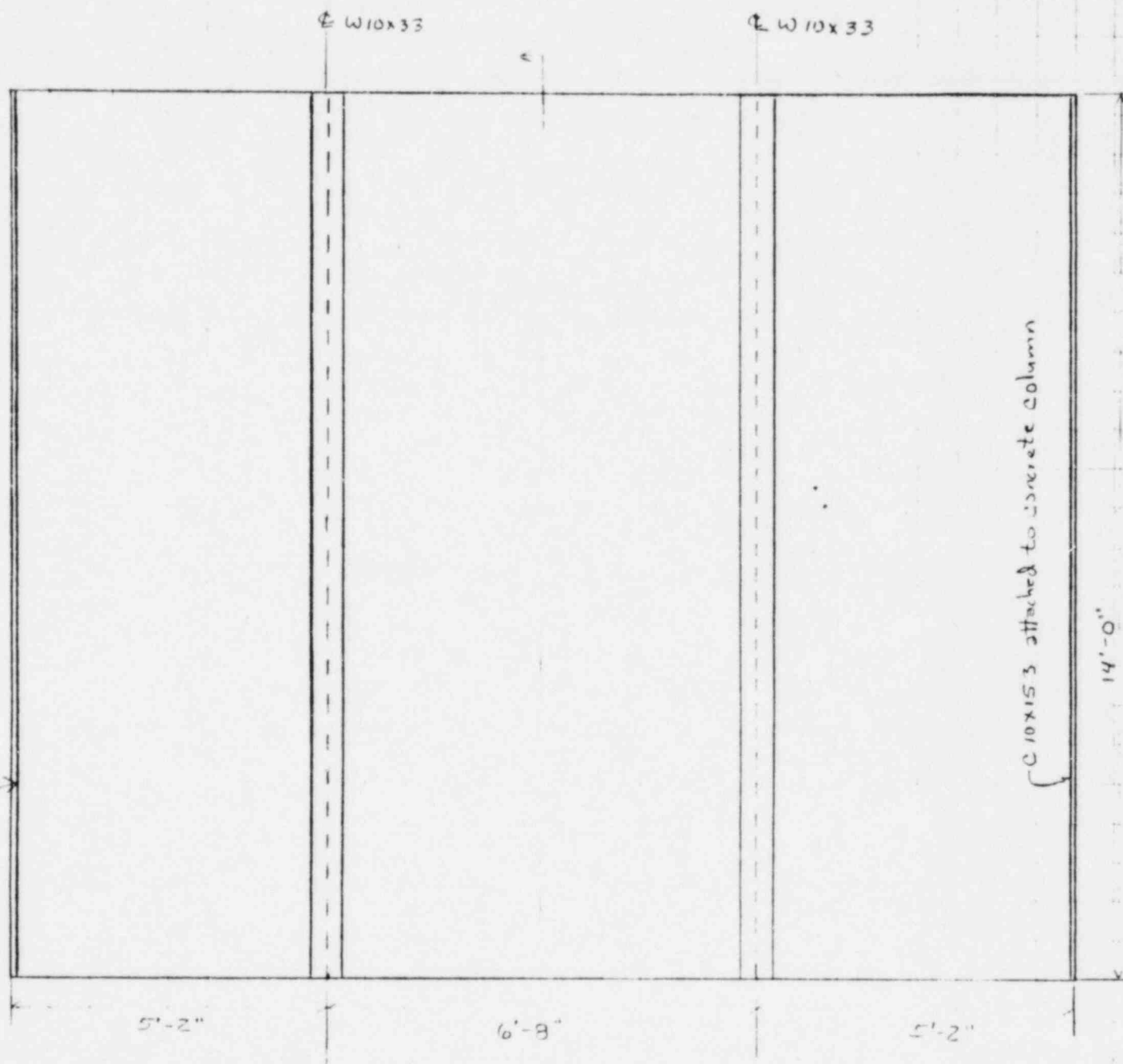
DIFF 1



Multiply Internal Value
by 2.79 for SSE

R2BLOCKD CRACKED SECTION

C10x15.3 attached to concrete column



Attachment V

Wall Geometry

Date

Pinned joint

Pinned boundary

9	18	27	36	45	54	63	72	81	90	99	108	117
8	8	16	24	32	40	48	56	64	72	80		
7	7	15	23	31	39	47	55	63	71	79		
6	6	14	22	30	38	46	54	62	70	78		
5	5	13	21	29	37	45	53	61	69	77		
4	4	12	20	28	36	44	52	60	68	76		
3	3	11	19	27	35	43	51	59	67	75		
2	2	10	18	26	34	42	50	58	66	74		
1	1	9	17	25	33	41	49	57	65	73		
	1	10	19	28	37	46	55	64	73	82	91	100

Pinned boundary

Attachment V SHEET 2

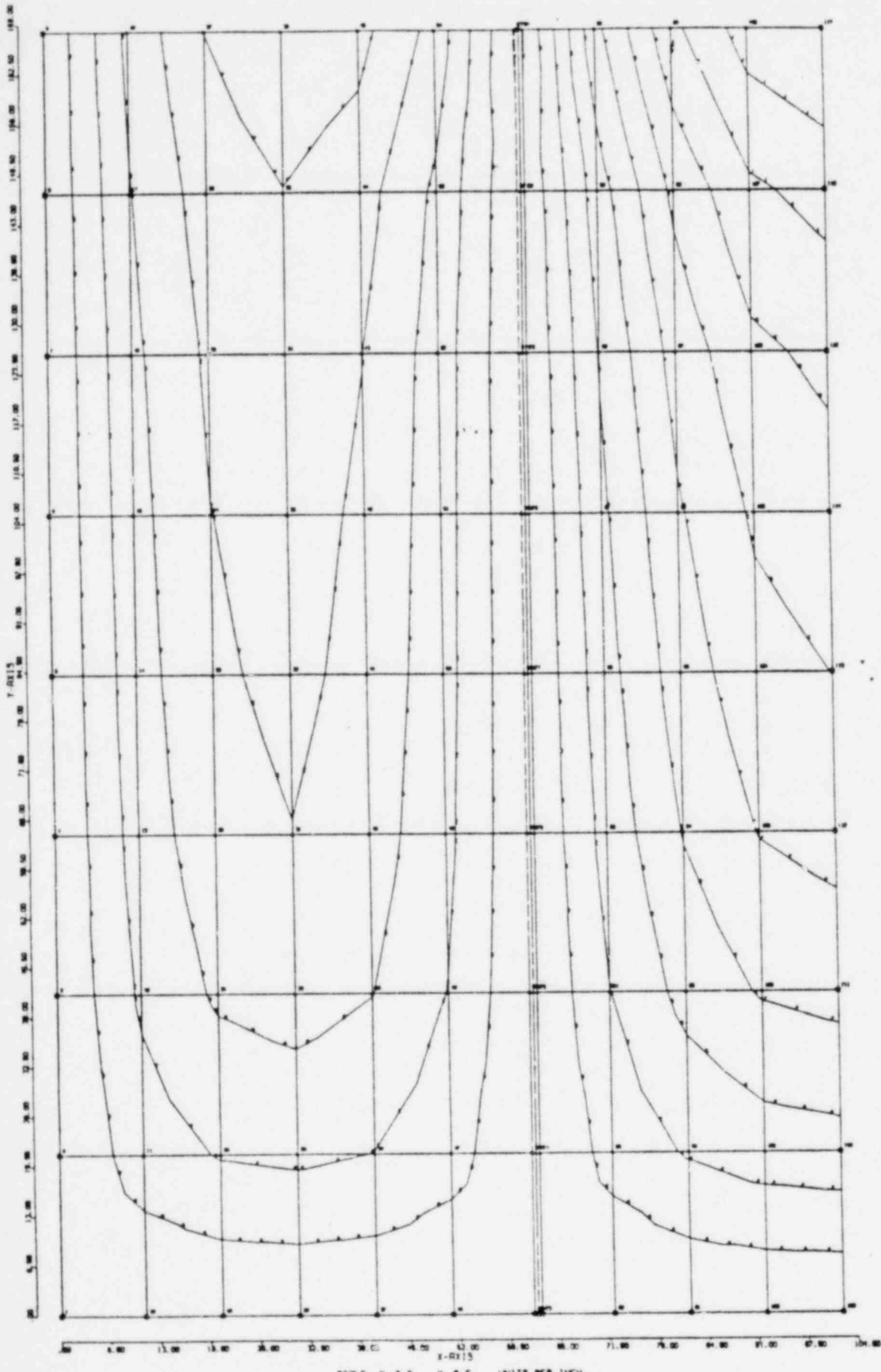
Model Grid

This wall panel is grouted core construction. The boundary conditions and member properties along joints 109 thru 117 are adjusted appropriately to take advantage of symmetry in the analysis. The following is an assessment of the results of the analysis for SSE conditions.

	Uncracked Section	Cracked Section
Maximum Horizontal Moment	336 inlb/in	664 in lb/in
Maximum Vertical Moment	404 inlb/in	272 in lb/in
Normal Allowable Moment Horizontal	727 inlb/in	658 inlb/in
SSE Allowable Moment Horizontal	969 inlb/in	877 inlb/in
Cracking Moment Horizontal	2180 inlb/in	N/A
Normal Allowable Moment Vertical	388 inlb/in	N/A
SSE Allowable Moment Vertical	518 inlb/in	N/A
Cracking Moment Vertical	1166 inlb/in	N/A

The following four sheets present the stress contours for the wall panel.

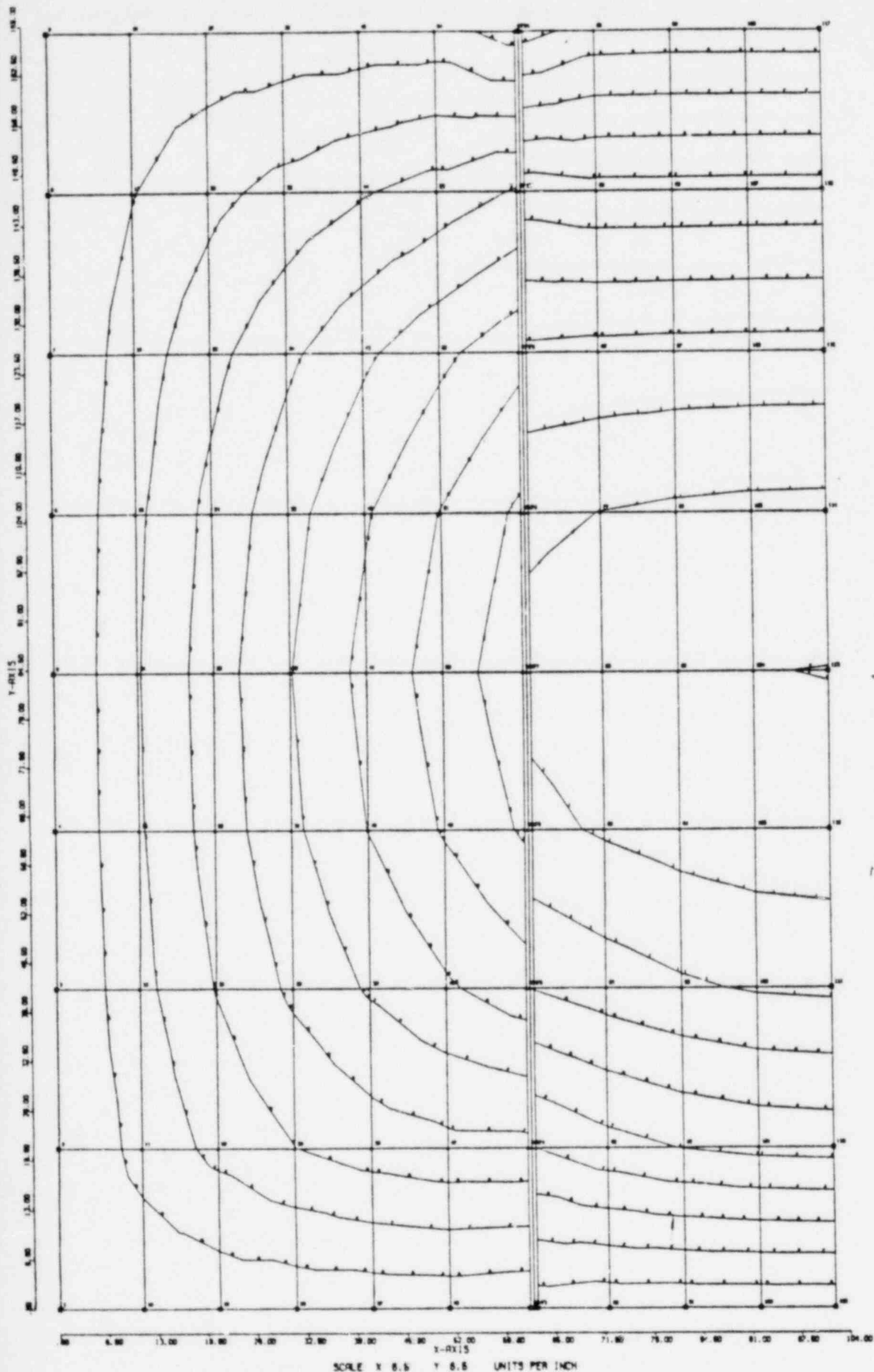
Sheet 4



LOADING	1
SURFACE	MIDDLE
STRESS COEFFICIENT	1
UNIT	LB
INTERVAL	VALUE
1	0.5
2	0.5
3	0.5
4	0.5
5	0.5
6	0.5
7	0.5
8	0.5
9	0.5
10	0.5
11	0.5
12	0.5
13	0.5
14	0.5
15	0.5
16	0.5
17	0.5
18	0.5
19	0.5
20	0.5
21	0.5
22	0.5
23	0.5
24	0.5
25	0.5
26	0.5
27	0.5
28	0.5
29	0.5
30	0.5
31	0.5
32	0.5
33	0.5
34	0.5
35	0.5
36	0.5
37	0.5
38	0.5
39	0.5
40	0.5
41	0.5
42	0.5
43	0.5
44	0.5
45	0.5
46	0.5
47	0.5
48	0.5
49	0.5
50	0.5
51	0.5
52	0.5
53	0.5
54	0.5
55	0.5
56	0.5
57	0.5
58	0.5
59	0.5
60	0.5
61	0.5
62	0.5
63	0.5
64	0.5
65	0.5
66	0.5
67	0.5
68	0.5
69	0.5
70	0.5
71	0.5
72	0.5
73	0.5
74	0.5
75	0.5
76	0.5
77	0.5
78	0.5
79	0.5
80	0.5
81	0.5
82	0.5
83	0.5
84	0.5
85	0.5
86	0.5
87	0.5
88	0.5
89	0.5
90	0.5
91	0.5
92	0.5
93	0.5
94	0.5
95	0.5
96	0.5
97	0.5
98	0.5
99	0.5
100	0.5

Multiply Interval Values
by 0.58 for SSE

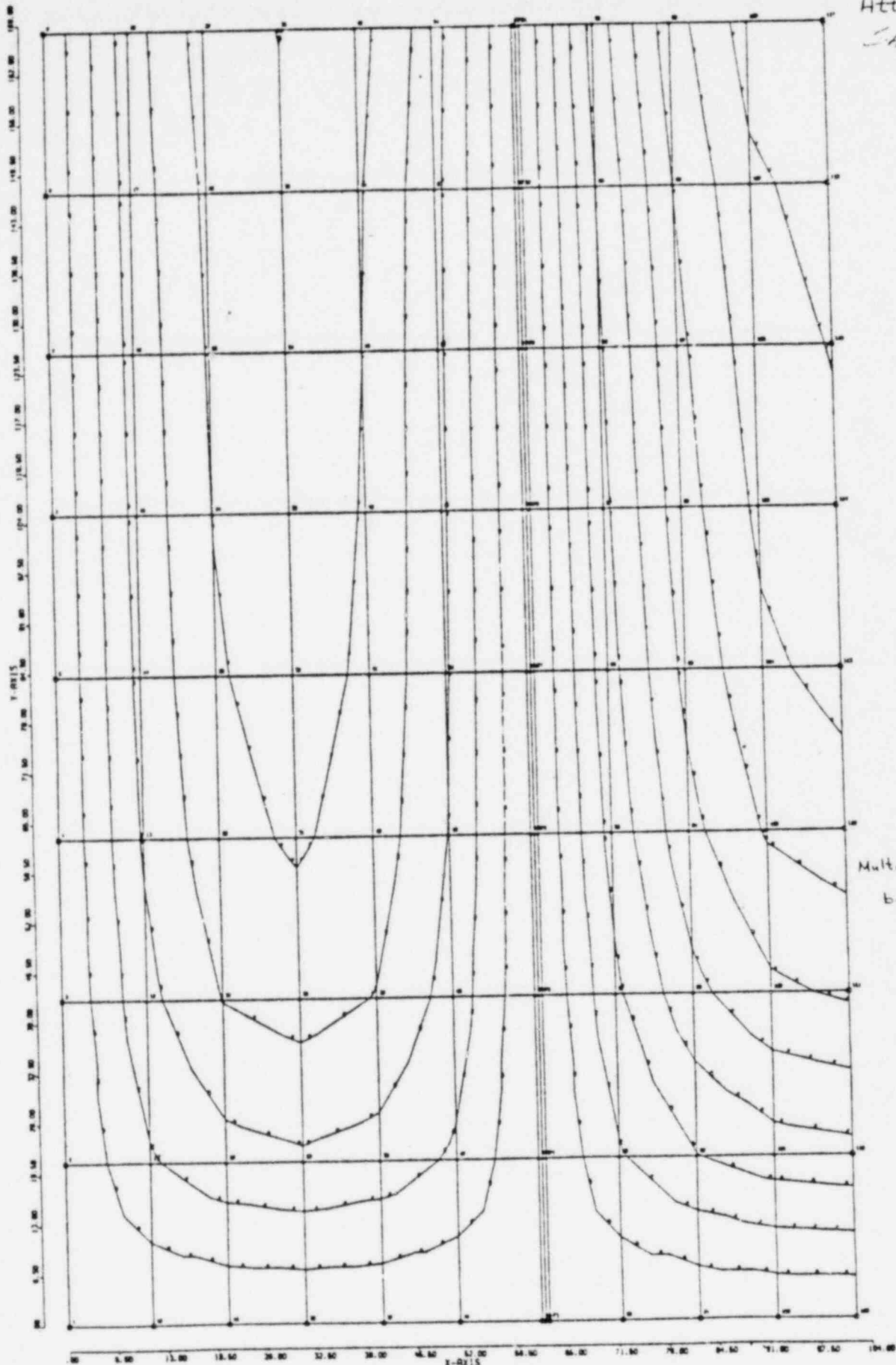
R2BLOCK UNCRACKED SECTION



LADING	1
SURFACE	MIDDLE
STRESS COUPLES 1/2	
UNITS LB INCH	
INTERNAL	VALUE
A	0.0
B	2.0000E-01
C	6.7000E-01
D	8.0000E-01
E	1.1470E-01
F	1.4900E-01
G	1.7200E-01
H	2.0000E-01
I	2.0000E-01
J	2.0000E-01
K	2.0000E-01

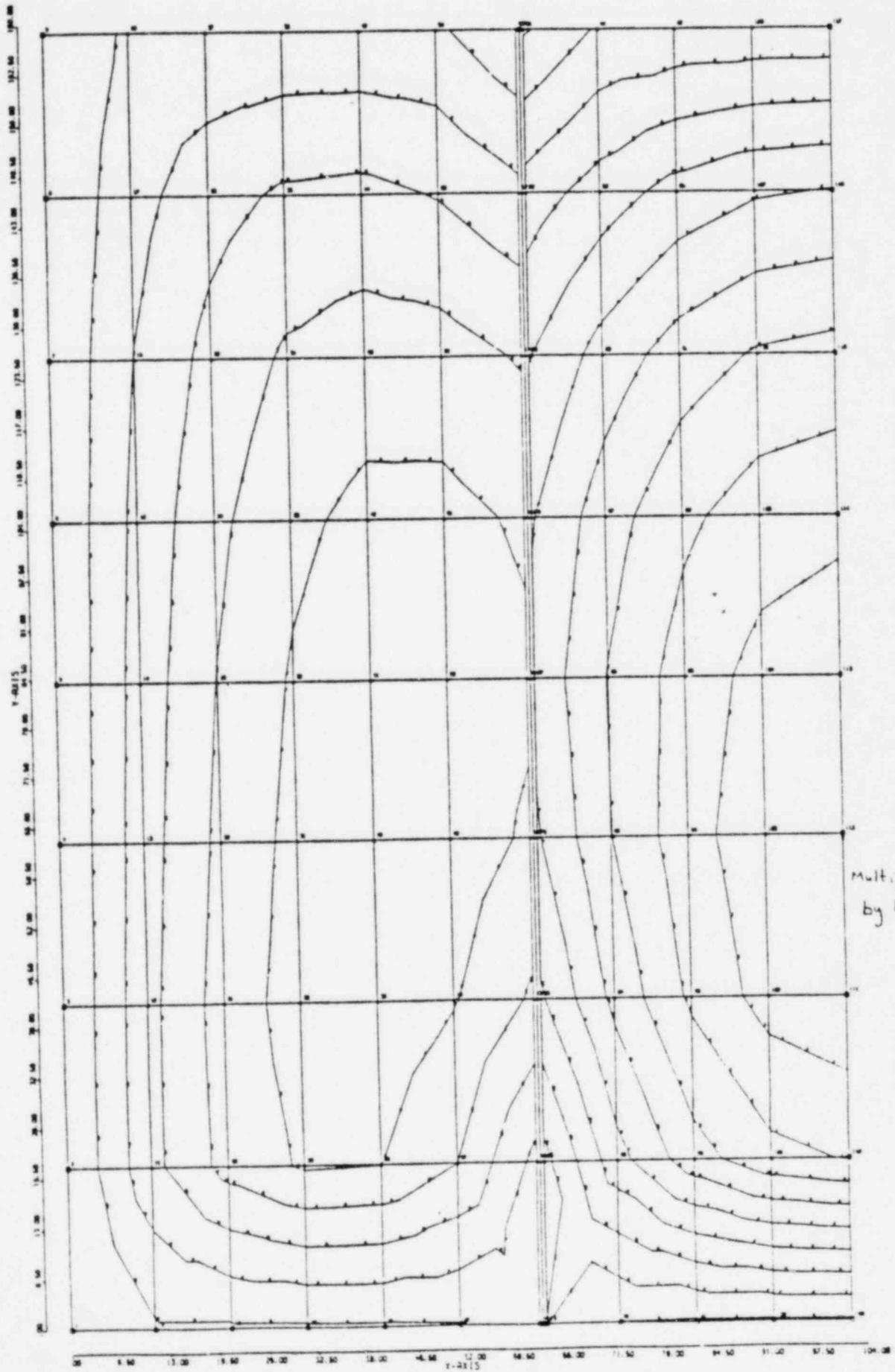
Multiply Internal Values
by 0.58 for SSE

R2BLOCKE UNCRACKED SECTION



Multiply Interval Value
by 1.41 for SSE

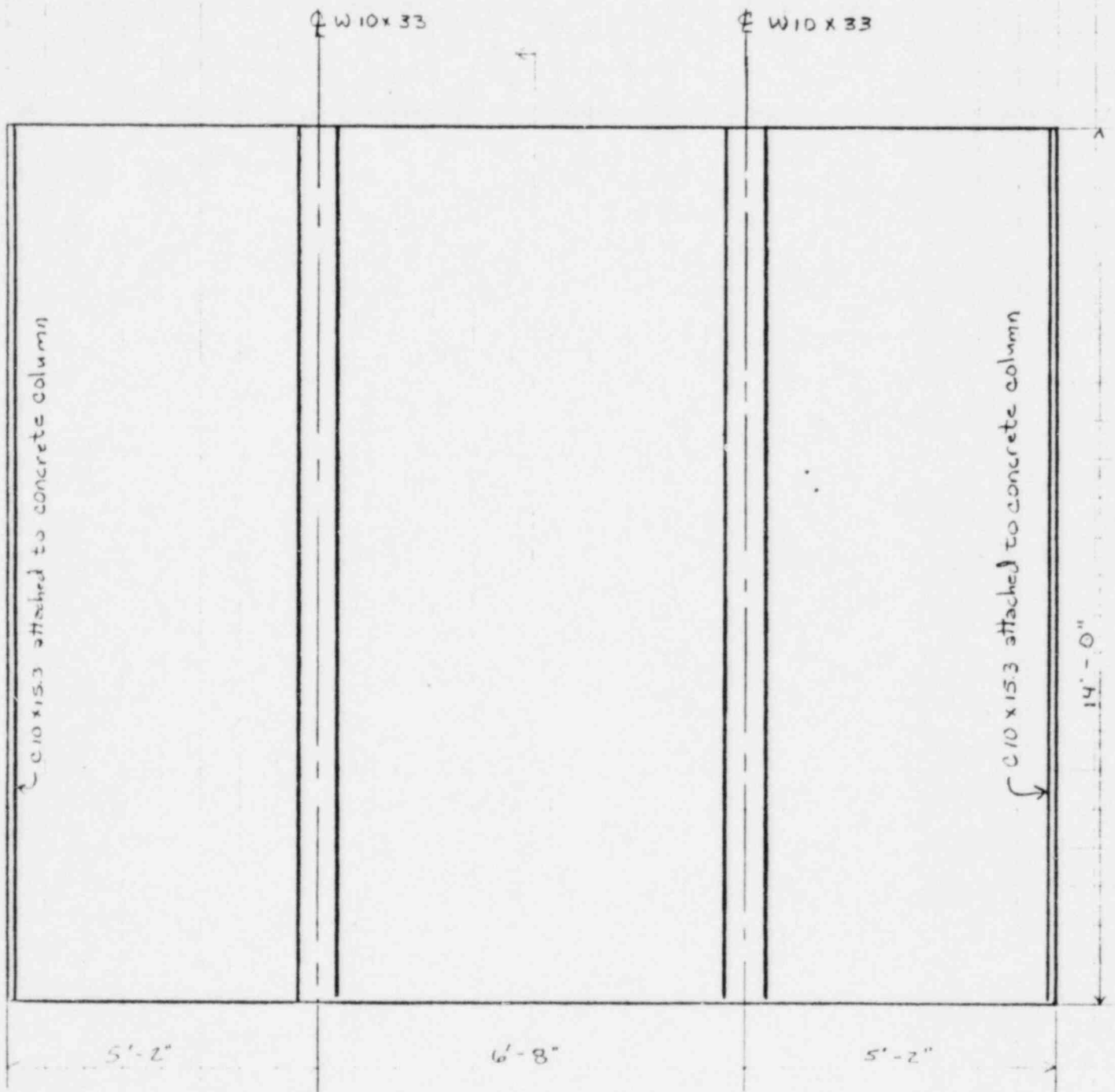
R2BLOCCE CRACKED SECTION



LOADING	1
SURFACE	11000
STRESS COMPLEX	1/
UNIT	1/2
INTERVAL	VALUE
A	0.0
B	1.000E-01
C	1.000E-01
D	1.000E-01
E	1.000E-01
F	1.000E-01
G	1.000E-01
H	1.000E-01
I	1.000E-01
J	1.000E-01

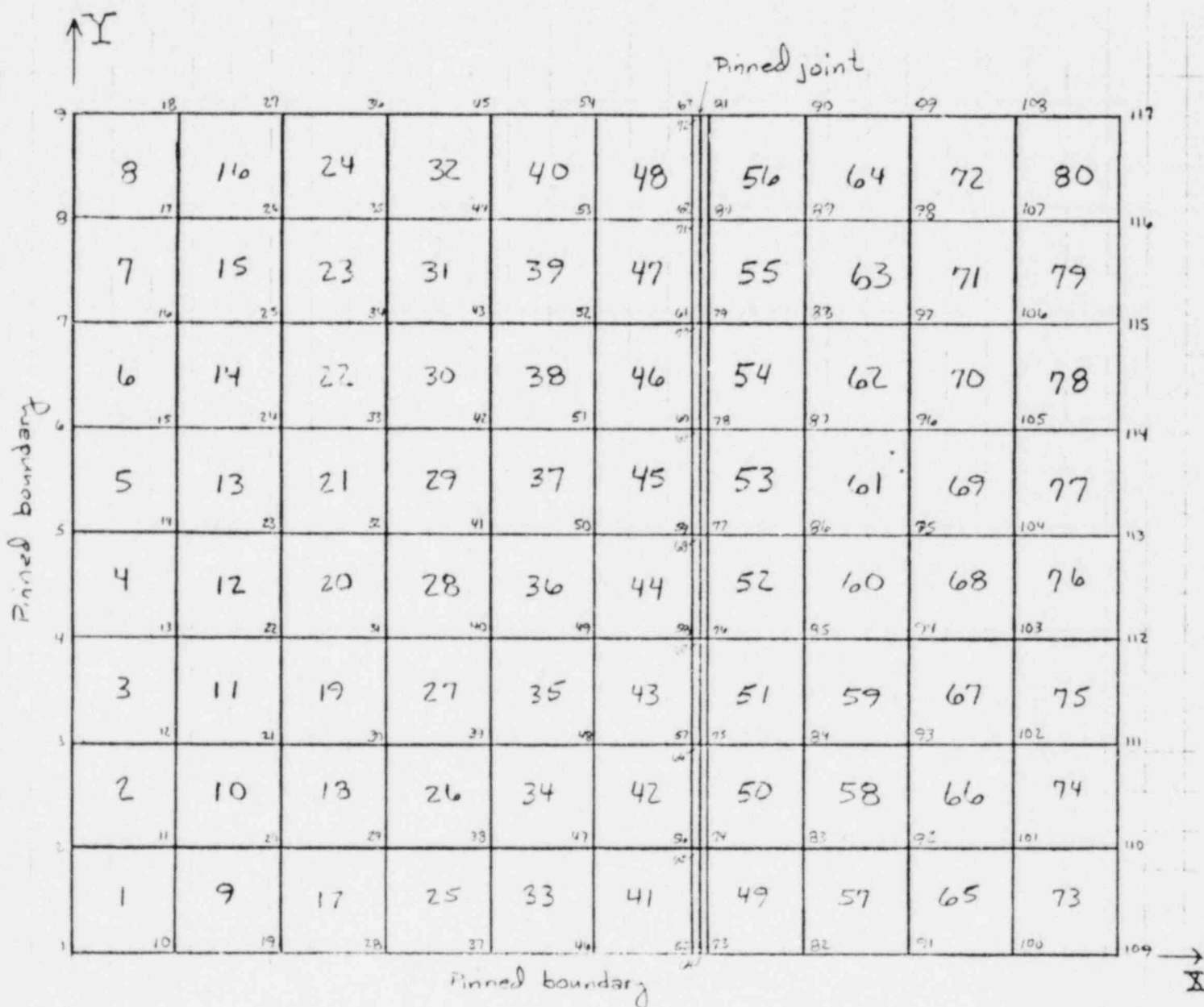
Multiply Interval Value
by 1.41 For SSE

CRACKED SECTION



Attachment VI - SHEET 1

Wall Geometry



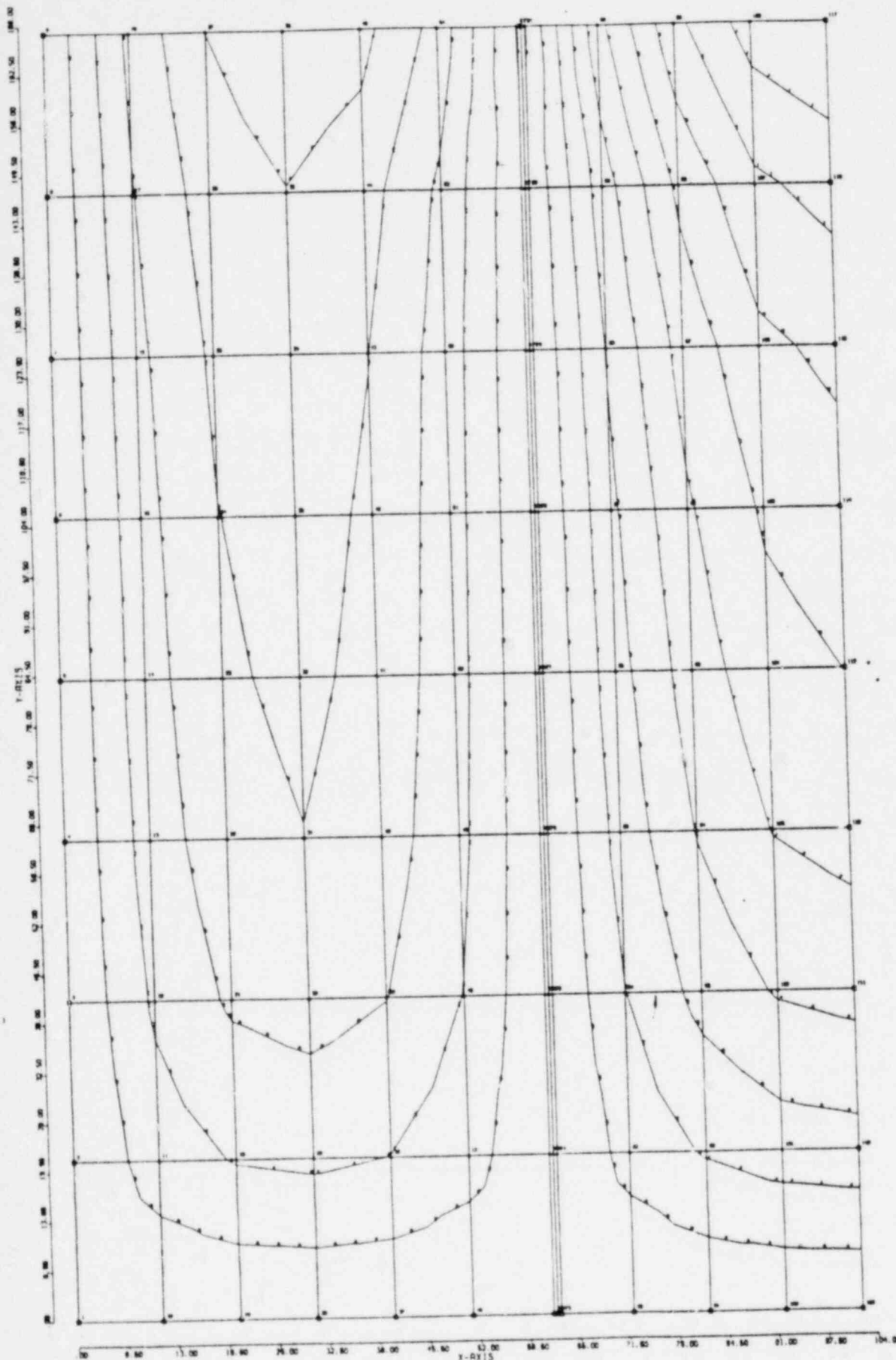
Attachment VI - SHEET 2

Model Grid

This wall panel is hollow core construction. The boundary conditions and member properties along joints 109 thru 117 are adjusted appropriately to take advantage of symmetry in the analysis. The following is an assessment of the results of the analysis for SSE conditions.

	Uncracked Section	Cracked Section
Maximum Horizontal Moment	111 inlb/in	234
Maximum Vertical Moment	124 inlb/in	99
Normal Allowable Moment Horizontal	412 inlb/in	658 inlb/in
SSE Allowable Moment Horizontal	550 inlb/in	877 inlb/in
Cracking Moment Horizontal	1237 inlb/in	N/A
Normal Allowable Moment Vertical	169 inlb/in	N/A
SSE Allowable Moment Vertical	225 inlb/in	N/A
Cracking Moment Vertical	506 inlb/in	N/A

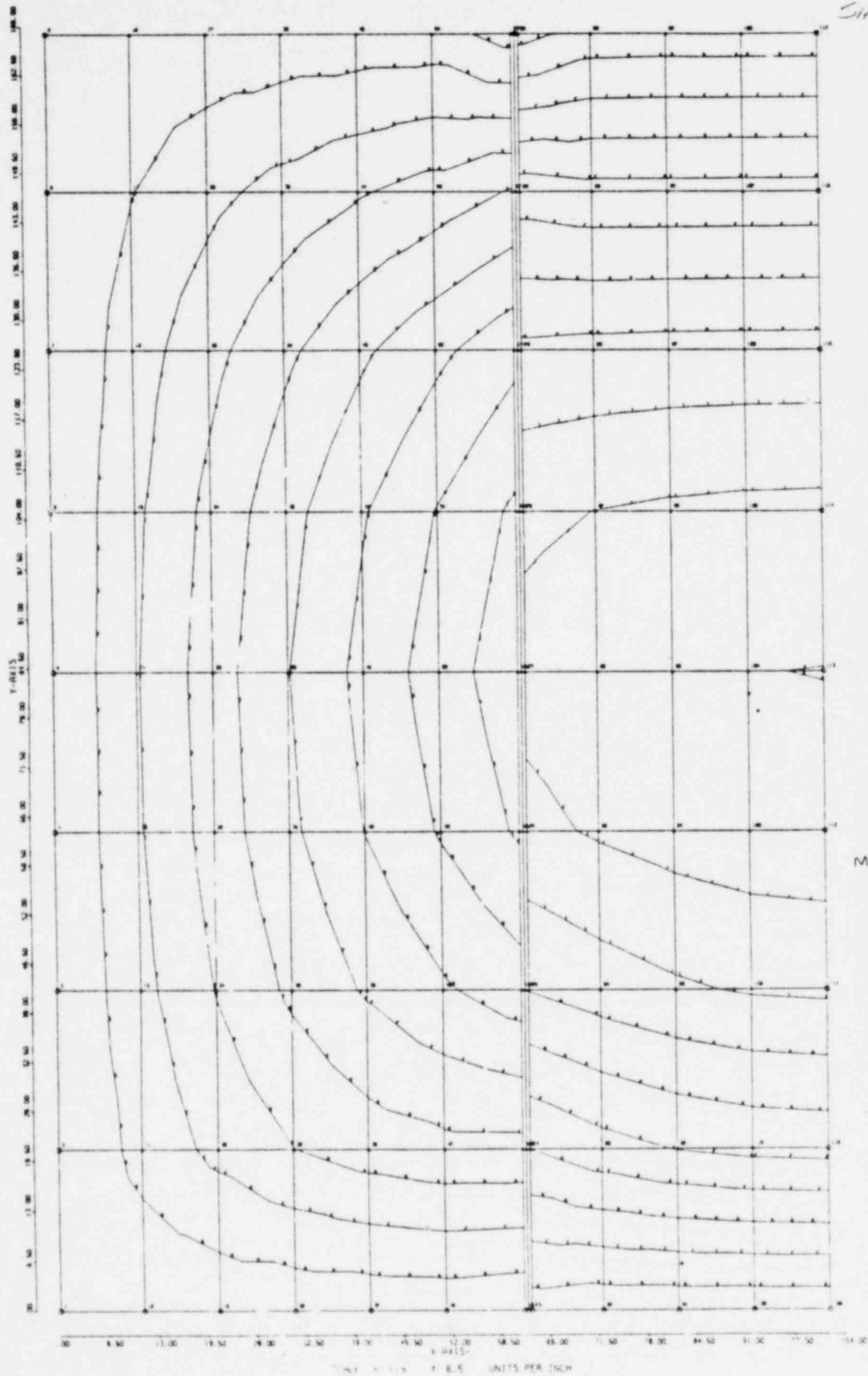
The following four sheets present the stress contours for the wall panel.



LINE NO.	1
SURFACE	MIDDLE
STRESS COEFFICIENT	1/
UNITS	LB INCH
INTERVAL	VALUE
0	0.0
1	0.0000E+00
2	0.0000E+00
3	0.0000E+00
4	0.0000E+00
5	0.0000E+00
6	0.0000E+00
7	0.0000E+00
8	0.0000E+00
9	0.0000E+00
10	0.0000E+00
11	0.0000E+00
12	0.0000E+00

Multiply Interval Values
by 0.43 for SSE

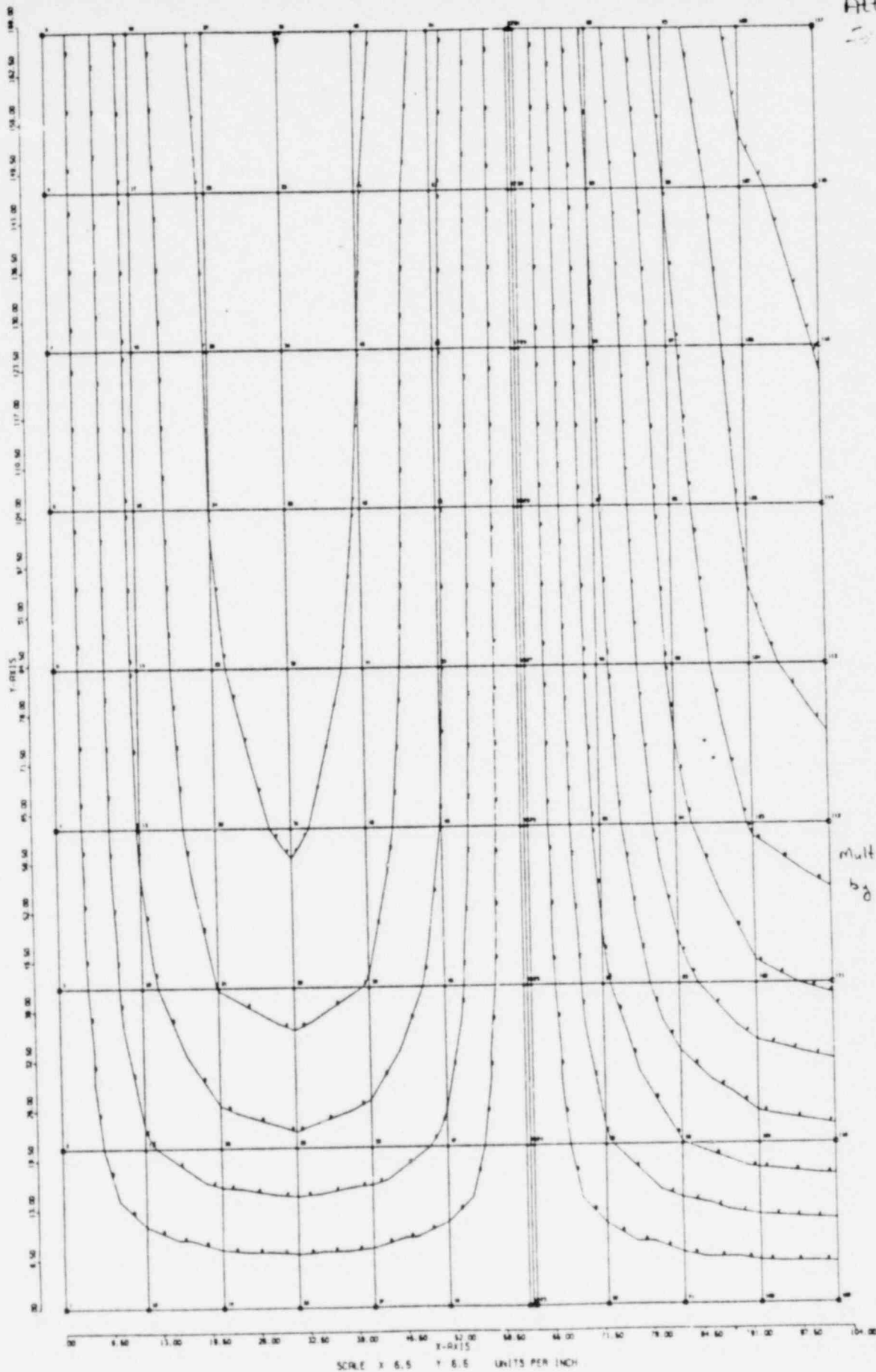
R2BLOCKF UNCRACKED SECTION



INTERVAL	VALUE
0	0.0
1	0.1
2	0.2
3	0.3
4	0.4
5	0.5
6	0.6
7	0.7
8	0.8
9	0.9
10	1.0

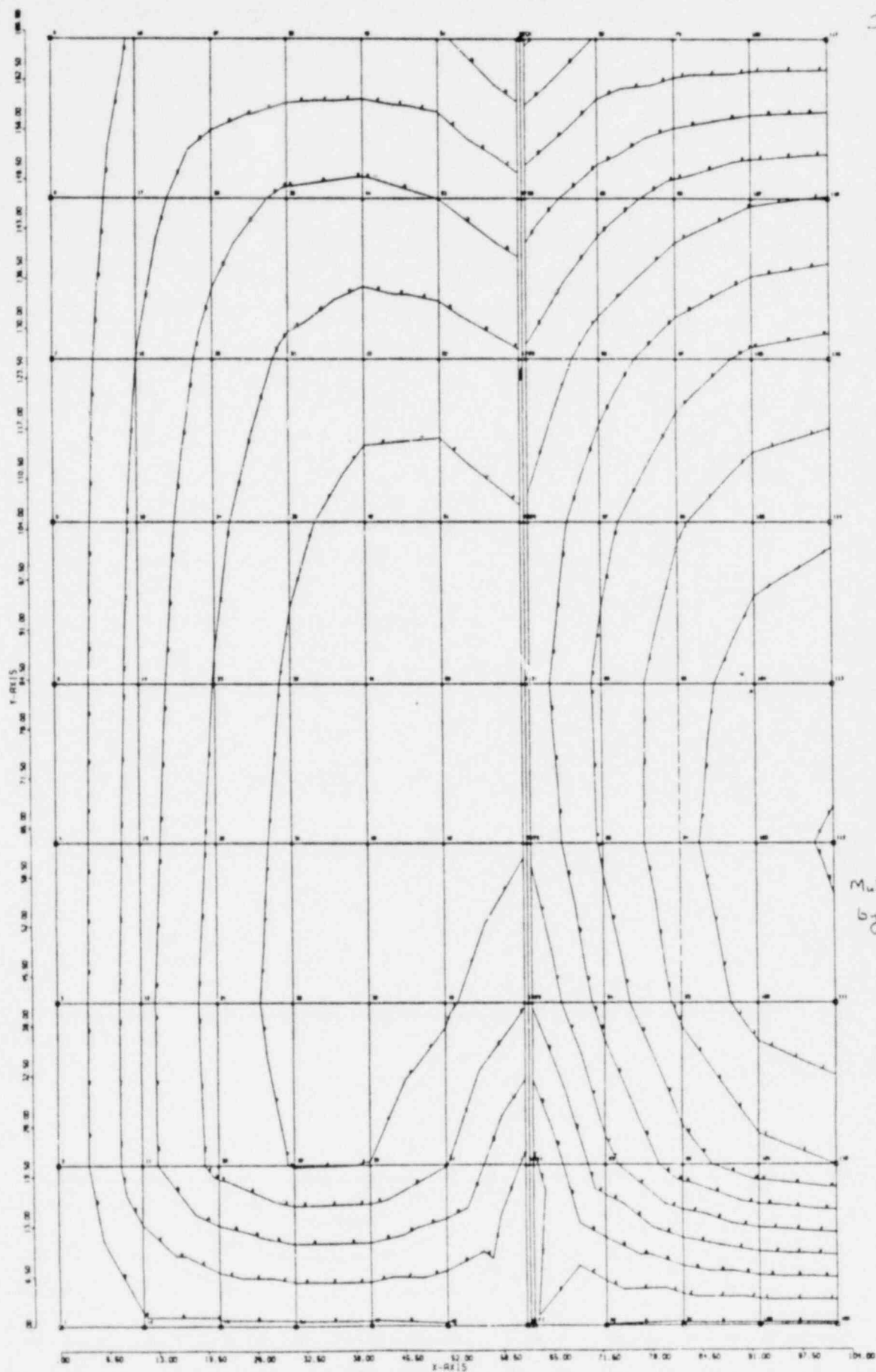
Multiply Interval Values
by 0.43 For SSE

S-17-6



R2BLOCKF CRACKED SECTION

LOADING 1	
SURFACE MIDDLE	
STRESS COUPLES IN	
UNITS LB INCH	
INTERVAL	VALUE
A	0.0
B	2.100E+01
C	4.200E+01
D	6.300E+01
E	8.400E+01
F	1.050E+02
G	1.260E+02
H	1.470E+02
I	1.680E+02
J	1.890E+02
K	2.100E+02



DEPTH	1
SURFACE	124.00
STRESS COUPLES 1/	
UNITS LB INCH	
INTERVAL	VALUE
1	0.0
2	0.0000-0.0000
3	0.0000-0.0000
4	0.0000-0.0000
5	0.0000-0.0000
6	0.0000-0.0000
7	0.0000-0.0000
8	0.0000-0.0000
9	0.0000-0.0000
10	0.0000-0.0000
11	0.0000-0.0000
12	0.0000-0.0000

Multiply Interval Value
by 1.07 for SSE

SCALE X 6.6 Y 6.6 UNITS PER INCH
R2BLOCKF CRACKED SECTION

Out-of-Plane Interstory Drift Effects:

Because of the small displacements of the primary structure and the fact that no continuous vertical reinforcing is provided to induce fixity at floor and ceiling, out-of-plane interstory drift is not a significant design consideration.

Inplane Interstory Drift Effects:

Reference: "An Investigation of the Interaction of Reinforced Concrete Frames with Masonry Filler Walls", Fiorato, Sozen, and Gamble, Technical Report to the Department of Defense, Contract DAKC 20-67-C-0136, University of Illinois, Urbana, Nov. 1970 SRS #370

This reference provides data on the performance of infilled frames with masonry walls. The gross shear strain seen by the wall panels is evaluated by establishing the "break point" on the load-deflection curves.

Based upon this published data, $\gamma = 1.1 \times 10^{-4}$ was assigned as the nominal crack point for masonry walls.

Example

The response of the building is assumed to be in phase.

The walls between elevation 594 and 611 are selected for the example. The walls in the N-S plane are subjected to the greatest differential deflection.

$$\Delta_{611} = 2.157 \times 10^{-3} \text{ ft}$$

$$\Delta_{594} = 1.587 \times 10^{-3} \text{ ft}$$

$$\Delta_{rel} = 0.57 \times 10^{-3} \text{ ft}$$

$$\text{panel height} = 14'$$

$$\gamma = \Delta_{rel} / \text{panel height} = 0.57 \times 10^{-3} / 14 = 4.1 \times 10^{-5}$$

$$\gamma_{\text{crack}} = 1.1 \times 10^{-4}$$

$$F.S. = 1.1 \times 10^{-4} / 4.1 \times 10^{-5}$$

$$F.S. = 2.7$$

Masonry Walls at CNS are acceptable for interstory drift

ATTACHMENT VIII

Design of Structural Wide Flange

Nominal 8" concrete block masonry has thickness of 7 5/8". Therefore try to select a wide flange shape with approximately 8" clear between the flanges.

Maximum masonry span = 80" assume grouted masonry construction. The peak acceleration from the 2% critical damping response spectra at elevation 838 will be used.

Beam length = 14'

Transverse horizontal acceleration = $1.435 \text{ g} \times 1.1 = 1.58 \text{ g}$
vertical acceleration = $0.437 \times 2/3 = \pm 0.3 \text{ g}$

Try W10 x 33:	$S_x = 35.0 \text{ in}^2$	$L_c = 8.4'$
7th Ed. AISC	$I_x = 171 \text{ in}^4$	$L_u = 20'$
Manual	$A_x = 9.71 \text{ in}^2$	$r_x = 4.20'$
	$d_x = 9.75 \text{ in}$	$r_y = 1.94''$
	$t_f = 0.433 \text{ in}$	
	$t_w = 0.292 \text{ in}$	
	$b_f = 7.964 \text{ in}$	

Section is non compact in A36 steel due to flange criteria
Section 1.5.14.1

$$b_f/2t_f = 7.964/2 (.433) = 9.20 > 52.2/\sqrt{36} = 8.7$$

$$b_f/2t_f = 9.2 < 95/\sqrt{36} = 15.8$$

Compression flange is unbraced through length $l = 14'$

$$L_u = 20' > 14' \rightarrow \text{Use } F_B = .6 F_y \text{ (Section 1.5.1.4.4)}$$

Beam is subjected to combination of axial and bending stresses.

Tabulated Loads

Transverse Load:

Masonry load: Grouted masonry wt @ 80 lb/ft²
Masonry spans are 80" \rightarrow simple spans

$$\text{Dead load} = (80/12) (80) = 533.3 \text{ lb/ft}$$

Steel load:

$$\text{Member self wt} = 33 \text{ lb/ft}$$

$$\text{Accelerated load: } 1.58 (533.3 + 33) = 895 \text{ lb/ft}$$

Axial load:

Masonry load: Masonry considered to carry own vertical load

Steel load: $1.3 (33) = 43 \text{ lb/ft}$

Total axial load = $14 (43) = 602 \text{ lbs}$

$$f_a = 602/9.71 = 62 \text{ lb/in}^2$$

$$f_b = \frac{Mc}{I} = \frac{M}{S}, M = \frac{895 (14)^2}{8} = 21.93 \text{ K-ft}$$

$$f_b = \frac{21.93 (12)}{35} = 7.52 \text{ K/in}^2$$

Check Stresses:

AISC Section 1.6 Combined Stresses

$$F_a = \frac{1 - \frac{Kl/r}{C_c}}{2} F_y$$

$$\frac{5}{3} - \frac{3 kl/r}{8C_c} - \frac{(Kl/r)^3}{8C_c^3}$$

$$C_c = 126.1$$

$$K = 1, l = 14' = 168'' \quad r = 1.94'' \quad (\text{neglect bracing by masonry})$$

$$Kl/r = 168/1.94 = 86.6 < C_c \rightarrow \text{use (1.5-1)}$$

$$F_a = 14.6 \text{ ksi}$$

$$f_a/f_a = .062/14.6 = .0042 < .15 \rightarrow \text{use 1.6-2}$$

$$\frac{f_a}{f_a} + \frac{f_{bx}}{f_{bx}} + \frac{f_{by}}{f_{by}} < 1$$

$$.0042 + \frac{7.52}{22} + 0 = 0.35 < 1 \quad \text{ok}$$

Therefore, W 10 x 33 is acceptable with no seismic increase in allowable stresses.

35. Provide a written commitment that requirements of Appendix B of 10 CFR Part 50 is met.

Response:

The Q.C. inspection program regarding block wall construction at Catawba meets the requirements of Appendix B of 10 CFR Part 50.

36. Discuss basis for selecting partial region of mat to represent total mat in auxiliary building design. Also, compare the approach above with conventional analysis techniques assuming rigid mat in one direction.

Response:

The Auxiliary Building foundation mat was modeled using a grid of Finite Elements supported at the mode points by springs. The reactions resulting from the overall analysis were used as loadings for this model. The resulting computer programs were run a number of times, with any springs found to be in tension removed before the next run was made. This process was continued until all springs remaining were in compression. The size of this model was chosen such that it corresponded with the natural boundaries of the building and/or extended past the last row of released springs far enough that the stresses calculated were negligible. This method was systematically applied at all critical areas of the mat foundation. Any overlapping of the areas was also considered. The major reason the mat was not modeled as a whole, using the finite element method, was because of the limited computer storage capacity at the time of the analysis.

The design resulting from the above analysis was compared to the design resulting from a conventional analysis along a typical frame line. The conventional analysis assumes a rigid mat in one direction. The results follow:

MAXIMUM COMPARATIVE RESULTS

ITEM	DESIGN CAPACITIES RESULTING FROM FINITE ELEMENT ANALYSIS	DESIGN CAPACITIES RESULTING FROM CONVENTIONAL ANALYSIS
Shear	900.K	500.K
Pos. Mom.	1930.K-FT	1416.K-FT
Neg. Mom.	2526.K-FT	2124.K-FT

As can be, seen the design provided is conserative.

37. Provide additional information regarding Question 220.45.

Response:

The design and analysis of the Spent Fuel Building structures is described in Sections 3.8.4.4, 9.1.2.1, 9.1.2.2, and 9.1.2.3. The design and analysis of the spent fuel racks is described in Sections 9.1.2.2 and 9.1.2.3. See attached Figures 9.1.2-7 and -8 for spent fuel rack plans and details. The spent fuel pool liner plate is described in Section 3.8.4.1 (A.2). The spent fuel storage racks are described in Sections 9.1.2.1 (8), 9.1.2.2, and 9.1.2.3.

See attached revised Section 9.1.2.1(1), 9.1.2.2, and 9.1.2.3.

ANSI N210-1976, "Design Objectives for Light Water Reactor Spent Fuel Storage Facilities at Nuclear Power Stations" Section 5.1.12.1 and 5.1.12.2 when a full loading of the assemblies described in Chapter 4 is considered. The computer codes and techniques utilized in the analysis have been validated against experimental data for water moderated UO_2 lattices with characteristics similar to the fuel analyzed.

In the analysis, the new fuel assemblies are assumed both to be in an infinite array and in their most reactive condition, namely unirradiated with 3.5 wt. percent enrichment U-235 and no control rods or supplemental neutron poisons present. All parameters are chosen to maximize K_{eff} , and the effects of reflectors other than water are included if their neglect would have been non-conservative.

The analysis concludes that a criticality accident during refueling and storage is not considered credible.

Since each unit has its own independent New Fuel Storage Facility and related racks, there are no safety considerations related to sharing of components.

Analysis and design of the New Fuel Storage Buildings and new fuel storage racks are performed as stated in Section 3.8.4. Details of the seismic analysis and design are provided in Section 3.7. Governing codes for design are as stated in Table 3.8.1-1.

9.1.2 SPENT FUEL STORAGE

9.1.2.1 Design Bases

Conformance with Regulatory Guide 1.13, "Fuel Storage Facility Design Basis" is as follows:

(1) Regulatory Position 1

Q220.45 | The spent fuel storage facility including the spent fuel storage racks and the spent fuel pool liner plate, as part of the Auxiliary Building, is analyzed and designed as a Category I structure (see Table 3.2.1-1). For details of the loading conditions and loading combinations of the spent fuel pool, refer to Table 3.8.1-2.

(2) Regulatory Position 2

- (a) Tornado winds are discussed in Section 3.3.2 and tornado missiles in Section 3.5.1.4.
- (b) The spent fuel pool superstructure and the New Fuel Building together provide protection from normal and tornado winds, and prevent tornado generated missiles from contacting fuel within the pool.

9.1.2.2 Facility Description

Each unit of the Catawba Station has an independent spent fuel storage system. The Fuel Handling System associated with the pool is discussed in Section 9.1.4, and Spent Fuel Cooling System is presented in Section 9.1.3. Radiation shielding and monitoring are presented in Sections 12.1 and 11.4, respectively. There are sufficient fuel storage racks to accommodate the number of fuel assemblies discharged from approximately 19 normal Catawba refueling cycles plus one complete Catawba core. Provisions are also made to store control rods and burnable poison rods. The dimensions and location of the fuel pool are included on Figures 9.1.2-2 and 9.1.2-3. For location of the fuel pool in the station complex see Figures 1.2.2-3 and 1.2.2-4. Major components, piping, valves and instrumentation in contact with the fuel pool water are stainless steel. The fuel pools, transfer canals, and cask pits are lined with stainless steel plate.

The spent fuel assemblies are held in a vertical position by the spent fuel pool storage racks. The fuel assemblies are supported within the fuel storage racks by a stainless steel plate located six inches above the fuel pool floor. Openings are provided that allow coolant water to flow through the rack and up around the fuel assembly. A lead-in assembly is provided at the top of each rack to guide fuel into its proper storage location.

Q220.45 The fuel racks are designed as free standing, self-supporting, independent modules which stand on the fuel pool floor. There are spaces available for the potential storage of 1418 fuel assemblies per unit. Spent fuel storage rack plans and details are provided in Figures 9.1.2-7 and 9.1.2-8.

9.1.2.3 Safety Evaluation

In the fuel storage racks, fuel is stored vertically in an array with a nominal center-to-center distance of 13.5 inches between assemblies to assure $K_{eff} < .95$ even if immersed in unborated water. The racks are designed to preclude insertion of fuel assemblies at other than permitted locations, thereby assuring the necessary spacing between assemblies. To further assure subcritical arrays in the fuel handling facilities, only one assembly can be manipulated at a time.

Spent fuel storage racks have been designed to prevent significant lifting forces from being applied to the racks. This is done by a design which eliminates protrusions in the racks including the elimination of projecting weld beads. In addition, tests are performed both in the shop after fabrication and in the fuel pool after installation to insure that there are no drag forces in excess of 50 pounds during removal of fuel assemblies from storage racks.

Since each unit has its own fuel pool, there are no safety considerations related to sharing of components.

To preclude the cask entering the spent fuel pool, the cask crane stops are located in a position to prevent the cask from being moved into the fuel pool

area. The cask area is separated from the spent fuel pool by a three-foot reinforced concrete wall (Reference Figures 9.1.2-2 and -3).

An evaluation has been performed to assess the possibility of the cask entering the spent fuel pool in the lifted (vertical) and tipped position. To evaluate the cask in the lifted position, the crane is assumed to impact against the crane stops traveling at the maximum crane speed of fifty feet per minute with the cask in a position to give the maximum swing and horizontal displacement.

Assuming that the cask rotates about the center of the crane drum and a rigid crane and rail stop, the cask center of gravity remains on the cask area side of the three-foot divider wall. For details of this cask position, refer to Figure 9.1.2-4. To evaluate the cask in the tipped position, the cask is assumed to catch the edge of the concrete wall of the cask area and tip toward the spent fuel pool. For this condition the maximum envelope (dimensions) are used for the possible casks to be used at Catawba. As shown in Figure 9.1.2-5, the center of gravity of the cask remains on the cask area side of the divider wall. Based upon this evaluation it is concluded that the cask would not enter the spent fuel pool due to dropping or tipping of the cask.

The design of the Catawba spent fuel pool racks complies with the NRC staff position on "Minimum Requirements for Design of Spent Fuel Racks" (Appendix D to Standard Review Plan Section 3.8.4) with the following exceptions:

- Q220.45
1. The materials used in the fabrication of the racks conform to the applicable ASTM specifications. These materials are not, however, designed or fabricated per ASME code.
 2. Duke's procedure for seismic design is as discussed in Section 3.7.2.
 3. Impact loads of fuel assemblies onto cell walls were not considered in the rack design. The small gap between assembly and cell, coupled with the cushioning effect provided by submergence, led to the conclusion that these impact loads are insignificant.

The fuel pool is designed to withstand the following:

- a. normal dead and equipment loads plus design seismic loads,
- b. all normal dead, equipment and live loads,
- c. normal dead and equipment loads plus tornado wind load,
- d. thermal stresses, and
- e. cask drop accident

Additionally, Section 9.1.3.3 presents a safety evaluation of the Spent Fuel Cooling System explaining in detail the provisions for continuous spent fuel cooling as required by Regulatory Guide 1.13 and further clarified in ANSI N211, "Design Criteria for Spent Fuel Storage Facilities." These provisions include:

DOCUMENT/ PAGE PULLED

ANO. 8204160397

NO. OF PAGES 2

REASON

☐ PAGE ILLEGIBLE

☐ HARD COPY FILED AT: PDR CF
OTHER _____

☐ BETTER COPY REQUESTED ON _____

☒ PAGE TOO LARGE TO FILM

☒ HARD COPY FILED AT: PDR CF
OTHER _____

☒ FILMED ON APERTURE CARD NO 8204160397-02

thru

8204160397-03

38. With respect to the seismic design of cable trays and supports, confirm that the OBE does not control the design accounting for the difference of damping values and stress allowables. Also, provide calculations for representative types of cable tray arrangements to show that the OBE does not control.

Response:

All existing cable tray and support calculations have been checked to confirm that OBE does not control the design accounting for the difference of damping values and allowable stresses.

This has been accomplished by comparison of the Allowable Stress Ratio (ASR) and a Peak Acceleration Ratio (PAR).

Allowable Stress Ratio: The ASR is a ratio of the SSE allowable stress to the OBE allowable stress. From FSAR Table 3.8.1-2.

SSE Loading Combinations

$$1.6S = D + L + E' = 0.96 F_y \quad \text{or} \quad 1.6 \text{ (AISC Allowables)}$$

OBE Loading Combinations

$$S = D + L + E = 0.6 F_y \times 1 \frac{1}{3} = 0.8 F_y \quad \text{or} \quad 1.333 \text{ (AISC Allowables)}$$

The 1/3 increase in stresses is in accordance with AISC Section 1.5.6, Wind and Seismic Stresses.

$$ASR = \frac{\text{SSE allowable stress}}{\text{OBE allowable stress}} = \frac{0.96 F_y}{0.8 F_y} = 1.20$$

Peak Acceleration Ratio: The PAR is a ratio of the SSE peak acceleration to the OBE peak acceleration. The SSE peak accelerations were taken from the response curves used in the existing calculations, which conform to damping values in FSAR Section 3.7.1.3. The OBE peak accelerations are taken from response curves which meet the recommendations of Regulatory Guide 1.61.

$$PAR = \frac{\text{SSE peak acceleration}}{\text{OBE peak acceleration}}$$

By comparison if the PAR is greater than the ASR, the SSE earthquake will govern the design. This is the case for all existing cable tray and support calculations. The PAR's range from 1.246 to 1.72, which are all greater than the ASR of 1.20.

In conclusion, the SSE earthquake loading governs in all cases and no further calculations are required.

39. Discuss the effects of relative displacements of adjacent supports of cable tray runs on the adequacy of the cable tray and support design.

Response:

Relative displacements of adjacent supports of cable tray runs will have little or no effect on the structural adequacy of the cable tray and support design.

In the Reactor Building, where cable trays span from one interior structure to another, the supports are provided with sliding connections to account for the differential movement between the individual structures.

Maximum total displacements in the Auxiliary Building range from 0.00" at El. 543+0 to 0.13" at El. 659+0. The relative displacement between floors would be much smaller than the maximums.

An assumed displacement of 1.0" was applied to a section of cable tray assumed to span between two adjacent floors. The resulting stress was less than 2 psi. An actual deflection of 0.006" was applied to a support that is connected between floors at El. 560.0 and El. 577.0. The resulting stress increase of 0.2% of the allowable is considered negligible.

40. For those cable tray runs and supports which are welded, provide key calculations to confirm that the intent of Regulatory Guide 1.61, dealing with the 4% damping for SSE, is met.

Response:

For cable tray supports that were assumed completely welded, response spectra curves with 2% damping were used to determine stresses resulting from the SSE in accordance with FSAR Section 3.7.1.3. This procedure is conservative since Regulatory Guide 1.61 recommends 4% damping for SSE and 2% damping for OBE.

With reference to Action Item 38, the calculations for welded supports have a Peak Acceleration Ratio (PAR) of 1.875, which is greater than the 1.20 Allowable Stress Ratio (ASR).

Therefore, the SSE earthquake governs the welded structure design of cable tray runs and supports.

41. Regarding the two cracks identified in masonry wall during the site visit on December 15, 1981, Duke will provide: A) location and description of the cracks; B) probable cause of the cracks; C) Duke's proposal for correcting the cracks.

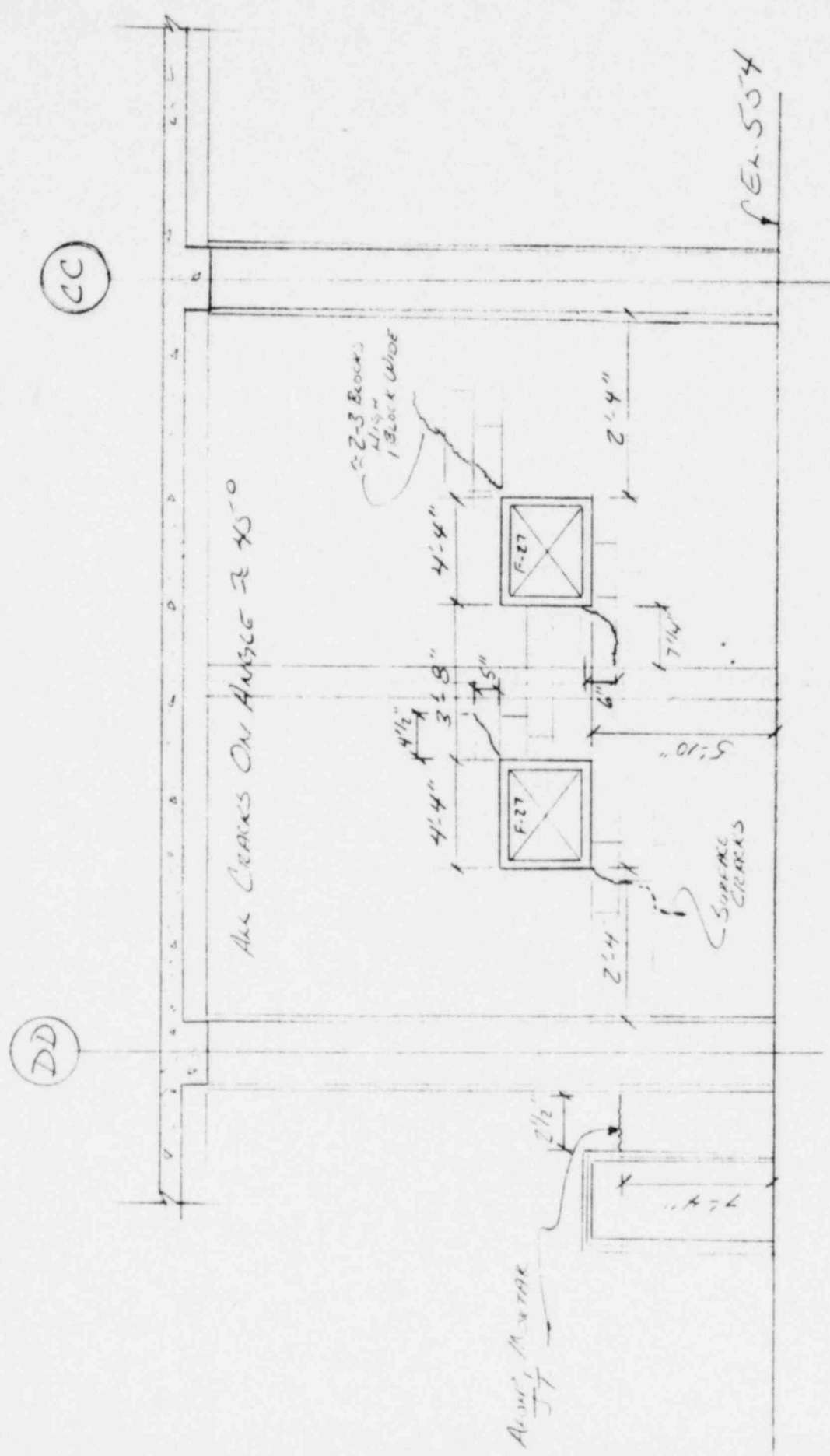
Response:

Attached is a figure detailing the locations of cracks identified during the December 15, 1981 site visit. An inspection of other block walls in this area did not reveal any other cracks.

The isolated cracks are thought to be caused from temperature expansion differential of the steel frames and the masonry.

Calculations were reviewed and due to the low accelerations experienced at this low elevation no repair is required. The cracks do not affect the structural integrity of the wall unit.

BATTERY ROOM CRACKS IN BLOCK WALL



12 ELEVATION ALONG LOC LINE 57
1002-1 N.T.S. LOOKING SOUTH
NOTE: CRACKS SHOWN ABOVE DO NOT
APPROX SAME ON BOTH SIDES OF WALL

42. In response to Question 220.35 justify your exclusion of the compressive and surface wave effects in consideration for seismic analysis of buried piping and electrical conduit runs.

Response:

See revised FSAR Section 3.7.3.12 (attached).

- (a) Inertial effects due to the dynamic behavior of the material in which the pipe is embedded. The model assumes that the seismic deformations of the surrounding material are imposed on the piping, which then conforms to this deformation away from the bends and changes in direction. Friction between the pipe and soil is accounted for in analyzing pipe lengths shorter than that required for the soil to develop the full axial friction force. For buried pipe bends or changes in direction and/or penetrations, the resistance of the surrounding soil to the displacement of the pipe is accounted for using the coefficient of subgrade reaction and equations for beams or elastic foundations.

Q220.35
Q241.10

The type of waves considered most appropriate in the analyses for buried pipeline systems are traveling body waves-compression (P) and shear (S) waves. The angles of incidence of the waves are selected to yield maximum values of strain, curvature or stress for a given condition of analysis. The wave propagation velocity with respect to the buried pipe or the ground surface is relevant for calculating the strains and curvatures induced in the buried pipeline as well as the relative displacements and rotations at the pipeline bends and junctions (References 18 and 19). The velocity of the traveling wave propagating through the entire soil/rock profile is a function of the wave length. The angle of incidence of body waves with respect to the ground surface was assumed to be in the range of 35° to 40° from vertical for short wave lengths (less than the depth to very dense soils/partially weathered rock) in order to compute a conservative lower bound velocity of propagation for analyses of the buried systems. For long wave lengths, the material velocity of the very dense soil-partially weathered rock, or a shear wave propagation velocity of 2000 ft per second, was assumed as the propagation velocity. The corresponding compression wave propagation velocity is 4200 ft/second.

Compressive or longitudinal wave effects are not excluded from consideration for seismic analyses of buried piping and electrical conduit runs, and are considered as explained in Reference 16. The pipe stresses calculated due to these compressive wave effects are less critical than those computed from the effects of shear waves.

Surface (Rayleigh) waves are not excluded from consideration for seismic analyses of buried piping and electrical conduit runs. For the Catawba site, the long period Rayleigh waves would propagate at the velocity of the bedrock, or 6000 fps for wave lengths equal to or greater than about 100 ft, twice the typical depth to rock. The pipe stresses calculated due to such Rayleigh waves are less critical than those computed from the effects of travelling body waves.

The equations of References 5, 7, and 16 are used to calculate the resulting stresses. A summary of information used in the analysis is as follows:

- A. Ground motions read from ground motion spectrum shown on Figure 11 of Reference 19, after scaling to appropriate maximum acceleration.

CNS

For each wave type, the full ground motion was assumed for calculating pipe stresses. This is conservative, since the ground motion is actually the result of summing the contribution from each of the wave types.

- 220.35
241.10
- B. Seismic shear wave propagation velocity - 2000 fps; compression wave propagation velocity - 4200 fps.
 - C. Maximum ground acceleration - Bedrock, 0.15g.
Backfill 0.40g.
 - D. Coefficient of subgrade reaction (K) for site backfill material (varies with pipe size).
Average value - 18,924 psi
 - E. Friction coefficient - 0.3
 - F. Poisson's ratio - 0.35 for soil, 0.25 for rock
 - G. Shear wave velocity of rock 7000 fps, Rayleigh wave velocity 6000 fps.

Information on the other properties of the subsurface materials is presented in Chapter 2.

The coefficient of subgrade reaction (K) was determined by the method described in Reference 16 and the seismic wave material velocity obtained from the site test data. Varying the velocity will result in an increase and decrease of the coefficient; this will respectively increase and decrease stress on the pipe. For calculation purposes the velocity was assumed to vary by $\pm 25\%$. The resulting maximum overstress value thus obtained is still less than the allowable pipe stress.

- (b) Static effects of displacements among structures to which the piping is attached. The Nuclear Service Water piping penetrates structures supported on continuous rock -

Auxiliary Building
Diesel Generator Buildings
NSW/SNSW Pump Structure

and structures supported on partially weathered rock -

NSW Intake Structure (lake)
SNSW Intake Structure (pond)
SNSW Discharge Structures.

There is also a non-seismic connection to the Low Pressure Service Water System piping for discharge during normal operation. The appropriate differential movements of the structure during the earthquake are imposed on the piping, assuming a fixed end connection at the point of entry into the structure.

CNS

16. Iqbal, M. Ayub, and Goodling, Evans C., Jr., "Seismic Design of Buried Piping," Proceedings, ASCE 1975 Conference on Structural Design of Nuclear Plant Facilities, held at New Orleans, LA., December 8-10, 1975, Vol. 1-A, pp. 142-168.
17. Teng, W. C., Foundation Design, Prentice-Hall, Inc., 1962, pp. 92-93.
18. Nuclear Reactors and Earthquakes, TID-7024, U. S. Atomic Energy Commission, Washington, D. C., 1963, pp. 191-195.
19. Newmark, Nathan M., Blume, John A. and Kapur, Kanwar K., "Seismic Design Spectra for Nuclear Power Plant," Proceedings of Power Division of ASCE, Vol. 99, No. P02, November 1973, pp. 287-303.
20. O'Rourke, Michael J., Bloom, Mary C., and Dobry, Ricardo, "Apparent Propagation Velocity of Body Waves," submitted to International Journal Earthquake Engineering and Structural Dynamics for possible publication, October 1980.
21. Wang, L. R., et al., Seismic Vulnerability Behavior and Design of Buried Pipelines, Technical Report (SVBDUPS Project) No. 9, Department of Civil Engineering, Rensselaer Polytechnic Institute, Troy, New York; March 1979.
22. Hall, William J. and Newmark, Nathan M., "Seismic Design Criteria for Pipelines and Facilities," Journal of the Technical Councils of ASCE, No. TC-1, November 1978, pp. 103.
23. Yeh, Gordon, C. K., "Seismic Analysis of Slender Buried Beams," Bulletin of the Seismological Society of America, Vol. 64, No. 5, October 1974, pp. 1551-1562.
24. Seed, H. B. and Lysmer, J., The Significance of Site Response in Soil-Structure Interaction Analyses for Nuclear Facilities, ASCE, Second Conference on Civil Engineering and Nuclear Power, Vol. II; Geotechnical Topics, held at Knoxville, Tennessee, Sept. 15-17, 1980.

43. Provide the MARC computer code description and documentation of its key assumptions, limitations and theoretical bases.

Response:

A description of the MARC computer code follows.

Catawba Nuclear Station
Duke Power Company

NRC Design Adequacy Audit
Action Item No. 43

CONTENTS

1. Organization of MARC-CDC Computer Code
2. Elements in MARC-CDC
3. Program Features
 - A. Material Library
 - B. Program Functions Library
 - C. Structural Procedures Library

GENERAL

MARC-CDC is a general purpose finite element program designed for the linear and nonlinear analysis of structures in the static and dynamic regime. Its extensive element library makes it useful in elastic analysis and its broad coverage of the structural mechanics area makes it invaluable as a nonlinear analysis tool. It is written in FORTRAN IV in general form with variable dimensions passed down to the subroutines. The user defines his own working space depending on element type, the size of the problem, and available memory.

Input data is divided into logical blocks. Each block is preceded by a code word. This procedure permits updating of input data previously read in. The input data is organized so that a user requiring only linear analysis need not be concerned with the nonlinear options in the program.

A library of elements is available directly in the program. These elements are called by a library code number in the input data.

The program may be used with a node-tying facility. This facility permits the tying together of different elements and the imposition of displacement constraints.

The elastic-plastic and large displacement analysis is effected in a series of piecewise linear increments (see reference 9 in Appendix G). Creep and thermal effects which cause initial strains are analyzed as a series of steps in which an increment of initial strain occurs at the start of each step. This initial strain can be a function of nuclear irradiation as well as of temperature. Optional facilities enable the lowest eigenvalue for buckling to be obtained after each applied increment of load. This eigenvalue furnishes the factor which must be used to scale the next increment of load to cause collapse.

The dynamic analysis may be carried out by either the modal or the direct integration procedure. The dynamic analysis can be carried out with any of the nonlinear features in the program that make physical sense. Nonlinear dynamic analysis may be performed by use of the direct integration procedure in MARC. Sometimes it is difficult to solve an ill-conditioned static problem. A possible approach to this dilemma is to solve the problem by converting it to a slow and heavily damped dynamics problem.

Controls have been added which allow the specification of loading or creep for a total number of increments or time steps, respectively. These controls are referred to as automatic load controls. The automatic load control for creep selects the time step for each increment so that the resulting stress and strain changes remain within a specified limit. A higher order step-by-step integration in time, known as the residual load correction, may be specified for creep and other nonlinear problems. This residual load correction feature stabilizes creep solutions.

An option allows the data for elements to be stored on the disk. In shell elements, this results in a significant saving of available core space. A restart option is provided and is recommended for problems with many load increments. Various output selection options exist. The program has a built-in two-dimensional mesh generator.

Perspective mesh display options allow data debugging. A post-processor facilitates the selective plot of results which are obtained from triangular or quadrilateral two-dimensional elements. Three-dimensional results are plotted by sectioning into planes.

USER SUBROUTINES

The MARC-CDC program is written so as to allow the user to write user subroutines to replace the standard coding at various points in the program if additional flexibility is required. The available user subroutines are described in Volume II, Section 3.

LINEAR ANALYSIS

The program, with its comprehensive element library and advanced constraint features, has been found useful for linear analysis. An option allows the user to qualify the mesh used in the analysis. It provides energy estimates of the quality of the analysis. The user who wishes only to use this feature in MARC should read the section in Chapter 2 on "Element Library" which covers the geometry of interest, Chapter 4 on "Input Data" and the Appendices on "Mesh Generation" and "Bandwidth Optimization". The other chapters deal with the more advanced features usually required in nonlinear analysis and may be read when its use is required. A useful guide to input data required in a linear analysis may be found in Section 1 of the MARC Program Input Manual (Volume II). The user who is only interested in linear analysis is advised to proceed to that chapter after reading the above named chapters.

DATA STORAGE

The user has at his disposition options in which certain data can be stored either in-core or out on disk or some other secondary storage. Three types of data can be treated in this way. The first type of data is connected with the storage of all element quantities. This data occupies a large amount of space for the more complex shell elements and yet putting it out on secondary storage does not cause large input/output times. Hence, when storage is in demand, this data should be the first to be stored in secondary storage. The second type of data is that concerned with the master stiffness matrix. This occupies the most amount of space but at the same time has a significant effect on the input/output time. The out-of-core solutions should be flagged if the problem cannot fit into core with the element data stored out-of-core. Finally, the third type of data is concerned with displacement and other nodal data. This data is needed so frequently that it should be moved out of core only as a last resort. On a machine with extended core storage (e.g. CDC 7600) this data should be written to extended core.

OUT-OF-CORE ELEMENT PROPERTIES OPTION

A considerable saving in core storage can be achieved by storage of element arrays (strains, stresses, temperatures, etc.) on an auxiliary device. This option is available by setting the ELSTO parameter card.

OUT-OF-CORE VECTOR OPTION

A considerable additional saving in core storage can be achieved by storage of all the displacement, load and coordinate vectors on an auxiliary storage device. This option is available by setting the VECSTO parameter card. In addition the PROGRAM statement in the main program should specify TAPE2.

MESH AND OUTPUT DISPLAY

The program contains an option to display the mesh being used for analysis. Plane, two-dimensional or perspective, three-dimensional plots are available. The mesh may be sectioned (only parts of the mesh plotted) to allow detailed views of parts - this feature is especially useful for debugging three-dimensional meshes since layers of elements may be extracted and viewed from various directions. Element and/or node numbers may be displayed. Displaced mesh plots and contour plots are obtained using the post-plotting features of this option. Details on this option may be found in Section 3 of this Volume.

The mesh display feature is obtained by including the MESH PLOT parameter card (Volume II, Section 2). The options are then selected by the mesh display option cards which are contained in Section 2.15 of Volume II. The program may be run with such plots included with an analysis, or for a mesh display mode only. The plot tape will be written as tape 4.

The plotter interface routines are written for CALCOMP plotters. For conversion to other plotting devices, these routines are listed and described in Volume II, Section 3.

FLOW SEQUENCE

The program is modular in nature. Its flow sequence is described in section 5 of this volume. The user should note the existence of a traceback feature and other diagnostic program messages.

AUXILIARY PROGRAMS

Two- and three-dimensional mesh generation (MARC Mesh3D) simplifies the modeling task.

HEAT TRANSFER

Finite element heat conduction elements allow a compatible heat conduction analysis to be carried out. An interface is provided for automatic control of the size of the temperature increment during the subsequent nonlinear thermal stress analysis.

GENERAL PURPOSE PROGRAM

To use the program effectively, the user should understand that the program is made up of three libraries, viz. the element, material and structural procedures library. The element library contains over 50 elements which allow the user to describe any geometry that may be encountered. The material library contains over 35 different material models which together cover the material behavior of most engineering materials in the linear and nonlinear regimes. Each structural procedure steers the program through its various modules in order to simulate a particular physical phenomena, such as temperature cycling, buckling, dynamic transient, and etc. The structural procedures library contains about 15 structural procedures. The program is arranged in such a way that the user may select and combine any components from any of the three libraries. This effectively allows an unlimited number of combinations and from the point of view of a user, provides a powerful multi-purpose analysis tool.

Table 1.2-1 gives the program functions that may be defined by the user. Table 1.2-2 to 1.2-4 summarizes the three libraries that make up the general purpose program. Further details of its components is given in Sections 2 and 3 of this volume.

The user should understand that apart from 1 card, and two separators, all input consists of optional blocks of data that select or turn on the various components of the three libraries. Thus, input is only entered if required and the task of input data preparation is proportional to the complexity of the analysis model.

TABLE 1.2-1. Program Functions

1. Incremental Mesh Generators
2. Kinematic Constraints
 - a) Transformation of degrees of freedom
 - b) Elastic foundation
 - c) Tying
 - d) Boundary constraints
3. Traction and Pressure Loading
 - a) Nodal loads
 - b) Surface loading
 - c) Volumetric loading
 - d) Thermal strain loading
4. Plotting Capabilities
 - a) Mesh display
 - b) Displaced position plots
 - c) Contour plots
 - d) Time history plots
5. Restart
6. Selective Assembly of Master Stiffness Equation
7. Incremental Function Generators

TABLE 1.2-2. Element Library

<u>Element</u>	<u>Code</u>
1. Two-node axisymmetric shell element	(1)
2. Axisymmetric triangular ring element	(2)
3. Two-dimensional (plane stress) four-node isoparametric quadrilateral element	(3)
4. Curved quadrilateral thin-shell element	(4)
5. Beam-column	(5)
6. Two-dimensional plane strain, constant stress triangle	(6)
7. Eight-node isoparametric three-dimensional hexahedron	(7)
8. Three-node triangular arbitrary shell	(8)
9. Three-dimensional truss element	(9)
10. Axisymmetric quadrilateral ring element (isoparametric)	(10)
11. Plane strain quadrilateral element (isoparametric)	(11)
12. Friction and gap element	(12)
13. Open-section beam	(13)
14. Closed-section beam	(14)
15. Isoparametric, two-node axisymmetric shell	(15)
16. Isoparametric, two-node curved beam	(16)
17. Pipe bend element	(17)
18. Four-node, isoparametric membrane	(18)
19. Generalized plane strain quadrilateral	(19)
20. Axisymmetric torsional quadrilateral	(20)
21. Three-dimensional 20-node brick	(21)
22. Curved quadrilateral thick-shell element	(22)
23. Three-dimensional 20-node rebar element	(23)
24. Curved quadrilateral shell element	(24)
25. Closed section beam in three dimensions	(25)
26. Plane stress, 8-node distorted quadrilateral	(26)
27. Plane strain, 8-node distorted quadrilateral	(27)
28. Axisymmetric, 8-node distorted quadrilateral	(28)
29. Generalized plane strain, distorted quadrilateral	(29)
30. Membrane, 8-node distorted quadrilateral	(30)
31. 6-Node Pipe Bend Element (not available)	(31)
32. Plane Strain 8-Node Distorted Quadrilateral Herrmann or Mooney Material Formulation	(32)
33. Axi-Symmetric, 8-Node Distorted Quadrilateral Herrmann or Mooney Material Formulation	(33)
34. Generalized Plane Strain, 8-Node Distorted Quadrilateral, Herrmann or Mooney Material Formulation	(34)
35. Three-Dimensional, 20-Node Brick. Herrmann or Mooney Material Formulation	(35)
36. Heat Transfer Element (Three-Dimensional Link)	(36)
37. Heat Transfer Element (Arbitrary Planar Triangle)	(37)
38. Heat Transfer Element (Arbitrary Axi-Symmetric Triangle)	(38)
39. Heat Transfer Element (Planar Bi-Linear Quadrilateral)	(39)
40. Heat Transfer Element (Axi-Symmetric Bi-Linear Quadrilateral Element)	(40)
41. Heat Transfer Element (8-Node Planar Bi-Quadratic Quadrilateral)	(41)
42. Heat Transfer Element (8-Node Axi-Symmetric Bi-Quadratic Quadrilateral)	(42)
43. Heat Transfer Element (Three-Dimensional 8-Node Brick)	(43)
44. Heat Transfer Element (Three-Dimensional 20-Node Brick)	(44)
45. Curved Timoshenko Beam Element in a Plane	(45)
46. Plane Strain Rebar Element	(46)
47. Generalized Plane Strain Rebar Element	(47)
48. Axi-Symmetric Rebar Element	(48)
49. Triangular Flat Plate Element	(49)
50. Rectangular Flat Plate Element	(50)
51. Quadrilateral Flat Plate Element	(51)
52. Elastic Beam	(52)

TABLE 1.2-2 Element Library

<u>Element</u>	<u>Code</u>
53. Plane stress, 8-node distorted quadrilateral with reduced integration	(53)
54. Plane strain, 8-node distorted quadrilateral with reduced integration	(54)
55. Axisymmetric, 8-node distorted quadrilateral with reduced integration	(55)
56. Generalized plane strain, 10-node distorted quadrilateral with reduced integration	(56)
57. Three-dimensional 20-node brick with reduced integration	(57)
58. Plane strain, 8-node distorted quadrilateral for Herrmann or Mooney material formulation with reduced integration	(58)
59. Axisymmetric, 8-node distorted quadrilateral for Herrmann or Mooney material formulation with reduced integration	(59)
60. Generalized plane strain, 10-node distorted quadrilateral for Herrmann or Mooney material formulation with reduced integration	(60)
61. Three-dimensional 20-node brick for Herrmann or Mooney material formulation with reduced integration	(61)
62. Axisymmetric, 8-node quadrilateral for arbitrary loading	(62)
63. Axisymmetric, 8-node quadrilateral for arbitrary loading, Herrmann formulation	(63)
64. Isoparametric, 2-node truss element	(64)
65. Heat transfer element, 2-node truss	(65)
66. 8-node axisymmetric with twist, Herrmann formulation	(66)
67. 8-node axisymmetric with twist	(67)

TABLE 1.2-3. Material Library

1. Engineering Materials at Room Temperature
2. Viscoelastic Behavior
 - a) Maxwell model
 - b) Kelvin model
3. Incompressible and Nearly Incompressible Material
 - a) Herrmann formulation
 - b) Large strain elasticity - Mooney material
 - c) Hypoelastic material
 - d) Anisotropic material (Taylor formulation)
4. Plasticity Behavior Models, Von Mises Yield Criterion
 - a) Prandtl-Ruess, Von Mises yield criterion
 - b) Temperature dependence
 - c) Isotropic hardening
 - d) Kinematic hardening
 - e) Combined kinematic and isotropic hardening
 - f) Definition of work hardening slopes
5. Creep behavior models
6. ORNL Constitutive Theories
7. Hydrostatic Yield Dependence
 - a) Linear Mohr Coulomb
 - b) Parabolic Mohr Coulomb
8. Large Displacement Analysis Effects
9. Anisotropic Behavior
 - a) Elastic
 - b) Plastic
10. Generalized Constitutive Relations
11. Low Tension and Cracking Behavior
 - a) Axisymmetric Analysis
 - b) Concrete Shell Analysis

TABLE 1.2-4. Structural Procedures Library

1. Linear Analysis
2. Nonlinear Analysis
 - a) Scaling for elastic-plastic analysis
 - b) Controls
3. Evaluation of J-Integral
4. Plasticity
5. Creep
6. Dynamic analysis
 - a) Modal analysis
 - b) Direct integration, implicit
 - c) Direct integration, explicit
7. Large Displacement
 - a) Incremental analysis
 - b) Buckling
 - c) Creep buckling, accumulated buckling
8. Fluid/Solid Interaction
9. Rigid, Perfectly Plastic Flow
10. Viscoplasticity
11. Heat Transfer, Diffusion Problems

INTRODUCTION

MARC-CDC contains an extensive element library. These elements provide coverage of plane stress and plane strain structures, axisymmetric structures (shell type or solid body, or any combination of the two), plate, beam and arbitrary shell structures, and full three-dimensional solid structures. A short description of each element and a summary of the data necessary for use of the element is included in this section. The reader will note that many elements serve the same purpose. Where possible we have indicated the preferred element that should be used. In general we have found that the quadrilateral elements give significantly better results in two dimensions. Because of the dependence of thermal and non-linear problems on the accuracy of stresses at the integration points, the higher order isoparametric element should be used for all such problems. Plate analysis can be performed by either degenerating one of the shell elements or by use of the reduced integration element (element 22). The elements with mid-side nodes require a large bandwidth for the solution of the master stiffness matrix. As a general comment, the user should be aware that the sophisticated elements in MARC will enable problems to be solved with many fewer elements when compared to solutions with constant stress elements. This requires the user to exercise his analytical skills and judgment. In return the user will be rewarded by a more accurate stress and displacement picture.

In this and subsequent sections, reference will be made to the first and second nodes, etc. of an element in order to define either the direction or sequence of the nodes. This order of the nodes is that which is defined by the connectivity matrix for the structure and is input by the CONNECTIVITY model definition block of Volume II, Section 2.

NOTE: For all elements right-handed coordinate systems are used. For all two-dimensional elements, right-handed rotation is anti-clockwise in the plane. In this chapter nodes are numbered in the order that they appear in the connectivity matrix. These numbers are of course replaced by the appropriate node numbers for an actual structural model. For all shell elements, stress and stiffness states are calculated at eleven representative points through the thickness.

NOTE: All shear strains are engineering values, not tensor values.

INCOMPRESSIBLE AND NEARLY INCOMPRESSIBLE ELEMENTS (Herrmann Formulation)

Certain elements in the program (Elements 32-35) allow the study of incompressible and nearly incompressible materials in plane strain and three-dimensional cases through the use of an augmented variational principle based on the Herrmann formulation (See Appendix G, Reference 26). The element is assumed to be elastic (or visco-elastic). However, the implementation is general enough for large displacements, creep and thermal strains to be taken into account. Note that although these elements only allow elastic and visco-elastic behavior, they may be used in conjunction with other elastic-plastic elements in the same mesh. It is also noted that these elements conform the basis for fluid flow analysis (See Appendix G, Reference 27). The elements may also be used to advantage for compressible materials, since their hybrid formulation usually gives more accurate stress predictions.

In the following, the element description appears in the sequence in which they were developed in the program. However, it is easier to recognize the applicability of each element by grouping it in its own structural class. This is shown in Table 2.0-1. Table 2.0-2 lists the element library in the sequence that the elements were developed.

REDUCED INTEGRATION ELEMENTS

For a number of isoparametric elements in the program (elements 22 and 53-61), a reduced integration scheme is used to determine the stiffness matrix of the element. In such a reduced scheme, the integration is not exact, the contribution of the highest order terms in the deformation field is neglected. Reduced integration elements have specific advantages and disadvantages. The most obvious advantage is the reduced cost for element assembly. This is specifically significant for the 3-dimensional elements (57 and 61). Another advantage is the improved accuracy which may be obtained with reduced integration elements. The increase in accuracy is due to the fact that the higher order deformation terms are coupled to the lower order terms, the coupling is strong if the elements are distorted. The higher order terms cause strain gradients within the element which are not present in the exact solution, and hence the stiffness is overestimated. Since the reduced integration scheme does not take the higher order terms into account, this effect is not present in the reduced integration elements.

This same feature also forms the disadvantage of the element. Each of the reduced integration elements has some specific higher order deformation mode(s) which do not give any contribution to the strain energy in the element. The 8-node quadrilateral elements have one such "breathing" mode, shown in fig. 2.53-3. The element 22 has two breathing modes, whereas the 20-node bricks have six breathing modes. Breathing modes may become dominant in meshes with a single array (8-node quads) or single stack (20-node bricks) of elements. In meshes of this type sufficient boundary conditions should be prescribed to suppress the breathing modes, or the exact integration element should be used. It may also be advantageous to combine reduced integration elements with the element with exact integration in the same mesh - this is always possible in MARC.

TABLE 2.0-1
Structural Classifications of Elements
(Continued)

Structural Type	Element Number	Displacement Function	Remarks	Element Number	Displacement Function	Remarks
	55	Quadratic	as 28 with reduced integration	62	Quadratic	8-node Arbitrary Loading
Membrane 3-D	18	Bilinear	4-node	30	Quadratic	8-node
Flat Plate	49	Constrained Cubic	3-node	50	Bicubic	4-node Isopara.
	51	Patch Cubic	8-node			
Curved	4	Bicubic	4-nodes	8	Constrained Cubic	3-node
	22	Quadratic	8-nodes reduced integration	24	Patch	8-node
3-D Solid	7	Tri-Linear	8-nodes isopara.	21	Quadratic	20-node
	57	Quadratic	As 21 with reduced integration			
Incompressible	32	Quadratic	8-node plane strain	33	Quadratic	8-node axisymmetric
	34	Quadratic	8-node generalized plane strain	35	Quadratic	20-node 3-D
	58	Quadratic	as 32 with reduced integration	59	Quadratic	as 33 with reduced integration
	60	Quadratic	as 34 with reduced integration	61	Quadratic	as 35 with reduced integration

TABLE 2.0-1
Structural Classifications of Elements
(Continued)

Structural Type	Element Number	Displacement Function	Remarks	Element Number	Displacement Function	Remarks
	66	Quadratic	8-node Axisym- metric with twist			
	67	Quadratic	8-node Axisym- metric with twist			
Pipe Bend	17	Cubic	2-nodes in plane 1-node out-of-plane			
Rebar Elements	46	Biquadratic	8-node	47	Quadratic	8-node
	48	Quadratic	8-node Axisymmetric	23	Quadratic	20-node
Heat Conduction Link	36	Linear	3-D 2-node	65	Quadratic	3-D 3-node

Table 2.0-2 Element Library Cont'd.

<u>Element</u>	<u>Code</u>
45. Curved Timoshenko Beam Element in a Plane	(45)
46. Plane Strain Rebar Element	(46)
47. Generalized Plane Strain Rebar Element	(47)
48. Axisymmetric Rebar Element	(48)
49. Triangular Flat Plate Element	(49)
50. Rectangular Flat Plate Element	(50)
51. Quadrilateral Flat Plate Element	(51)
52. Elastic Beam	(52)
53. Plane stress, 8-node distorted quadrilateral with reduced integration	(53)
54. Plane strain, 8-node distorted quadrilateral with reduced integration	(54)
55. Axisymmetric, 8-node distorted quadrilateral with reduced integration	(55)
56. Generalized plane strain, 10-node distorted quadrilateral with reduced integration	(56)
57. Three-dimensional 20-node brick with reduced integration	(57)
58. Plane strain, 8-node distorted quadrilateral for Herrmann or Mooney material formulation with reduced integration	(58)
59. Axisymmetric, 8-node distorted quadrilateral for Herrmann or Mooney material formulation with reduced integration	(59)
60. Generalized plane strain, 10-node distorted quadrilateral for Herrmann or Mooney material formulation with reduced integration	(60)
61. Three-dimensional 20-node brick for Herrmann or Mooney material formulation with reduced integration	(61)
62. Axisymmetric, 8-node quadrilateral for arbitrary loading	(62)
63. Axisymmetric, 8-node quadrilateral for arbitrary loading, Herrmann formulation	(63)
64. Isoparametric, 2-node truss element	(64)
65. Heat transfer element, 2-node truss	(65)
66. 8-node axisymmetric with twist, Herrmann formulation	(66)
67. 8-node axisymmetric with twist	(67)

TABLE 2.0-2. Element Library

<u>Element</u>	<u>Code</u>
1. Two-node axisymmetric shell element	(1)
2. Axisymmetric triangular ring element	(2)
3. Two-dimensional (plane stress) four-node isoparametric quadrilateral element	(3)
4. Curved quadrilateral thin-shell element	(4)
5. Beam-column	(5)
6. Two-dimensional plane strain, constant stress triangle	(6)
7. Eight-node isoparametric three-dimensional hexahedron	(7)
8. Three-node triangular arbitrary shell	(8)
9. Three-dimensional truss element	(9)
10. Axisymmetric quadrilateral ring element (isoparametric)	(10)
11. Plane strain quadrilateral element (isoparametric)	(11)
12. Friction and gap element	(12)
13. Open-section beam	(13)
14. Closed-section beam	(14)
15. Isoparametric, two-node axisymmetric shell	(15)
16. Isoparametric, two-node curved beam	(16)
17. Pipe bend element	(17)
18. Four-node, isoparametric membrane	(18)
19. Generalized plane strain quadrilateral	(19)
20. Axisymmetric torsional quadrilateral	(20)
21. Three-dimensional 20-node brick	(21)
22. Curved quadrilateral thick-shell element	(22)
23. Three-dimensional 20-node rebar element	(23)
24. Curved quadrilateral shell element	(24)
25. Closed section beam in three dimensions	(25)
26. Plane stress, 8-node distorted quadrilateral	(26)
27. Plane strain, 8-node distorted quadrilateral	(27)
28. Axisymmetric, 8-node distorted quadrilateral	(28)
29. Generalized plane strain, distorted quadrilateral	(29)
30. Membrane, 8-node distorted quadrilateral	(30)
31. 6-Node Pipe Bend Element (not available)	(31)
32. Plane Strain 8-Node Distorted Quadrilateral Herrmann or Mooney Material Formulation	(32)
33. Axisymmetric, 8-Node Distorted Quadrilateral Herrmann or Mooney Material Formulation	(33)
34. Generalized Plane Strain, 8-Node Distorted Quadrilateral, Herrmann or Mooney Material Formulation	(34)
35. Three-Dimensional, 20-Node Brick, Herrmann or Mooney Material Formulation	(35)
36. Heat Transfer Element (Three-Dimensional Link)	(36)
37. Heat Transfer Element (Arbitrary Planar Triangle)	(37)
38. Heat Transfer Element (Arbitrary Axisymmetric Triangle)	(38)
39. Heat Transfer Element (Planar Bi-Linear Quadrilateral)	(39)
40. Heat Transfer Element (Axisymmetric Bi-Linear Quadrilateral Element)	(40)
41. Heat Transfer Element (8-Node Planar Bi-Quadratic Quadrilateral)	(41)
42. Heat Transfer Element (8-Node Axisymmetric Bi-Quadratic Quadrilateral)	(42)
43. Heat Transfer Element (Three-Dimensional 8-Node Brick)	(43)
44. Heat Transfer Element (Three-Dimensional 20-Node Brick)	(44)

AXI-SYMMETRIC SHELL, ISOPARAMETRIC FORMULATION - ELEMENT 15

This is a two-node axi-symmetric, thin-shell element, with a cubic displacement assumption based on the global displacements and their derivatives with respect to distance along the shell. The strain-displacement relationships used are suitable for large displacements with small strains. The stress-strain relationship is integrated through the thickness by Simpson rule, the first and last points being on the surfaces. Three-point Gaussian integration is used along the element.

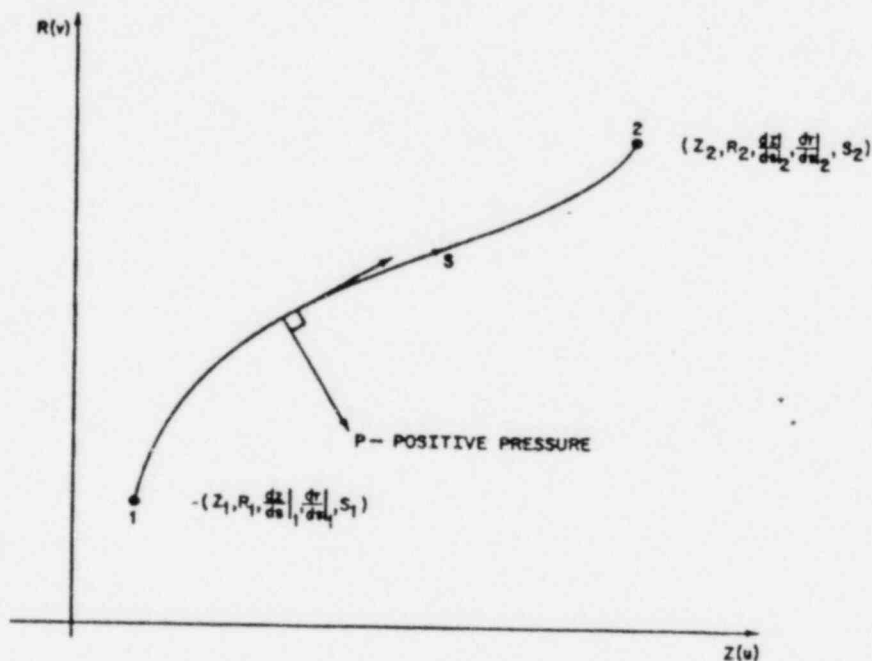


Figure 2.15-1. Axi-symmetric, Curved Thin-Shell Element

QUICK REFERENCE

. TYPE 15:

Axi-symmetric, curved thin-shell element.

- CONNECTIVITY:

Two nodes per element.

- GEOMETRY:

Linear thickness variation along the element. Thickness at first node of the element stored in the first data field (EGEOM1).

Thickness at second node in the third data field (EGEOM3).

If EGEOM3=0, constant thickness assumed. Notice that the linear thickness variation is only taken into account if the ALI POINTS option is used since, in the other case, section properties formed at the centroid of the element are used for all integration points.

The second data field is not used (EGEOM2).

- COORDINATES:

1 = z

2 = r

3 = $\frac{dz}{ds}$

4 = $\frac{dr}{ds}$

5 = s

(Note: The redundancy in the coordinate specification is retained for simplicity of use with mesh generators).

- DEGREES OF FREEDOM:

1 = u = axial (parallel to symmetry axis)

2 = v = radial (normal to symmetry axis)

3 = $\frac{du}{ds}$

4 = $\frac{dv}{ds}$

- TRACTIONS:

Distributed loads. Selected with IBODY as follows:

Uniform pressure - IBODY=0

Non-uniform pressure - IBODY=5

Pressure assumed positive in direction of normal obtained by rotation of -90° from direction of increasing s (see Figure 2.15-1).

Uniform load in 1 direction - IBODY = 1

Non-uniform load in 1 direction - IBODY = 3

Uniform load in 2 direction - IBODY = 2

Non-uniform load in 2 direction - IBODY = 4

In the non-uniform cases (IBODY = 3, 4 or 5) the load magnitude must be supplied by user subroutine FORCEM.

Concentrated loads applied at the nodes must be integrated around the circumference.

OUTPUT OF STRAINS:

Generalized strains are:

1 = meridional membrane (stretch)

2 = circumferential membrane (stretch)

3 = meridional curvature

4 = circumferential curvature

OUTPUT OF STRESSES:

Output of stress at points through thickness (first and last points are on surfaces), first point on surface up positive normal, positive normal is opposite to positive pressure shown in Figure 2.15-1.

1 = meridional stress ; 2 = circumferential stress

TRANSFORMATION:

The degrees of freedom may be transformed to local directions.

OUTPUT POINTS:

Centroid or three Gaussian integration points. First Gaussian point is closest to first node, second is at centroidal section, third is closest to second node.

MESH GENERATOR:

None available.

SECTION STRESS INTEGRATION:

Use SHELL SECT parameter card to set number of points for Simpson rule integration through the thickness. 3 points is enough for linear material response--7 points for simple plasticity or creep analysis, 11 points for complex plasticity or creep (e.g. dynamic plasticity). The default is 11 points.

In the following section, we outline the features available in MARC-CDC. Because the program covers a large area, it is not possible to present all the relevant theory here. The user who is interested in the theory behind a particular feature may obtain it from the references given in this volume. It may be useful to note that there are two volumes connected with the theory behind the program (Volume IV, MARC Course Manual and Volume V, Collected Papers). These volumes may be purchased from MARC Analysis.

This section is divided into two parts and describes the materials and the structural procedures library. The materials library allows the user to select from among a large number of elastic and inelastic models. The material behavior models may be anisotropic. In the inelastic models, the yield functions may be dependent on temperature on mean hydrostatic stress (e.g. concrete soils).

The structural procedure determines which features of the program will be used in a particular analysis. The structural procedures library covers the whole range of physical phenomena found in structural mechanics. This includes linear and nonlinear (piecewise incremental) behavior in the static and dynamics regime. The user of a general purpose program should bear in mind the ability to select from the three libraries viz. element, materials and structural procedures. The use of each library presents its own difficulties in ensuring a correct analysis. To ensure correct use of the element library, the user must select the appropriate element and ensure that the element and nodal data are correct. These may be checked with the aid of the mesh display feature.

To ensure correct use of the material library, the user must check that the proper material constants are input. The dependence of the material on temperature and other state variables should also be checked. It is a good practice to check the correctness of the material problem by solving a simple one element truss problem with the same material model. To ensure correct use of the procedures library, the user must pay attention to two aspects. First of all, the correctness of the kinematic constraints and the loading must be verified. Then, the correct setting of the control tolerances and load increment size must be specified. Wherever possible, the program attempts to relieve the user of manual control. The user should take advantage of all the automatic controls provided. In the absence of any specialized information on the problem, the user should follow and use the default tolerances provided by the program. Here again, it is a wise procedure to solve a similar problem with a one-element problem to establish the appropriateness of the structural procedure.

In this section we describe the material models that are available in the program's material library. For normal modeling of an engineering metal at room temperature, the user need only enter the PROPERTY block of input data. This is described in Section 2, page 2.6-6 of Volume II.

Material Library

1. Engineering materials at room temperature
2. Viscoelastic behavior
 - a) Maxwell model
 - b) Kelvin model
3. Incompressible and Nearly Incompressible Material
 - a) Herrmann formulation
 - b) Large strain elasticity - Mooney material
 - c) Hypoelastic material
 - d) Anisotropic material (Taylor formulation)
4. Plasticity Behavior Models, Von Mises Yield Criterion
 - a) Prandtl-Ruess, Von Mises yield criterion
 - b) Temperature dependence
 - c) Isotropic hardening
 - d) Kinematic hardening
 - e) Combined kinematic and isotropic hardening
 - f) Definition of work hardening slopes
5. Creep Behavior Models
6. ORNL Constitutive Theories
7. Hydrostatic Yield Dependence
 - a) Linear Mohr Coulomb
 - b) Parabolic Mohr Coulomb
8. Large Displacement Analysis Effects
9. Anisotropic Behavior
 - a) Elastic
 - b) Plastic
10. Generalized Constitutive Relations

A generalized constitutive material for plasticity has been implemented. It is described in this section under the viscoplasticity procedure.
11. Low Tension and Cracking Behavior
 - a) Axisymmetric Analysis
 - b) Concrete Shell Analysis

VISCOELASTICITY - GENERALIZED KELVIN MATERIAL BEHAVIOR

In addition to the non-linear Maxwell type model allowed in the CREEP option, a general Kelvin model may be included through the use of the VISCO ELAS parameter card. In this case the program assumes an additional creep strain ϵ_{ij}^K , governed by

$$\frac{d}{dt} \epsilon_{ij}^K = A_{ijkl} s_{kl} - B_{ijkl} \epsilon_{kl}^K$$

where [A] and [B] are defined by the user in the subroutine described below.

s_{ij} are the deviatoric stress components

$$s_{ij} = \sigma_{ij} - \delta_{ij} \frac{\sigma_{kk}}{3}$$

and the total strain is

$$\epsilon_{ij} = \epsilon_{ij}^e + \epsilon_{ij}^p + \epsilon_{ij}^c + \epsilon_{ij}^K + \epsilon_{ij}^{th}$$

ϵ_{ij}^{th}	= thermal strain components	} instantaneous response
ϵ_{ij}^e	= elastic strain components	
ϵ_{ij}^p	= plastic strain components	
ϵ_{ij}^c	= creep strains defined via CRPLAW and VSWELL routines and using CREEP option	
ϵ_{ij}^K	= Kelvin model strain components as defined above	

KELVIN USER SUBROUTINE.

The matrices [A] and [B] above are defined by the user in subroutine CRPVIS. The header cards are:

```
SUBROUTINE CRPVIS (CRPR, TSIG, SINC, AE, BE, NGENS, DT, DTOL, N, NN, MAT, TIME,
TIMINC) DIMENSION CRPR(1), TSIG(1), SINC(1), AE (NGENS, NGENS), BE (NGENS, NGENS)
```

Where

CRPR are the Kelvin creep strain components

TSIG(1) is the second invariant of deviatoric stress = $(\frac{3}{2} s_{ij} s_{ij})^{1/2}$

TSIG(2) is the hydrostatic stress = $\frac{1}{3} \sigma_{kk}$

SINC are the deviatoric stress components (s_{ij})

AE is the matrix $A_{ij \ k}$ above, to be defined here by the user

BE is the matrix $B_{ij \ k}$ above, to be defined here by the user

NGENS is the number of stress (strain) components

DT are the total state variables at this point (temperature first)

DTDL are the increments of state variables at this point during the step of the solution

N element number

NN integration point number

MAT material identification number (from PROPERTY option)

TIME total time

TIMINC time increment

Only AE and BE are to be defined by the user - the other variables are provided to assist in calculations, for example when a nonlinear Kelvin model is used.

This routine is called at each point of each element when necessary, when the VISCO ELAS parameter card is present. Note that the use of the VISCO ELAS option also requires the use of the CREEP option in the model definition data as well. The CREEP option is required to set the tolerance control for the maximum strain in any increment. In viscoelastic two-dimensional analysis the stress does not change appreciably so that all time steps are controlled by the maximum increment in strain. The recommended and default value of this strain increment is 0.05 of the total elastic strain. Note that this value is ten times smaller than the default value for normal creep problems. Because of the use of the CREEP option, Maxwell models may be included in series with the Kelvin model. The ordering of stress and strain components is given in Volume B, section 1 for each element.

When used with membrane or doubly curved shell elements (curvilinear coordinates) the above relation is written in a mixed formulation:

$$\frac{d}{dt} (\epsilon_{\alpha \beta}^{\delta} K) = A_{\alpha \beta \delta}^{\gamma} S_{\gamma}^{\delta} - B_{\alpha \beta \delta}^{\gamma} \epsilon_{\gamma}^{\delta} K \quad \alpha, \beta \text{ etc.} = 1, 2$$

with two shear components stored,

$$\epsilon_1^1, \text{ then } \epsilon_1^2$$

Note, curvilinear coordinates are only used in MARC in plane stress (membranes and thin shells), hence the range 1, 2 on Greek indices above.

INCOMPRESSIBLE AND NEARLY INCOMPRESSIBLE FORMULATION (Herrmann Formulation)

Certain elements in the program (elements 32-35 and 58-61) allow the study of incompressible and nearly incompressible materials in plane strain and three-dimensional cases through the use of an augmented variational principle based on the Herrmann formulation (see Appendix G, reference 26). This section gives the details of the formulation.

It is assumed that the instantaneous behaviour is isotropic elastic. Then the total Lagrange strain is written as

$$E_{ij} = E_{ij}^e + E_{ij}^{ne}$$

where

E_{ij}^e are the elastic strain components

E_{ij}^{ne} are the non-elastic strain components
i.e. creep and thermal strains.
(Currently plasticity is not included
in the formulation of these elements).

The elastic constitutive theory is

$$S_{ij} = 2G(E_{ij}^e + \nu H\delta_{ij}) \quad (1)$$

where S_{ij} are Kirchhoff stress components

G is the shear modulus

ν is the Poisson ratio (close to, or equal to 0.5)

H is the Herrmann mean pressure variable = $\frac{\sigma_{kk}}{2G(1+\nu)}$ (2)

The equilibrium equation is

$$\sigma_{ij,j} + F_i = 0 \quad (3)$$

F_i = body force per unit volume

σ_{ij} = Cauchy stress components

The dilatational relation is

$$E_{kk}^e - (1-2\nu)H = 0 \quad (4)$$

We introduce a virtual displacement field δu_i on the equilibrium equation, and a variation $(-2\nu G\delta H)$ on the dilatational relation to give an augmented virtual work equation:

$$\int_V (\sigma_{ij,j} + F_i) \delta u_i dV - \int_{V^0} (E_{kk} - E_{kk}^{ne} - (1-2\nu)H) 2\nu G\delta H dV^0 = 0$$

here V is the current volume, V^0 is the initial volume occupied by the same material.

Using the Gauss theorem, with $\sigma_{ij} n_j = T_i$ (the surface tractions), gives

$$\begin{aligned} & \int_{V^0} (S_{ij} \delta E_{ij} + (E_{kk} - (1-2\nu)H)2\nu G\delta H) dV \\ &= \int_{S^0} T_i \delta u_i dS^0 + \int_{V^0} F_i \delta u_i dV^0 \\ &+ \int_{V^0} E_{kk}^{ne} 2\nu G\delta H dV^0 \end{aligned} \quad (5)$$

Here $\delta E_{ij}(u, \delta u) = \frac{1}{2} (\delta u_{i,j} + \delta u_{j,i} + u_{k,i} \delta u_{k,j} + \delta u_{k,i} u_{k,j})$

is the first variation of Lagrange strain.

Substitute the elastic constitutive theory (equation (1)) to obtain

$$\begin{aligned} & \int_{V^0} 2G(\delta E_{ij} E_{ij} + \nu H \delta E_{kk} + \nu E_{kk} \delta H - \nu (1-2\nu)H\delta H) dV^0 \\ &= \int_{S^0} T_i \delta u_i dS^0 + \int_{V^0} F_i \delta u_i dV^0 \\ &+ \int_V 2G(E_{ij}^{ne} \delta E_{ij} + \nu E_{kk}^{ne} \delta H) dV^0 \end{aligned} \quad (6)$$

Equation (6) is the governing variational principle. It is shown below that in the small displacement case with no creep effects this reduces to the Herrmann formulation of reference 26. First, however, note that the above equation includes large displacement and large strain effects and is solved incrementally in the program. Taking a Taylor expansion of (6) in displacement to first order terms gives:

$$\begin{aligned} & \int_{V^0} 2G(\Delta E_{ij} \delta E_{ij} + E_{ij} \Delta \delta E_{ij} + \nu H \Delta \delta E_{kk} \\ &+ \nu \Delta E_{kk} \delta H - \nu (1-2\nu) H \delta H) dV^0 \\ &= \int_{S^0} \Delta T_i \delta u_i dS^0 + \int_{V^0} \Delta F_i \delta u_i dV^0 \\ &+ \int_{V^0} 2G(\Delta E_{ij}^{ne} \delta E_{ij} + E_{ij}^{ne} \Delta \delta E_{ij} + \nu \Delta E_{kk}^{ne} \delta H) dV^0 \end{aligned}$$

where F are the total forces on the right-hand side of (6) and I is the left-hand side of (6). Note the assumption of constant G and ν : the extension to, say, temperature dependent properties is quite straightforward

$$\text{Here, } \Delta E_{ij} = \frac{1}{2} (\Delta u_{i,j} + \Delta u_{j,i} + \Delta u_{k,i} u_{k,j} + \Delta u_{k,j} u_{k,i})$$

$$\text{and } \Delta \delta E_{ij} = \frac{1}{2} (\Delta u_{k,i} \delta u_{k,j} + \Delta u_{k,j} \delta u_{k,i})$$

Equation (7) is linear in Δu_i and so may be solved by the finite element method. Note that equation (7) is the same as the general incremental equation of the program (equation 3.1 of reference 25, section G), particularized to linear elastic isotropic behavior, if the constitutive theory is re-written as

$$\begin{Bmatrix} \Delta S_{11} \\ \Delta S_{22} \\ \Delta S_{33} \\ \Delta S_{12} \\ \Delta S_{23} \\ \Delta S_{31} \\ \Delta I \end{Bmatrix} = 2G \begin{bmatrix} 1 & 0 & 0 & 0 & 0 & 0 & \nu \\ 0 & 1 & 0 & 0 & 0 & 0 & \nu \\ 0 & 0 & 1 & 0 & 0 & 0 & \nu \\ 0 & 0 & 0 & 1/2 & 0 & 0 & 0 \\ 0 & 0 & 0 & 0 & 1/2 & 0 & 0 \\ 0 & 0 & 0 & 0 & 0 & 1/2 & 0 \\ \nu & \nu & \nu & 0 & 0 & 0 & -\nu(1-2\nu) \end{bmatrix} \begin{Bmatrix} \Delta E_{11} \\ \Delta E_{22} \\ \Delta E_{33} \\ \Delta E_{12} \\ \Delta E_{23} \\ \Delta E_{31} \\ \Delta H \end{Bmatrix} \quad (8)$$

where the shear strain increments are written in engineering notation

$$(\Delta E_{12} = \Delta u_{1,2} + \Delta u_{2,1} + u_{k,1} \Delta u_{k,2} + u_{k,2} \Delta u_{k,1})$$

and ΔI is the increment of 'dilatational restraint force' - the Lagrange multiplier term in the augmented virtual work equation (5) above.

Equivalence of above formulation to Herrmann's principle for small displacement, non-creeping behavior.

The Herrmann principle is (reference 26, equation (9)):

$$\begin{aligned} \delta \left(\int_V G (\theta_1^2 - 2\theta_2 + 2\nu H \theta_1 - \nu(1-2\nu) H^2 - 6\nu e_T H - 2\theta_1 e_T) dV \right. \\ \left. - \int_V F_i u_i dV - \int_{S_T} T_i u_i dS \right) = 0 \end{aligned} \quad (9)$$

with e_T is thermal strain ($= e_T \delta_{ij}$)

$$\text{and } \theta_1 = e_{kk}, \theta_1^2 - 2\theta_2 = \epsilon_{ij} \epsilon_{ij}$$

This reduces to

$$\int_V 2G(\epsilon_{ij} \delta\epsilon_{ij} + \nu H \delta\epsilon_{kk} + \nu \epsilon_{kk} \delta H - \nu(1-2\nu) H \delta H) dV$$

$$= \int_S T_i \delta u_i dS + \int_V F_i \delta u_i dV + \int_V 2G(e_T \delta\epsilon_{kk} + 3\nu e_T \delta H) dV \quad (10)$$

This is the same as (6) above if second order terms in E_{ij} and displacement dependent terms in δE_{ij} are neglected, and we write $E_{ij}^{ne} = e_T \delta_{ij}$.

Thus, the formulation described in this section may be particularized to the Herrmann principle for small displacement, non-creeping problems.

Note that the elements based on the above principle assume isotropic behaviour, so that anisotropic option cannot be used in them. Note also that currently these elements allow elastic time independent behaviour only - creep is allowed but not plasticity (although they may be used in conjunction with other elastic-plastic elements in the same mesh).

LARGE STRAIN ELASTICITY - MOONEY MATERIAL

The program offers the Mooney finite strain thermo-elastic constitutive theory for incompressible hyperelastic materials (e.g. rubber, solid propellant) undergoing large strain and displacement. The basic linearized incremental procedure of MARC is utilized, in conjunction with a hybrid variational principle defined below, similar in form to the Herrmann incompressible elastic formulation. Both these formulations are incorporated in Elements 32 (Plane Strain), 33 (Axi-Symmetric), 34 (Generalized Plane Strain) and 35 (Three-Dimensional). All these elements use bi- or tri-quadratic displacement interpolation, and bi- or tri-linear interpolation for the pressure variable, and are isoparametric in formulation -- See Volume I, Section 2. These elements may be used in combination with other elements in the library (suitable tying may be necessary) and with each other. Note that where different materials are joined the nodes must be uncoupled to allow the mean pressure discontinuity -- tying must be used to couple the displacements only.

The formulation is complete for arbitrarily large displacements and strains; however, the user should remember that the solution is obtained as a series of piecewise linear increments, so that suitably small load steps must be taken. Since residual load correction is important for accurate solutions, and the elements are higher order (linear stress), the ALL POINTS parameter card is recommended. (See Volume IV for details of the theory).

INCOMPRESSIBLE AND NEARLY INCOMPRESSIBLE ANISOTROPIC FORMULATION(TAYLOR FORMULATION)

With the hybrid elements in MARC, it is also possible to analyze incompressible and approximately incompressible anisotropic elastic materials. The option is used for the hybrid elements if the ANISOTROPI parameter card is included. Similar to the compressible anisotropic material, the orientation of the elastic constants used by the MARC program is provided by the user in the subroutine ORIENT.

In the most generally allowed case, the stress strain law in the preferred orientation is

$$\begin{Bmatrix} \epsilon_{11} \\ \epsilon_{22} \\ \epsilon_{33} \\ \gamma_{12} \\ \gamma_{23} \\ \gamma_{31} \end{Bmatrix} = \begin{matrix} A_{11} & A_{12} & A_{13} & 0 & 0 & 0 \\ & A_{22} & A_{23} & 0 & 0 & 0 \\ & & A_{33} & 0 & 0 & 0 \\ & & & A_{44} & 0 & 0 \\ \text{Symmetric} & & & & A_{55} & 0 \\ & & & & & A_{66} \end{matrix} \begin{Bmatrix} \sigma_{11} \\ \sigma_{22} \\ \sigma_{33} \\ \tau_{12} \\ \tau_{23} \\ \tau_{31} \end{Bmatrix}$$

The arrangement of the $\{\epsilon\}$ $\{\sigma\}$ vectors is defined for each element in the Element Library section of the manual. The A_{ij} are supplied by the user in the subroutine ANELAS. The A_{ij} may be defined as a function of temperature.

The necessary header cards for ANELAS are

```
SUBROUTINE ANELAS(N, NN, LAYER, A, IRDIM, T)
  DIMENSION A(IRDIM, IRDIM)
  User coding
  RETURN
  END
```

Here:

N is the element number.

NN is the integration point number.

LAYER is the layer number(always 1 for the hybrid elements).

A is the A_{ij} to be defined by the user, the number of allowable A_{ij} being given in Table 3-1.

IRDIM is the dimension of the R array for the current elements.

T is the current temperature.

All parameters except the A array are defined by the program. A must be defined by the user in the routine. The formulation used to derive the stress as a function of strain for these materials is due to Taylor et al, Appendix G, reference 29.

HYPOELASTIC MATERIAL

The program allows hypoelastic material behaviour in any element (including Herrmann formulation elements) through the use of a user subroutine HYPELA. For this class of constitutive theory, the program assumes

$$\dot{\sigma}_{ij} = c_{ijkl} \dot{\epsilon}_{kl}^e + g_{ij}$$

where c_{ijkl} and g_{ij} are functions of elastic strain and temperature

The user subroutine is used to define c_{ijkl} and g_{ij} as functions of elastic strain and temperature. Note that for the Herrmann formulation, $\dot{\sigma}_{ij}$ is augmented by \dot{H} , the mean pressure variable, so that the extra term in g_{ij} (corresponding to \dot{H}) should be added as necessary.

The parameter card HYPOELAS is needed for this option. In order to obtain accurate solutions, the user should provide a second stiffness over the increment:

$$\Delta\sigma_{ij} = \bar{c}_{ijkl} \Delta\epsilon_{kl}^e + \bar{g}_{ij}$$

where \bar{c} and \bar{g} are mean values over the (finite) increment. In addition, the total stress

$$\sigma_{ij}(\epsilon_{ij}^e, T)$$

should be defined as its exact value at the end of the increment to allow the residual load correction to work effectively.

PLASTICITY

The behavior is the classical theory of isotropic, elastic-plastic, time-independent materials, with a Mises or Mohr-Coulomb (extended Mises) yield criterion, isotropic strain hardening, temperature-dependent elastic properties, and strain-rate dependent yield stress. Perfect plasticity is assumed when no strain hardening is specified.

The stress-strain relation is then

$$\{\dot{\sigma}\} = [D] (\{\dot{\epsilon}\} - \{\dot{\epsilon}^T\}) + \{\dot{h}\} \dot{T}$$

where

- $\{\dot{\sigma}\}$ The stress rate
- $\{\dot{\epsilon}\}$ The total strain rate
- $\{\dot{\epsilon}^T\}$ The thermal strain, given by

$$\dot{\epsilon}_{ij} = \alpha \dot{T}, \quad i = j$$

$$\dot{\epsilon}_{ij} = 0, \quad i \neq j$$

[D] is either [C], the elastic stress-strain relation, if the point is not loading into the plastic range, or $[D]_d = [c] \{s\} [s] [c]$ when the point is loading into the plastic range.

Here,

$$d = \left(\frac{2}{3} \bar{\sigma}\right)^2 \frac{\partial \bar{\sigma}}{\partial \ln \bar{p}} + [s] [c] \{s\},$$

$\bar{\sigma}$ The equivalent tensile stress.

$\frac{\partial \bar{\sigma}}{\partial \ln \bar{p}}$ The slope of the tensile isothermal stress-strain curve, at the point defined by $\bar{\sigma}$.

$\{s\}$ The deviatoric stresses.

Also, if the point is not loading into the plastic range,

$$\{h\} = \{G\} = \left[\frac{dc}{dT} \right] [c^{-1}]^T \{\sigma\}$$

= rate of change of elastic constants with temperature, multiplied by the current total stress,

or when plastic loading is taking place,

$$\{h\} = [G] - \frac{1}{d} [c] \left(\{s\} [s] \{G\} - \frac{2\bar{\sigma}}{3} \frac{\partial \bar{\sigma}}{\partial T} - \frac{2}{3} \frac{\partial r}{\partial T} \frac{\partial \bar{\sigma}}{\partial \epsilon_p^0} d\epsilon_p \right)$$

where

$G, c, s,$
 d and $\bar{\sigma}$ As defined above.

$\frac{\partial \bar{\sigma}}{\partial T}$ The temperature rate of change of the equivalent yield stress at the current temperature of this point.

r is the ratio of the workhardening slope at temperature to the slope at initial temperature

$$r = \frac{\frac{\partial \bar{\sigma}}{\partial \epsilon_p^T}}{\frac{\partial \bar{\sigma}}{\partial \epsilon_p^0}}$$

where subscripts T and 0 denote temperatures at T and initial temperature respectively.

The above rate equation is used as an incremental equation in the program, with $[D]$ and $\{h\}$ modified as weighted means for those increments which are elastic and plastic. The temperature dependence of the workhardening slopes can be used in cases where the workhardening slopes change appreciably with temperature. The theory assumes that the workhardening slopes change with temperature for a given equivalent plastic strain. The equivalent plastic strain is assumed to be unaffected by changes in temperature. The data is given in the form of rate of change of the ratio r with respect to temperature in the TEMPERATURE EFFECTS option block. More details on this part of the program (for the isothermal case) may be found in reference 10 of Appendix G.

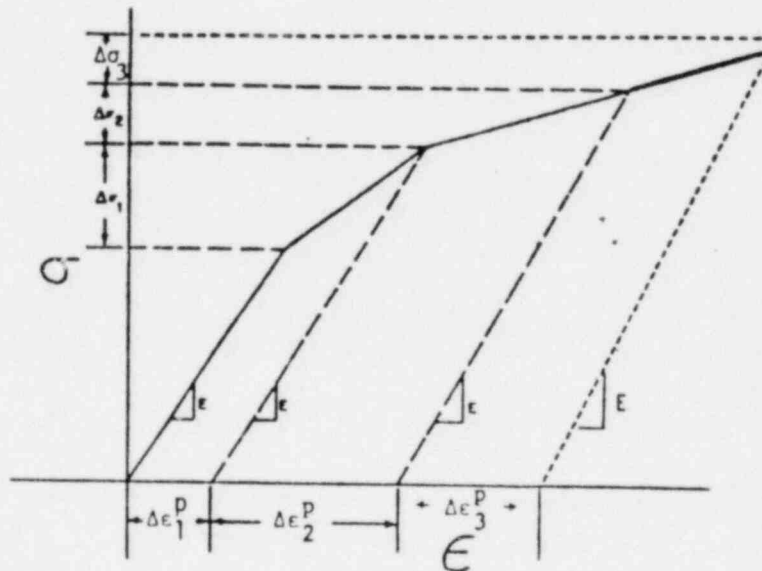
It should be noted that because of the use of the rate equations directly in incremental form, the condition of perfect plasticity can never be achieved. However, provided the strain increments are left small (by using small load increments), the departure from the true yield surface is negligible.

An option exists for selecting kinematic hardening instead of isotropic hardening. Essentially the same programming is used for kinematic hardening. However, a shift in the yield center is performed prior to calculating the strain and stress rates. The program uses only the number of stresses already present in the element. The kinematic hardening formulation always works in full nine-dimensional stress space.

Combined isotropic and kinematic hardening is also available as an option, where a nonlinear hardening slope is treated as isotropic superposed on kinematic, the kinematic slope being taken as that as $\bar{\epsilon}^p \rightarrow \infty$.

DEFINITION OF WORK-HARDENING SLOPES

Work-hardening slopes must be input for uniaxial stress data as change in stress per unit of plastic strain: see the diagram below:



$$\text{1st work hardening slope} = \frac{\Delta\sigma_1}{\Delta\epsilon_1^P}, \text{ breakpoint} = 0.0$$

$$\text{2nd work hardening slope} = \frac{\Delta\sigma_2}{\Delta\epsilon_2^P}, \text{ breakpoint} = \Delta\epsilon_1^P$$

$$\text{3rd work hardening slope} = \frac{\Delta\sigma_3}{\Delta\epsilon_3^P}, \text{ breakpoint} = \Delta\epsilon_1^P + \Delta\epsilon_2^P$$

NOTE: The slopes of the work hardening curves should be based on a plot of the stress versus plastic strain curve for a tensile test. The elastic components of the stress strain curve should not be included and the first breakpoint of the work hardening slope should be 0.0

CREEP

Creep behavior is based on a Mises yield criterion with isotropic behavior described by the equivalent creep law

$$\dot{\epsilon} = f(\bar{\sigma}, \bar{\epsilon}^C, T, t).$$

Thus, the material behavior is described by:

$$\{\dot{\epsilon}^C\} = \dot{\epsilon}^C [u]$$

where:

[u] The unit outward normal to the current J_2 stress surface.

$\frac{\dot{\epsilon}^C}{\epsilon}$ The equivalent creep strain rate, assumed to be described by a piecewise linear approximation to:

$$\frac{\dot{\epsilon}^C}{\epsilon} = A \cdot f(\bar{\sigma}) \cdot g(\bar{\epsilon}^C) \cdot h(T) \cdot k(t)$$

(Any of the functions, f , g , h , or k may be set to unity by setting the number of piecewise linear slopes for that relation to zero on the input data.)

The above relationship is used in the program by an initial strain technique; that is, a load vector due to the creep strain increment is added to the right-hand side of the stiffness equation.

Particular creep laws may be provided by the user through subroutines CRPLAW and VSWELL. CRPLAW assumes purely deviatoric creep while VSWELL assumes purely volumetric creep.

ORNL CONSTITUTIVE THEORIES

The Oak Ridge National Laboratory currently recommended constitutive theories for inelastic design analysis of FFTF components, as defined in ORNL-TM-3602, have been incorporated into the MARC-CDC Constitutive Library. The data and user-subroutine modifications needed to use this constitutive option are documented in Volume II, Sections 2 and 3. Note that as a result of the introduction of two distinct yield conditions, two sets of base values, workhardening curves and yield vs. temperature tables must be input.

The user is required to input the Blackburn Creep Law as a user subroutine (CRPLAW). This subroutine is discussed in Volume II, Section 3. Users should note that the parameter EQCP (first parameter in CRPLAW) will be defined as:

$$\bar{\epsilon}^C = \left(\frac{2}{3} \sum_{ij} \Delta \epsilon_{ij}^C \sum_{ij} \Delta \epsilon_{ij}^C \right)^{1/2}$$

when the ORNL constitutive option is flagged by use of the ORNL parameter card, but in all other cases the definition

$$\bar{\epsilon}^C = \sum \left(\frac{2}{3} \Delta \epsilon_{ij}^C \Delta \epsilon_{ij}^C \right)^{1/2}$$

is retained. Note that the equivalent primary creep strain is passed into CRPLAW in EQCPNC, the second parameter. This parameter must be redefined in that routine as the equivalent (total) creep strain increment, while the first parameter (EQCP) must be redefined as the equivalent primary creep strain increment. Again, this only applies when the ORNL constitutive option is flagged. During analysis with the ORNL Option, equivalent creep strain is used to store the distance between the two shifted origins in creep strain space (ϵ in ORNL-TM-3602). The sign on this value indicates which origin is currently active, so that a negative sign indicates use of the 'negative' origin ($-\epsilon_{ij}$).

HYDROSTATIC YIELD DEPENDENCE

The MARC program includes an option for elastic-plastic behavior based on a yield surface with hydrostatic stress dependence. Such behavior is observed in a wide class of soil and rock-like materials: these materials are generally classified as Mohr-Coulomb materials (generalized Mises materials). Ice in so far that it exhibits a dependence on hydrostatic stress is also thought to be a Mohr-Coulomb material.

The generalized Mohr-Coulomb behavior implemented in MARC is due to Drucker and Prager [17]:

The yield function is assumed to be perfectly plastic but is now a linear function of the hydrostatic stress.

$$f = \alpha J_1 + J_2^{1/2} - \frac{\bar{\sigma}}{3} = 0$$

where

$$J_1 = \sigma_{ii}$$

$$J_2 = \frac{1}{2} S_{ij} S_{ij}, \quad S_{ij} = \sigma_{ij} - \frac{1}{3} \delta_{ij} \sigma_{kk}$$

See the MARC theoretical manual for a relation between α and $\bar{\sigma}$ with the more traditional Mohr constants.

The above constitutive description is available in MARC by setting column 15 of the MOHRC parameter card to 1, the value of $\bar{\sigma}$ is read in by the PROPERTY option as the equivalent yield stress (cols. 51-60 of the third card of the option) and the value of α is read in on the same option in the field labelled 'density'. Notice that the convention, tensile direct stress is positive, is maintained throughout the program, contrary to many soil mechanics texts.

The hydrostatic dependence has been generalized still further to give a yield function of the form $f(J_1, J_2) = 0$. In the case of plane strain, this gives a yield envelope which is parabolic. The general yield surface used in MARC is described by

$$f = (3J_2 + \sqrt{3} \alpha J_1)^{1/2} - \bar{\sigma} = 0$$

The parabolic type yield surface may be obtained in MARC by setting the MOHRC parameter card column 15 to 2.

STRESS-STRAIN RELATION FOR LARGE DISPLACEMENT ANALYSIS

The large displacement option in MARC-CDC makes use of a Lagrangian (initial coordinate frame of reference). For this reason the fundamental stress and strain measures used are Kirchhoff stress and Lagrange strain. Therefore, the user must ensure that any stress-strain data input utilizes these measures. This distinction becomes significant for strains above one percent.

For the usual tensile test results, the conversions are straightforward, as indicated below:

In a tensile test, with a specimen of initial gauge length L_0 , current gauge length L and stretch of $u = L - L_0$, initial area A_0 , current area A , current load P , we have

$$\text{Engineering strain} = \frac{u}{L_0}$$

$$\text{True strain} = \ln \left(1 + \frac{u}{L_0} \right)$$

$$\text{Lagrange strain} = \frac{u}{L_0} + 1/2 \left(\frac{u}{L_0} \right)^2$$

$$\text{Engineering stress} = \frac{P}{A_0}$$

$$\text{True stress} = \frac{P}{A}$$

$$\text{Kirchhoff stress} = \frac{P}{A_0 \left(1 + \frac{u}{L_0} \right)}$$

Thus, the most usual conversions would be:

(a) Given Engineering stress-strain curve

$$\text{stress} = S_E = \frac{P}{A_0}, \text{ strain} = e_E = \frac{u}{L_0}$$

$$\text{Kirchhoff stress} = \frac{S_E}{(1 + e_E)}, \text{ Lagrange strain} = e_E \left(1 + 1/2 e_E \right)$$

Thus to produce the appropriate stress-strain curve for MARC-CDC, for a point on the Engineering stress-strain curve corresponding to an engineering strain value e_E , the stress must be divided by $(1 + e_E)$ and the strain multiplied by $(1 + 1/2 e_E)$.

b) Given True stress strain curve

$$\text{stress} = S_T = \frac{P}{A}, \text{ strain} = e_T = \ln \left(1 + \frac{u}{L_0} \right)$$

$$\text{Kirchoff stress} = S_T \frac{A}{A_0 \exp(e_T)}$$

Hence to produce the stress-strain curve for MARC-CDC, for a point on the True stress-strain curve corresponding to a True strain value e_T , the stress must be multiplied by $\frac{A}{A_0 \exp(e_T)}$

and the strain measure converted as $e_L = (\exp(e_T) - 1)(1 + 1/2(\exp(e_T) - 1))$.

For details of the large displacement formulation in the program, see Reference 24, Appendix G.

ANISOTROPIC MATERIAL BEHAVIOR

Anisotropic, time-independent behavior is available in MARC for both elastic, elastic-plastic and creep response. The generality extends to the specification of nine independent elastic constants and six yield sizes in those elements allowing a complete stress space. The user may also supply a transformation into a preferred orientation at each point used for stress-strain calculation. The dimensionality of the transformation and the number of allowable independent elastic and yield constants for each element are tabulated in Table 3-1.

The transformation matrix should be supplied as defined by:

$$v_i = g_{ij} \bar{v}_j \quad \text{for rectangular, Cartesian systems}$$

or

$$v_i = g_i^j \bar{v}_j \quad \text{for curvilinear systems (doubly curved shell)}$$

where v_i is a vector in the preferred orientation in which the constitutive properties will be supplied, and \bar{v}_i is a vector in the orientation used by MARC at the current point. The allowable dimension of the g_i^j matrix is shown in Table 3-1 for each element in the library. User subroutine ORIENT supplies the matrix. Note that g_i^j is given as $G(I, J)$ in such a matrix. If ORIENT is not supplied, $v_i = \bar{v}_i$ is assumed, i.e., the orientation used by the MARC program for the particular elements in the analysis is assumed to be that in which the anisotropic constants will be supplied. Note also that output remains in the global system even if ORIENT is used. The POST tape gives the user access to stresses and strains and may be used to obtain them in a local system.

The elastic anisotropy is defined by the specification of elastic constants in the preferred orientation. The number of such constants available for each element is shown in the table. These constants are input by supplying, in the user subroutine ANELAS, the ratios of the terms in the corresponding isotropic stress-strain law. These ratios all default to unity if they are unspecified; they are also assumed not to be temperature dependent, so that the temperature dependence of the elastic stress-strain law is only introduced isotropically through $E(T)$, $\nu(T)$.

The yield anisotropy is defined by the specification, again by user subroutine, of the tensile and shear yield values in the preferred orientation. The number of such yield values allowable in any element is shown in the table. As in the elastic case, ratios of anisotropic to isotropic yield must be supplied, with the program defaulting to a unit ratio for those undefined by the user. The ratios are given in subroutine ANPLAS. The ratios are assumed to be temperature independent, so that temperature dependence of the yield function is introduced isotropically only. Anisotropy of the yield function is included in association with deviatoric stress only, so that the Mohr-Coulomb (generalized Mises) options of the program may be used in conjunction with the anisotropic behavior.

The creep anisotropy assumes the anisotropic stress potential defined by ANPLAS, as described in the yield definition above.

Anisotropic thermal expansion is specified by the user subroutine ANEXP, giving the increments of thermal strain components directly in the preferred orientation set up in subroutine ORIENT. Any values not specified in ANEXP are given their isotropic values, using the instantaneous coefficient of thermal expansion (corrected for temperature) set up in the PROPERTY and TEMPERATURE EFFECTS options.

ELASTIC ANISOTROPY - USER SUBROUTINE ANELAS

In the most generally allowed case, the preferred orientation the isothermal stress-strain law is:

$$\begin{Bmatrix} \sigma_{11} \\ \sigma_{22} \\ \sigma_{33} \\ \tau_{12} \\ \tau_{23} \\ \tau_{31} \end{Bmatrix} = \begin{bmatrix} r_{11} D_{11} & r_{12} D_{12} & r_{13} D_{13} & 0 & 0 & 0 \\ & r_{22} D_{22} & r_{23} D_{23} & 0 & 0 & 0 \\ & & r_{33} D_{33} & 0 & 0 & 0 \\ \text{Symmetric} & & & r_{44} D_{44} & 0 & 0 \\ & & & & r_{55} D_{55} & 0 \\ & & & & & r_{66} D_{66} \end{bmatrix} \begin{Bmatrix} \epsilon_{11} \\ \epsilon_{22} \\ \epsilon_{33} \\ \gamma_{12} \\ \gamma_{23} \\ \gamma_{31} \end{Bmatrix}$$

The arrangement of the $\{\sigma\}$, $\{\epsilon\}$ vectors is defined for each element in the Element Library section of the manual. The D_{ij} are those appropriate for isotropic elasticity (derived from $E(T)$, $\nu(T)$). The r_{ij} are supplied by the user in subroutine ANELAS.

The necessary header cards for ANELAS are:

```
SUBROUTINE ANELAS (N, NN, LAYER, R, IRDIM)
  DIMENSION R (IRDIM, IRDIM)
    user coding
  RETURN
  END
```

Here:

N is the element number

NN is integration point number

LAYER is the layer number (always 1 for continuum elements)
 R is the r_{ij} to be defined by the user; the number of allowable r_{ij}
 being given in Table 3-1.
 IRDIM is the dimension of the R array for the current element.

ALL parameters except the R array are defined by the program. R must be defined by the user in this routine.

Note that the R matrix has the dimension appropriate to the number of stress components associated with the particular element (see Table 301). Thus, for example, in elements 3, 4, 8 or 18, the R matrix would be of size 3 x 3, and the stress strain law would take the form:

$$\begin{Bmatrix} \sigma_{11} \\ \sigma_{22} \\ \sigma_{12} \end{Bmatrix} = \begin{bmatrix} r_{11} & D_{11} & r_{12} & D_{12} & 0 \\ & & r_{22} & D_{22} & 0 \\ \text{Symmetric} & & & r_{33} & D_{33} \end{bmatrix} \begin{Bmatrix} \epsilon_{11} \\ \epsilon_{22} \\ \epsilon_{12} \end{Bmatrix}$$

Yield surface and creep stress potential Anisotropy -- user subroutine ANPLAS

The anisotropic yield function and stress potential are assumed as:

$$a_1(\sigma_y - \sigma_z)^2 + a_2(\sigma_z - \sigma_x)^2 + a_3(\sigma_x - \sigma_y)^2 + 3a_4 \tau_{yz}^2 + 3a_5 \tau_{zx}^2 + 3a_6 \tau_{xy}^2 = 2\bar{\sigma}^2$$

(R. Hill - "Mathematical Theory of Plasticity," Oxford, 1950)

where:

$\bar{\sigma}$ is the equivalent tensile yield stress for isotropic behavior
 $(\bar{\sigma} = \bar{\sigma}(\epsilon^p, T))$

and, for Mohr-Coulomb behavior, $\bar{\sigma} = \bar{\sigma}(J_1)$, $J_1 = (\frac{\sigma_x + \sigma_y + \sigma_z}{3})$.

The user defines ratios of actual to isotropic yield (in the preferred orientation) in the array YRDIR for direct tension yielding, and YRSHR for yield in shear (ratio of actual shear yield to $\bar{\sigma}/\sqrt{3}$ = isotropic shear yield). Then the a_i above are derived as (Hill):

$$\begin{aligned}
 a_1 &= \frac{1}{YRDIR(2)**2} + \frac{1}{YRDIR(3)**2} - \frac{1}{YRDIR(1)**2} \\
 a_2 &= \frac{1}{YRDIR(3)**2} + \frac{1}{YRDIR(1)**2} - \frac{1}{YRDIR(2)**2} \\
 a_3 &= \frac{1}{YRDIR(1)**2} + \frac{1}{YRDIR(2)**2} - \frac{1}{YRDIR(3)**2} \\
 a_4 &= \frac{2}{YRSHR(3)**2} \\
 a_5 &= \frac{2}{YRSHR(2)**2} \\
 a_6 &= \frac{2}{YRSHR(1)**2}
 \end{aligned}$$

Note that YRDIR and YRSHR should be given in the order appropriate for the element (see Library Element description).

On the output, the Mises intensity is not affected by these material parameters.

Subroutine ANPLAS is written with the following header cards:

```

SUBROUTINE ANPLAS(N, NN, LAYER, NDI, NSHEAR, YRDIR, YRSHR)
DIMENSION YRDIR (NDI), YRSHR (NSHEAR)
  user coding
RETURN
END

```

Here:

N is the element number
 NN is the integration point number
 LAYER is the layer number (always 1 for continuum elements)
 NDI is the number of direct stresses
 NSHEAR is the number of shear stresses
 YRDIR is the array of tensile yield ratios
 YRSHR is the array of shear yield ratios

All parameters except YRDIR, YRSHE are defined by the program. YRDIR and YRSHR are defined by the user in this routine.

SPECIFICATION OF PREFERRED ORIENTATION - SUBROUTINE ORIENT

User subroutine ORIENT is used to supply a preferred orientation so that ANELAS and ANPLAS may supply anisotropic material constants in this orientation.

The required cards are:

```
SUBROUTINE ORIENT (N, NN, LAYER, G)
  DIMENSION G (3,3)
      user coding
  RETURN
  END
```

where:

N is the element number
NN is the integration point number
LAYER is the layer number (always 1 for continuum elements)
G is the transformation to the preferred orientation from the usual MARC orientation for this element

All parameters except G are passed in by the program--the user must supply the G matrix. The allowable transformations are shown in Table 3-1. Note that rectangular, Cartesian systems may be transformed orthogonally only. For curvilinear systems G is defined by $G(I,J) = g_i^j$. For planar transformations, $G(3,I)=G(I,3)=0$, $G(3,3)=1$, $I=1,2$ must be given.

ANISOTROPIC THERMAL EXPANSION - SUBROUTINE ANEXP

User subroutine ANEXP is used to specify anisotropic thermal strain increments in the orientation defined in subroutine ORIENT. The user is given the temperature at the beginning of the increment, the temperature increment, and the base value of thermal expansion coefficient given on the PROPERTY OPTION: he must supply the incremental thermal strain vector Δe_{ij} (Δe_i^j) for curvilinear systems, doubly curved shell and membrane elements) in the subroutine. Any components of the incremental thermal strain vector not defined in the routine assume their isotropic values.

The necessary header cards for ANEXP are:

```
SUBROUTINE ANEXP (N, NN, LAYER, T, TINC,
  ICOED, NDI, NSHEAR, EQEXP)
  DIMENSION EQEXP(1), TINC(1)
      user coding
  RETURN
  END
```

where:

N is the element number.
NN is the integration point number.
LAYER is the layer number for shells or beams (always 1 for continuum elements).
T(1) is the total temperature at the beginning of the increment
T(2) etc are the total values of other state variables at the beginning of the increment.
TINC(1) is the temperature increment.
TINC(2) etc. are the increments of other state variables.
COED is the base value of the coefficients of thermal expansion, given on the PROPERTY option.
NDI is the number of direct components of strain at this point.
SHEAR is the number of shear components of strain at this point.
EQEXP is the thermal strain increment vector, to be defined by the user in this subroutine.

All parameters except EQEXP are supplied by the program. EQEXP should be defined by the user in this routine. Note that for curvilinear coordinate elements (doubly curved shells, membranes, e.g. elements 4, 8, 18, 24, 30) the mixed strain tensor with two tensor shear components, $\epsilon_1^2, \epsilon_2^1$, is stored. Otherwise shear components are engineering shear strain

Table 3-1. Allowable Anisotropy

Library Element Number	Allowable Transformations To Preferred Operation	Size of R. Matrix (IRDIM) for IRDIM=1 No Anisotropy Possible	Number of Direct Yield Ratios (NDI)	Number of Shear Yield Ratios (NSHEAR)
1	None	2	3	0
2	Orthogonal in z-r plane	4	3	1
3	Orthogonal in x-y plane	3	3	1
4	Any in $\theta^1 - \theta^2$ surface	3	3	1
5	None	1	1	0
6	Orthogonal in x-y plane	4	3	1
7	Orthogonal in (x,y,z) space	6	3	3
8	Any in $\theta^1 - \theta^2$ surface	3	3	1
9	None	1	1	0
10	Orthogonal in z-r plane	4	3	1
11	Orthogonal in x-y plane	4	3	1
12	None	3	1	2
13	None	1	1	0
14	None	2	1	1
15	None	2	3	0
16	None	1	1	0
17	None	2	3	0
18	Any in surface	3	3	1
19	Orthogonal in (x,y,z) space	6	3	3
20	Orthogonal in (x,y,z) space	6	3	3
21	Orthogonal in (x,y,z) space	6	3	3
22	Orthogonal in (x,y,z) space	5	3	2
23	None			
24	Any in $\theta^1 - \theta^2$ surface	3	3	1
25	None	2	1	1
26	Orthogonal in x-y plane	3	3	1
27	Orthogonal in x-y plane	4	3	1
28	Orthogonal in z-4 plane	4	3	1
29	Orthogonal in x-y plane	4	3	1
30	Any in surface	3	3	1

Table 3-1. Allowable Anisotropy

Library Element Number	Allowable Transformations To Preferred Operation	Size of R. Matrix (IRDIM) for IRDIM=1 No Anisotropy Possible	Number of Direct Yield Ratios(NDI)	Number of Shear Yield Ratios (NSHEAR)
31	Element not available at this time			
32	Orthogonal in x-y plane	4	-	-
33	Orthogonal in z-r plane	4	-	-
34	Orthogonal in x-y plane	4	-	-
35	Orthogonal in (x,y,z) space	6	-	-
36-44	Use subroutine ANKOND to supply anisotropic conductivity			
45	None	1	1	0
46-48	None			
49	Any in \underline{v}^1 - \underline{v}^2 plane	3	3	1
50	Any in \underline{v}^1 - \underline{v}^2 plane	3	3	1
51	Any in \underline{v}^1 - \underline{v}^2 plane	3	3	1
52	None	Not Available		
53	Orthogonal in x-y plane	3	3	1
54	Orthogonal in x-y plane	4	3	1
55	Orthogonal in z-r plane	4	3	1
56	Orthogonal in x-y plane	4	3	1
57	Orthogonal in (x,y,z) space	6	3	3
58	Orthogonal in x-y plane	4	-	-
59	Orthogonal in z-r plane	4	-	-
60	Orthogonal in x-y plane	4	-	-
61	Orthogonal in (x,y,z) space	6	-	-

LOW TENSION AND CRACKING

a) Axisymmetric Models

This cracking option in MARC-CDC allows the user to perform a cracking analysis on an axisymmetric model using elements 10 or 28. The cracking model can predict both diametric and in plane (r-z plane) cracks of an axisymmetric structure subjected to mechanical and/or thermal loadings. During a load increment, if all three principal stresses at an integration point of an element are lower than the ultimate stress of the material, then no cracks will be initiated at this point. A crack is assumed to take place when one of the principal stresses reaches the ultimate stress. The direction of the crack is assumed to be perpendicular to the principal direction. Both constitutive equations and state of stress are modified to compensate for the loss of stiffness in the cross-crack direction at the location of the crack. The analysis of an axisymmetric reinforced concrete structure can be simulated by using this option in conjunction with the axisymmetric REBAR ELEMENT (Element 48).

After the initiation of a crack at a point in the structure, an initial crack strain is estimated in the cross-crack direction. During subsequent load increments, the strain in the cross-crack direction is compared with the initial crack strain for the determination of the closing of the crack. A crack is considered to be closed if the strain in the cross-crack direction is less than the initial crack strain. The material at the location of the crack is then assumed to be completely healed from cracking in the compressive direction. For the prediction of subsequent cracks at this point, the original state of material properties would be used.

b) Concrete Shell Analysis

Analytical procedures which may accurately determine stress and deformation states in concrete structures are complicated due to many factors. Among them are (1) the low strength of concrete in tension resulting in progressive cracking under increasing load, (2) the nonlinear load-deformation response of concrete under multi-axial compression. Since concrete is mostly used in conjunction with steel reinforcement, an accurate analysis requires the consideration of the components forming the composite structure. The steel reinforcement bars are introduced as anisotropic and overlapping shell elements.

Reinforcement Bars

The reinforcement bars are modeled by overlapping shell elements. These overlapping shell elements must be input with a separate element number but with the same element type number and connectivity, respectively. User subroutines ANELAS and ORIENT are also included to give the shell section the equivalent smeared value of elastic property at the 11 equally-space representative points through the thickness of the shell. The user provides elastic constants to determine the anisotropy due to the rebars in subroutine ANELAS. These elastic constants should be set to a very small number for the representative point through the shell thickness that does not have a reinforcement bar. Refer to section on ANISOTROPIC MATERIAL BEHAVIOR for further details (Volume I, 3.8-1).

Failure Criterion

For the analysis with concrete, the first step is to develop yield and failure criteria for concrete. On the basis of the generalized Mohr-Coulomb behavior, the failure law for concrete of the following form is proposed (see Reference 1):

$$3J_2 + \sqrt{3} B \sigma_1 J_1 + \alpha J_1^2 = \sigma_0^2 \quad (1)$$

where B , α , and σ_0 are material constants. For the biaxial stress conditions using the experimental data provided by Kupfer, et.al [2], and Liu, et.al [3], these constants were determined by a numerical trial procedure. The best fit was found by

$$B = \sqrt{3}, \quad \alpha = 1/5, \quad \text{and} \quad \sigma_1 = P/3$$

(P is the uniaxial compressive strength of concrete).

In the MARC program, for the doubly-curved shell elements, in which the stress condition is essentially two-dimensional, the assumed failure envelope for concrete is as shown in Figure 3.9-1. In compression-compression zone there is a marked nonlinearity in the failure curve expressed by Equation (1). In this region, the failure of concrete is defined by "crushing."

In tension-compression zone, consistent with the experiments, the failure is represented by a straight line connecting the points $\sigma_1 = P$ (compression) and $\sigma_2 = 0.10 P$ (tension).

In the tension-tension zone concrete behaves as an elastic material and the failure may be defined by the maximum tensile stress criterion.

THERMAL EXPANSION COEFFICIENT - DEFINITION

The MARC program always uses an instantaneous thermal expansion coefficient definition

$$\left. \begin{aligned} d\epsilon_{ij}^{th} &= \alpha_{ij} dT && \text{in general} \\ \text{or } d\epsilon_{ii}^{th} &= \alpha dT && \text{for the isotropic case -} \\ &&& \text{no sum on } i. \end{aligned} \right\} 1$$

In many cases the user is given data in terms of a reference temperature

$$\epsilon^{th} = \alpha(T - T^0) \quad 2$$

where α is a function of temperature: $\alpha = \alpha(T)$.

Clearly, in this case

$$d\epsilon^{th} = \left[\alpha + \frac{d\alpha}{dT}(T - T^0) \right] dT \quad 3$$

so when the user is given data in this reference temperature, total expansion form, the necessary conversion procedure is

1. Compute and plot equation 2 in the form 3

$$\alpha + \frac{d\alpha}{dT}(T - T^0) \quad 4$$

as a function of temperature.

2. Model 4 in user subroutine ANEXP, or with piecewise linear slopes and breakpoints in the TEMPERATURE EFFECTS option.

Progressive Cracking

Progressive cracking of concrete is based on the element representation. That is for each element (for each integration point of the element) the stress state is transformed to the principal stress space and the failure criterion is then checked for tension-tension and tension-compression zones. If the failure criterion is met then a crack is defined at that integration point, the crack being oriented perpendicular to the principal tension direction (Figure 3.9-2). To account for the presence of the crack in succeeding increments of loading, the incremental stiffness matrix is modified such that the element cannot transmit tensile stresses normal to the crack direction. In the shear term of the stiffness matrix a shear retention factor ($0 < \lambda < 1$.) is incorporated to account for the aggregate interlocking on the cracked surfaces.

Yield Criterion

Up to about 30 to 35 per cent of the compressive strength, concrete under uniaxial compression behaves as linear elastic. In biaxial loading, the elastic range in the compression-compression zone expands due to the micro-cracking confinement caused by lateral restraint.

The yield surface for concrete in biaxial loading may be obtained by scaling the failure curve. Equation (1) down to a size where uniaxial yield point, $\bar{\sigma}$, corresponds to about one-third of the uniaxial compressive strength. Therefore, the yield condition is

$$3J_2 + \sqrt{3} B \bar{\sigma} J_1 + \alpha J_1^2 = \bar{\sigma}^2 \quad \bar{\sigma} > 0. \quad (2)$$

when
$$\bar{\sigma} = P_y = \frac{1}{3} P \text{ (compression)}$$
 failure in

Yield condition (2) may be applied in both compression-compression, and compression-tension zones, with no loss of accuracy (see Reference 1).

Input To The MARC Program

This capability is used in the program by the following input.

- (1) The CRACKING parameter card is used to switch on the option.
- (2) The shear retention coefficient is input in column 21-30 of the same card series. In most cases this coefficient may be taken as 0.5.
- (3) The rest of the input is supplied in the PROPERTY option of the model definition cards (column 51-60 of the 3rd card series). The yield stress P_y is input as a positive value. The program then assumes $P=3$ is the cylinder strength of concrete under uniaxial compression. The values of α and B in (1) and (2) are pre-set to $\alpha=1/5$ and $B=\sqrt{3}$ for all concrete elements. These elements are identified by the CRACKING option for their model definition data.

References

1. Buyukozturk, O., "Prediction of Yield and Failure of Concrete Under Combined Stress," Development Report #TR75-1D, Marc Analysis Research Corporation, Providence, Rhode Island, January, 1975.
2. Kupfer, H., Hilsdorf, H. K., and Rush, H., "Behavior of Concrete Under Biaxial Stresses," ACI Journal, Proc. Vol. 66, No. 8, August 1969, pp. 656-666.
3. Liu, T.C.Y., Nilson, A.H., Slate, F.O., "Stress-Strain Response and Fracture of Concrete in Uniaxial and Biaxial Compression," ACI Journal, Proc., Vol. 69, No. 5, May 1972, pp. 291-295.

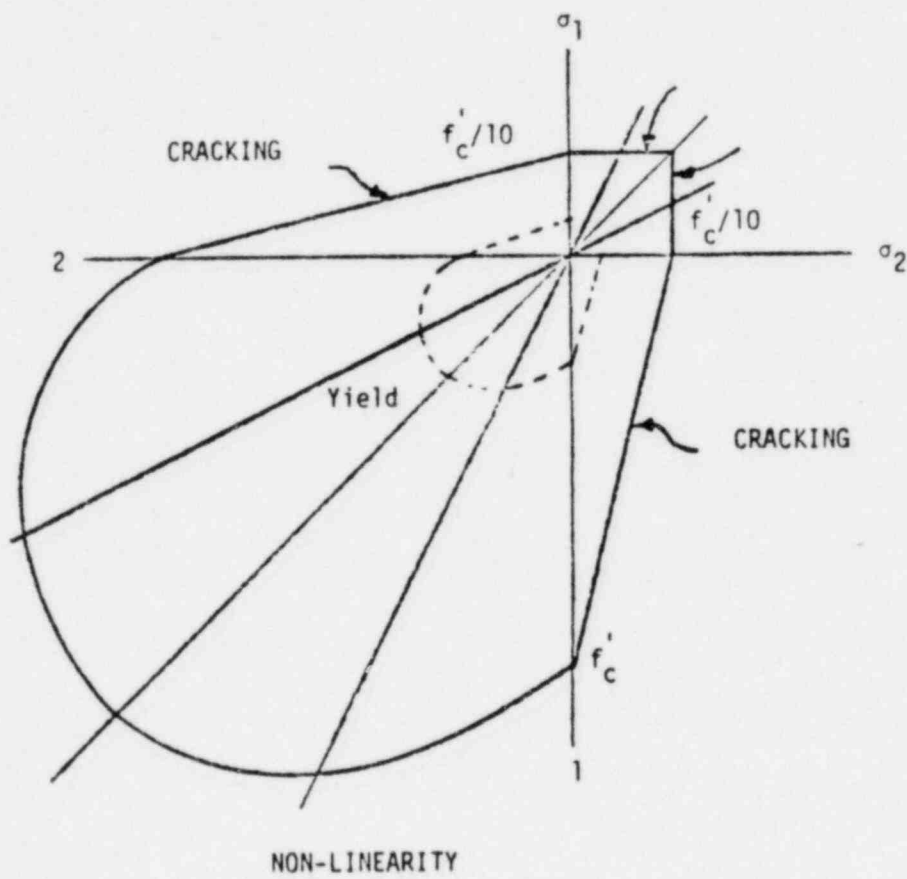


FIGURE 3.9-1. Failure Envelope

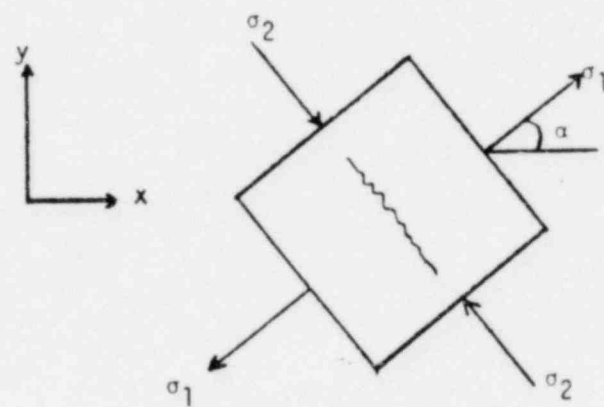


FIGURE 3.9-2. Crack Development

PROGRAM FUNCTIONS AND STRUCTURAL PROCEDURES LIBRARY

In this section we first describe the features available in the program for implementing the direct stiffness method. This is then followed by a description of the Structural Procedures Library.

A. Program Functions

1. Incremental Mesh Generators
2. Kinematic Constraints
 - a) Transformation of degrees of freedom
 - b) Elastic foundation
 - c) Tying
 - d) Boundary Constraints
3. Traction and Pressure Loading
 - a) Nodal loads
 - b) Surface loading
 - c) Volumetric loading
 - d) Thermal strain loading
 - e) Centrifugal Loading
4. Plotting Capabilities
 - a) Mesh display
 - b) Displaced position plots
 - c) Contour plots
 - d) Time history plots
5. Restart
6. Selective Assembly of Master Stiffness Equation
7. Incremental Function Generators

INCREMENTAL MESH GENERATOR

A collection of aids to mesh generation have been included in the program. These aids are referred to collectively as incremental mesh generators. In principle, they generate connectivity lists by repeating patterns and generate nodal coordinates by interpolation. Each of the aids may be used directly during the model definition phase of the input.

In the use of the incremental mesh generators, the user makes use of the element and node numbers that will be used in the actual analysis. The structure is divided into regions or blocks for which a particular mesh pattern can be generated with ease. The element connectivity lists that are sufficient to establish a pattern for each region is input via the CONNECTIVITY option. The incremental generators are then used to generate the rest of the connectivity lists.

The nodal coordinates are then generated. The critical node points that define the outline of the regions or blocks are entered by means of the COORDINATES option. The incremental generators are then used to complete the rest of the mesh. As a final operation, the regions are joined together by merging nodes which are close together.

A special connectivity interpolator option allows elements with mid-side nodes to be generated first without the mid-side nodes, and then filling in the mid-side nodes. Sometimes the difficulty of determining the position of a node requires a separate mesh generation run followed by mesh display plotting prior to the analysis run.

The following incremental generators are provided:

- 1) Element Connectivity Generator. This repeats the pattern of the connectivity data for previously-defined master elements. One element may be removed per series of the master elements. This allows the generation of tapering meshes. In the case of 3 node elements, two elements can be removed per master series.
- 2) Element Connectivity Interpolator. This completes the filling of connectivity list by generating mid-side nodes. It is used to generate elements with mid-side nodes by first generating the simpler quadrilateral or cubic elements without the mid-side nodes and then filling in the mid-side with this option.
- 3) Coordinate Generator. This creates a new set of nodes by copying the spacing of another specified set of nodes.
- 4) Coordinate Interpolator. This takes the line defined by two end nodes and divides the line by a specified number of equally-spaced nodes. The spaces between the nodes may be varied according to a geometric progression.
- 5) Coordinate Generation for Circular Arcs. This option generates the coordinates for a series of nodes which lie on a circular arc.
- 6) Nodal Merge. This option merges all nodes which are closer than a specified distance. It closes up all gaps in the nodal numbers.

TRANSFORMATION OF DEGREES OF FREEDOM

The program allows transformation of individual nodes from the global to a local direction through an orthogonal transformation. This facilitates the application of sliding boundary conditions and the tying together of shell and solid elements.

Note that transformations are assumed to be orthogonal, and that when transformation is invoked on a node, all loads and kinematic conditions at the node must be input in the transformed system, and displacement output will be in the transformed system. Transformation should not be imposed on nodes with default constraints.

ELASTIC FOUNDATION

The elements in MARC may be specified as being supported on a frictionless, elastic foundation. The foundation supports the structure with a force per unit area given by

$$\dot{p}_n = K(u_n) \dot{u}_n$$

where K is the equivalent spring stiffness of the foundation (per unit surface area) and u_n is the normal displacement of the surface at a point in the same direction as p_n .

The same conventions apply to the elastic foundation specification as are used for pressure specification, in terms of the face of the element which will be used. The force is not one-sided, that is, it will be applied whether tensile or compressive. The stiffness K may be made non-constant, by programming subroutine USPRNG.

Elastic foundations are specified as follows:

- (1) In the parameter card set, the ELAS FOUND card must be included to give the number of elements for which elastic foundation will be specified (see Volume II, Section 2).
- (2) In the model definition input blocks, the FOUNDATION block must be used to specify the elements which will rest on such an elastic foundation (see Volume II, Section 2).

TYING OF DEGREES OF FREEDOM

The program contains a generalized constraint condition option: any constraint involving linear dependence of nodal displacements may be included in the stiffness equations. Examples of the use of such a facility are:

- . The imposition of sliding boundary conditions
- . Imposition of particular displacement forms on parts of the structure (as a special case, rigid body motion of some surface)
- . The compatible joining of shell and solid type elements, shells to shells, beam stiffeners on shells, or different element types (e.g., 8- and 20-node bricks)
- . Use of one element type, but joining a fine and a coarse mesh, where the interface has more nodes in the fine mesh than in the coarse mesh, so that for compatibility, the extra nodes in the fine mesh must be properly constrained

The user may take advantage of this facility either by using the constraints which are available directly in the program, or by overriding these with his own constraint equations which are supplied in a short user subroutine. The constraint equations that are available directly in the program are summarized in this section. Table 3-2 summarizes these constraints.

Table 3-2. SUMMARY OF STANDARD TYING TYPES

Tying Code	No. of Retained Nodes	Purpose	Remarks
I<NDEG	1	Tie the Ith degree of freedom at the tied node to the Ith degree of freedom at the retained node.	NDEG = No. of degrees of freedom per node.
100	1	Tie all degrees of freedom at the tied node to the corresponding degrees of freedom at the retained node.	
23	1	Tie axi-symmetric solid node to axi-shell (element type 1) node.	Both tied and retained nodes must be transformed to local system. TRANSFORMATION option must be invoked. (See Section 3, Volume I)
18	2	Joining together the boundaries of intersecting shells, element type 4, 8 or 24. Fully moment carrying joint.	Tied node is also second retained node. (See Section 3, Volume I, and Section D-37A Volume IV)
28	2	Joining intersecting shells, element type 4, 8 or 24. Pinned joint.	Tied node is also second retained node. (See Section 3, Volume I and Section D-37A Volume IV)
19	2	Use beam element 13 as a stiffener on shell elements 4 or 8. Tied node is beam node: 1st retained node is shell node, 2nd is beam node again. Beam node should be on, or close to, the normal to the shell at the shell node.	Tied node is also second retained node.
20	3	Create an extra node in a shell type 8 element tied to the interpolation function of the shell. Used in conjunction with tying type 21 to tie a beam element 13 or a stiffener across a shell element.	Always used after tying type 21.
21	2	Same as type 19, but tying beam to an interpolated shell node not at a vertex of an element - element type 8 only. Must be followed by type 20 to tie the interpolated shell node into the shell mesh.	Must be followed by a tying type 20.
22	2	Join intersecting shells, element type 22.	Tied node is also second retained node. Thickness vector must be specified at tied and retained nodes.

TABLE 3-2
Summary of Standard Tying Types
(Continued)

Tying Code	No. of Retained Nodes	Purpose	Remarks
31	2	Refine mesh of first order (linear displacement) elements	Tie interior nodes on refined side to corner nodes on coarse side.
32	3	Refine mesh of second order (quadratic displacement) elements in 2-D.	Tie Interior nodes on refined side to the edge of an element on the coarse side.
33	4	Refine mesh of 8-node bricks	Tie interior node on refined side to the edge of an element on the coarse side
34	8	Refine mesh of 20-node bricks	Tie interior nodes on refined side to the 8 (4 corner, 4-mid-side nodes of an element on the coarse side.
24	2	Join intersecting shells or beams, element types 15-17.	Tied nodes is also 2nd retained node.
25	1	Join solid mesh to shell or or beam (type 15 or 16)	Similar to 23 above but no transformation needed.
49	2	Join intersecting plates, element type 49.	Tied node is also retained node.
50	2	Join intersecting plates, element type 50, corner nodes of element moment carrying joint.	Tied node is also retained node, type 51.
51	2	Join intersecting plates, midside nodes element type 51, moment carrying joint.	Tied node is also retained node.

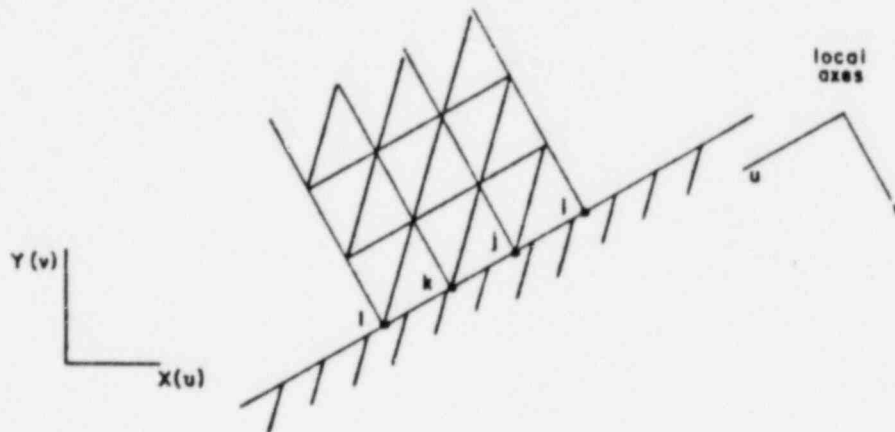
TABLE 3-2
Summary of Standard Tying Types
(Continued)

Tying Code	No. of Retained Nodes	Purpose	Remarks
52	1	Pin joint for beam types 14, 25, or 52.	
53	1	Full moment-carrying joint for beam types 14, 25 or 52.	
13	2	Joining two elements type 13 under an arbitrary angle. Full moment carrying joint.	Tied node is also 2nd retained node
>100	1	Generate several tyings of type <u>N</u> DEG	Tying code is first dof multiplied by 100 added to last dof, ie., 209 means tie 2nd to 9th dof at tied node to resp. 2nd to 9th dof at retained node.

WARNING -- TRANSFORMATION MUST NOT BE USED AT NODES INVOLVED IN TYING TYPES 13, 18, 19, 20, 21, 22, 24, 25, 49, 50, 51, 52 or 53.

Examples of each of the constraint equations available directly in the program follow:

1. Equal displacement at two nodes in a particular direction. This option may be used to impose sliding boundary conditions, as in the example below.



In this example we wish to enforce rigid sliding on the boundary, i.e., in the local coordinates defined above:

$$u_i = u_j = u_k = u_l$$

$$v_i = v_j = v_k = v_l = 0$$

The second equation is simply a set of fixed boundary conditions. The first equation is a constraint equation and is treated as follows:

We rewrite it as the set of equations

$$u_i = u_j$$

$$u_k = u_j$$

$$u_l = u_j$$

i.e., expressing all the u displacements in terms of u_j . Then on the TIE parameter card, columns 11 through 15, we specify the number of equations -- in this case, 3. In addition, we also complete the TYING card series.

<u>Card Series</u>		<u>Columns</u>	<u>Description</u>
TIE		11 through 15	Number of constraints.
		16 through 20	We only have one type of constraint.
		21 through 25	Two nodes are involved in each constraint equation.
TYING	2	1 through 5	The code for the tying type is equal to the degree of freedom being constrained. This automatically brings in a simple constraint equation. Thus, assuming the nodal displacement transformation facility has been used to rotate into local coordinates at these nodes (see TRANSFORM parameter card), we now specify 1 in column 5.
	2	6 through 10	In each equation, one node is retained on the right-hand side.
	3	1 through 5	$\left. \begin{matrix} 1 \\ i \\ j \end{matrix} \right\} \text{ repeated for } k \text{ and } l$
	4	1 through 5	

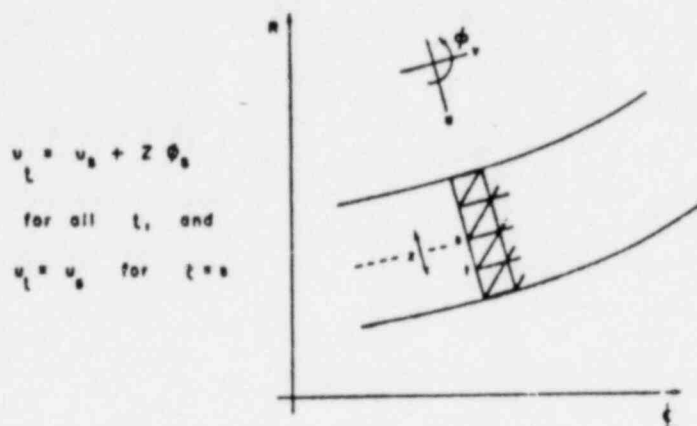
This completes the constraint condition.

- Specify the tying type as 100 to constrain node i to node j by the matrix equation

$$\{u_i\} = \begin{bmatrix} 1 & & 0 \\ & \ddots & \\ 0 & & 1 \end{bmatrix} \{u_j\}$$

- Specify tying type 23 for axisymmetric shell-solid interface. This example shows the use of a compatible combination of library elements 1 (axisymmetric shell) and 2 (triangular ring), or 10 (quadrilateral ring).

The constraint of compatibility between the two different elements may be imposed by nodal constraints on the transition plane, which may be written in terms defined as follows:



$$u_t = u_s + Z \phi_s$$

for all t , and

$$u_t = u_s \text{ for } t = s$$

These constraints are in the program as tying type 23: they are programmed in local coordinates as defined above, thus displacements at nodes on the transition plane must be rotated into these new directions, as shown in the data for this example. The tying is then done directly by specifying:

Tying type 23

Constrained node = off-center node on transition plane

Retained node = central node on transition plane

for each node except the central node on each transition plane.

The TRANSFORMATION option must be invoked with this tying type.

4. Specify tying type 18 or 28 for joining together the boundaries of intersecting shells (element type 4, 8 or 24).

Tying type 18 provides a moment carrying joint, type 28 a pinned joint at intersections of shell surfaces.

The user should note the following:

- a) For surfaces with the same normal at the intersection, tying type 18 and 28 both tie all rotations and membrane strains. The program does not, in this case, provide a pinned joint capability. In addition, since all first derivatives are constrained, the tying is not correct if the surface thickness changes discontinuously at the intersection. Experience shows the latter to be a small effect if the thickness does not change by more than 50%-100%. For more accuracy, the user should provide his own constraints (via UFORMS) for this case.
- b) For element type 4 no attempt is made by the program to tie

the cross derivative terms $\frac{\partial^2 u_i}{\partial \theta^1 \partial \theta^2}$. These can only be con-

strained if the (θ^1, θ^2) lines are orthogonal in both surfaces at the line of intersection. If this is the case, the user should include these additional constraints via UFORMS.

- c) No tying is provided for the mid-side nodes of element type 24. This constraint should be provided by the user via subroutine UFORMS.
- d) It is possible to use tying types 18 or 28 to use element types 8 and 4 in the same mesh.

See Volume IV for theoretical development of these constraints.

- 5. Tying types 19, 20, 21 - use of element 13 as a beam stiffener on elements 8 or 4.

Tying type 19 allows element 13 to be applied as a stiffener to element types 8 or 4 with the beam node on (or close to) the normal to the shell surface at a shell node. Tying type 21 ties the beam to a node introduced independently at any point in the shell surface (element type 8 only). Type 20 is then used to constrain this new node to the 4 element vertices of the shell element in which it appears. See Volume IV for complete description of these constraint theories.

Then introduce the tangent to the shell surface, closest in direction to \underline{b}_1 , by

$$\underline{c}_1 = \underline{b}_1 - (a_3 \cdot b_1) \underline{a}_3 \quad (1)$$

where $\underline{a}_3 = \underline{a}_1 \times \underline{a}_2 = \text{unit normal to shell at } s$.

$$|\underline{a}_1 \times \underline{a}_2|$$

Choose a normal to \underline{c}_1 in the shell surface

$$\underline{c}_2 = \underline{a}_3 \times \underline{b}_1 = - (b_1 \cdot a_2) \underline{a}_1 + (b_1 \cdot a_1) \underline{a}_2 \quad (2)$$

Let u_1^s, u_2^s, u_3^s , be the components of displacement of the point S in the direction $\underline{c}_1, \underline{c}_2, \underline{a}_3$ respectively, and let s_1, s_2 be measures of distance in the shell surface from S in the directions \underline{c}_1 and \underline{c}_2 . At B , let s measure distance along the beam axis, ϕ be the angle of twist about the beam axis, and u_1^b, u_2^b, u_3^b be the components of displacement of B along \underline{b}_1 and parallel to \underline{c}_2 and \underline{a}_3 . The offset of the beam node B from the shell node S is defined as

$$d = \underline{SB} \cdot \underline{a}_3 \quad (3)$$

where \underline{SB} is the vector from S to B .

With this notation, the basic displacement constraint equations are written as follows:

$$\text{Rotation: about } \underline{c}_3, \quad \frac{du^b}{ds} = \frac{\partial u^s}{\partial s_1} \quad (4)$$

$$\text{about } \underline{c}_2, \quad \frac{du^b}{ds} = \frac{\partial u^s}{\partial s_1} \quad (5)$$

$$\text{about } \underline{c}_1, \quad \phi = \frac{\partial u^s}{\partial s_1} \quad (6)$$

$$\text{Displacement: } u_3^b = u_3^s \quad (7)$$

$$u_1^b = u_1^s - d \cdot \frac{\partial u^s}{\partial s_1} \quad (8)$$

$$u_2^b = u_2^s - d \cdot \frac{\partial u^s}{\partial s_2} \quad (9)$$

Thus, the node B appears as both a tied and retained node, with 6 degrees of freedom tied out by use of Equations (6) - (9) and (12), appropriately transformed to the global Cartesian and surface coordinate systems. This tying type has been programmed in MARC in two forms: with the shell node S coincident with one of the vertices of the triangles defining the shell surface (tying type 19) and with S at some other point in the interpolated surface (tying type 21). For the latter case it is also necessary to constrain the shell node to the vertices of the triangle defining the part of the surface on which it is placed: this is done by constraints of type (b) below.

b. Constraint of an interpolated shell node (for element 8 only).

In order to allow a beam element to be constrained to interpolated shell nodes, S, at points other than the triangular vertices on the surface, it is necessary that the degrees of freedom introduced at S be properly constrained to the interpolated deformation of the shell. This may be achieved directly by use of interpolation functions and their first derivatives with respect to the surface coordinates, for the element 8 used in MARC. Thus the equation

$$\{u\}_S = \begin{bmatrix} F(\theta^1_S, \theta^2_S) \end{bmatrix} \begin{Bmatrix} u_a \\ u_b \\ u_c \end{Bmatrix} \quad (13)$$

are used to form the vector of displacements at the interpolated node from the displacements of the vertices of the triangle to which it belongs (in the $\theta^1 - \theta^2$ plane). Since the constraint matrix F is an appropriate ordering of the interpolation function and its derivatives, which are function of position ($\theta^1 - \theta^2$), these are the only coordinates needed to generate F in (13). However, the beam-shell constraint equations require the interpolated shell surface to be defined at node S. This is achieved by using (13) to generate the Cartesian coordinates and their derivatives with respect to surface coordinates at S in terms of these quantities at the triangle vertices with precisely the same matrix F (θ^1_S, θ^2_S), since the element is of isoparametric formulation.

This constraint is available as type 20 in the MARC program. The node S may be on the interior or the boundary of a triangle in the (θ^1, θ^2) plane.

Note that for any constraint type 21 (beam node tied to an interpolated shell node) there must also exist a constraint type 20 to tie the interpolated shell node into the surface. If this is not provided by the user, the program aborts with a message.

There are thus six constraints between the beam and shell node. The beam node is treated as a tied node, with both shell node, S, and the beam node as retained nodes. When the degrees of freedom at B are transformed to the global set, the global displacement components will be constrained by equations (7), (8) and (9), and likewise ϕ will be constrained by (6). However, (4) and (5) become two constraints between the three components of displacement derivatives. These must be used to remove two of these degrees of freedom at the beam node. The procedure adopted is as follows:

We write

$$\begin{Bmatrix} \frac{du_2^b}{ds} \\ \\ \frac{du_3^b}{ds} \end{Bmatrix} = [D] \begin{Bmatrix} \frac{d\bar{u}_1^b}{ds} \\ \frac{d\bar{u}_2^b}{ds} \\ \frac{d\bar{u}_3^b}{ds} \end{Bmatrix} \quad (10)$$

where \bar{u}_i^b are the global displacement components at the beam node, and $[D]$ is a transformation matrix defined from the orientation of \underline{b}_1 , \underline{c}_2 and \underline{a}_3

The equation may be rewritten as

$$\begin{Bmatrix} \frac{du_2^b}{ds} \\ \\ \frac{du_3^b}{ds} \end{Bmatrix} = \{D_i\} \frac{d\bar{u}_i^b}{ds} + [D^*] \begin{Bmatrix} \frac{d\bar{u}_j^b}{ds} \\ \\ \frac{d\bar{u}_k^b}{ds} \end{Bmatrix} \quad (11)$$

where one global degree of freedom has been isolated. Inverting $[D^*]$ (a 2 x 2 matrix) results in

$$\begin{Bmatrix} \frac{du_j^b}{ds} \\ \\ \frac{du_k^b}{ds} \end{Bmatrix} = [D^*]^{-1} \begin{Bmatrix} \frac{du_2^b}{ds} \\ \\ \frac{du_3^b}{ds} \end{Bmatrix} - [D^*]^{-1} \{D_i\} \frac{d\bar{u}_i^b}{ds} \quad (12)$$

provided $[D^*]$ is not singular. In the coding, this problem is avoided by choosing the combination of columns of $[D]$ as the one with the largest determinant. Equation (12) may be used as a constraint on $\frac{d\bar{u}_j^b}{ds}$ and $\frac{d\bar{u}_k^b}{ds}$, which become tied degrees of freedom at node B.

See the description of the FORMS subroutine Volume II, Section 3 for more detail on the constraint equations when the technique of including any arbitrary constraint is detailed.

It should be noted that when kinematic constraint coordinates (tying constraints) are applied between degrees of freedom at a node A and degrees of freedom at other nodes and the same node A (e.g., in the use of arbitrary shell intersection), node A must be specified last in the list of retained nodes.

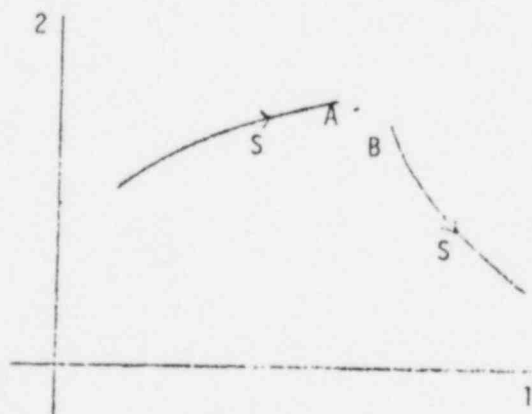
6. Specify tying type 22 to join the boundaries of intersecting shells modeled with element type 22.

This is the same as tying type 18 for elements of type 4 or 8. It gives a fully moment carrying joint between two shells modeled with element type 22. A node is provided in each surface at each node location along the line of intersection. Each of these pairs of nodes is then tied with tying type 22. One node of the pair is given as the tied node, with the other node of the pair, then the first node of the pair, both given as the two retained nodes.

Note that in order for the program to find the line of intersection, it is necessary that the surface normal coordinates (coordinates 4, 5, 6) at each node of the line of intersection be given.

7. Specify tying type 24 to join intersecting surfaces modeled with elements of type 15, 16 or 17.

This tying provides a fully moment carrying joint between two such surfaces. Since the surfaces are discontinuous, two nodes are needed at the intersection point -- one in each surface. Then one of these nodes is given as the tied node, and the other node, then the first node again, are given as the two retained nodes.



Tying Type 24

Tie Shell to Shell or Beam to Beam. Moment Carrying (24)

$$\begin{aligned} \text{Rotation at A} &= -\frac{du^A}{ds^1} \frac{dx^A}{ds^2} + \frac{du^A}{ds^2} \frac{dx^A}{ds^1} \\ &= \text{rotation at B} \end{aligned} \quad (1)$$

$$\text{Disp}^1 \text{ at A} = \text{disp}^1 \text{ at B} = \underline{u} \quad (2)$$

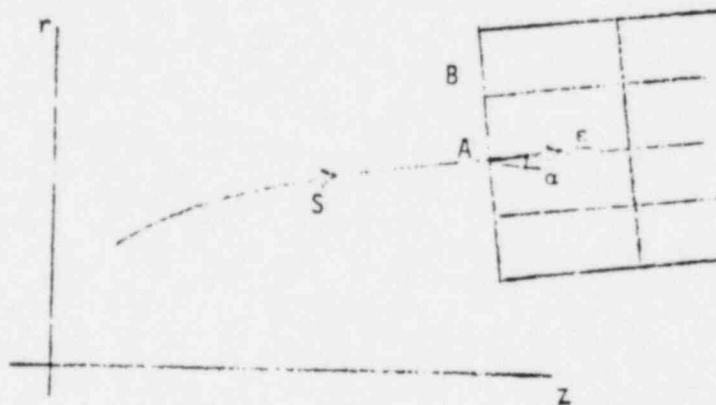
```

So:      S(1,1)=1.
          S(2,2)=1.
          A=-XORD(4,1)
          B=XORD(3,1)
          I=1
          ABS(A).GT.1.E-3)GO TO 2
          A=XORD(3,1)
          B=(XORD(4,1)
          I=2
2         S(I,3)=-XORD(4,2)/A
          S(I,4)=XORD(3,2)/A
          J=NDEG+5-I
          S(I,J)=-B/A
          RETURN

```

8. Specify tying type 25 to join a solid mesh (continuum elements) to a shell or beam mesh (element types 15 or 16).

This tying is similar to tying type 23 for element 1, except that the transformation of nodes is not needed. It imposes tangential tying but no normal constraint. The latter must be provided by using the same node on the middle surface for the shell and for a point of the solid (continuum) mesh. Then each solid mesh node off the middle surface on the interaction face is given in turn as tied nodes with the shell node as retained node.



Tying Type 25

Tie Solid (10 or 28) to Shell (15)

B = solid node, A = shell node

\underline{t} = tangent to shell

$= \cos \alpha \underline{\hat{i}} + \sin \alpha \underline{\hat{j}}$ ($\underline{\hat{i}}$ $\underline{\hat{j}}$ = unit vectors along axes)

$$\text{Rotation at A} = \phi = - \frac{du_z}{ds} \sin \alpha + \frac{du_r}{ds} \cos \alpha \quad (1)$$

$$\text{Complete time} = \underline{u}^B = \underline{u}^A - \underline{AB} \phi^A \quad (2)$$

$$\underline{u} = \text{disp}^1 \text{ vector} = u_z \hat{i} + u_r \hat{j}$$

$$\underline{AB} = \text{vector from A to B}$$

$$= (z^B - z^A) \hat{i} + (r^B - r^A) \hat{j}$$

Plane stress - don't tie normal disp¹, only tangential.

So (2) becomes

$$\underline{u}^B \cdot \underline{t} = \underline{u}^A \cdot \underline{t} - \underline{AB} \phi^A \cdot \underline{t} \quad (3)$$

and normal displacement is transmitted by making a node in the solid mesh as well as the shell mesh.

So only tying is tie B to A and B via (3), which is

$$\begin{aligned} u_z^B \cos \alpha + u_r^B \sin \alpha &= u_z^A \cos \alpha + u_r^A \sin \alpha - [(z^B - z^A) \cos \alpha \\ &+ (r^B - r^A) \sin \alpha] \left(- \frac{du_z^A}{ds} \sin \alpha + \frac{du_r^A}{ds} \cos \alpha \right) \end{aligned}$$

$$\text{with } \cos \alpha = \frac{dz}{ds}, \quad \sin \alpha = \frac{dr}{ds}$$

hence UFORMS:

```

COSA = XORD(3,2)
SINA = XORD(4,2)
A=COSA
B=SINA
I=1
IF(ABS(COSA).GT.1.E-3)GO TO 2
A=SINA
B=COSA
I=2

2      CONTINUE
S(I,1)=COSA/A
S(I,2)=SINA/A
OFFSET = (XORD(1,1)-XORD(1,2))*COSA
1      + (XORD(2,1)-XORD(2,2))*SINA
S(I,3)=SINA*OFFSET/A
S(I,4)=COSA*OFFSET/A
J=NDEG+5-I
S(I,J)=-B/A
RETURN

```

9. Tying types 31, 32, 33 and 34 join the extra nodes in a fine mesh to the nodes of a coarse mesh for compatibility along the interface. Tying types 31 and 32 apply to the mesh refinement of first order (linear displacement and second order quadratic displacement) two dimensional elements. Types 33 and 34 give fine mesh to coarse mesh compatibility for 8 node and 20 node brick elements.

Example

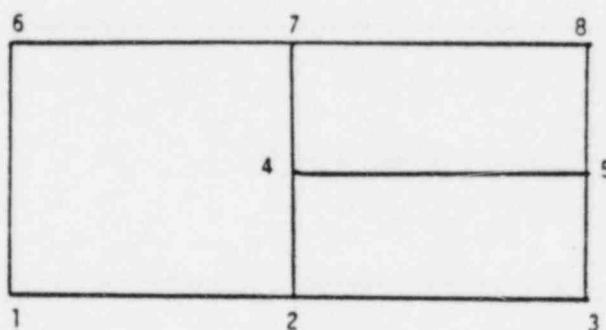


Figure 3.12-6

- a) Tying Type 31 - first order, 2D elements
2 retained nodes: nodes 2 and 7 tied node: node 4

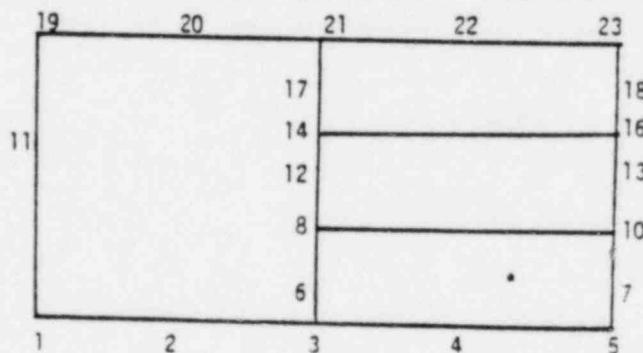


Figure 3.12-7

- b) Tying Type 32 - second order s 2D element

- a) 3 retained nodes: nodes 3, 12, 21
tied node: node 6
- b) 3 retained nodes: nodes 3, 12, 21
tied node: node 8
- c) 3 retained nodes: nodes 21, 12, 3
tied node: node 14
- d) 3 retained nodes: nodes 21, 12, 3
tied node: node 17
- 4 constraint eqs.

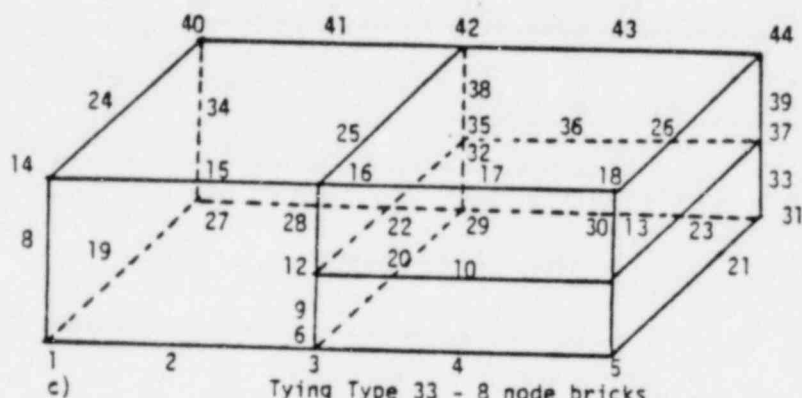


Figure 3.12-8

2 constraint equations

- a) 4 retained nodes: nodes 2, 7, 15, 10
tied node: node 4
- b) 4 retained nodes: nodes 15, 10, 2, 7
tied node: node 12

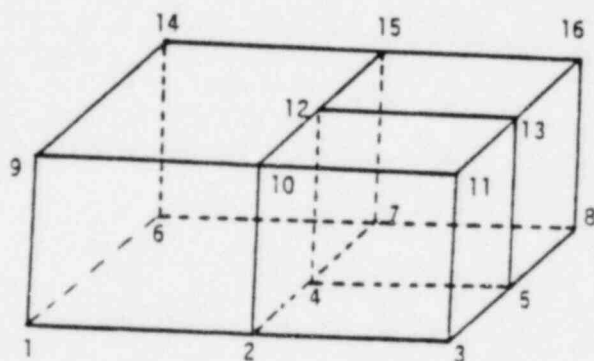


Figure 3.12-9

5 constraint equations

- a) 8 retained nodes: nodes 14, 3, 27, 40, 7, 18, 33, 23
tied node: node 10
- b) 8 retained nodes: nodes 14, 3, 27, 40, 7, 18, 33, 23
tied node: node 4
- c) 8 retained nodes: nodes 40, 14, 3, 27, 23, 7, 18, 33
tied node: node 20
- d) 8 retained nodes: nodes 27, 40, 14, 3, 33, 23, 7, 18
tied node: node 30
- e) 8 retained nodes: nodes 27, 40, 14, 3, 33, 23, 7, 18
tied node: node 36

10. Tying type 13 - joining two elements type 13 under arbitrary angle.

Tying type 13 allows two elements type 13, which are not on one line but under an arbitrary angle, to be tied. Only the first 7 degrees of freedom are related, the 8th torsional degree of freedom is left free. See Volume F for complete description of the constraint theory.

11. Tying types ≥ 100

Tying type 100 ties all degrees of freedom at the tied node to the corresponding degree of freedom at the retained node.

Tying types ≥ 100 tie a number of degrees of freedom at the tied node to the corresponding degree of freedom at the retained node. This number is determined as follows:

From dof $\times 100 + \text{To dof} = \text{tying type}.$

EXAMPLE: We want to equate only dof 2 until 8 of two points.
Use tying type 209.

BOUNDARY CONDITIONS

The program allows the nodal displacement to be specified for a particular degree of freedom. If a displacement value is not given when the Boundary Condition Option is specified, the value of the fixed displacement is set to zero. An option allows boundary conditions to be specified at the time of two-dimensional mesh generation. (See Section 2.5-1, Volume II)

TRACTION, PRESSURE LOADINGS

The loads on a structure may be applied in four ways:

a) NODAL LOADS

The loads may be applied directly to the nodes.

b) SURFACE PRESSURE

Pressures may be specified for element surfaces. These pressure loadings vary with the element types. A full description of the types of pressure loadings is given in the description of each element type. See Section 2 of this volume. Some of the shell elements allow a linearly varying pressure over the element surface.

c) BODY FORCES

Certain body forces (volumetric loading) such as acceleration forces may be specified. In this category we also include the pseudo body forces such as thermal and creep strains. Thermal loading may be specified and entered under the THERMAL option.

d) CENTRIFUGAL LOADING

The load stiffness matrix for centrifugal loading is obtained by using the CENT parameter card and specifying in the model definition block, ROTATION A, the direction of the axis of rotation and a point on that axis. The actual load is then invoked in the TRACTIONS option by specifying an IBODY load type = 100 and entering the quantity, ω^2 (square of rotation speed in radians per time), for the magnitude of the distributed load. This load type is not yet available for elements 1,2,5,6,17, and 36 through 61.

This capability is intended for use in dynamics analysis, particularly with modal extraction, where the natural frequencies of the structure are strongly affected by this centrifugal load contribution. Since the load stiffness matrix is a large displacement effect, it is only formed after increment 0. To obtain the modes and frequencies including all the large displacement terms, the user should input the centrifugal load in the TRACTIONS block on increment 0, and then have one or two steps of zero increments of load. This will update the stiffness matrix so that the user can then invoke the MODAL SHAPE option in the next increment. Note that the FOLLOW FOR option should also be invoked since centrifugal loading is a follower force effect.

The user is also provided with a number of user subroutines for special load specifications.

1. FORCEM. User subroutine for specification on non-uniform pressure loads.
2. FORCDT. User subroutine for input of time dependent loads or displacements.

MARC-CDC PLOTTING CAPABILITIES

Extensive capability is built into the program to allow plotting of input and output for data checking and output display. A significant feature of the plotting is the plotter interface package. All plotting from the program generates plot device driver instructions through a small set of low level interface subroutines. This design allows simple conversion to any plot device (e.g. Calcomp, Complot, SC4020, etc.) through the re-coding of the interface routines and their use as user subroutines. The standard default interface routines cause a tape (logical unit 4) to be written to drive an off-line Calcomp plotter, and are listed in Volume II, Section 3. On many machines these routines will also drive an on-line Houston Instrument (Complot) plotter.

The plotting capability is invoked by including a MESH PLOT parameter card in the input deck. A flag on this card indicates if the user wants pre-plotting or post-plotting (or both).

PRE-PLOTTING

The pre-plotting is available for mesh display, to allow the user to view his mesh and check the accuracy and suitability of his model. The SECTIONING option allows various parts of the model (chosen by element type, element number, or location) to be plotted separately, thus making it easy to examine modeling details, particularly for shell or three-dimensional solid elements. The user has options to display element and/or node numbers, for identification purposes. For curved elements, (mid-side node solid elements, or shell elements) the actual curve fitted by the program through the user's nodal coordinate data is displayed thus allowing a check of the reasonableness of the curve fit to the actual structure.

POST-PLOTTING

The post-plotting capability is provided in three main features -- displaced position plots and contour plots in MARC, and time history plots in MARC PLOT. For the description of the latter, see the MARC-PLOT section. The first two concepts are described below.

Displaced position plots allow the user to compare the structure after deformation (shown in heavy lines) the structure before deformation (shown in dotted lines). The same capability allows examination of buckling modes or dynamic mode shapes, and velocity or acceleration profiles. This displaced position capability provides a very realistic view of the effect of loading on a structure.

Contour plots show the user the variation in a particular parameter of the solution (e.g. stress or strain) over the structure. The program allows contouring of any variable over any element type. In order that the resulting plots be correctly interpreted, it is often important for the user to know the technique used to produce the contour plots. For this reason, the following paragraphs describe the contouring technique.

In order to produce a two-dimensional plot, any three-dimensional structure must first be sectioned. In the case of doubly curved shell elements, the user must choose a layer from the 11 layers used by the program through the thickness of the shell, so that the variable may be contoured on that layer. For a solid, three-dimensional element, the user will usually invoke the SECTIONING option to provide an uncluttered view of part of the structure. He must choose a slice through the element to be plotted, so that contours may be given on the slice. The slices possible are shown in the pictures below for the two types of three-dimensional solid elements in the program. Note that the slice specification is related to the face (or node) ordering of the element. This usually provides convenient plots, especially with a generated mesh. The slices pass through the integration points of the elements.

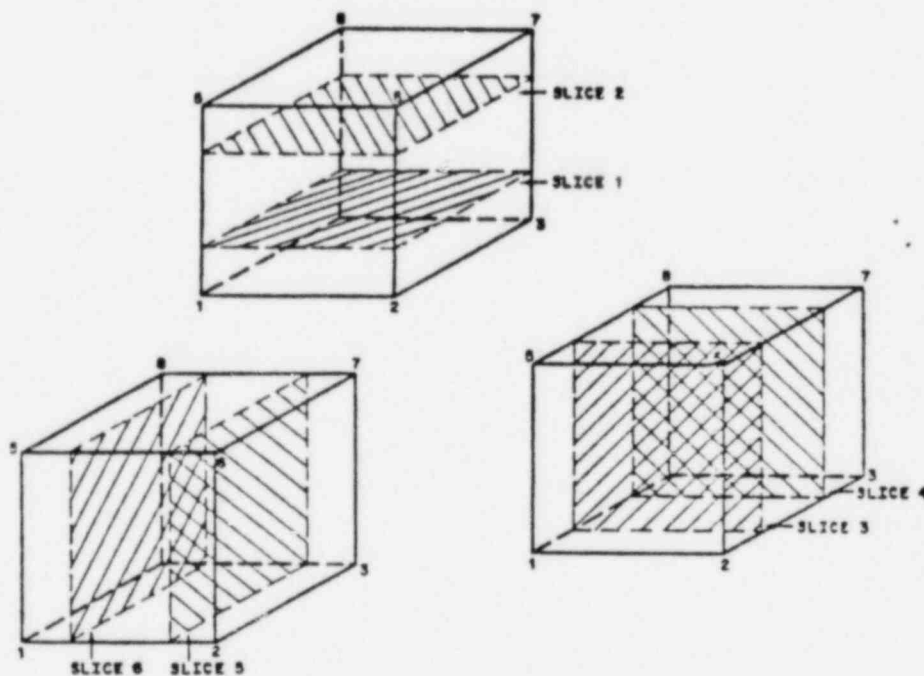


Figure 3.15-1. Slice Specification for the Eight Node Brick (Element 7) and the Twenty Node Bricks With Reduced Integration (Elements 57, 61)

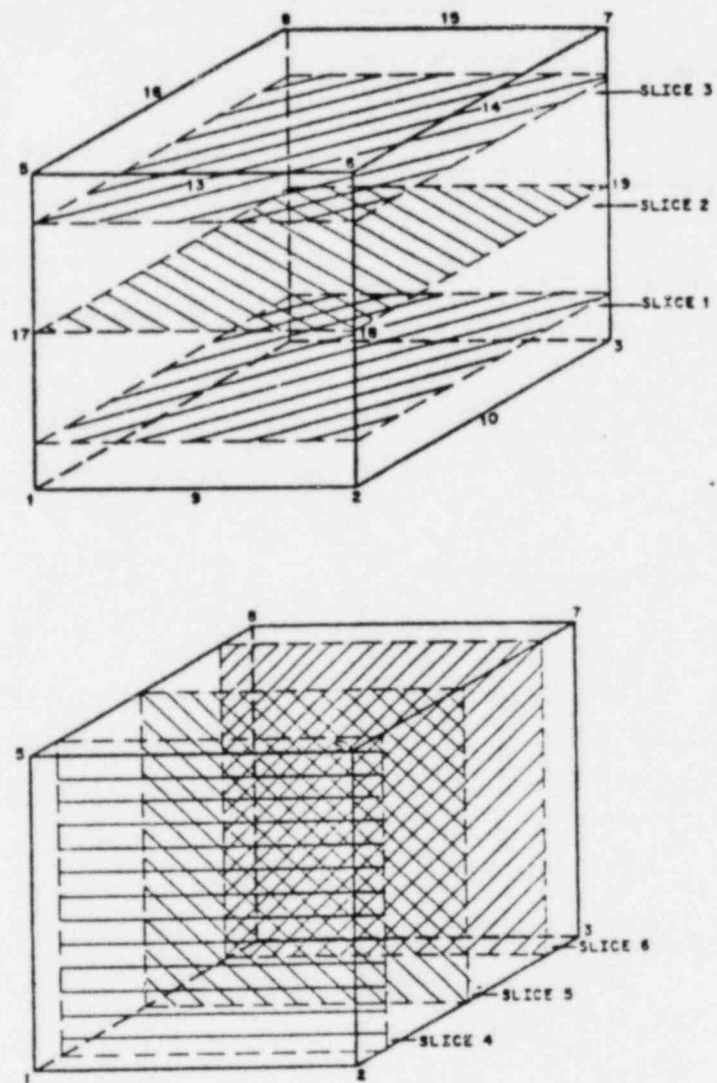


Figure 3.15-2. Slice Specification for the Twenty Node Brick (Elements 21, 35)

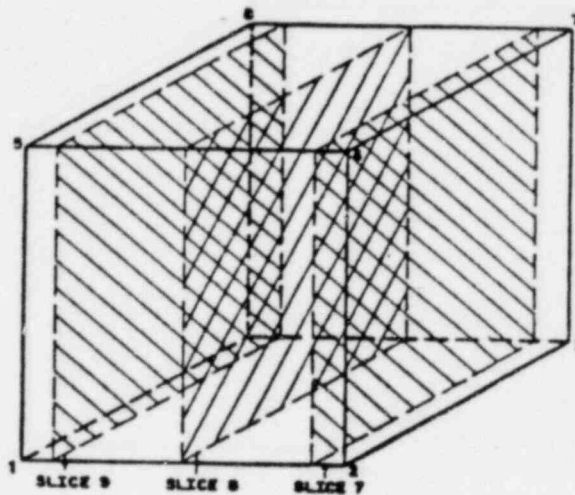
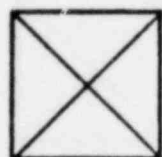


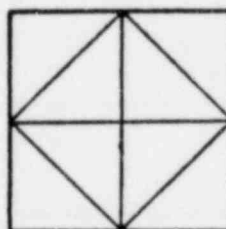
Figure 3.15-3. Slice Specification for the Twenty Node Bricks (Element 21, 35) (cont'd)

Once a section is defined (by slicing or layer choice if necessary), the contour plot is generated as follows:

1. Nodal values are computed by extrapolation of the integration point values of the chosen variable to the nodes of the element, then average nodal values are calculated, the average being weighted by the included angle subtended at the node by each element contributing to the node. The averaging only considers the elements in the section chosen, if the SECTIONING option is invoked. Note that such averaging is physically unreasonable if discontinuities are present. In such a case SECTIONING should be used to avoid averaging across the discontinuity.
2. Contouring is performed on a linear triangle basis. That is, a first order quadrilateral (e.g. element 3, 10, 11, etc.) is divided into four triangles, a second order quadrilateral (e.g. element 21, 22, 24, 26, etc) is divided into 8 triangles, as shown below. In each triangle contours are drawn assuming linear variation between values of the variable at the nodes of the triangle obtained by the averaging process in (1) above.



**FIRST ORDER
QUADRILATERAL**



**SECOND ORDER
QUADRILATERAL**

Figure 3.15-3. Sub-Triangles Used for Contouring Quadrilateral Elements

3. A contour plot is produced with the mesh shown in dotted lines. Because straight line contouring is used, meshes containing higher order (curved edge) elements are stylized to show straight line element edges for consistency.
4. All contours may be labeled, or a selected set of contours labeled. The latter option may often be useful to avoid excessive labeling in regions of high gradients.
5. The mesh (or section of the mesh) is shown in dotted lines. A mesh outline only is not available, since the algorithm is based on a single element data base.

RESTART

The restart option in the MARC-CDC program is used with nonlinear analysis. The purpose of the restart option is to allow the incremental solution to be split into steps of a few increments per step, thus allowing flexibility in the analysis. Restart also provides an opportunity to store intermediate values in case error occurs after several increments have been successfully completed. When this option is chosen, the restart tape may be used to restart at any increment for which restart data has been successfully completed.

The restart is controlled by the RESTART parameter card in conjunction with the RESTART model definition option. Tapes used for restart (output and/or input) must also be given on the main PROGRAM card.

In a problem to be restarted, the data to control the loads during the next increment (after the current set of increments is completed) must be provided after the END OPTION card. In a restarted problem, the data cards are supplied as in a normal run (except for the restart controls). The increments which are written on the restart tape are controlled by the 2nd Card Series, Columns 6-10, under the RESTART option, Volume II, Section 2.

SELECTIVE ASSEMBLY RESTART OPTION

This feature of the program allows the user to assemble the system matrices selectively, spreading the assembly over several runs. This is particularly useful for large problems, as a protection against system failure and to avoid complete reassembly upon re-analysis with small design changes which only affect some elements. The latter feature is available since the program allows selected elements to be re-computed and thus overwrite their original stiffness values on the back-up element stiffness tape.

The feature is invoked with the EDIT parameter card in conjunction with the REGEN option. The EDIT parameter card tells the program how many elements will be newly computed during this run of the problem, as well as giving the last element to be reached during this run, and the back-up tape upon which all element stiffness (except those currently being generated), up to and including the last element given, will be found. Note that the program will complete the analysis if the last element specification in the EDIT card is left blank. If that specification is made, execution ends at the element given.

The tape on which element stiffnesses are written has a default unit number of 11. The tape containing previously generated stiffnesses has a default unit number of 12. During equation solution, tapes 11 and 12 are overwritten, so that if required the user must provide a back-up tape.

This option should only be used during a single increment. For non-linear analysis, the RESTART option must also be involved to perform one increment at a time.

As an example of the use of this feature -- suppose an analysis with 1000 elements is to be performed. The user chooses to protect himself against errors and system failures by only assembling 200 elements per run. The required cards should then be:

RUN 1

EDIT Parameter Card

Columns 15	Set to 1 to write back-up tape.
Columns 16-20	Set to 200 elements to be assembled.
Columns 26-30	Leave blank (not needed).
Columns 31-35	Leave blank (use default tape 11).

REGEN Option

Number of lists = 1
First element in list = 1
Last element in list = 200
Increment in list = 1

After successful completion of this run, elements 1-200 are kept on tape 11. Run 2 is then executed.

RUN 2

EDIT Card

Columns 15 Set to 2 to read previous tape and continue assembly.
Columns 16-20 Set to 200 elements to be assembled.
Columns 21-25 Set to 400 to stop after that element is assembled.
Columns 26-30 Leave blank (use default tape 12).
Columns 31-35 Leave blank (use default tape 11).

REGEN Option

Number of lists = 1
First element in list = 201
Last element in list = 400
Increment in list = 1

This run will then read elements 1-200 from tape 12 (which was written on tape 11 in run 1) and write all elements up to number 200 on tape 11. Note that in the last run, execution will continue through equation solution and output (thus overwriting tapes 11 and 12) if columns 21-25 of the EDIT card are blank, but execution will halt after complete assembly if 1000 is entered in these columns. Five such runs will complete the 1000 element job.

INCREMENTAL FUNCTION GENERATORS

A collection of aids to generation of program functions have been included in the program. These aids are referred to collectively as incremental function generators. In principle they generate the function data, i.e. the boundary conditions, point loads, tying, transformation and mass point data either by repeating patterns or by interpolation respectively. In general two schemes have been included to generate the function data for the nodes. The first scheme refers to the nodes indirectly and points to the nodes via element numbers and positions of the nodes on the connectivity list. This is initiated by model definition data with header cards which have GENER as its last word, e.g. BC GENER, TIE GENER, etc.

The following incremental function generators are available using the indirect element reference scheme.

- a) Boundary Condition Generator (BC GENER). This applies the same boundary conditions to the nodes of an element as that which had been previously applied to a master element.
- b) Tie Generator (TIE GENER). This applies the tying constraint to corresponding nodes on successive pairs of elements using a prescribed pair of elements as master. The tying for the nodes of the master pair of elements must have been specified previously.
- c) Initial Condition Generator (INIT GENER). This applies the same initial conditions to the nodes of an element using the initial conditions of another element as a master. A code is also included to select initial displacement and/or initial velocity.
- d) Mass Point Generator (MASS GENER). This applies the same mass points to the nodes of an element in a series of elements using another element as a master.
- e) Traction Generator (TRAC GENER). This applies the same point loads to the nodes of an element in a series of elements using another element as a master.
- f) Node Transformation Generator (TRANS GENER). This applies the same transformation to one of the nodes of a series of elements. The transformation only makes the use of the nodes of the element and the pattern of the transformation is established by the position of the node on the connectivity list.

The second scheme uses an incremental procedure to repeat or interpolate function data previously specified for critical starting and ending nodes of a series. If end node conditions are specified, the input requires that this be interpolated linearly for a particular node. The input is initiated by model definition data with header cards which have FILL as its last word, e.g. BC FILL, TIE FILL and etc. The following incremental function generators are available using the interpolation scheme.

- 1) Boundary Condition Interpolator (BC FILL). This applies the same boundary conditions to the succeeding nodes of a series as was previously applied to the first and last node. If a non-zero value of displacement is given for the boundary condition on the last node, this is used to define an applied displacement at the node by linear interpolation. The interpolation is based on a count of nodes and not on physical spacing between the nodes.
- 2) Initial Condition Interpolator (INIT FILL). This applies the same initial conditions to the succeeding nodes of a series as was previously applied to the first and last node. If a non-zero value of displacement is given for the initial condition on the last node, it is used to define the initial condition at the node by linear interpolation. The interpolation is based on an integer count of nodes and not on physical spacing between the nodes. A code is also included to select initial displacement and/or initial velocity.
- 3) Mass Point Interpolator (MASS FILL). This applies the same mass points to the successive nodes of a series that was previously applied to the first and last node. If a non-zero value of mass point is given for the last node, it is used to define a mass point at the node by linear interpolation with the value given for the first node. The interpolation is based on an integer count of nodes and not on physical spacing between the nodes.
- 4) Tie Interpolator (TIE FILL). This applies the tying constraint to a series of tied and retained nodes. This repeats the tying pattern previously established for the first tied nodes on the list.
- 5) Traction Interpolator (TRAC FILL). This applies the same point loads on a series of nodes as that applied to the first node. If a non-zero value is specified for the last node in the series, the value is used to define the value at the other nodes by interpolation. Interpolation is based on the integer count of the nodes using the values specified for the beginning and end nodes of the series.
- 6) Transformation Interpolator (TRANS FILL). This applies the same transformation to a series of nodes by defining two series of additional nodes which help to establish the transformation directions.

8. Structural Procedures Library

1. Linear Analysis
2. Nonlinear Analysis
 - a) Scaling for elastic-plastic analysis
 - b) Controls
3. Evaluation of J-Integral
4. Plasticity
5. Creep
6. Dynamic Analysis
 - a) Modal Analysis
 - b) Direct integration, implicit
 - c) Direct integration, explicit
7. Large Displacement
 - a) Incremental analysis
 - b) Buckling
 - c) Creep buckling, accumulated buckling
8. Fluid/Solid Interaction
9. Rigid, Perfectly Plastic Flow
10. Viscoplasticity
11. Heat Transfer, Diffusion Problems

LINEAR ANALYSIS

In the solution of a linear problem the user is primarily interested in selecting from the element library. The minimum data required for an elastic analysis may be found in Section 1 of Volume II.

In order to provide for more efficient usage of core in a linear analysis, the program is stripped of the storage which is required only for a nonlinear analysis. This option also allows repeated solutions with different loads, using the already assembled and decomposed stiffness matrix. See the ELASTIC parameter card, Volume II, Section 2, to achieve the most efficient usage of core in a linear analysis.

The program makes extensive use of higher order elements. These elements yield information on the quality of an analysis. A feature has been included in the program to enable the user to determine the quality of an analysis. This is described on the following page.

QUALIFICATION OF MESH AND ERROR OF ANALYSIS IN HIGHER ORDER ELEMENTS

This option measures the energy content in the higher displacement modes and compares it to the energy in the constant strain mode for a linear elastic analysis. This value can be regarded as the rate of change of energy with respect to increase (by actually taking a decrease corresponding to the degrees of freedom in the higher displacement modes) in the degrees of freedom in the region covered by the element^[1]. The program also points out the energy density of the higher displacement modes for each integration point. This energy density can be plotted as contours by selecting the plot type code 41. The energy density distribution can be used as a guide to mesh refinement, more elements being placed around integration points with high energy density due to the higher displacement modes.

A two line output summarizes the average higher mode energy content and identifies the element with the largest higher mode energy content. This element should receive the most attention in mesh refinement. The above output should guide the user in determining the appropriateness of the particular elastic analysis and will yield the following information.

- a) By observing the average higher energy mode content, the user will be able to estimate if a sufficient number of elements were used. This higher energy mode can be regarded as an estimate of the energy change provided by a doubling of the degrees of freedom.
- b) By observing the regions with large higher energy modes and then comparing this with the structure average, the user can estimate the need for further refinement in the region.
- c) By observing the regions with low higher energy modes, the user can determine regions that can be left out in further refined mesh analysis of a structure.

This option is used for including the parameter card for mesh qualification. The use of the option does not result in significant increase in computing (under 5%).

[1] Melosh, R. J. and Marcal, P. V., "An Energy Basis for Mesh Refinement of Structural Continua," to be published.

ARBITRARY LOADING OF AXISYMMETRIC SOLIDS BY FOURIER EXPANSION

The standard solid ring capability in MARC is expanded to accommodate arbitrary mechanical and thermal loading. Expressing the circumferential distribution of displacements and forces in terms of Fourier series, the three-dimensional analysis decouples into a series of independent two-dimensional analyses. Thus, the Fourier series approach to displacement and load representation allows for an efficient solution to the analysis of axisymmetric structures under arbitrary loading. Since this formulation is based on the principle of superposition, only linear problems are permitted. Also, the material properties must remain constant in the circumferential direction. Consequently, the formulation is restricted to axisymmetric structures characterized by axisymmetric, linear elastic material behavior and small strains and small displacements.

The general form of the Fourier series expansion of the function $F(\theta)$ is shown below:

$$F(\theta) = a_0 + \sum_{n=1}^{\infty} (a_n \cos n\theta + b_n \sin n\theta) \quad (1)$$

The above expression is used for the expansion of the displacement functions. The sine and cosine terms are separated to simplify the derivation. For each value of n a symmetric and an antisymmetric problem is formulated.

Focusing on the symmetric case, the displacements expressed in terms of their nodal values are:

$$\begin{aligned} u^n &= [N_1, N_2, \dots] \cos n\theta \{u^n\}^e \\ v^n &= [N_1, N_2, \dots] \cos n\theta \{v^n\}^e \\ w^n &= [N_1, N_2, \dots] \sin n\theta \{w^n\}^e \end{aligned} \quad (2)$$

nodal forces are written as follows:

$$\begin{aligned} Z &= Z_0 + \sum_{n=1}^n Z^n \cos n\theta \\ R &= R_0 + \sum_{n=1}^n R^n \cos n\theta \\ T &= T_0 + \sum_{n=1}^n T^n \sin n\theta \end{aligned} \quad (3)$$

For $n=0$ the formulation defaults to the fully axisymmetric two-dimensional analysis if only the symmetric expansion terms are used. The antisymmetric case for $n=0$ yields a solution for the variable w only corresponding to constant loading in tangential direction. Axisymmetric solids under pure torsion are analyzed in this fashion.

In order to utilize the Fourier expansion analysis feature in MARC, the input must contain the following information:

1. FOURIER parameter card to allocate storage for the series expansions.
2. FOURIER model definition block as many series as are needed to describe tractions, thermal loading and boundary conditions are input. The following are three different ways to describe the series:
 - a) Specify coefficients a_0, a_1, b_1, \dots on cards.
 - b) Describe $F(\theta)$ in point wise fashion by an arbitrary number of pairs $[\theta, F(\theta)]$ given on cards. The corresponding series coefficients are formed by the MARC Program.
 - c) Use user subroutine UFOUR to generate an arbitrary number of $[\theta, F(\theta)]$ parts and let the program calculate the series coefficients.
3. TRACTIONS, THERMAL LOADS AND BOUNDARY CONDITIONS

For each group of the above specifications a different series representation can be used. The series are numbered sequentially in the order they are encountered during the FOURIER model definition input.

The numbers of analysis steps (increments) is dependent on the number of harmonics chosen. For a full analysis with symmetric and anti-symmetric load cases the total number of increments equals twice the number of harmonics. The table below shows which FOURIER coefficients are used for a given increment.

INC.	LOAD TERMS		
	1st DOF, 2	2nd DOF, r	3rd DOF, θ
0	a_0	a_0	0
1	0	0	a_0
2	a_1	a_1	b_1
3	b_1	b_1	b_1
\vdots	\vdots	\vdots	\vdots
$2n$	a_n	a_n	b_n
$2n+1$	b_n	b_n	a_n

FOURIER coefficients - Increment Number

The magnitude of concentrated forces should correspond to the value of the ring load integrated around the circumference. Thus, if the Fourier coefficients for such a varying ring load $p(\theta)$ are found from the $[a, p(\theta)]$ distribution, where $p(\theta)$ has the units of force per unit length, the force magnitude given in the TRACTION block should be equal to the circumference of the loaded ring. If $p(\theta)$ is in units of force per radian the TRACTION magnitude should be equal to 2π .

For varying pressure loading the Fourier series can be found from $[a, p(\theta)]$ input with p expressed in force per unit area. The equivalent nodal forces are calculated by the MARC program and also integrated around the circumference. Thus, the distributed load magnitude in the TRACTION block should be 1.0.

After the completion of all increments required by the analysis, the "incremental" data can be used to generate the final results by super position at any station around the circumference. For this the restart tape containing all the data of the individual harmonics is used together with the CASE COMBINATION option.

~~CONFIDENTIAL~~

The user should realize at the outset that nonlinear analysis is more difficult to perform than linear elastic analysis because it imposes severe demands on computing time and judgment. Most nonlinear analysis requires at least two passes of the program. Thus, care and patience should be exercised in equal measure in a nonlinear analysis. It is recommended that nonlinear analyses be accomplished in no less than two runs. The first run should be designed to extract the maximum information with the minimum cost of computing. Fewer degrees of freedom should be used wherever possible. The number of load increments can be halved by doubling the size of each load increment. For example, in an elastic-plastic analysis, the first coarse run can be performed to estimate the collapse load. The result is available from the flattened load displacement and load strain curves. In a large displacement analysis, a coarse run determines the regime of most rapid change where additional load increments must be specified. In general, the increment size should be planned in the final run (bearing in mind that the analysis is performed as a series of piecewise linear steps), with the following rule of thumb: there should be as many load increments as required to fit the nonlinear results by the same number of straight lines.

This rule should be modified to restrict elastic-plastic loads to increments below one-tenth the load to cause first yield. The reason for this is that the yield criterion has been linearized so that the error term is quadratic, and changes of the order of $(1/10)^2$ of the yield stress provide negligible wandering from the yield locus. This drift from the yield locus can be checked by recording the output of equivalent (total) stress in an element and comparing it with the current value of the yield stress. When the load vector changes drastically, such as from a pressure to a thermal load increment, it is advantageous to iterate at least once for each load increment in order to calculate the correct stress-strain relation for the transition region [10], i.e., the region which yields in the current increment of load. The nonlinear geometric analysis is carried out in the initial coordinate system.

A new load increment should be specified after each increment of load. If the same increment of load should be repeated for the next time step, it is sufficient to end the load option by a CONTINUE card. From one increment to the next, load input options allow:

- . The displacement boundary conditions to be specified

- The node tying operations to be changed
- New tractions and temperatures to be input
- Creep to occur
- The buckling load to be estimated with the stress and displacement state before the application of the last load increment.

The automatic load control procedure permits the number of load increments or the total creep time to be specified. The results of the first analysis may be scaled up to cause first yield by specifying such scaling in the input data (SCALE parameter card).

The residual load correction is obtained by calculating the difference between internal forces and external loads from the equation

$$\{R\} = \{P\} - \int [\alpha]^T [B]^T \{\sigma\} dV$$

where

$[\alpha]$ is the nodal displacement to undetermined coefficient transformation matrix

$[B]$ is the differential operator which transforms displacements to strains

$\{\sigma\}$ are the generalized stresses

$\{P\}$ is the load vector

$\{R\}$ is the residual load correction

This residual load correction is almost always automatically turned on for nonlinear solutions. In order to satisfy the above equation the integral must be evaluated by summing the contribution from all integration points. Thus, this feature requires that all element states such as stresses be stored at all the integration points. This storage is flagged by the ALL POINTS input parameter card.

It is strongly recommended that ALL POINTS be used with any nonlinear analysis involving any but the simple constant stress elements.

CONTROLS FOR NONLINEAR ANALYSIS

MARC handles nonlinear static problems in two ways:

- (a) tangent modulus method
- (b) initial strain method

Examples of the tangent modulus method are elastic-plastic analysis, nonlinear springs and foundations, gaps.

An example of the initial strain method is creep or visco-elastic analysis.

For the tangent modulus method, the program forms a mean stiffness, based on estimates of the displacement, strain, etc., increments. It then solves the equations and checks the tolerance again.

Clearly, two controls are needed for this technique -- a tolerance on convergence and a limit to the allowable number of cycles. These are input on the CONTROL model definition block. The convergence tolerance is based on a comparison of the energy change predicted when forming the mean stiffness, and the energy change which results from the incremental solution. Experience indicates that a 10% tolerance gives satisfactory solutions -- clearly, accuracy and cost may be traded by changes to this tolerance.

The limit to the number of cycles is provided to avoid excessive cycling in a hopeless case, such as reaching limit load, or a buckling collapse. Usually three cycles is quite sufficient as a maximum. If more cycles are required, it is recommended that smaller load steps be used instead (a re-cycle costs the same as a single cycle step), since this is a more accurate piecewise linear tracking of the actual nonlinear history.

In addition to the above two controls, a minimum number of cycles may be specified. This allows fixed re-cycling in cases where the user is aware of severely nonlinear effects, or of non-proportional loading, where the extrapolation used for the initial mean stiffness may be in serious error.

CREEP CONTROL TOLERANCES -- AUTO CREEP OPTION

The program runs a creep solution (under constant load conditions) via the AUTO CREEP history definition card set. This option chooses time steps automatically, based on a set of tolerances and controls provided by the user. These are as follows:

1. Stress Change Tolerance (CONTROL Model Definition Set, Card 3, Columns 21-30)

This tolerance controls the allowable stress change per time step during the creep solution, as a fraction of the total stress at a point. Since the stress changes during the transient creep, and because the creep strain rate is usually very strongly dependent on stress, this tolerance should be considered an accuracy tolerance, governing the accuracy of the transient creep response. If the user desires an accurate tracking of the transient, a tight tolerance -- say 1% or 2% stress change per time step -- should be specified. If the steady-state solution only is sought, a relatively loose tolerance - 10%-20% - may be supplied.

2. Creep Strain Increment Per Elastic Strain (CONTROL Model Definition Set, Card 3, Columns 11-20, Also CREEP Model Definition Set, Card 2, Columns 36-50)

The program uses explicit integration of the creep rate equation, and hence requires a stability limit. This tolerance provides that stability limit. In almost all cases the default of 50% represents that limit, and hence the user need not provide any entry for this value.

3. Maximum Number of Recycles for Satisfaction of Tolerances (CONTROL Model Definition Set, Card 2, Columns 16-20), Also CREEP Model Definition Set, Card 7, Columns 6-10)

The program is choosing its own time step during AUTO CREEP, based on the algorithm described below. In some cases the program may recycle in order to choose a time step to satisfy tolerances, but it is rare for the recycling to occur more than once per step. If excessive recycling occurs, it may be because of physical problems (such as creep buckling), bad coding of user subroutine CRPLAW, or excessive residual load correction as may occur when the creep solution begins from a state which is not in equilibrium. This entry allows the user to avoid wasting machine time under such circumstances -- if, after this many attempts at stepping forward, there is no satisfaction of tolerances, the program will stop. The default of 5 is reasonable in most normal cases.

4. Low Stress Cut-Off (CONTROL Model Definition Set, Card 3, Columns 31-40, Also CREEP Model Definition Set, Card 2, Columns 51-65)

This control is intended to avoid excessive iteration and small time steps caused by tolerance checks based on small (round off) stress states. A simple example is a beam column in pure bending -- the stress on the neutral axis will be a very small roundoff-number, and it would make nonsense of the automatic time stepping scheme to base time step choice on satisfying tolerances at such points. The default here of 5% is satisfactory for most cases - it tells the program not to check those points where the stress is less than 5% of the highest stress in the structure.

5. Choice of Element For Tolerance Checking (CREEP Model Definition Set, Card 7, Columns 1-5).

The default option for creep tolerance checking is that all integration points in all elements are checked. In many cases the user may wish to save time by only checking tolerances in one selected element -- this field is then used to select that element. Usually the most highly stressed element is chosen.

NOTE:

1. All stress and strain measures used in tolerance checks are second invariants of the deviatoric state (i.e. equivalent Mises uniaxial values).
2. All tolerances and controls may be reset upon restart.
3. When a tolerance or control may be entered in two places (i.e. on the CREEP or CONTROL model definition set) the values or defaults provided by the last of these options in the input deck are used.

AUTO CREEP

This history definition set chooses time steps according to an automatic scheme based on the tolerances described above, designed to take advantage of the usually diffusive characteristics of most creep solutions -- rapid initial gradients which settle down with time. The algorithm is as follows:

For a given time step Δt , a solution is obtained.

The largest values of stress change per stress $\left| \frac{\Delta \sigma}{\sigma} \right|$ and creep strain change per elastic strain, $\left| \frac{\Delta \epsilon^C}{\epsilon^e} \right|$ are found. These are compared to the tolerance values set by the user, T_σ and T_ϵ .

Then the value p is calculated as the bigger of

$$\left| \frac{\Delta \sigma}{\sigma} \right| / T_\sigma \quad \text{or} \quad \left| \frac{\Delta \epsilon^C}{\epsilon^e} \right| / T_\epsilon$$

- a) Clearly if $p > 1$, the solution is violating one of the user's tolerances in some part of the structure. In this case the program resets the time step as

$$\Delta t_{\text{new}} = \Delta t_{\text{old}} * .8/p$$

i.e. as 80% of the time step which would just allow satisfaction of the tolerances. The time increment is then repeated. Such repetition continues until tolerances are successfully satisfied, or until the maximum recycles control is exceeded -- in the latter case the run is ended. Clearly, the first repeat should satisfy tolerances - if it does not, the cause could be

- . excessive residual load correction
- . creep buckling - creep collapse
- . bad coding in subroutine CRPLAW or VSWELL

and appropriate action should be taken before the solution is restarted.

- b) If $p \leq 1$ the solution is satisfactory in the sense of the user supplied tolerances. In this case the solution is stepped forward to $t + \Delta t$ and the next time step begun. The time step used in the next increment is chosen as

$$\Delta t_{\text{new}} = \Delta t_{\text{old}} \quad \text{if} \quad 0.8 \leq p \leq 1.0$$

$$\Delta t_{\text{new}} = 1.25 * \Delta t_{\text{old}} \quad \text{if} \quad 0.65 \leq p \leq 0.8$$

$$\Delta t_{\text{new}} = 1.5 * \Delta t_{\text{old}} \quad \text{if} \quad p \leq 0.65,$$

The idea here being to take advantage of the usually diffusive nature of the creep solution to generate a series of monotonically increasing time steps.

J-INTEGRAL EVALUATION

The program allows the evaluation of the J-Integral by calculating the change in strain energy per nodal movement during any analysis. Several values may be obtained simultaneously, for use in 3-dimensional analysis or for multi-path comparisons. For elastic-plastic analysis the plastic strains are included in the definition of the strain energy, thus evaluating the J-integral for the equivalent nonlinear elastic material. This feature is invoked through the use of the J-INT parameter card and the J-INTEGRAL model definition set.

See Volume IV, Section D4-29, for details of the formulation.

PLASTICITY

The program solves the elastic-plastic problem by means of the tangent stiffness method. A piecewise linear incremental procedure is used. The program can scale the result of a linear elastic analysis to give first yield. Subsequent increments are performed so as to limit the stress changes to tolerable value. This class of problems may also be solved by using the viscoplastic procedures described in this section. A wide number of yield function models have been implemented in the program. These have been described during the description of the material library. Finally, we note that a generalized plasticity feature has been implemented which allows the user to define a new yield function and a new flow rule. The flow rule may be an associated or a non-associated flow rule.

CREEP

The program solves the creep problem by calculating the increment of the initial strain force vector. This force vector is a function of the time step. Control of this time step is the most important aspect of a creep analysis. Two quantities must be controlled. First of all, the stress increment is controlled for accuracy, then the maximum strain increment is controlled for stability of the time integration process. The automatic time increment control option performs this dual control. The user may specify that this control be based on a named element. The default control considers all the elements. If both stress and strain changes are below 80 percent of their respective tolerances, the next time step is chosen to be 1.25 times the current increment size. Likewise, if both are below 65 percent of their respective tolerances, the time step multiplier is 1.5. If the stress or strain change is greater than the specified tolerance, the calculation is repeated with a time step that is 0.8 of the increment, computed by linear interpolation, that would just satisfy tolerances.

Example 3.3 in Volume III illustrates the use of the automatic creep controls. The user can get an appreciation of the tolerances that may be set for economic computing by referring to that example.

DYNAMIC ANALYSIS

The MARC-CDC program includes dynamic analysis by either the modal or the direct integration procedure. At present it can perform modal analysis by the inverse power sweep procedure. Subsequent time integration is performed with the Duhamel Integral which integrates any linear problem exactly. The direct integration is carried out using the Newmark Beta method of stop-by-step integration ($\beta=1/4$, $\gamma=1/2$) or the Houbolt operator, or the central difference (explicit) operator.

The modal extraction (MODAL SHAPE option) may be invoked immediately in the analysis, or after several increments of static large displacement analysis. The latter feature allows the dynamics of prestressed structures to be studied (small vibrations about a deformed, prestressed position), such as the vibration of rotating machinery. Note that a step with zero load should be taken just before the MODAL SHAPE option, to update the stiffness matrix completely, since MODAL SHAPE does not reform the stiffness.

Nonlinear problems should only be attempted with the direct integration procedure. The method relies on the tangent modulus stiffness approach and in order to save from having to reassemble the stiffness matrix after each time increment [21] the user is given the ability to specify a fixed number of increments before reassembly can take place.

EIGENVALUE EXTRACTION

The eigenvalues are extracted using the inverse power sweep method. An initial vector is created by the program. This vector is multiplied by the mass matrix (or differential stiffness matrix in a buckling analysis) and the decomposed stiffness matrix to obtain a new vector. The process is repeated until convergence has been reached according to either of two criteria:

- a) Single eigenvalue convergence. At each iteration an eigenvalue is computed. If the values at two successive iterations are within a tolerance, convergence is assumed.
- b) Double eigenvalue convergence. It is assumed that the trial vector is a linear combination of two eigenvectors. Using the three latest vectors, two eigenvalues are calculated. These two values are compared with the two values calculated in the previous step and convergence is assumed if they are within the prescribed tolerance.

When an eigenvalue has been calculated the program will either exit from the extraction loop if a sufficient number of vectors has been extracted or create a new guess vector for the continued calculations. If a single eigenvalue was obtained, the program will use the double eigenvalue routine to obtain the best guess vector for the next eigenvalue. If two eigenvalue were obtained, an arbitrary guess vector orthogonal to the previously obtained vectors is created.

When the first eigenvalue has been calculated, the program will orthogonalize the trial vector to previously extracted vectors at each iteration (Gram-Schmidt orthonormalization).

For the dynamic option the user may also select a power shift method. If more than 6 modes are required it is probably necessary to decompose the stiffness matrix around more than one eigenvalue in order to converge to the higher modes. The user controls the analysis by specifying three parameters:

- a) The initial shift frequency. This is normally set to zero unless the structure has rigid body modes which prohibits a decomposition around the frequency zero.
- b) The number of modes to be extracted between each shift. A value smaller than five is probably not economical because a shift requires a new decomposition of the stiffness matrix.
- c) Auto shift parameter. When a new shift point is selected it is set to the highest frequency squared plus a scalar times the difference between the highest and next highest distinct frequency squared. The scalar is preset to one in the program but can be changed by the user.

MODAL DAMPING

The natural frequencies are extracted by the MODAL SHAPE Option (Volume II, Section 2), for the undamped system. During the time-history response obtained on the basis of the extracted modes, the user may include damping associated with each mode. This is achieved through the use of the DAMPING optional block. In this option, the user inputs the fraction of critical damping to be used with each mode. Then, during the integration of the time history, the program associates the corresponding damping fraction with each mode, basing the integration on the usual assumption that the damping matrix of the system is a linear combination of the mass and stiffness matrices, so that the modes of the system are not changed by the damping.

DIRECT INTEGRATION DAMPING

As in the modal option, the user may introduce damping in the direct integration options, using the same assumption that the system damping matrix is a linear combination of the mass and stiffness matrices of the system:

$$C = \alpha M + \beta K,$$

where

C is the damping matrix,

M is the mass matrix

K is the instantaneous stiffness matrix

and

α, β are scalar factors

In this notation, the governing equation is

$$Ma + cv + I = F,$$

$$K = \frac{dI}{du}$$

where

I is the integral $\int B^T \sigma dV$

The user inputs the α and β factors in the DAMPING block; then the program forms and includes C each time the system matrices are reformed, basing the βK combination on the current value of instantaneous stiffness, K.

CONCENTRATED MASS

The user may input concentrated masses directly, to be included in the dynamic analysis. The number of such point masses is input with the MASS POINT parameter card, and the list of the masses magnitudes with the MASSES Option. Note that a point mass must be input in association with each appropriate degree of freedom at a node.

DIRECT INTEGRATION OPERATORS

Three direct integration operators are available (see DYNAMIC parameter card, Volume II, Section 2). The first (IDYN=2) is the Newmark β method, with $\gamma = 1/2$, $\beta = 1/4$ (trapezoidal rule), while the second (IDYN=3) is the Houbolt operator (displacement approximated over 3 time-steps by a cubic). Both of these operators are implicit (i.e., matrix solution is required to step the solution forward) and both are unconditionally stable with respect to time step size for linear problems. The Houbolt operator introduces artificial damping, the amount of such damping increasing with the ratio of time step to period of the natural modes of the system. Thus the Houbolt operator effectively removes higher mode response from the system. The usual recommendation is to extract the Eigen modes and frequencies of the system (using the MODAL SHAPE Option) and then decide on which modes are important to the response. The time step should then be chosen as $1/15$ to $1/30$ of the period of the highest such mode. However, in nonlinear problems, the mode shapes and frequencies are strong functions of time, through plasticity and large displacement effects, so that the above guideline may be quite a coarse approximation. A more general rule would be to repeat a part of the analysis with a significantly different time step ($1/5$ to $1/10$ of the original), and compare response. This is easily achieved through the use of the RESTART Option.

Both the Newmark and the Houbolt operators introduce periodicity errors, again reversing with the ratio of time step to period of the natural mode involved. With the above guideline, minor errors would occur for the modes below that used for time step estimates.

The derivations of the equations used in MARC to solve the system, based on the Newmark and Houbolt operators can be found in Volume 4 of the MARC manuals. The following summary shows the equations used.

NEWMARK BETA OPERATOR

The generalized form of the Newmark β operator is

$$u^{n+1} = u^n + \Delta t v^n + \left(\frac{1}{2} - \beta\right) \Delta t^2 a^n + \beta \Delta t^2 a^{n+1}$$

$$v^{n+1} = v^n + (1-\gamma) \Delta t a^n + \gamma \Delta t a^{n+1}$$

where superscript n denotes a value at the n th step and u , v and a take on the usual meaning.

The particular form of the dynamic equations corresponding to the trapezoidal rule

($\gamma = \frac{1}{2}$, $\beta = \frac{1}{4}$) is:

$$\left(\frac{4}{\Delta t^2} M + \frac{2}{\Delta t} C + K\right) \Delta u = F^{n+1} - I^n + M \left(a^n + \frac{4}{\Delta t} v^n\right) + C v^n \quad (1)$$

where

$$I = \int B^T \sigma dV$$

Equation (1) allows implicit solution of the system: $u^{n+1} = u^n + \Delta u$

Without the residual load correction, we have

$$\left(\frac{4}{\Delta t^2} M + \frac{2}{\Delta t} C + K\right) \Delta u = \Delta F + M (2a^n + \frac{4}{\Delta t} v^n) + 2 C v^n \quad (2)$$

The damping uses the assumption that

$$C = \alpha M + \beta K \quad (\alpha, \beta \text{ scalars})$$

HOUBOLT OPERATOR

The Houbolt operator is based on the use of a cubic fitted through three previous points and the current (unknown) point in time.

This results in the equation

$$\begin{aligned} \left(\frac{2}{\Delta t^2} M + \frac{11}{6\Delta t} C + K \right) \Delta u = F^{n+1} - I^n + \frac{1}{\Delta t^2} (3 u^n - 4 u^{n-1} + u^{n-2}) M \\ + \frac{1}{\Delta t} \left(\frac{7}{6} u^n - \frac{3}{2} u^{n-1} + \frac{1}{3} u^{n-2} \right) C \end{aligned} \quad (3)$$

This equation provides an implicit solution scheme. Solve (3) for Δu , hence obtain $u^{n+1} = u^n + \Delta u$ and so obtain v^{n+1} and a^{n+1} . Two points should be kept in mind -

1. (3) is based on uniform time steps and so must be modified when the time step is changed.
2. A special starting procedure is necessary since u^n , u^{n-1} and u^{n-2} appear in (3).

Without the residual load correction, we have

$$\begin{aligned} \left(\frac{6}{\Delta t^2} M + \frac{3}{\Delta t} C + K \right) \Delta u = \Delta F + \frac{1}{\Delta t} M (6v^n + 3\Delta t a^n) \\ + c (3v^n + \frac{1}{2} \Delta t a^n) \end{aligned} \quad (4)$$

The damping again assumes that

$$C = \alpha M + \beta K$$

CENTRAL DIFFERENCE OPERATOR

Here the operator is written as

$$a^t = (v^{t+1/2} - v^{t-1/2})/\Delta t$$

$$v^t = (u^{t+1/2} - u^{t-1/2})/\Delta t$$

so that

$$a^t = (\Delta u^{t+1} - \Delta u^t)/\Delta t^2$$

where

$$\Delta u^t = u^t - u^{t-1}$$

and the program solves

$$\frac{M}{\Delta t^2} \Delta u^{t+1} = F^t - I^t + \frac{M}{\Delta t^2} \Delta u^t$$

Since the program uses a Lagrangian formulation, the mass matrix is only triangularized once. Also, since the operator is only conditionally stable, the stability limit of the initial linear system is always computed (by a power sweep for the highest mode of the system), and the time step selected by the user is checked for stability and, if necessary, corrected.

LARGE DISPLACEMENT ANALYSIS

The large displacement formulation is based on the initial coordinate system. The analysis is performed by piecewise linear solutions. Incremental stiffness matrices are formed to account for initial stress and change of nodal coordinate effects. Follower forces may be applied. In special cases, such as rigid plastic flow for metal working, updating of the nodes for a deforming system is provided by a user subroutine (UPNOD).

BUCKLING

This procedure is used for estimating the maximum load that can be applied to a geometrically nonlinear structure.

The buckling option solves the following eigenvalue problem by a power sweep method.

$$([K] + \bar{\lambda} [\Delta K_G (\Delta u, u, \Delta \sigma)](d) u = 0$$

ΔK_G is assumed to be a linear function of the load increment ΔP to cause buckling. The stiffness ΔK_G for the buckling load is developed on the basis of the stress and displacement state at the start of the last increment. The load increment ΔP and the corresponding Δu just calculated are used. However, the stress and strain states are not updated until after the buckling analysis. The buckling load is therefore estimated by:

$$P_{\text{buckling}} = P_{\text{last}} + \bar{\lambda} \Delta P$$

where:

$\bar{\lambda}$ is the value obtained by the power sweep

It should be noted that the load vector ΔP need not be proportional to the load P . In the case of linear elastic buckling, $P_{\text{last}} = 0$. The buckling load is estimated with the initial displacement stiffness matrix. This matrix accounts in a linearized manner for the effects of displacements prior to buckling. This is very important in geometrically sensitive structures.

An estimate of the buckling load can be achieved after every load increment, if it is desired.

For details of this method of estimating elastic geometric collapse, see Reference 25, Appendix G.

GENERALIZED SHANLEY BUCKLING

In the generalized Shanley Buckling we consider the buckling of elastic-plastic structures which deform with a symmetric mode but bifurcate with an asymmetric bending mode. For example, a plate when loaded in its plane, deforms with in-plane displacements (symmetric mode). However, it bifurcates out-of-plane (asymmetric mode). In the presence of plasticity, and as shown by Shanley, this bifurcation can only take place in the presence of an increasing load. Shanley also argued that bifurcation took place with continued plastic loading; however after the bifurcation, elastic unloading of parts of the yielded zone takes place. Some increase of load takes place before the structure buckles.

The program simulates the process in the following manner. First of all, by testing for buckling at each load increment the Shanley bifurcation point is found. A restart tape is written after each increment. The program is then restarted at the bifurcation increment and the PROPORTIONAL LOAD increment is used to increase the total displacement by a scaled displacement corresponding to the bending mode. The program presents the user with a displacement vector of the same length as the total displacement vector. The user should remember that this implies a large bending displacement. A very small increment of load is then applied in order to allow the full asymmetric displacement to take place. The buckling load can then be found by further increments. An alternate approximate procedure has been added to the program. This option demands that, for the next increment, only half the plate or shell is allowed to yield; thus, placing an upper bound on the strengthening due to elastic unloading. Therefore, an eigenvalue analysis will give an upper bound estimate of the load for collapse.

In the check examples, this load did not differ significantly from the bifurcation load (+5%). However, no general statement can be made.

CYCLIC CREEP BUCKLING

The incremental stiffness ΔK_G in the earlier equation is a function of increments of stress $\Delta\sigma$ and displacement Δu . A reasonable estimate of the creep buckling time can be found by calculating the $\Delta\sigma$ and Δu due to an increment of time when a steady creep state has been reached. This incremental quality is then used to estimate the eigenvalue λ by which the increment of time has to be scaled in order to cause buckling.

An even better estimate of the buckling time can be obtained by repeating the buckling analysis after a certain interval and extrapolating from a plot of actual creep time and estimated creep buckling time.

In the case of a repeated cyclic load, the same procedure may be repeated, but now the program allows for the accumulation of the stress and displacement increments over a whole cycle. The accumulated quantities are used to form a geometric stiffness matrix. At the end of a whole cycle, the next increment is applied, followed by a buckling analysis. This gives an eigenvalue which may be interpreted as the number of whole cycles to cause buckling.

FLUID/SOLID INTERACTION

This capability allows the study of structures immersed in, or containing a fluid. The model allows for the effect of pressure waves in the fluid, which is assumed to be inviscid and incompressible. It is only relevant to dynamic analysis, since the only effect of the fluid is to augment the mass matrix of the structure. The complete theory is given in Volume IV. Examples of the use of this feature are -- vibration of dams, ship hulls, and tanks containing liquids.

In MARC the fluid is modeled with heat transfer elements (potential theory) and the structure modeled with normal stress -- displacement elements. The element choice should ensure the interface between the structural and fluid models has compatible interpolation, i.e., first order solid and fluid elements, or both second order. If necessary, the tying option may be used to achieve compatibility. The FLU LOAD parameter card and FLUID SOLID model definition set are necessary to identify the interfaces between the fluid and the structure. Then on the zeroth increment, the program calculates the stiffness matrix for the structure, and the mass matrix for the structure augmented by the fluid effect. On subsequent increments, the usual dynamic options may be invoked (eg. MODAL SHAPE, DYNAMIC CHANGE) depending on the type of dynamic analysis requested on the DYNAMIC parameter card.

Note that the calculation of the structural mass augmentation requires the triangularization of the fluid potential matrix, which is singular unless some boundary condition (such as a free surface) is available on the fluid pressure.

RIGID, PERFECTLY PLASTIC FLOW

Creeping, steady state flow (neglecting inertia effects) of rigid, perfectly-plastic materials may be modeled by use of the incompressible elements. The velocity field (and stress field) is obtained as the solution. Iteration is performed to converge on the equivalent viscosity. This iteration is based on the velocity field, so that the method only converges for velocity boundary conditions. See Volume IV for theory.

The use of this option is flagged by the R-P FLOW parameter card. Convergence controls are input in the CONTROL option for controlling the iteration on the velocity field.

For pseudo-steady flow problems, user subroutine UPNOD is available for updating the mesh.

VISCOPLASTICITY

The creep option has been modified to enable problems with viscoplasticity to be solved. In its most common form of application, it is used to implement the initial stress or initial strain procedure of elastic-plastic analysis. The method is modified to allow for the solution of elastic-plastic problems with non-associated flow rules which result in unsymmetric stress strain relations. In the method as implemented no attempt has been made to distinguish between elastic-plastic and creep strains. It therefore should not be used for problems with combined elastic-plastic and creep behavior.

The procedure solves the equation

$$[K] \{du\} = \{dF\};$$

where $\{dF\}$ is the incremental initial stress or strain force vector. This force vector is formed from the viscoplastic strain increments formed at the element integration point level by subroutine CRPLAW.

$$\int_V [B]^T [S] \{de\}_i dV$$

where $[B]$ is the strain to displacement transformation matrix

$[S]$ is the elastic stress strain relation

and $\{de\}_i$ is the viscoplastic strain increment

The following load incrementation procedure is to be followed in solving a viscoplastic problem.

1. Apply an elastic load increment. This will exceed the steady state yield stress.
2. Relieve the high yield stresses by turning on the AUTO CREEP option. Steps 1 and 2 may be repeated in succession for as many times as required to achieve the required load program.

Note that the size of the load increments are not altered during the AUTO CREEP process so that further load increments can be effected by using the PROPORTIONAL INCREMENT feature.

The viscoplastic approach converts an iterative elastic-plastic method to one where a fraction of the initial force vector is applied at each increment by virtue of the time step controls. The success of the method depends on the proper use of the automatic creep time step controls. This means that selection of an initial time step that will result in just satisfying the tolerances placed on the allowable stress changes is necessary.

The initial time step $dt = \frac{\text{allowable stress change} \times 0.7}{\text{maximum viscoplastic strain rate} \times \text{Young's modulus}}$

The allowable stress change is specified in the creep controls. The maximum strain rate is usually obtained from the most highly stressed element. It is also important to select a total time that will give sufficient increments to work off the effects of the initial force vector. A total time of 30 times the estimated dt is usually sufficient.

HEAT TRANSFER

MARC contains a solid body heat transfer capability, based on the formulation given in Volume IV, Section D3-1. This section describes the use of this capability. The following features form the heat transfer option.

- a) Choice of backward difference (modified Crank-Nickolson) or Lees three level time integration; unconditionally stable for linear problem; automatic time step choice.
- b) Temperature, time dependent materials (including latent heat effects) and boundary conditions. User subroutines available for variable film coefficient and flux inputs.
- c) Choice of quasi-linearization or extrapolated averaging for evaluation of temperature dependent properties with Crank-Nickolson operator.
- d) Allowance for all types of boundary conditions and external flux, e.g., prescribed temperature/time history, volumetric flux, surface flux, film coefficients, radiation.
- e) Convenient output of nodal and integration point temperatures. This allows the solution to be interfaced with any stress analysis package. The format of the output is described below. MARC contains a special time interpolation capability to provide direct input of such time-temperature histories to a nonlinear (e.g., elastic-plastic) stress analysis via MARC.
- f) Ability to handle linear, homogeneous constraints on temperature (tying).
- g) Contour or time/temperature history plots via the MESH PLOT option or MARC-PLOT respectively.

ELEMENTS

The library elements available for heat transfer are as follows:

- 1-D - Linear temperature variation
- 2-D - Plane and axi-symmetric bi-linear and bi-quadratic quadrilaterals
- 3-D - Tri-linear (8-node) and tri-quadratic (20-node) bricks.

These elements are described in Volume I, Section 2.

DATA DEFINITION

The following data definition sets are available for heat transfer analysis with MARC. They are described in detail in Volume II.

a) Parameter Cards

HEAT

This card must be included to indicate that the analysis to be performed is a heat transfer analysis. The following cards must also be included:

SIZING	To give the overall problem size
END	To indicate the end of the parameter cards.

The following parameter cards may be used optionally with heat transfer:

TIE, RESTART, ELSTO, VECSTO, ECS, PRINT, ALL POINTS,
FORCOT, INPUT TAPE, ANISOTROPI, MESH PLOT, EDIT, TITLE,
TAPES, MATERIAL, NOTES, FILMS, FLUXES, CONTACT

b) Model Definition Cards

The following Model Definition sets may be used as necessary to define the heat transfer problem:

MESH2D, CONNECTIVITY, GEOMETRY, PROPERTY, COORDINATES,
BOUNDARY C, TEMPERATURE, CONTROL, RESTART, END OPTION,
TYING, UFXORD, RENUMBER, INITIAL CO, FORCOT, REGEN,
OPTIMIZE, POST, PRINT CHOICE, FILMS, FLUXES, SERVO LINK

c) Time History Input

The history input for the heat transfer problem is defined on these cards. The following sets are necessary for time history input:

TRANSIENT

This set defines the period of time and end conditions for this part of the solution.

The automatic time stepping scheme is based on a maximum temperature change per step given on the control option. The scheme is as follows:

After a solution is obtained for a step, the maximum temperature change in the step is calculated. This is then checked against the control specified value. If the actual maximum change exceeds the specified maximum, the step is repeated with a smaller time step--this continues until the specified maximum is not violated, or until the maximum recycles given on the control option is reached: in the latter case the program stops. If the actual maximum temperature change is between 80% and 100% of the specified maximum, the program goes on to the next step, using the same time step. If the actual maximum is between 65% and 80% of the specified maximum, the next step is tried with a time step of 1.25 times the current step: if it is below 65% of the specified maximum, the next step is tried with a time step 1.5 times the current step. The purpose of the scheme is to increase the time step as the diffusion solution proceeds: see Volume IV theoretical notes on heat transfer.

CONTINUE

This card indicates the end of a data definition set for transient control.

In addition, the following set may be used optionally.

BOUNDARY CHANGE, TYING CHANGE, PRINT CHOICE, FLUXES

The user should note that in heat transfer analysis total values are always input; e.g., total temperature boundary conditions, or total fluxes. For time varying temperature, flux or film input, the user may use subroutines FORCDT, FLUX, or FILM. Thus, external parameters (fixed temperature, fluxes or film coefficients) are set up using the necessary Model Definition or Time History Input cards. Conditions remain in effect until modified by subsequent Time History Input cards, or by user subroutine.

STEADY STATE SOLUTIONS

For steady state problems, the TRANSIENT option must still be input. Either set the specific heats to zero or use an 'infinite' time step. If the problem is nonlinear, the tolerance for property recycling on the control model definition set should be used to obtain an accurate solution.

OUTPUT

The program provides, as printed output, the nodal point temperatures and the temperatures at the element centroid or integration points, if the ALL POINTS option is invoked. The frequency and amount of output may be changed at any time with the PRINT CHOICE option; the default is to print all nodes and elements at each time step.

In addition, the user may utilize the POST processor model definition card set to provide himself with a tape of element and nodal point temperatures. This allows interface to MARC PLOT for temperature-time history plotting, or to stress analysis. For the latter case, the format of the POST tape is defined in Volume II, Section 8.1. Note that, in the definition of element variables in the POST option, only one element variable -- temperature - (code 9) is available in heat transfer.

A user subroutine NASSOC allows the user to specify a non associated flow rule for use with the equivalent creep strains (viscoplastic) calculated by subroutine CRPLAW. In order to use the viscoplastic option a flag is set in the CREEP parameter card.

The viscoplasticity feature can be used to implement very general constitutive relations with the aid of user function subroutines -- ZERO and YIEL.

In summary, the requirements for solution of the viscoplastic problem are:

1. Inclusion of the CREEP parameter card and creep controls.
2. Combined use of load incrementation immediately followed by a series of creep increments specified by AUTO CREEP.
3. Use of User Subroutine CRPLAW.
4. Optional use of User Subroutine NASSOC.

44. Provide a comparison of the stiffness obtained for the computer model to that of hand calculated ring segment at elevation 668+10 of the reactor building shell wall.

Response:

The interior structure of the Catawba reactor buildings was analyzed using a lumped mass model which considered the torsional effects present in the structure. The structural properties used as input to the lumped mass model are area, shear area, moments of inertia about the plan axis, and the polar moment of inertia. In addition, lateral stiffnesses are calculated for use in locating the center of rotation and for use in the distribution of lateral seismic shear forces. The torsional stiffness is also calculated for use in finding the polar moment of inertia and for use in the distribution of shears due to torsion. The above calculations were completed by a computer program developed in-house, specifically for this use. The program uses everyday methods of engineering mechanics and procedures developed in "Design of Multi-story Reinforced Concrete Buildings for Earthquake Motion" by Blume-Newmark & Corning. Plan #8, attached, shows a typical plan section at elevation 668+10 for which the above method was used.

The methods outlined in the above reference are intended for use with "Regular" buildings; that is, buildings of beam-slab-wall-column construction. The interior structure consists of many elements which fall into this category but it also has in its upper portion a closed ring, continuous section. The results from this program and a closed form hand solution for this ring are given in Table 44-1.

Discussion of results in Table 44-1.

The area, shear area, and lateral moments of inertia are, for all practical purposes, the same, the differences owing only to the differences in the two sections used in the calculations. The lateral stiffnesses, torsional stiffness, and the polar moment of inertia show an increase in the hand calculations or an under estimate by the computer program.

The increase in lateral stiffness has two effects in these calculations. (One), it moves the center of rigidity closer to the center of the structure and (two), it increases the amount of the total shear distributed to the ring. The movement of the center of rigidity will reduce the overall torsional effects in the building. This coupled with an increase in the polar moment of inertia will decrease the total shear on the structure.

The increase in stiffnesses, K_x , K_y , and K_p increase the percentage of total shear and torsional shear that is carried by the crane wall cylinder. The loads in question, both shear and torsion, are small in relation to the capacities of these structural elements in question. As noted above, the decrease in shear and torsion should, when coupled with the increase in stiffness, leave the design unaffected.

TABLE 44-1

PROPERTY	RING SECTION ² HAND CALC. RESULTS	PROGRAM RESULTS ¹
Ax (Ft ²)	810.53	832.00
As (Ft ²)	423.10	439.64
Ix (Ft ⁴)	750247.67	768050.
Iy (Ft ⁴)	750247.67	788490.
Ip (Ft ⁴)	1,500,495.33	570,180.
Kx (K/Ft)	11,851,829.51	7,397,700.
Ky (K/Ft)	11,851,829.51	7,373,400.
Kp ($\frac{K-Ft}{RAD}$)	4.2101×10^{10}	1.5998×10^{10}

NOTES:

¹ The program used the Section of Plan #8 for calculation.

² Figure 44-1 used in hand calculations.

Ax = Area

As = Shear Area

Ix = Moment of inertia about x-x

Iy = Moment of inertia about y-y

Ip = Polar moment of inertia (Izz)

Kx = Stiffness in direction x

Ky = Stiffness in direction y

Kp = Rotational stiffness

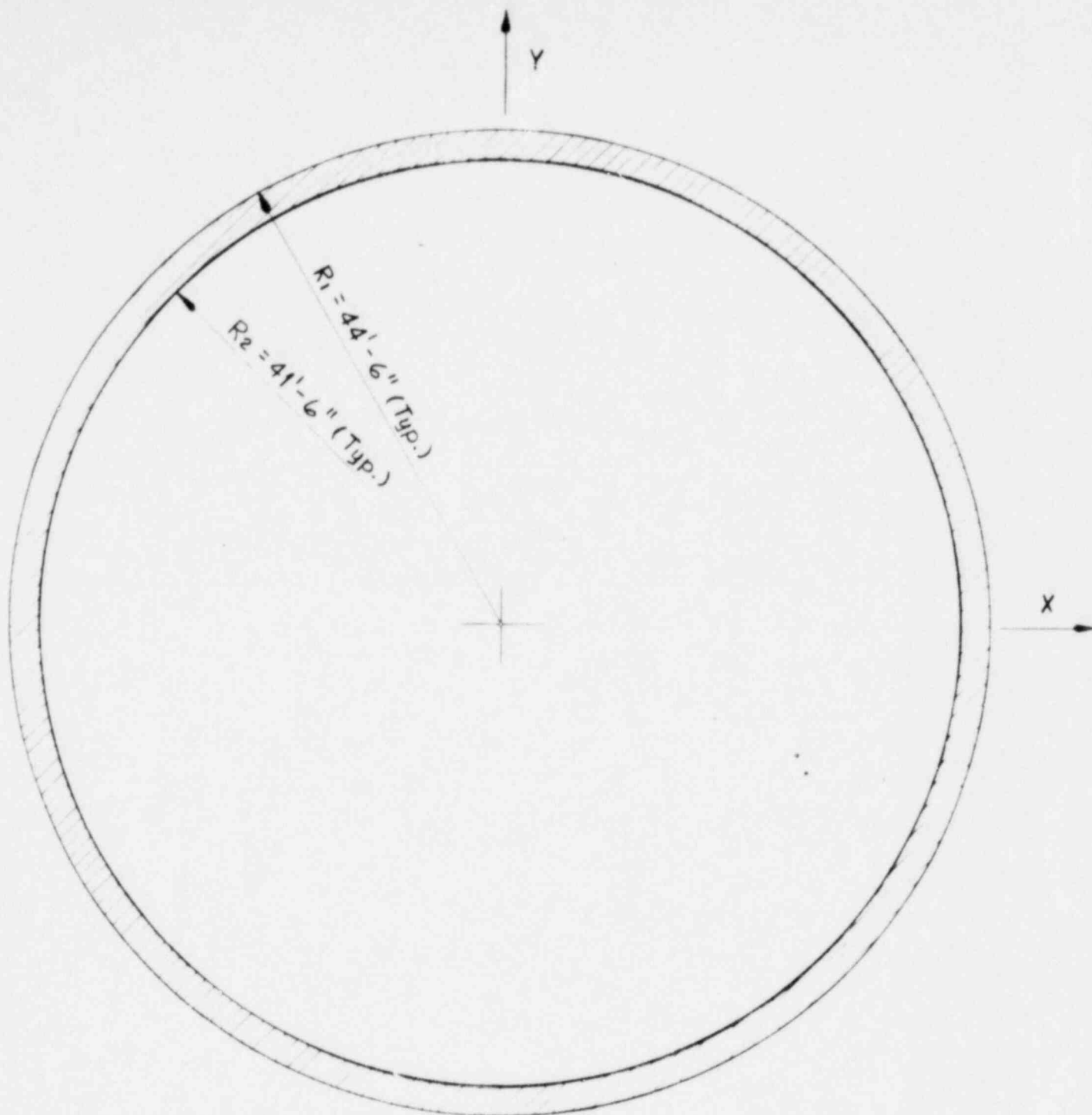
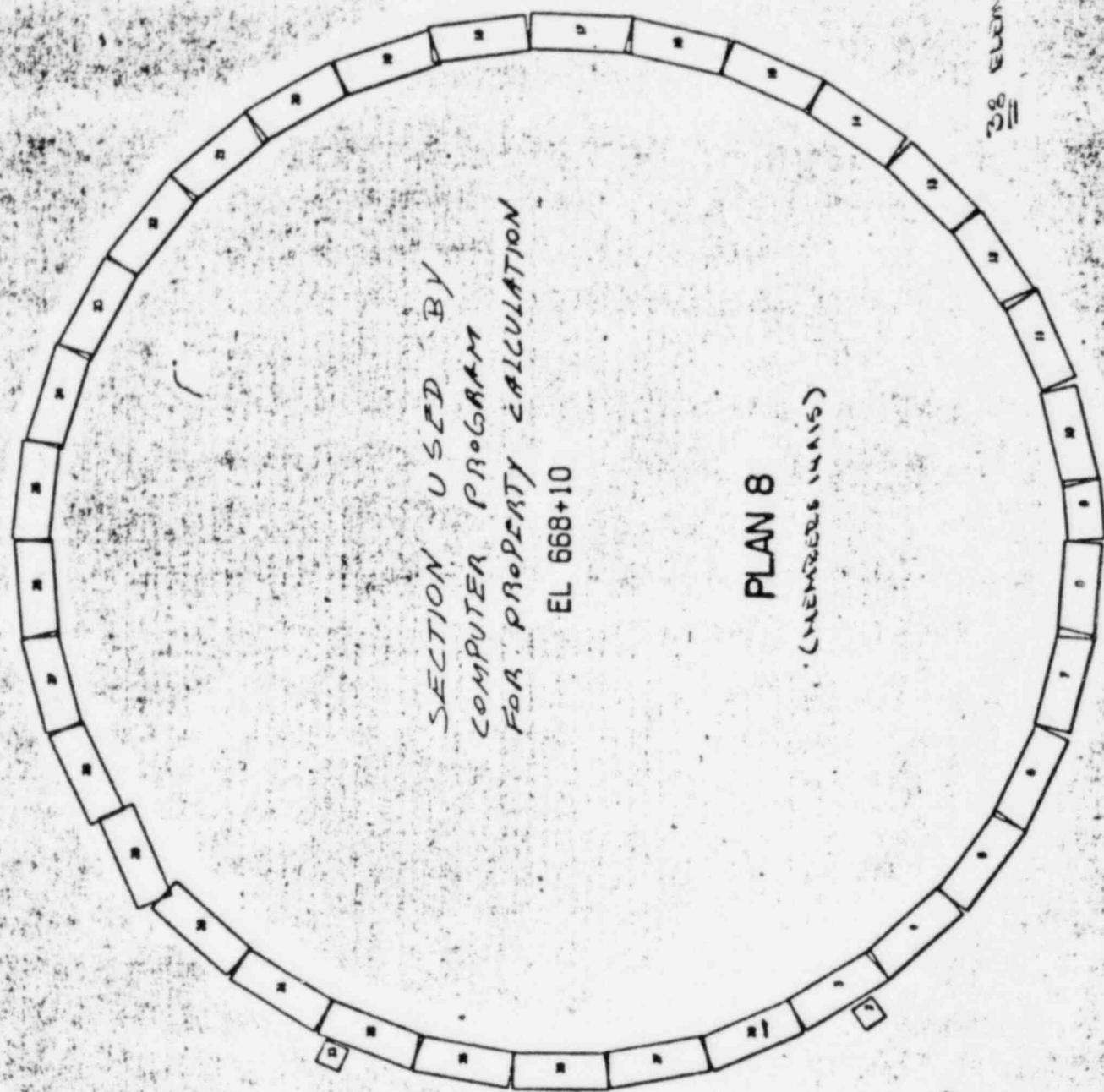


Figure 44-1
Section Used For
Hand Calculations

SHEET NO. 34 (of 54)

Rev. #3

0000059 0965



PLAN 8

(MEMBERS IN AIS)

SECTION USED BY
COMPUTER PROGRAM
FOR PROPERTY CALCULATION

EL 668+10

38 ELEMENTS